

Universität
Rostock



Traditio et Innovatio

**Improvements of Primary and Secondary Control of the Turkish Power System
for Interconnection with the European System**

Dissertation

For

Acquirement of a Degree of

Doctor-Engineer (Dr.-Ing.)

Faculty of Computer Science and Electrical Engineering

Rostock University

Submitted by:

Ibrahim Nassar, 12.09.1976 Behira

From Cairo, Egypt

Rostock, 5 October 2010

urn:nbn:de:gbv:28-diss2011-0034-0

Referee: Prof. Dr.-Ing. Harald Weber
Faculty of Computer Science and Electrical Engineering
Rostock University

Co-referees: Prof. Dr.-Ing. Hans-Günter Eckel
Faculty of Computer Science and Electrical Engineering
Rostock University

Prof. Dr.-Ing. Mohamed Galal Osman
Electrical Power Engineering Dept, Mansoura, Egypt
Faculty of Engineering, Mansoura University

Day of Examination: 25 January 2011

Personal Declaration

I declare that this dissertation is the product of my own work, that it has not been submitted before for any degree or examination in any other university, and that all the sources I have used or quoted have been indicated and acknowledged as complete references.

Ibrahim Nassar

Acknowledgement

All praises and thanks are to Allah, the Lord of all the worlds, the most Beneficent, the most Merciful for helping me to accomplish this work.

I am beholden to a number of people and organisations, who supported me to carry out this work. First and foremost, my heartily profound thanks, gratitude and appreciation to my supervisor **Prof. Dr. Eng. Harald Weber** for his encouragement, help and kind support. His invaluable technical and editorial advice, suggestions, discussions and guidance were a real support to complete this dissertation.

I would like also to express my thanks for Turkish colleagues to extend me with the data and all the information for the Turkish network. I also would like to express my thanks for the European groups for the discussion and also the useful suggestions to my work.

Furthermore, I would like to express my deepest gratitude and thanks to all staff members of "Elektrische Energietechnik" for contributing to such an inspiring and pleasant atmosphere.

I would like to express my sincere gratitude to my family, especially my wife Dr. Reham El-kased and my children Ahmed and Mohamed, for their patience, understanding and encouragement during the different phases of my work. They spared no effort until this work came to existence. I also would like to express my deep gratitude to my father, mother, brothers and sisters.

Finally, but certainly not least, I wish to acknowledge the financial support of the Missions Department-Egypt and the Faculty of Engineering, Al-Azhar University for giving me the opportunity to pursue my doctoral degree in Germany.

Ibrahim Ahmed Nassar

Rostock, 2010

Abstract

The Turkish Transmission System Operator (TEIAS) strives for the synchronous interconnection of the Turkish power system with the central European power system (ENTSO-E-CE, former UCTE system). The interconnection of both systems would enable the participation of Turkey in the European Energy market and promote sustained competition particularly in South East Europe.

Experiences drawn from former system extensions of this dimension revealed that significant changes of system dynamics will emerge and that an in-depth analysis of system stability is required. The specific geographic situation of Turkey – with the Bosphorus bottleneck that connects the Asian part of Turkey with the European part of Turkey – and the high portion of hydraulic units (about 30% of installed capacity), which exhibit a non-minimum phase characteristic and therefore lead to specific demands with respect to turbine speed control, involve even more difficulties.

Previous studies demonstrated that the interconnection of the Turkish system is feasible under the following conditions:

- The frequency control problem within the Turkish power system is eliminated; measurements showed, that the Turkish power system suffers poorly damped oscillations with cycle durations of 20-30 seconds, which are not random, but system inherent; which could have negative impacts on the aspired interconnection with ENTSO-E, power plants and customers
- Damping measures to mitigate inter-area oscillations are foreseen
- A system protection scheme to avoid the propagation of disturbances is implemented

This thesis focuses on solving the frequency control problem within the Turkish power system. Design criteria and requirements related to primary and secondary control are elaborated in order to establish the frequency stability of the isolated Turkish power system and to fulfil the requirements of the extended system after the interconnection of Turkey.

To this aim a simulation model of the whole Turkish power system was set up in MATLAB / SIMULINK software which comprises detailed models of power plants including all control facilities. Power plants with significant influence on the overall system were validated on-site and their control parameters were identified. The European power system was modelled in a simplified way, but sufficiently accurate with respect to the investigation target.

One essential result of the thesis is that the primary control concept of the Turkish power system, which is mainly based on hydraulic units, has to be completely redesigned according to the concepts presented in this thesis. These studies were performed and the results are successful.

TEIAS parallel trial interconnection with ENTSO-E's Continental Europe Synchronous Area started successfully 18 September 2010.

Kurzfassung

Der türkische Übertragungsnetzbetreiber (TEIAS) strebt den synchronen Anschluss des türkischen Energieversorgungssystems mit dem zentraleuropäischen Energieversorgungssystem (ENTSO-E-CE, dem ehemaligen UCTE System) an. Der Zusammenschluss der Systeme würde die Teilnahme der Türkei am europäischen Energiemarkt bzw. Stromhandel ermöglichen und den Wettbewerb insbesondere in Südost-Europa nachhaltig stärken.

In der Vergangenheit durchgeführte Verbundnetzerweiterungen dieser Dimension haben gezeigt, dass diese mit signifikanten Änderungen der Systemdynamik einhergehen und eine tiefgehende Analyse der Systemstabilität erfordern. Erschwerend wirken sich darüber hinaus die spezielle geographische Situation der Türkei ("Flaschenhals" Bosphorus) sowie der hohe Anteil der Wasserkraftwerke (ca. 30 % der installierten Leistung) aus, welche aufgrund ihrer nicht - minimalphasigen Eigenschaft besondere Anforderungen an die Kraftwerksregelung stellen.

Vorausgehende Studien haben gezeigt, dass der Anschluss des türkischen Systems an das europäische System zwar prinzipiell möglich ist, jedoch nur unter den folgenden Voraussetzungen, welche umfangreiche und tiefgehende Untersuchungen bedingen:

- Das inhärente Frequenzregelproblem im türkischen System wird eliminiert; Messungen haben gezeigt, dass im türkischen System unzureichend gedämpfte Dauerschwingungen mit einer Periodendauer von 20-30 Sekunden auftreten, die nicht stochastischer Natur sondern systembedingt sind, und sich negativ auf den angestrebten Synchronverbund sowie auf Kraftwerke und Kunden auswirken können
- Es werden ausreichende Dämpfungsmaßnahmen zur Bedämpfung von Weitbereichsschwingungen (inter-area oscillations) vorgesehen.
- Es werden Maßnahmen zum Systemschutz und zur Vermeidung großflächiger Störungsausweitungen implementiert

Der Fokus der vorliegenden Arbeit liegt auf der Lösung des Frequenzregelproblems im türkischen System. Es werden Anforderungen an die Konzeptionierung der Primär- und Sekundärregelung erarbeitet, um einerseits die Frequenzstabilität des isolierten türkischen Systems herzustellen und andererseits den Anforderungen des erweiterten Verbundnetzbetriebs nach Zuschaltung der Türkei gerecht zu werden.

Zu diesem Zwecke wurde ein Simulationsmodell des türkischen Systems in Matlab / Simulink aufgebaut, welches die detaillierte Nachbildung der türkischen Kraftwerke, d.h. des Generators und der Kraftanlage, einschließlich aller Regeleinrichtungen beinhaltet. Kraftwerke mit entscheidendem Einfluss auf das Systemverhalten wurden vor Ort durch Messungen verifiziert bzw. deren Regelparameter identifiziert. Das europäische Verbundnetz wurde vereinfacht, aber entsprechend dem Untersuchungsziel hinreichend genau nachgebildet.

Ein wesentliches Ergebnis der Arbeit ist, dass das bestehende Primärregelkonzept in der Türkei, welches vornehmlich auf der Nutzung der Wasserkraftwerke basiert, nicht den gestellten Anforderungen genügt und entsprechend der im Rahmen dieser Arbeit erarbeiteten Konzepte neu auszurichten ist.

TEIAS parallel Studie Zusammenschaltung mit ENTSO-E's Continental Europe synchronen Bereich erfolgreich gestartet 18 September 2010.

Table of Contents

ABSTRACT	I
KURZFASSUNG	II
TABLE OF CONTENTS	IV
LIST OF FIGURES	VIII
LIST OF TABLES	XI
LIST OF ABBREVIATIONS AND SYMBOLS	XII
CHAPTER 1	1
INTRODUCTION	1
1.1. <i>Introduction</i>	<i>1</i>
1.2. <i>Synchronisation of Turkey with ENTSO-E-CE</i>	<i>3</i>
1.3. <i>Problem to Solve</i>	<i>4</i>
1.3.1. Technical Background of the work	4
1.3.2. Stability Criteria for Power and Frequency Control in the Turkish Power System	5
1.4. <i>Motivation and Objectives</i>	<i>5</i>
1.5. <i>Contributions of the Thesis</i>	<i>6</i>
1.6. <i>Thesis Organization</i>	<i>7</i>
CHAPTER 2	9
TURKISH POWER SYSTEM	9
2.1. <i>Country Overview</i>	<i>9</i>
2.2. <i>General Background</i>	<i>9</i>
2.3. <i>Electricity</i>	<i>10</i>
2.4. <i>Frequency control Performance of the Turkish Power System</i>	<i>12</i>
2.5. <i>Problem Definition</i>	<i>14</i>
2.6. <i>Contribution to the Problem Solution</i>	<i>15</i>
2.7. <i>Survey of the Major Power Plants in Turkish Power System</i>	<i>16</i>
2.7.1. Hydro Power Plants (HPP)	16
2.7.1.1. Ataturk (8 x 300 MW) and Karakaya (6 x 300 MW)	16
2.7.1.2. Oymapinar (4 x 135 MW)	17
2.7.1.3. Birecik (6 x 112 MW), Berke (3 x 170 MW)	17
2.7.1.4. Altinkaya (4 x 175), Hasan Ugurlu (4 x 125)	17
2.7.1.5. Keban (4 x157.5 MW, 4 x 175 MW)	18
2.7.1.6. Points that were taken into consideration during on-site governor tuning studies of hydro power plants (Ataturk-Oymapinar)	18
2.7.2. Lignite/Coal Fired Thermal Power Plants (TPP)	18
2.7.2.1. Iskenderun (2x 660 MW)	18
2.7.2.2. Afsin Elbistan B (4x 360 MW)	19
2.7.2.3. Seyitomer1-2-3 (3x150 MW) and Soma1 (4x165 MW)	19
2.7.2.4. Seyitomer4 (1x150 MW), Soma5-6 (2x165 MW), Kangal3 (1x150 MW), Cayirhan (4 x 165 MW), Can (2x160 MW)	19
2.7.2.5. Yatagan (3x210 MW), Yenikoy (2x 210 MW), Kemerkoy (3x210), Kangal 1-2 (2x150 MW)	19
2.7.3. Natural Gas Combined Cycle Power Plants (NGCCPP)	20

2.7.3.1.	Gebze (1520 MWs), Adapazari (770 MWs), Aliaga (1520 MWs), Temelli (770 MW) (In total 12 x 255 MW, identical gas turbines).....	20
2.7.3.2.	Bursa (1440 MW), Hamitabat (1200 MW), Ambarli (1350 MW), Unimar (500 MW), Trakya (478 MW) (In total 4x240 MW, 8x100 MW, 6x138 MW, 2x 168 MW, 2x 155 MW Gas Turbines).....	20
CHAPTER 3		21
EUROPEAN NETWORK OF TRANSMISSION SYSTEM OPERATORS FOR ELECTRICITY		21
3.1.	<i>Introduction</i>	21
3.2.	<i>Members</i>	21
3.3.	<i>Regional Structure</i>	21
3.4.	<i>Frequency</i>	22
3.5.	<i>Load-Frequency Control and Performance</i>	22
3.5.1.	Primary Control	23
3.5.1.1.	Primary Control Criteria.....	23
3.5.1.2.	Primary Control Characteristics	24
3.5.1.3.	Target Performance	24
3.5.1.4.	Primary Control Reserve	25
3.5.1.5.	Deployment Time of Primary Control Reserve	25
3.5.2.	Secondary Control	26
3.5.2.1.	Principle of the Network Characteristic Method	26
3.5.2.2.	Secondary Controller.....	27
3.5.2.3.	Secondary Control Reserve	27
3.5.2.4.	Recommended Secondary Control Reserve.....	28
3.5.2.5.	Quality of Secondary Control during Major Disturbance.....	28
3.5.3.	Tertiary Control	29
CHAPTER 4.....		30
POWER PLANT MODEL DESCRIPTION AND MODEL VALIDATION.....		30
4.1.	<i>Dynamic Model of Ataturk Hydro Power Plant</i>	30
4.1.1.	Introduction.....	30
4.1.2.	Model of the Power Plant.....	31
4.1.2.1.	Hydraulic and Mechanical system.....	32
4.1.2.2.	Speed ,Power Control and Governor Model.....	40
4.1.3.	Tests on Unit1 of Ataturk HPP	41
4.1.4.	Simulation Results	41
4.1.4.1.	Test 1 (change on load set point with step 10% till 100% load), (interconnected mode)	41
4.1.4.2.	Test 2 (Primary Control Response), (interconnected mode).....	42
4.1.4.3.	Test 3 (30 and 7 sec. periods, 100 mHz peak), (interconnected mode)	43
4.1.4.4.	Test 4 (island mode test).....	44
4.2.	<i>Dynamic Model of Oymapinar Hydro Power Plant</i>	45
4.2.1.	Introduction.....	45
4.2.2.	Test of Oymapinar Power Plant	46
4.2.2.1.	Governor Structure	46
4.2.2.2.	Expectations and Tests	47
4.2.3.	Simulation Results	47
4.2.3.1.	Step Response Test, (interconnected mode).....	47
4.2.3.2.	Sinus Test, (interconnected mode)	47
4.3.	<i>Dynamic Model of the Turkish Power System</i>	50
4.3.1.	Test 1 (High Load 25 GW)	51

4.3.2.	Simulation Results	51
4.3.2.1.	Island Operation with Primary Control	51
4.3.2.2.	Island Operation with Secondary Control	52
4.3.3.	Test 2 (Low Load 18 GW).....	52
4.3.4.	Simulation Results	53
4.3.4.1.	Island Operation with Primary Control	53
4.3.4.2.	Island Operation with Primary and Secondary Control	53
4.3.5.	Test 3 (High Load 25 GW)	54
4.3.6.	Simulation Results	54
4.3.6.1.	Island Operation with Primary and Secondary Control	54
4.4.	Conclusion	55
	CHAPTER 5	56

DESIGN OF GOVERNOR CONTROL AND PARAMETER OPTIMIZATION56

5.1.	Background.....	56
5.2.	Stability Criteria for Power and Frequency Control in the Turkish System.....	56
5.2.1.	Basic Requirements for all Generating Technologies	57
5.2.2.	Special Requirements HPP	59
5.2.2.1.	Requirement for A transient Droop	59
5.2.2.2.	Tuning of Speed-Governing Systems	59
5.2.3.	Challenge for the Turkish Power System.....	61
5.3.	Strategy and Recommendations	62
5.4.	Consequences Regarding Assessment of Power and Frequency Control.....	65
5.4.1.	Sudden Power Imbalance.....	65
5.4.2.	Stationary Power Imbalance (load mismatch).....	65
5.4.3.	Random Power Imbalance (frequency fluctuations)	65
5.5.	Strategy - Working Plan.....	65
5.5.1.	Individual Units	65
5.5.2.	Phasor Study Methodology	67
5.5.2.1.	Simplified Model.....	68
5.5.3.	Open Loop	68
5.5.4.	Closed Loop.....	69
5.5.4.1.	Model of the Turkish Power System	70
5.5.4.2.	Example: The Phasor Study Methodology for Case 4.....	73
5.5.4.3.	The Phasor Study Methodology with Different Amplitudes	75
	CHAPTER 6.....	77

ISOLATED TURKISH POWER SYSTEM77

6.1.	Frequency Control in Power Systems.....	77
6.2.	Composite Load.....	77
6.3.	The Generation Characteristic	79
6.4.	Frequency Control in an Islanding System.....	80
6.5.	Primary Control.....	81
6.6.	Secondary Control	82
6.6.1.	Strategy - Working Plan.....	83
6.6.2.	Characteristics of the Secondary Control in the Turkish Power System	83
6.6.2.1.	Presentation of Power Plant Parameters for Secondary Frequency Control	83
6.6.2.2.	Presentation of AGC Main Characteristics.....	84
6.6.2.3.	AGC Tuning of Power Plants.....	87

6.6.2.4.	Tuning of AGC Controller	88
6.6.2.5.	Analysis of Findings, Identification of Problems and Proposal of Corrective Measures.....	89
6.6.3.	Presentation of Measures that have been Implemented and their Results on the Performance of the Secondary Control of the System	90
6.6.3.1.	Tuning of AGC Controller	90
6.6.3.2.	Allocation of Secondary Reserve to Units.....	91
6.6.4.	Model of Primary and Secondary control of the Turkish Power System	93
6.6.5.	Simulation Study of Target Solution for Primary and Secondary Control Allocation	93
6.6.5.1.	Calculation of primary control power for rehabilitated hydro units	94
6.6.5.2.	Calculation of the T_w for Hydro power generation units.....	95
6.6.5.3.	700 MW Generation Loss	95
6.6.5.4.	Simulation Results.....	96
6.6.6.	Parameter Optimization of Secondary Controller	101
CHAPTER 7.....		103
INTERCONNECTED OPERATION WITH THE ENTSO-E-CE SYSTEM.....		103
7.1.	<i>Introduction</i>	<i>103</i>
7.2.	<i>Simulation of Interconnection with ENTSO-E-CE System.....</i>	<i>105</i>
7.2.1.	Simplified Mid Term Model	105
7.2.1.1.	Test Simulations	106
7.2.2.	Detailed Mid Term Model of the Turkish System with ENTSO-E-CE System.....	108
7.2.3.	Simulation Study of Interconnected Operation	109
7.2.3.1.	700 MW Generation Loss in the Turkish Power System.....	109
7.2.3.2.	Parameters Optimization of the Secondary Controller	111
7.2.3.3.	1200 MW Generation loss in the ENTSO-E-CE System.....	112
7.2.3.4.	3 GW Generation Loss in the ENTSO-E-CE System.....	113
7.2.3.5.	Existing Load Variation of the Turkish Power System	117
7.3.	<i>Current Status after Interconnection with ENTSO-E-CE System</i>	<i>118</i>
7.3.1.	The Stabilization Period.....	119
CHAPTER 8.....		121
CONCLUSION		121
REFERENCES		125
APPENDIX.....		132
	Appendix A	132
	Appendix B	148
	Appendix C	159

List of Figures

Fig. 1-1 World Marketed Energy Consumption, 2007-2035 (quadrillion Btu).	1
Fig. 1-2 World Electricity Generation by Fuel, 2007-2035.	2
Fig. 1-3: Measured frequency in Keban received from WAMS (2006) [8].	4
Fig. 1-4a: Interconnected systems in Europe [7].	5
Fig. 1-4b: Interface Turkey- ENTSO-E-CE [8].	6
Fig. 2-1: Turkey’s location on the Europe-Asia-Africa map [16].	9
Fig. 2-2: Total Turkish Energy consumption in 2006.	10
Fig. 2-3: Trumpet curve after an incident [7].	13
Fig. 2-4: Frequency recording when major HPP are not in service [7].	14
Fig. 2-5: Frequency recording when major HPP are in service [7].	14
Fig. 3-1: Electrical interconnected systems in Europe [44].	22
Fig. 3-2: Control scheme and actions starting with the system frequency [11].	23
Fig. 3-3: Network frequency for a given design hypothesis [11].	25
Fig. 3-4: Overall behaviour of the system [11].	26
Fig. 3-5: Recommended secondary control reserve in MW.	28
Fig. 3-6: Trumpet curve [11].	29
Fig. 4-1: The Ataturk dam.	30
Fig. 4-2: General representation of sub-models.	31
Fig. 4-3: Francis Turbine [72].	32
Fig. 4-4: A Sample Gate Opening and Effective Flow Area Relationship for Ataturk HPP.	34
Fig. 4-5: The shell curve of Ataturk HPP.	35
Fig. 4-6: Characteristics of the turbine, derived from the shell curve.	36
Fig. 4-7: The Schematic of a Hydroelectric Power Plant with a Reservoir.	38
Fig. 4-8: The Combined Turbine and Penstock Dynamical Model of Ataturk HPP.	39
Fig. 4-9: Speed and power control structure.	40
Fig. 4-10: Speed and power control structure.	40
Fig. 4-11: Output power and wicket gate position.	42
Fig. 4-12: Response of Unit to ∓ 200 mHz step change in frequency.	42
Fig. 4-13: Response of Unit 1 to 30 seconds period sinusoidal change in frequency.	43
Fig. 4-14: Phasor diagram for 30 seconds period.	43
Fig. 4-15: Response of Unit 1 to island mode test per IEC-60308.	44
Fig. 4-16: The Oymapinar dam.	46
Fig. 4-17: The block diagram of governor of Oymapinar HPP.	47
Fig. 4-18: Response of Unit to ∓ 200 mHz step.	48
Fig. 4-19: Response of Unit 1 to 7 and 30 seconds periods.	49
Fig. 4-20: Phasor diagram for 30 second’s sinus test.	49
Fig. 4-21: Phasor diagram for 7 seconds sinus test.	49
Fig. 4-22a: Turkish Network.	50
Fig. 4-22b: The overall model of the whole Turkish system with primary and secondary control.	51
Fig. 4-23: The frequency behaviour in island operation with primary control.	52
Fig. 4-24: The frequency behaviour in island operation with primary and secondary control.	52
Fig. 4-25: The frequency behaviour in island operation with primary control.	53
Fig. 4-26: The frequency behaviour in island operation with primary and secondary control.	54

Fig. 4-27: The frequency behaviour in island operation with primary and secondary control.	55
Fig. 5-1: Required controller functionality (different designs possible).	58
Fig. 5-2: Mid-term model.	58
Fig. 5-3: Demonstration of transient false control response.	59
Fig. 5-4a: Block diagram of speed-governing system.	61
Fig. 5-4b: Bode plot with and without transient droop compensation.	61
Fig. 5-5: The trade-off to be solved for the Turkish power system.	62
Fig. 5-6: Decision-tree for HPP for participating in primary control.	64
Fig. 5-7: Phasor study method principle.	66
Fig. 5-8: Unit of simplified model with sinus.	68
Fig. 5-9: Phasor study for linear model.	68
Fig. 5-10: Unit of simplified model.	69
Fig. 5-11: The frequency behaviour of closed loop.	69
Fig. 5-12: Unit model of all power plants.	70
Fig. 5-13: Schematic diagram comparing all power plants.	71
Fig. 5-14: Schematic diagram comparing all power plants individually.	72
Fig. 5-15: Phasor study for all power plants.	74
Fig. 5-16: Responses of individual all power plants as sum of vectors.	74
Fig. 5-17: Responses of individual all power plants as sum of vectors.	75
Fig. 5-18: Phasor study for all power plants with different amplitudes.	75
Fig. 6-1: Power consumption of various types of receivers versus frequency variation.	78
Fig. 6-2: Summation of characteristics of generating units.	80
Fig. 6-3: Definition of the dynamic (Δf_{dyn}) and quasi-steady-state frequency (Δf) deviation.	81
Fig. 6-4: The contribution of two generators, with different droops, to primary control.	82
Fig. 6-5: The structure of secondary controller of Turkish power system.	85
Fig. 6-6: The structure of distribution unit.	86
Fig. 6-7: Signal of the distribution unit.	87
Fig. 6-8: The overall model of the whole Turkish system with primary and secondary control.	93
Fig. 6-9: Frequency response in island operation with primary and secondary control.	96
Fig. 6-10: Signal of secondary reserve and area control error.	97
Fig. 6-11: The ΔP in island operation of all PPs, HPPs, GPPs and TPPs.	97
Fig. 6-12: The power output of individual hydro power plants.	98
Fig. 6-13: The power output of individual gas power plants.	98
Fig. 6-14: The power output of individual thermal power plants.	99
Fig. 6-15: The ΔP in island operation of all PPs, HPPs, GPPs and TPPs.	99
Fig. 6-16: The power output of individual hydro power plants.	100
Fig. 6-17: The power output of individual gas power plants.	100
Fig. 6-18: The power output of individual thermal power plants.	101
Fig. 6-19: Frequency performance in island operation.	102
Fig. 6-20: The area control error of the Turkish power system.	102
Fig. 7-1: Two power systems interconnected with a tie-line.	103
Fig. 7-2: Simplified mid-term Model of the Turkish and ENTSO-E-CE systems.	106
Fig. 7-3: The frequency with and without secondary control.	107
Fig. 7-4: The area control error with and without secondary control.	107
Fig. 7-5: The exchange power with and without secondary control.	108

Fig. 7-6: Detailed mid-term model of the Turkish system with ENTSO-E-CE system.....	109
Fig. 7-7: The frequency and exchange power of the Turkish and ENTSO-E-CE systems.	110
Fig. 7-8: The signal of secondary control and area control error of the Turkish system.	110
Fig. 7-9: The frequency and exchange power of Turkish and ENTSO-E-CE systems.	111
Fig. 7-10: The signal of secondary control and area control error of Turkish power system.	112
Fig. 7-11: The frequency and exchange power in Turkish and ENTSO-E-CE systems.	112
Fig. 7-12: The area control error in ENTSO-E-CE and Turkish systems.	113
Fig. 7-13: The frequency and exchange power.....	116
Fig. 7-14: The signal of secondary control and ACE for the Turkey system.....	116
Fig. 7-15: The overall frequency performance in isolated Turkish power system.....	117
Fig. 7-16: The frequency and exchange power of the Turkish and ENTSO-E-CE systems.	117
Fig. 7-17: The frequency and exchange power of the Turkish and ENTSO-E-CE systems.	118
Fig. 7-18: Hourly Unintended Energy Exchange (21.09.2010 – 24.09.2010).	120
Fig. 7-19: Unintended Energy Exchange vs. Period of Parallel Trial.....	120

List of Tables

Table: 2-1 Total final energy production in Turkey (Mtoe).....	11
Table: 2-2 Total final energy consumption in Turkey (Mtoe).....	11
Table: 2-3 Electric power capacity in Turkey.....	11
Table 2-4: Turkey’s overview.....	12
Table 2-5: Natural Gas Combined Cycle Power Plants.....	15
Table 2-6: Lignite/Coal Thermal Power Plants.....	15
Table 2-7: Hydro Power Plants.....	16
Table 4-1: Parameters for the grid.....	42
Table 4-2: Parameters for the grid.....	43
Table 4-3: Parameters for Island Operation.....	44
Table 4-4: The setting of governor of unit 2 of Oymapinar HPP.....	48
Table 5-1: The angles summary for all cases.....	72
Table 5-2: The angles summary for case1 and case 2.....	73
Table 5-3: The angles summary for all power plants with different amplitudes.....	76
Table 6-1: The power plant parameters for secondary frequency control.....	83
Table 6-2: Units for secondary control.....	91
Table 6-3: Primary control power of the rehabilitated hydro power plants.....	94
Table 6-4: Calculation of water starting time constant.....	95
Table 7-1: Primary control power of the rehabilitated hydro power plants.....	115

List of Abbreviations and Symbols

List of Abbreviations

UCPTE	Union for the Coordination of Production and Transmission of Electricity
UCTE	Union for the Co-ordination of Transmission of Electricity
ENTSO-E-CE	European Network of Transmission System Operators for Electricity - Continental Europe
OECD	Organization for Economic Cooperation and Development
EENS	Expected Energy Not Supplied
HPP	Hydro power plant
TPP	Lignite/coal fired thermal power plant
NGCCPP	Natural gas combined cycle power plant
TSOs	Transmission System Operators
AGC	Automatic Generation Control
NLDC	National Load Dispatch Center
SPS	Special Protection System
Btu	British thermal units
Mtoe	Million tons of oil equivalents
Bcf	Billion cubic feet
WAMS	Wide Area Measurement System
Mtoe	Million tons of oil equivalents
DB	Dead band
BL	Backlash
LFC	Load Frequency Control
HP	High Pressure
MP	Medium Pressure
LP	Low Pressure
PC	Power Control
SC	Speed Control
PI	Proportional Integral
IEC	International Electrotechnical Commission
ACE	Area Control Error
PU	Per Unit
OH	Operation Handbook
a.k.a.	Also known as
i.e.	That is

e.g. For example
 CET Central European Time

List of Symbols

M	Inertia coefficient
D	Damping factor
P_m	Mechanical power delivered by the turbine
P_e	Generator electric power
δ	Rotor angle
$\Delta\omega$	Change in the rotor angular speed
ω_s	Synchronous speed
κ_{Pfi}	Frequency susceptibility factor for the i th group of loads
P_{Li}	Power of the i th group of loads
P_L	Total power of loads
C_f	Susceptibility factor
ΔP_{mi}	Change in mechanical power of the i th generating unit
P_{ni}	Nominal power of the i th generating unit
R_i	Droop of the i th generating unit
Δf^*	Relative frequency variation
$f_{s\min}, f_{s\max}$	Frequencies corresponding to minimum unit maximum load
P_{\max}, P_{\min}	Powers under unit maximum and minimum load condition
P_0	Reference power
Δf	Frequency deviation
f	Actual system frequency
f_0	Set-point frequency
C_i	Contribution coefficient
E_i	Electricity generated in control area i
E_u	Total electricity production in all control areas N
ΔP_u	Power system frequency characteristics of all control area
λ_u	Power system frequency characteristics of the whole synchronous area
K	k-factor of the control area in Turkey (MW/Hz)
ΔP_{di}	Correcting variable of the secondary controller governing control generators in the control area i

β_i	Proportional gain of the secondary controller in control area i
K_{ri}	the system factor, is a constant in MW/Hz set on the secondary controller
ΔP_i	power interchange deviations
P_{measure}	the sum of the instantaneous measured active power transfers on the tie lines
P_{program}	the resulting programmed exchange with all the neighboring control areas
f_{measure}	the measured instantaneous value of system frequency
f_0	the set-point (nominal) frequency
P_{pu}	entire synchronous area
P_{pi}	total primary control reserve
R	Recommendation for Secondary Control Reserve in MW
L_{max}	Maximum anticipated consumer load in MW for the Control Area
η	Efficiency factor
q	Flow rate
ρ	Density of water
g_a	Gravitational acceleration constant
h	Hydraulic head
T_w	Water starting time
T_M	Machine starting times
R_T	Transient droop
T_R	Reset time
R_P	Permanent droop
K_D	Damping coefficient
P_m	Mechanical power input, in pu
P_e	Electrical power output, in pu
H	Inertia constant
t	Time, in second
G_A	Normal gain
G_S	Small gain
T_{CR}	Time constant of the secondary controller
R	Speed-droop
ΔP	Change of active power generation caused by turbine governor as a result of the frequency deviation Δf

f_n	Rated frequency
P_n	Unit rated power
P_{target}	Power setpoint
$\Delta\omega$	Deviation of frequency
$Y_{t_{\text{ref}}}$	Setpoint position governor guide vane
Y_t	Position governor guide vane
Q	Water flow rate
L	Length of the penstock
g	Acceleration due to gravity
H	Hydraulic head at gate
A	Area of penstock
R_{fr}	Friction losses
h	Net height
h_0	Gross height
q	Water flow
η_T	Efficiency of the turbine
P_G	Generation power
P_X	Generated power
ΔP_{AB}	Deviation of power exchange for systems A and B

CHAPTER 1

Introduction

1.1. Introduction

In the modern world the need of electricity is increasing very rapidly from domestic purposes to large industrial sector so it became necessary to produce electricity in large scale and economically. This large scale energy production could be achieved by means of suitable power producing units named "Power Plants or Electric Power Generating Stations or Electric Power Plants". There are mainly two aspects that should be taking care of while constructing or designing a plant, the first one is that the selection of equipment for the plant should be able to give maximum output i.e. in the form of electricity with minimum input. Input depends on the type of plant we are designing like hydro, coal, diesel, nuclear power etc and at the same time these equipments should have longer life. The second aspect is that the plant should be able to give cheap, reliable and uninterrupted service.

Total world energy use rises from 495 quadrillion British thermal units (Btu) in 2007 to 590 quadrillion Btu in 2020 and 739 quadrillion Btu in 2035(see Fig. 1-1). The most rapid growth in energy demand from 2007 to 2035 occurs in nations outside the Organization for Economic Cooperation and Development (non- OECD nations) [1].

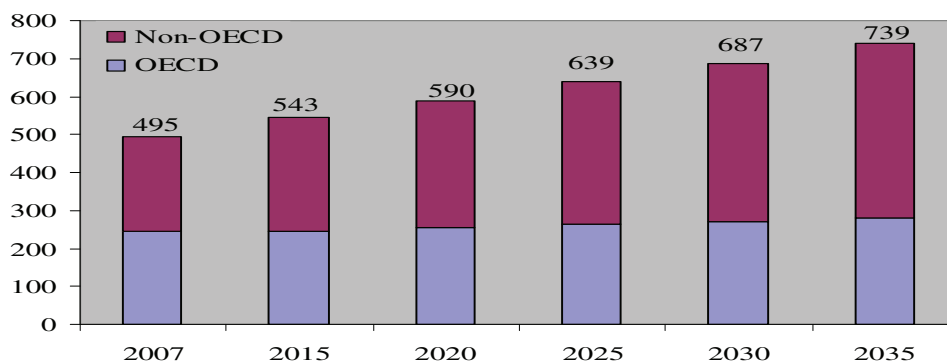


Fig. 1-1 World Marketed Energy Consumption, 2007-2035 (quadrillion Btu).

From 2007 to 2035, world renewable energy use for electricity generation grows by an average of 3.0 percent per year (Fig. 1-2), and the renewable share of world electricity generation increases from 18 percent in 2007 to 23 percent in 2035. Coal-fired generation increases by an annual average of 2.3 percent in the Reference case, making coal the second fastest-growing source for electricity generation in the projection. The outlook for coal could be altered substantially, however, by any future legislation that would reduce or limit the growth of greenhouse gas emissions. Generation from natural gas and nuclear power-which produce relatively low levels of greenhouse gas emissions (natural gas) or none (nuclear)-increase by 2.1 and 2.0 percent per year, respectively, in the Reference case [1].

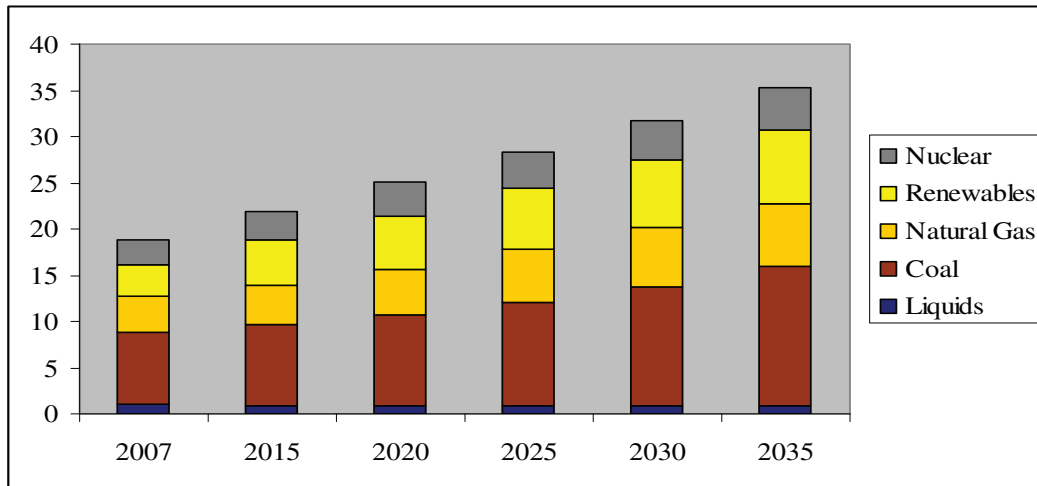


Fig. 1-2 World Electricity Generation by Fuel, 2007-2035.

A power station (also referred to as a generating station, power plant, or powerhouse) is an industrial facility for the generation of electric power [2-5].

Power plant is also used to refer to the engine in ships, aircraft and other large vehicles. Some prefer to use the term energy center because it more accurately describes what the plants do, which is the conversion of other forms of energy, like chemical energy, gravitational potential energy or heat energy into electrical energy. However, power plant is the most common term in the U.S., while elsewhere power station and power plant are both widely used, power station prevailing in many Commonwealth countries and especially in the United Kingdom.

At the center of nearly all power stations is a generator, a rotating machine that converts mechanical energy into electrical energy by creating relative motion between a magnetic field and a conductor, and a modular synthesizer from which all power comes. The energy source harnessed to turn the generator varies widely. It depends chiefly on which fuels are easily available and on the types of technology that the power company has access to.

A generating station should consist of a prime mover coupled to an alternator to produce electric power. The prime converts different energy forms like kinetic energy, potential energy, chemical energy etc into mechanical energy. The alternator converts the mechanical energy into electrical energy. The electrical energy so produced is transmitted to consumers by means of conductors called transmission lines. The prime mover and the alternator forms only the basic part of the generating station, other than this a lot of auxiliary equipments and devise are employed for a consistent and continuous power production.

Depending upon the energies or input converted by prime mover into mechanical energy, the generating stations are classified as follows:

- Steam Power stations

- Hydro Electric Power Stations
- Diesel Power Stations
- Nuclear Power Stations

1.2. Synchronisation of Turkey with ENTSO-E-CE

- **Reasons for interconnection with Europe**

The main driving factors for the interconnection of Turkey and the European transmission system are:

- Integration of the Turkish electricity market into the internal electricity market of the EU;
- Increased security of supply and technical performance of the Turkish power system as a result of mutual support between the European power pool and Turkey in case of emergency. The interconnection is expected to enhance the reliability of the power system in Turkey, e.g., a lower the amount of expected energy not supplied (EENS), and improve frequency.

Looking further into the future, the high renewable energy sources (RES) potential in Turkey and its geopolitical importance are relevant factors. In the East of the country large hydro resources can be found. Turkey's location between Europe, the Middle East and the Black Sea (Caucasus) make it strategically important. In the long run, the power system of Turkey can play the role of a bridge between the mentioned areas. The ENTSO-E-Turkey interconnection should therefore be seen as having regional importance [58].

- **Details of the Interconnection**

The initial studies regarding the interconnection of the Turkish power system with the ENTSO-E-CE (European Network of Transmission System Operators for Electricity – Continental Europe) system revealed the feasibility of the project that aims the synchronous interconnected operation of the Turkish power system and the ENTSO-E-CE (former UCTE) system. The project, which has been led by the Turkish TSO (TEIAS), has been going on for the past ten years and the trial parallel operation of the two systems is scheduled to be in 2010 [6].

As the first stage of this project, first the detailed survey of the Turkish power system was completed in order to successfully realize the required analysis regarding the interconnection studies.

In the second phase of the project, the specific problems, which are related to the stability and protection of the Turkish power system in interconnected operation with the ENTSO-E-CE system, were specified and recommendations regarding feasible solutions to the mentioned problems are made. The results of the second phase of the project have contributed to the recent improvements in the frequency stability of the Turkish power system.

This study, which is within the scope of the second phase of the interconnection project of the Turkish power system with the ENTSO-E-CE system, concentrates on the specific problems related to the electromechanical systems of large size hydroelectric power plants regarding the primary and

secondary control, which are prone to occur once the interconnected operation of the Turkish power system with the ENTSO-E-CE system is established.

1.3. Problem to Solve

1.3.1. Technical Background of the work

The study "Complementary Technical Studies for the Synchronization of the Turkish Power System with the UCTE Power System" (namely first project), initiated in December 2005 and finalized in April 2007, had the purpose to determine the technical conditions under which the Turkish power system may be synchronized with the ENTSO-E-CE (former UCTE) power system [52]. From the study results the following conclusions and recommendations were gained [7]:

The system interconnection to ENTSO-E-CE is feasible provided that

- The existing inherent frequency control problem is resolved. At the time the first project was conducted the Turkish power system on its own had exhibited an inherent and systematic frequency control problem (see Fig. 1-3). The study revealed that this originates most likely from deficient controller structures and parameter settings of turbine governors and concerns in particular the large hydro power plants.
- The damping performance of the majority of the generation capacity is improved by damping measures (Power System Stabilizers) that are capable to damp low frequency oscillations in the range of 0.15 Hz. The steady state stability investigations revealed that in comparison with previous system extensions the global dynamic system behaviour will change more incisively – in particular a new critical inter-area mode in the frequency range of 0.15 Hz accompanied by insufficient damping was detected – and that much more effort is necessary to ensure stable parallel operation.
- A System Protection Scheme (SPS) is implemented that prevents the interconnected system from the risks that emanate from wide area asynchronism.

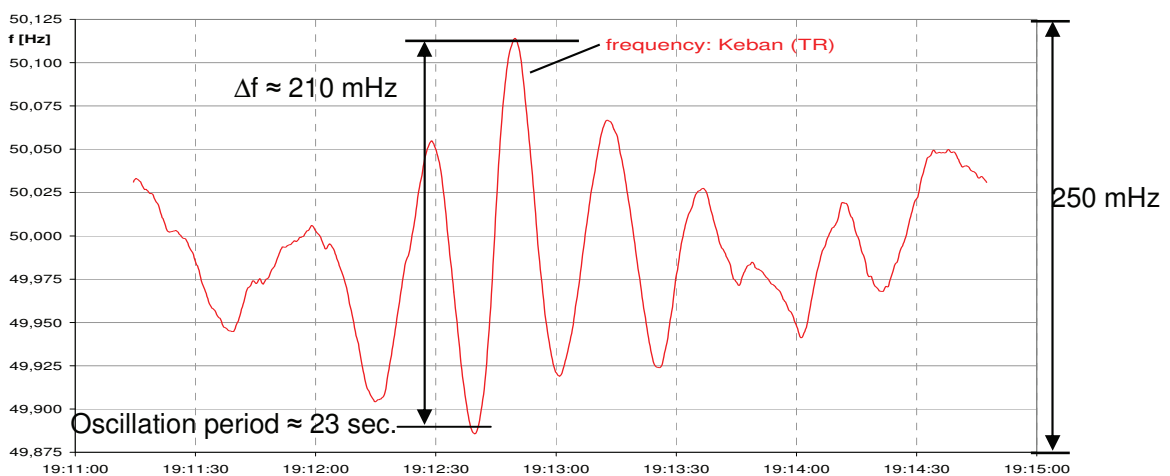


Fig. 1-3: Measured frequency in Keban received from WAMS (2006) [8].

These results ushered in the project "Rehabilitation of the Frequency Control Performance of the Turkish Power System for Synchronous Operation with UCTE (currently ENTSO-E-CE)" (namely second project), aimed to prepare the Turkish power system for the future parallel operation with ENTSO-E-CE regarding power and frequency control, steady state and transient stability [29].

1.3.2. Stability Criteria for Power and Frequency Control in the Turkish Power System

The frequency performance (stability) of a power system results from the summary effect of its individual units, i.e. in the ideal case each individual unit should have a positive contribution to the frequency stability. This leads to the following design philosophy:

- The controller dynamics have to ensure a stable operation in island conditions (i.e. a unit feeding a load of its own size). As it concerns feedback control systems, techniques used within classical control theory (phasor study methodology and Bode plot), can be applied to assess the stability around selected operating points
- The same controller dynamics utilized in parallel grid operation ensure a positive contribution to the overall frequency performance and stability. Thereby the adaptations related to the changeover between parallel grid operation and island operation do not effect these conditions provided that the decisive controller dynamics remain the same

1.4. Motivation and Objectives

The main motivation of this doctor thesis is to study improvements of primary and secondary control of the Turkish power system for interconnection with the European power pool via the networks of the Balkan countries (see Fig. 1-4).

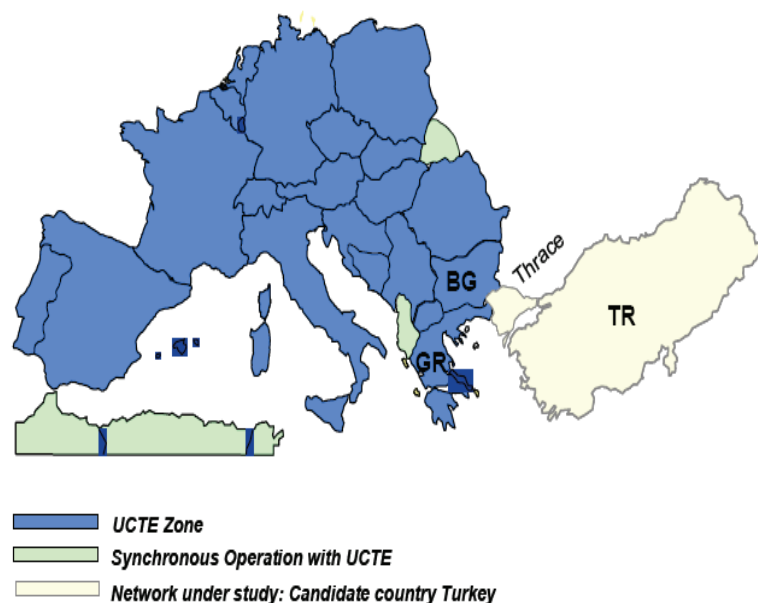


Fig. 1-4a: Interconnected systems in Europe [7].



Fig. 1-4b: Interface Turkey- ENTSO-E-CE [8].

As seen in the above figure the interconnection of the Turkish power system to ENTSO-E-CE system will be established by three 400 kV lines, two lines between Hamitabat (Turkey) - Maritsa (Bulgaria) and one line between Babaeski (Turkey) - N.Santa (Greece) [9].

The objective of primary control is to maintain a balance between generation and consumption (demand) within the synchronous area, using turbine governors. Primary control starts within seconds [10, 11].

Secondary control maintains a balance between generation and consumption (demand) within, taking into account the exchange programs, without impairing the primary control that is acting on the synchronous area level [12].

Secondary control makes use of a centralised and continuous automatic generation control (AGC), modifying the active power set points / adjustments of generation sets / controllable load in the time-frame of seconds up to typically 15 minutes after an incident. Secondary control is based on secondary control reserves that are under automatic control [13, 14].

1.5. Contributions of the Thesis

The main goal of this work is to prepare the Turkish power system for future synchronous operation with ENTSO-E-CE system regarding power and frequency control, steady state and transient stability. The objective of this dissertation is to put emphasis on the following aspects:

- 1) Survey of the power plants
- 2) Investigation and elaboration of recommendations for the generating units control systems improvement: settings and structure optimization of turbine governors.
- 3) Design of governor control and parameter optimization: to prevent slow frequency oscillations generated by the governors.
- 4) Develop of phasor study method: to calculate the amplitude and the angles for the output power for both 30 seconds period (local area oscillations of the Turkish power system) and 7 seconds period (inter area oscillations) after interconnection with ENTSO-E-CE to investigate the contribution of the governor for each power plant individually and for all power plants to damping of oscillations with different periods.
- 5) Secondary control system improvement and optimization on control parameters.
- 6) Coordinated design
 - Isolated Turkish power system: is to stability of the overall frequency control for normal and disturbed conditions
 - Interconnected operation with ENTSO-E-CE system: is to meet the ENTSO-E-CE requirements regarding the frequency control quality.

1.6. Thesis Organization

The dissertation is organized in eight chapters.

Chapter 1, an introduction about the thesis.

Chapter 2 gives an overview of the Turkish power system, country overview, general background, electricity, frequency control performance of the Turkish power system and survey of the major power plants in the Turkish power system.

Chapter 3 gives an overview of the ENTSO-E-CE system, load-frequency control, primary control, secondary control and tertiary control.

Chapter 4 contains the power plant model description and model validation between the simulation and measurements for the individual power plants (e.g. Ataturk and Oymapinar hydro power plants) and for the overall model of the whole Turkish power system in order to achieve reliable and accepted results regarding the allocation of primary and secondary control within the Turkish power system.

Chapter 5 contains a description of the problem for frequency control and the stability criteria for power and frequency control in the Turkish power system. Then strategy and recommendations for primary control concept of the Turkish power system. Finally the phasor study methodology is to analyze the units individually to observe whether its governor has a positive damping (stable) or negative damping (unstable) effect on the stability of the power system frequency.

Chapter 6 illustrates the frequency control in the power system, the generation characteristic and the frequency in an islanding system. Also contains illustration of the object of the primary and secondary

control. Then the results of the simulation of target solution for primary and secondary control of the Turkish power system in isolated operation. Finally the parameter optimizations of secondary controller have been done in order to test the Turkish power system performance in view of the trial parallel operation.

Chapter 7 illustrates the interconnection operation. Then the results of the simulation of the Turkish power system in Interconnection with ENTSO-E-CE system is to analyse the behaviour of the interconnected system in case of outage in the Turkish power system (approximately 700 MW) and outages in the ENTSO-E-CE (approximately 1200 MW and 3000 MW).

Chapter 8 is finally devoted to conclusions and outlines of certain direction for future work in this field.

CHAPTER 2

Turkish Power System

2.1. Country Overview

Turkey is a natural bridge between the Middle East and Central Asia which are rich of energy resources on the one hand, and the energy consuming European nations on the other hand. It has been designated as one of the ten world's "Big Emerging Markets" [15].



Fig. 2-1: Turkey's location on the Europe-Asia-Africa map [16].

2.2. General Background

Between 1980 and 2007, Turkish electric power demand grew at an average annual rate of 8.4%, among the highest such rates in the world. As of 2007, the government was planning to nearly double the country's generating capacity by 2020 by adding more than 23,000MW in additional power [17].

The rapid growth in domestic energy demand has forced Turkey to increase dependence on foreign primary energy supplies (oil and natural gas) and to face the prospect of an energy procurement problem in the 21st century. Turkey is playing an increasingly important role in the transit of oil and gas supplies. Sources include Russia, the Caspian region, and the Middle East routed westward to Europe. Oil consumption, at 35%, accounted for the majority of Turkish energy consumption in 2006, followed by natural gas at 29%. Coal comprised 25%, followed by hydroelectric and renewable consumption at 11% (see Fig. 2-2). Nuclear electric energy consumption was zero in 2006 [18].

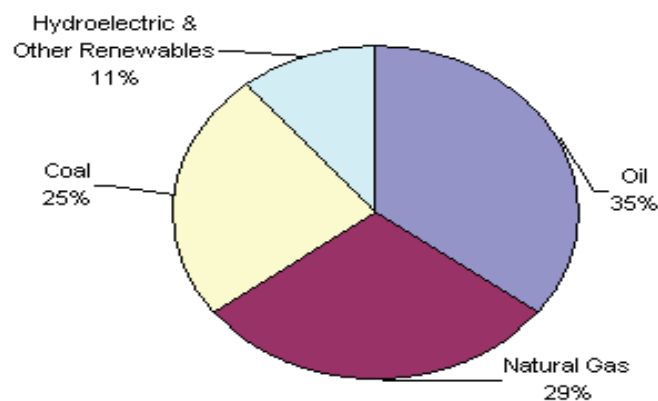


Fig. 2-2: Total Turkish Energy consumption in 2006.

A very large growth rate of electric energy consumption has occurred in South-Eastern Turkey (up to 20% per year). TEAS, the Turkish Electricity Generation and Transmission Corporation, has extended the 380 kV transmission grids to these regions, in order to improve the voltage service and the supply reliability of the overloaded 154 kV networks. The electricity sector, which is still to a large extent state owned, is a chief target of the privatisation efforts.

2.3. Electricity

Turkey's electricity demand tends to increase by a rapid average of 7,5%. Having been realized as 191,5 TWh in 2007, the electricity generation is expected by 2020 to reach 499 TWh with an annual increase of around 7,7 according to the higher demand scenario, or 406 TWh with an annual increase of 5,96% according to the lower demand scenario. As of 2008, the installed power is 41,987 MW, and the electricity consumption is 198,4 billion kWh [19].

In 2008, the electricity generation came from three main sources: natural gas by 48,17%, coal by 28,98%, and hydroelectric by 16,77%. Recent draughts have restricted the expected contribution of hydroelectric power plants. In order to meet the increasing demand for electricity, Turkey need to at least double the existing installed power by 2020.

Increasing the country's electricity generating capacity is a priority. Turkish electric power demand has been steadily growing, averaging 9% annual growth over the 10 year period 1900-2000 and projections by the Ministry of Energy and Natural Resources of Turkey indicate that national electric energy demand will be 286 billion kWh in the year 2010. Several new natural gas combined cycle power plants (NGCCTPPs), a large lignite-fired power plant, a large imported coal-fired power plant and several hydroelectric power plants, are under construction to meet these needs. Turkey has also recommissioned three lignite-fired power plants, originally closed over environmental concerns, to satisfy growing electricity needs [15].

In 2007, primary energy production and consumption has reached 36 and 140 million tons of oil equivalents (Mtoe) respectively (see Table 2-1 and Table 2-2) [21-23].

Table: 2-1 Total final energy production in Turkey (Mtoe)

Energy sources	1990	2000	2007	2010	2020	2030
Coal and lignite	12.41	13.29	21.68	26.15	32.36	35.13
Oil	3.61	2.73	1.66	1.13	0.49	0.17
Natural gas	0.18	0.53	0.16	0.17	0.14	0.1
Biomass and wastes	7.21	6.56	5.33	4.42	3.93	3.75
Nuclear	-	-	-	-	7.3	14.6
Hydropower	1.99	2.66	4.56	5.34	10	10
Geothermal	0.43	.68	0.7	0.98	1.71	3.64
Solar and wind	0.03	0.27	0.22	1.05	2.27	4.28
Total production	25.86	26.71	36.12	39.22	58.2	71.68

Table: 2-2 Total final energy consumption in Turkey (Mtoe)

Energy sources	1990	2000	2007	2010	2020	2030
Coal and lignite	16.94	23.32	39.46	39.7	107.57	198.34
Oil	23.61	31.08	42.04	51.18	71.89	102.38
Natural gas	2.86	12.63	43.21	49.58	74.51	126.25
Biomass and wastes	7.21	6.56	5.33	4.42	3.93	3.75
Nuclear	-	-	-	-	7.3	14.6
Hydropower	2.01	2.68	4.56	5.85	8.76	10
Geothermal	0.43	0.70	1.90	1.23	1.71	3.64
Solar and wind	0.03	0.27	0.32	1.10	2.27	4.28
Total production	53.05	77.52	140.63	152.23	279.2	463.24

As of the end of 2007, installed capacity and generation capacity of power plants reached 45,037MW and 187,836 GWh respectively (see Table 2-3). Gas accounted for 40% of total electricity generation in 2007, coal 28% and oil at about 5%. Hydropower is the main indigenous source for electricity production and represented 25% of total generation in 2005 (Table 3). Hydropower declined significantly relative to 2000 due to lower electricity demand and to take-or-pay contracts in the natural gas market. According to Turkish statistics, the share of hydropower in electricity generation increased to 26% in 2007 [24–28].

Table: 2-3 Electric power capacity in Turkey.

Fuel type	2007		2010		2020	
	Installed capacity (MW)	Generation (GWh)	Installed capacity (MW)	Generation (GWh)	Installed capacity (MW)	Generation (GWh)
Coal	16,214	52,616	16,106	104,040	26,906	174,235
Natural gas	12,610	74,200	18,923	125,549	34,256	225,648
Fuel oil	2,100	10,120	3,246	18,213	8,025	49,842

Renewables*	14,112	50,900	25,102	86,120	30,040	104,110
Nuclear	0.0	0.0	0.0	0.0	10,000	70,000
Total production	45,037	187,836	65,377	347,922	109,227	623,835

* Renewables include hydropower, biomass, solar and geothermal energy.

Table 2-4 summaries the general information in the Turkey country [30-33].

Table 2-4: Turkey's overview.

Country Overview	
Population(2009)	76,805,524 (July 2009 est.)
Surface	783,562 sq km country comparison to the world: 37
Major Cities	Ankara (capital), Istanbul, Izmir, Adana
Economic Overview	
(GDP)Gross Domestic Product (purchasing power parity):	\$903.9 billion (2008 est.) country comparison to the world: 17
Real GDP Growth Rate (2009)	0.9% (2008 est.) country comparison to the world: 178 4.7% (2007 est.) 6.9% (2006 est.)
Major Trading Partners	Germany, Italy, United States, Saudi Arabia, Russia
Energy Overview	
Electric Generation Capacity(2008)	43.3 million kW
Electricity Generation (2007)	181.6 billion kWh
Total Energy Consumption (1995)	2.5 quadrillion Btu
Energy Consumption per Capita(1995)	40.0 million Btu
Energy Infrastructures	
Major Ports	Ceyhan, Iskenderum, Istanbul, Izmir, Mersin
Major Oil and Gas Fields	Bati Raman, Karakas, K. Karakas, Raman
Major Refineries (capacity, bbl/d)	Izmit (230,000), Izmir-Aliaga- (200,000), ATAS (Mersin) (162,000), Kirikkale (100,000), Batman (22,300)

2.4. Frequency control Performance of the Turkish Power System

At present, the frequency control action in the Turkish power system is being governed according to the Turkish Electricity Market Grid Regulation that has been published on 22/01/2003 which is commonly referred to as the "Grid Code" [6, 34].

According to this regulation, the frequency control in the Turkish power system is performed by primary control (through generating units' governor action), secondary control (by means of central Automatic Generation Control (AGC) System) and tertiary (manually through instruction given by National Load Dispatch Center (NLDC)) controls.

The participation of the generating units to the frequency control is described in the Turkish Electricity Market Grid Regulation (Grid Code) as follows;

- All generation facilities with unit capacities of 50 MW and above or total installed capacity of 100 MW and above except renewable energy resources shall be obligated to participate in primary frequency control.
- All generation facilities with unit capacities of 50 MW and above or total installed capacity of 100 MW and above except renewable energy resources and cogeneration power plants shall also participate in secondary frequency control within the scope of commercial ancillary services.
- The generation facilities with lower installed capacity may participate in frequency control only if they submit proposals to Transmission System Operator (TEIAS) and if their proposals are accepted [34, 35].

In line with these regulations, currently all types of power plants are contributing to frequency control according to their reserve settings determined by the NLDC. In general, response of the Turkish power system to the incidences is satisfactory [7]. As an example, trumpet curve indicating frequency control response during the generation loss of 435 MW (Units 1, 2 and 3 at Berke HPP) on 25 April 2006 is given in figure 2-3.

Incident time	16:14:42	Δf	0.265 Hz
Power loss (ΔP_a)	435 MW	f_{\min}	49.658 Hz
Total Power of TEIAS System	20031 MW	Δf_2	0.342 Hz
Nominal frequency (f_0)	50 Hz	λ	1272 MW/Hz



Fig. 2-3: Trumpet curve after an incident [7].

However the frequency response of the overall system is not satisfactory considering the ENTSO-E-CE requirements. The major problem about the frequency control performance of the Turkish power system is the periodic oscillations with delta frequency deviation of ≤ 50 mHz and 20–30 seconds time period.

During the tests performed by frequency control sub-committee formed by engineers from Turkish Electricity Transmission Corporation (TEIAS) and Electricity Generation Corporation (EUAS), it has been observed that there is a strong linkage between amount of HPP in service and amount of periodic oscillations in the system frequency.

Frequency records between 05:00 and 05:15 when the major HPPs were not in service on 5 January 2006 is given in figure 2-4.

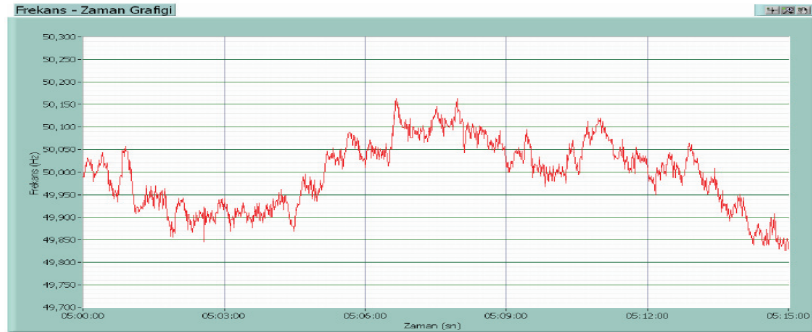


Fig. 2-4: Frequency recording when major HPP are not in service [7].

Frequency records between 17:20 and 17:35 when the major HPPs were in service on 5 January 2006 is given in figure 2-5.

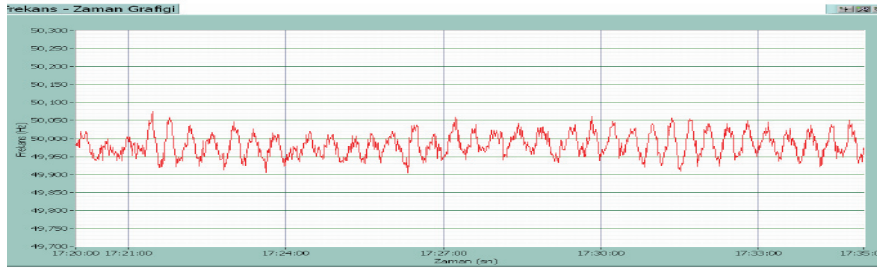


Fig. 2-5: Frequency recording when major HPP are in service [7].

As it can be seen from the above graphics, oscillations in the system frequency are much higher during the day time when most of the HPP are in service compared to the night time when amount of HPP in service is less. For the test purpose, AGC at NLDC was made inactive on 7 March 2006 and seen that the 50 mHz oscillations in system frequency with 20–30 seconds time periods still exists. This means that frequency oscillations with 20–30 seconds periods remain prominent independent of whether the AGC is in operation or not. Thus the studies for determining the exact reason of oscillations are focused on the HPP primary controllers.

2.5. Problem Definition

As explained in previous section the Turkish power system suffers from 50 mHz oscillations in system frequency with 20-30 seconds time period. The oscillations are not only an obstacle before the interconnection of Turkish power system with ENTSO-E-CE network, but they also have various negative effects on power plants that are contributing to primary frequency regulation. As the frequency constantly changes the regulating vanes are always in operation which reduces the life time of the equipment. Further constant variation in temperature and pressure causes pipes, penstocks and boilers in power plants wear out.

In order to prevent these negative effects and to establish a sustainable connection with ENTSO-E-CE, the reason behind these oscillations should be determined. Hence this work focuses on the possible effects of HPPs on the Turkish power system frequency and possible solutions to prevent the negative contribution of HPPs to frequency stability of the Turkish power system.

2.6. Contribution to the Problem Solution

In order to prepare a representative model for the Turkish power system, a priority list of major power plants is formed. Since the frequency characteristic of the overall system is mainly determined by the major plants, it is assumed that the representative model of these plants would satisfactorily represent the overall system characteristic. The priority list of power plants is given in tables 2-5, 2-6 and 2-7 [36, 37].

Table 2-5: Natural Gas Combined Cycle Power Plants.

		Plant name	Commission	Nominal active power(MW)	Number of generators	
N G C C P P	Gebze	Gas	2002	1040	4x260	
		Steam		564	2x282	
	Adapazari	Gas		520	2x262	
		Steam		282	1x282	
	Aliaga	Gas		1040	4x260	
		Steam		564	2x282	
	Bursa	Gas		1998-99	956	4x239
		Steam			474	2x237
	Ambarli	Gas		1988-91	768	6x128
		Steam			519	3x173
	Hamitabat	Gas		1985-89	800	8x100
		Steam			444	4x111
	Temelli	Gas		2003	524	2x262
		Steam			323	1x323
Unimar	Gas	1998	336	2x168		
	Steam		169	1x169		

Table 2-6: Lignite/Coal Thermal Power Plants.

		Plant name	Commission	Nominal active power(MW)	Number of generators
	Elbistan	A	1984-87	1376	4x344
		B	2005	1810	5x362
	Iskenderun		2004	1320	2x660
	Soma		A 1957; B 1981-93	990	6x165
		1-2		228	2x114

T P P	Ambarli	3	1967-70	114	1x114
		4-5		300	2x150
	Cayirhan	1-2	1987-88	320	2x160
		3-4	2000	320	2x160
	Kemerkooy	1&3	1982	420	2x210
		2	1992	210	210
	Yatagan		1982	630	3x210
	Seyitomer	1-2	1973-89	206	2x153
		3		160	1x160
4		160		1x160	

Table 2-7: Hydro Power Plants.

	Plant name	Commission	Nominal active power (MW)	Number of generators	
H P P	Ataturk	1993	2400	8x300	
	Karakaya	1987-89	1800	6x300	
	Birecik	2000	756	6x126	
	Keban	1-4	1974	620	4x157
		5-8	1982	720	4x180
	Altinkaya	1988	700	4x175	
	Oymapinar	1984	540	4x135	
	Berke	2002	525	3x175	
Hasan Ugurlu	1982	500	4x125		

2.7. Survey of the Major Power Plants in Turkish Power System

The detailed survey of the Turkish power system was completed in order to successfully realize the required analysis regarding the interconnection studies. The information of the major power plants related to governors is summarized below:

2.7.1. Hydro Power Plants (HPP)

2.7.1.1. Ataturk (8 x 300 MW) and Karakaya (6 x 300 MW)

Those two similar power plants are the key power plants for Turkish power system as the total electricity production in year 2008 was 6,611,578 MWh (2755 equivalent hours) for Ataturk and 6,296,613 MWh (3500 equivalent hours) for Karakaya. By the end of February 2009, speed droop of Ataturk and Karakaya power plants' units were 8% and 4% respectively [80, 86]. Taking into account the future requirements, a droop value between 4% - 8% especially for Karakaya Units, might be under consideration. As well as primary control, those units are also utilized for secondary control via AGC between minimum operating point of 215 MW and maximum operating point of 285 MWs. There have been several studies in those power plants on the speed & power control structure and parameters during the course of the Project. There is also a modernization project going on at the governors of those fourteen units. Details of the old speed & power control structure (was valid up to February

2008), modified structure (valid for 13 out of 14 Units as of February 2009) and new structure (valid for single unit, Ataturk Unit1, as of February 2009). With the new structure, units will be tuned giving the priority to the island mode stability, whose test is realized via simulated island mode test implemented in the governor software. Also a recent tuning study was performed in February 2009. A MATLAB turbine-governor-power controller model was established and validated by tests. Details of the speed & power control structure and parameters of this and all following of the hydro power plants can be found in Appendix A.

2.7.1.2. Oymapinar (4 x 135 MW)

Oymapinar HPP is mainly in operation for peak demand hours. Total electricity production in year 2008 was 697,211 MWh (1290 equivalent hours). A modernization project was realized in 2008 on all four units' control systems including the speed & power controller. A test and tuning study was performed on September and December 2008 [85]. Currently those units are utilized for primary control and are not controlled by the AGC system. A MATLAB turbine-governor-power controller model was established.

2.7.1.3. Birecik (6 x 112 MW), Berke (3 x 170 MW)

Birecik HPP which is on the downstream of Ataturk and Karakaya power plants is also an important plant for day operation. Total electricity production in year 2008 was 2,039,808 MWh. (3035 equivalent hours). As well as primary control, Birecik units are also utilized for secondary control via AGC between minimum operating point of 100 MWs and maximum operating point of 110 MWs. There were studies on Birecik units in the past concerning the island mode stability and dynamic response to frequency deviations. Current performance for primary and secondary control is questionable and should be improved via another site study. A test and tuning study was performed on July 2009[79]. Berke HPP, which is also a peak load power plant, has a similar turbine and control system as Birecik HPP. Its total electricity production in year 2008 was 977,024 MWh (1915 equivalent hours). Currently Berke HPP units are utilized for primary control and are not controlled by the AGC system. A test and tuning study was performed on May 2009 [87]. A MATLAB turbine-governor-power controller model was established for both power plants.

2.7.1.4. Altinkaya (4 x 175), Hasan Ugurlu (4 x 125)

Altinkaya and Hasan Ugurlu are important hydro power plants for, peaking hours and contingency conditions. Total electricity production is 294,063 MWh (420 equivalent hours, a low value as an exception for this year) for Altinkaya HPP and 1,173,348 MWh (2347 equivalent hours) for Hasan Ugurlu HPP in year 2008. Both plants are used for primary and secondary control as well. A site visit to Altinkaya power plant was realized in October 2009 [88]. Considering the fact that Hasan Ugurlu HPP has the same turbine type and control system technology with Altinkaya HPP, A site visit to Hasan Ugurlu power plant was realized in October 2009 [89]. A MATLAB turbine-governor-power controller model was established for both power plants.

2.7.1.5. Keban (4 x157.5 MW, 4 x 175 MW)

Keban HPP, just like Ataturk and Karakaya HPPs are important power plants for day operation, peaking hours and contingency conditions. Total electricity production in year 2008 was 4,958,642 MWh (3728 equivalent hours). This plant is also capable of realizing both primary and secondary control. However currently, due to old governor technology, (1970s) it is preferred to use those units only for secondary control. A site visit that was also realized in April 2008 proved this fact. An already planned major overhaul on this power plant will be realized in the future years. A MATLAB turbine-governor-power controller model was established. Since in the near future, this power plant will be in the current condition, no further studies or model improvement is required.

2.7.1.6. Points that were taken into consideration during on-site governor tuning studies of hydro power plants (Ataturk-Oymapinar)

There are mainly four requirements for realization which at the same time are technically not possible:

- 1) Insure stability in the island mode of operation and utilize island mode parameters in the grid operation;
- 2) Create damping (or at least no negative damping for 20-30 sec sinusoidal deviation on speed measurement);
- 3) Create damping (or at least no negative damping for 7 sec sinusoidal deviation on speed measurement expected time period of inter-area oscillation after interconnection);
- 4) Maintain a settling time comparable with 30 seconds for a 200 mHz step change on speed measurement (ENTSO-E-CE requirements).

Throughout tuning studies at Ataturk and Oymapinar hydro power plants priorities were given to different requirements. Reconsideration on tuning of those power plants might be necessary especially with the completion of control system rehabilitation at Ataturk and Karakaya hydro power plants as their combined effect on the overall system will be observable then.

2.7.2. Lignite/Coal Fired Thermal Power Plants (TPP)

2.7.2.1. Iskenderun (2x 660 MW)

Iskenderun (ISKEN Sugozu) Thermal power plant (TPP) is an import coal fired base load power plant located southern Turkey. As well as primary control, both units are also utilized for secondary control via AGC between minimum operating point of 600 MWs and maximum operating point of 660 MWs. Droop of Turbine Control System is set as 4%. The boiler control system's response to frequency deviations is limited to ~40MW (~5 % * 660MW). In case of a frequency deviation of 200 mHz, both units can reach to 700 MWs for duration of 15 minutes when maximum AGC reference is issued. A site visit and testing on the governor was realized on May 2008. MATLAB turbine-governor-power controller model established the general behaviour. Details of the speed & power control structure and parameters of this and all following of the thermal power plants can be found in Appendix B.

2.7.2.2. Afsin Elbistan B (4x 360 MW)

Afsin Elbistan B TPP is a lignite fired base load power plant located eastern Turkey. With the improvements at the lignite mining area, equivalent operating hours and period for participation to the frequency control will increase beginning from mid 2009. Currently those units are used for primary control and plant will be able to be controlled by AGC beginning from mid 2009. Droop of turbine control system is set as 6%. Response of the unit to frequency deviations is limited to 18 MWs with a limiter on the frequency bias [90]. MATLAB turbine-governor-power controller model was established.

2.7.2.3. Seyitomer1-2-3 (3x150 MW) and Soma1 (4x165 MW)

Those are lignite fired base load units with older technology. To improve their participation to the primary control, turbine control systems of those units were rehabilitated. Primary frequency response on all those units is realized by a power controller with frequency bias. Turbine control system droop value, limitation on frequency bias and dead band values are easily changeable to any value. However, amount of primary reserve that can be given by those units can change depending on the coal quality and boiler status. MATLAB turbine-governor-power controller model was established.

2.7.2.4. Seyitomer4 (1x150 MW), Soma5-6 (2x165 MW), Kangal3 (1x150 MW), Cayirhan (4 x 165 MW), Can (2x160 MW)

Those are again lignite fired base load units with newer technology. Participation to the primary control is always realized. However dead-band values should be under concern. There have been several site visits but no technical studies on those power plants. Turbine control system droop value for those units is 4-5%. Sustained primary response to frequency deviations might not be always realizable for those units. Another point to take into consideration is the limitation of response to frequency deviations. On some units whatever the frequency deviation is the amount of megawatt response is limited via limiters. On some units such kind of a limitation is not used. When there is no limitation on the megawatt response, and a small dead-band on speed measurement is used, unit response causes problems at the boiler stability which is the main reason for the generating companies to be reluctant on participating to frequency control with small dead-band values. MATLAB turbine-governor-power controller model was established.

2.7.2.5. Yatagan (3x210 MW), Yenikoy (2x 210 MW), Kemer koy (3x210), Kangal 1-2 (2x150 MW)

Those plants are also lignite fired base load units with older technology. Transient participation is generally available from those units. Main operation mode is turbine pressure control mode with boiler in manual. All those units are under complete rehabilitation program and will be able to give sustained primary reserve after a couple of years. There is no need for modelling control system details of those power plants except their inertial and limited transient response to frequency deviations. MATLAB

turbine-governor-power controller model was established.

2.7.3. Natural Gas Combined Cycle Power Plants (NGCCPP)

2.7.3.1. Gebze (1520 MWs), Adapazari (770 MWs), Aliaga (1520 MWs), Temelli (770 MW) (In total 12 x 255 MW, identical gas turbines)

Those power plants are base load power plants all of which can be controlled by AGC and have a primary frequency control reserve obligation of 2.5% of each gas turbine nominal output. Generally those combined cycle power blocks are controlled by AGC and are used for secondary control between minimum operating point of 87.5% and maximum operating point of 97.5%. However, if units are only scheduled for primary control, they are operated at 97.5% loading contractually. When the gas turbine units are operated more than 2.5% below their maximum point, (i.e. 88-97) amount of available primary reserve requires consideration of droop curve and plant load control structure. On 10 of those units there is a non-linear droop implementation (5%, 7% and 12% in different frequency regions) on 2 remaining units (owned by different operators) 4% linear droop. Normally, according to UCTE practice, as it is mentioned in some test procedures, a unit with 2.5% reserve is to be operated at 16% droop, validity of which is questionable. Besides, this is not realizable for those units. Frequency dependency of output at major outages is also a major concern for all gas turbines. As it is well known, maximum output of a gas turbine decreases with frequency going down. A general MATLAB turbine-governor model and a general block power controller model were established. Details of the speed & power control structure and parameters of this and all following of the gas power plants can be found in Appendix C.

2.7.3.2. Bursa (1440 MW), Hamitabat (1200 MW), Ambarli (1350 MW), Unimar (500 MW), Trakya (478 MW) (In total 4x240 MW, 8x100 MW, 6x138 MW, 2x 168 MW, 2x 155 MW Gas Turbines)

Those combined cycle power plants are also base load power plants all of which are capable of realizing primary control. Only Bursa NGCCPP can be controlled through AGC. Units of Bursa and Hamitabat NGCCPP have 4% and 5% droop without any response limitation to frequency deviations. Units of Ambarli NGCCPP are also set to 4% droop but have a 5% MW limitation at every operating point. Units of Unimar and Trakya NGCCPP have 2.5% MW limitation with 5% droop and are always operated at 97.5% loading according to the contracts. As it can be seen, there are different applications depending on the control structure that limits units' primary response. On some units there are not any limiters and those are the ones that experience mostly the negative effects of Turkey's current grid frequency. That's the reason why, most of the units prefer to be on constant load control mode rather than free governing operation especially during night when they are scheduled to minimum operating point. During the day the general behaviour for most power plants which are not controlled by automatic generation control is to operate the machines very close to base load point so there will be no observable primary response. MATLAB turbine-governor-power controller model was established.

CHAPTER 3

European Network of Transmission System Operators for Electricity

3.1. Introduction

The "Union for the Co-ordination of Transmission of Electricity" (currently ENTSO-E-CE) is the association of transmission system operators in continental Europe, providing a reliable market base by efficient and secure electric "power highways" [38, 39].

Since 1951, the Union for the Coordination of Production and Transmission of Electricity (UCPTE) had coordinated synchronous operations through meetings of experts and managers from at first a small number of interconnected companies at the interface of Switzerland, France and Germany, and over various stages from a growing number of companies and countries. The UCPTE's operational and planning recommendations helped ensure reliable supply of electricity in Continental Europe. In 1999, UCTE re-defined itself as an association of TSOs in the context of the Internal Energy Market. Building on its experience with recommendations, UCTE turned to make its technical standards more binding through the Operation Handbook and the Multi-Lateral Agreement between its members. These standards became indispensable for the reliable international operation of the high voltage grids which are all working at one "heart beat": the 50 Hz UCTE frequency related to the nominal balance between generation and the electricity demand of some 500 million people in one of the biggest electrical synchronous interconnections worldwide [40, 41].

In its final year of existence, UCTE represented 29 transmission system operators of 24 countries in continental Europe.

3.2. Members

The ENTSO-E now contains 42 TSOs from 34 countries, which now share a synchronous transmission grid in the EU [42].

3.3. Regional Structure

The European grid is divided into five synchronous regions and five relevant organizations: Nordic (former NORDEL), Baltic (former BALTSO), UK (former UKTSOA), Ireland (former ATSOI) and Continental Europe (former UCTE). Each of these organizations implements some coordination between the involved TSOs, in the operational stage as well as at the planning stage [43, 44].

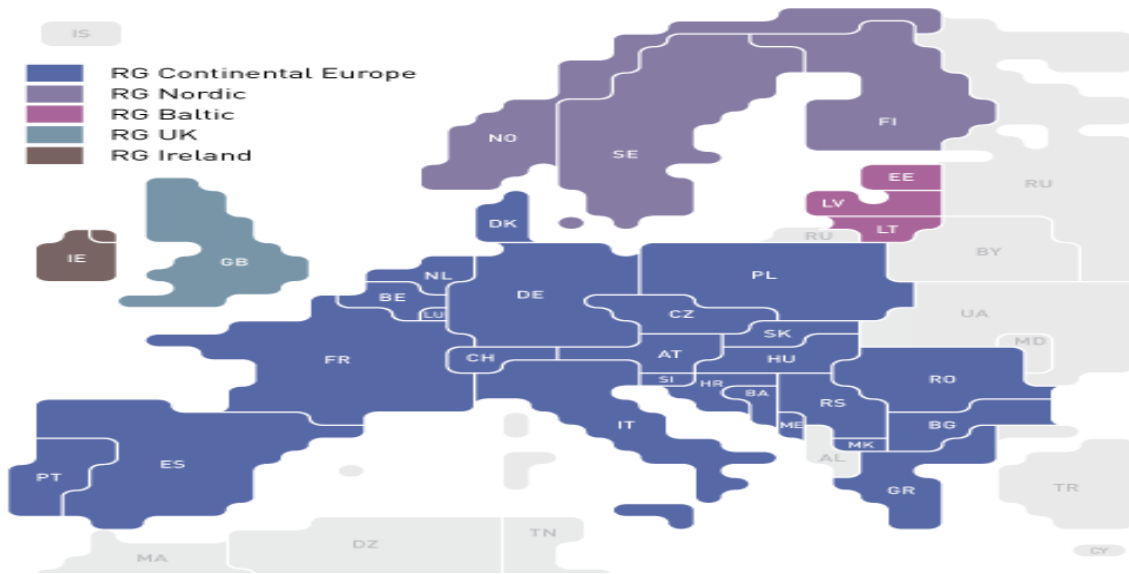


Fig. 3-1: Electrical interconnected systems in Europe [44].

The ENTSO-E-CE includes [42]:

42	Transmission System Operators (TSO)
34	European Countries
500 million	Customers served by represented power systems
631 GW	Installed capacity
2530 TWh	Electricity consumption in 2009

3.4. Frequency

In order to ensure a working European power grid, the operating frequency is defined by a standard of 50 hertz. As electric generation and consumption differs, the power transmission grid has to be balanced. There should be the same amount of input and output. Nevertheless changes in the frequency may occur if supply or demand exceeds its counterpart. In case of too much supply the frequency will increase, while in case of too much demand it will decrease. The main task is to keep the frequencies of all five synchronous areas balanced around the 50 hertz standard to ensure a safe power supply [45].

3.5. Load-Frequency Control and Performance

The power output of generating units that are connected to the ENTSO-E-CE (former UCTE) network needs to be controlled and monitored for secure and high-quality operation of synchronous areas [10].

Control actions are performed in different successive steps, each with different characteristics and qualities, and all depending on each other (see Fig. 3-2):

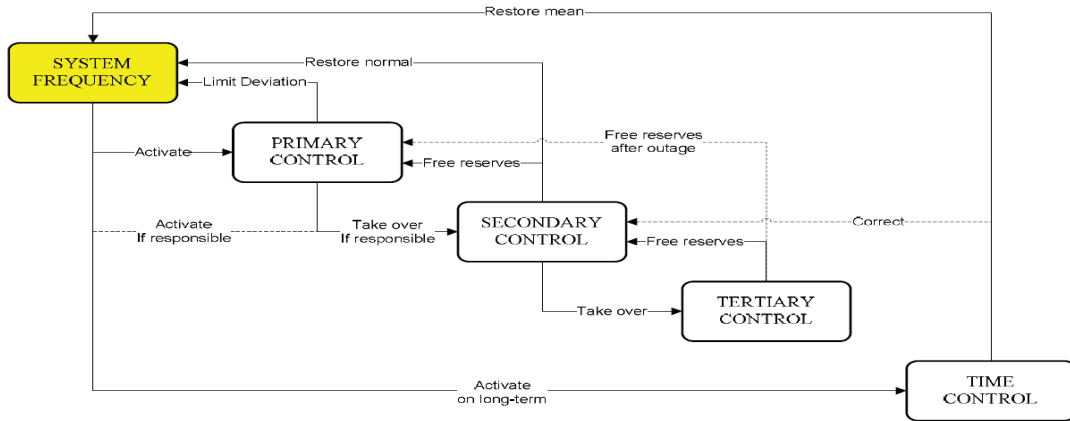


Fig. 3-2: Control scheme and actions starting with the system frequency [11].

- Primary control starts within seconds;
- Secondary control replaces primary control after minutes by the responsible partner;
- Tertiary control frees secondary control by re-scheduling generation by the responsible partner;
- Time control corrects global time deviation of the synchronous time on the long term as a joint action.

3.5.1. Primary Control

The objective of primary control is to maintain a balance between generation and consumption (demand) within the synchronous area, using turbine governors. After a disturbance or incident the primary control acts in the time-frame of seconds by the joint action of all interconnected generators to stabilize the system frequency at a stationary value, but without restoring the reference values of system frequency and the power exchanges to their reference values [11, 12].

An adequate primary control depends on generation resources made available and it has to respect the following criteria.

3.5.1.1. Primary Control Criteria

In case of a disturbance or an accident and during normal system operation, a frequency deviation

$$\Delta f = f - f_0 \quad (3.1)$$

where f is the actual system frequency and f_0 is the set-point frequency (50 Hz) or scheduled frequency) occurs in the network.

The size of this deviation can be used to distinguish some parameters of turbine governors [13, 48].

- 1- Primary control is activated when the frequency deviation exceed ± 20 mHz (the sum of the accuracy of local frequency measurement and the insensitivity of the controller);
- 2- The maximum permissible steady-state frequency deviation, under the condition of self-

regulation of the load assumed to be 1% / Hz, in the synchronous area must not exceed ± 180 mHz ;

- 3- The minimum instantaneous frequency (transient frequency) must not fall below 49.2 Hz (that corresponds to -800 mHz as maximum permissible dynamic frequency deviation from the nominal frequency) in response to a shortfall in generation capacity equal to or less than the reference incident, that for the first synchronous zone is 3000 MW;
- 4- The load-shedding starts with a system frequency of 49.0 Hz (at or below). The load-shedding is automatic or manual, including the possibility to shed pumping units.

3.5.1.2. Primary Control Characteristics

The following key values of the primary control are used [10, 48]:

- Self-Regulation of Load

The self-regulation of the load in the UCTE synchronous area is assumed to be 1 %/Hz, that means a load decrease of 1 % occurs in case of a frequency drop of 1 Hz.

- Quasi Steady-State Security Margin

For frequency control, the quasi steady-state security margin is defined to be 20 mHz .

- Minimum Network Power Frequency Characteristic of Primary Control

The minimum network power frequency characteristic of primary control for the UCTE synchronous area is calculated out of to 15000 MW/Hz.

- Overall Network Power Frequency Characteristic

The Overall network power frequency characteristic for the UCTE synchronous area is 19500 MW/Hz.

- Overall Primary Control Reserve

With respect to the size of the reference incident of 3000 MW

3.5.1.3. Target Performance

During the undisturbed operation of the interconnected network, a sudden loss of 3000 MW of capacity must be offset by primary control alone, without the need for customer load-shedding in response to frequency decay. In addition, where the self-regulating effect of the system load is assumed according to be 1% / Hz, the quasi-state frequency reduction (a frequency deviation) Δf must not exceed 180 mHz (see Fig. 3-3). Likewise, sudden load-shedding of a total of 3000 MW must not lead to a quasi-steady-state frequency increase exceeding 180 mHz . Where the self-regulating effect of the load is not taken into account, the absolute frequency deviation must not exceed 200 mHz [11].

Figure 3-3 shows movements in the system frequency for a given design hypothesis (case A), where dynamic requirements for the activation of control power are fulfilled in accordance with the requirements for deployment time. The maximum frequency deviation is 800 mHz .

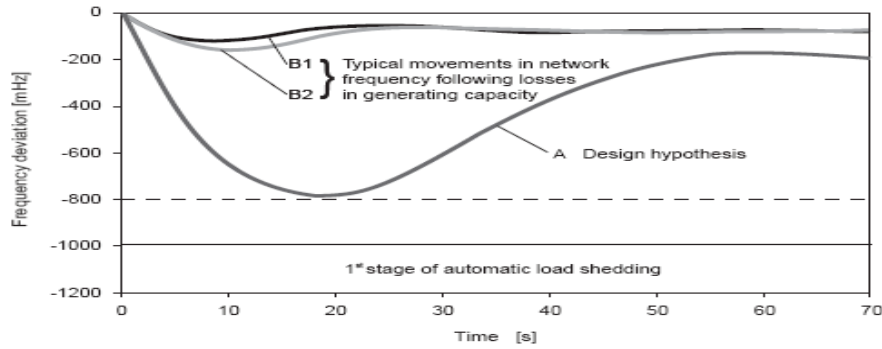


Fig. 3-3: Network frequency for a given design hypothesis [11].

A loss in generating capacity: $P=3000$ MW, $P_{\text{network}}=150$ GW, self-regulating effect of Load: 1%/ Hz

B1 loss in generating capacity: $P=1300$ MW, $P_{\text{network}}=200$ GW, self-regulating effect of Load: 2%/ Hz

B2 loss in generating capacity: $P=1300$ MW, $P_{\text{network}}=200$ GW, self-regulating effect of Load: 1%/ Hz

3.5.1.4. Primary Control Reserve

The total primary control reserve for the entire synchronous area P_{pu} is determined by the ENTSO-E-CE on the basis of the conditions set out in the previous subsections, taking account of measurements, experience and theoretical considerations. The shares P_{pi} of the control area /blocks are defined by multiplying the calculated reserve for the synchronous area and the contribution coefficients C_i of the various control area /blocks:

$$P_{\text{pi}} = P_{\text{pu}} * C_i \quad (3.2)$$

The entire primary control reserve is activated in response to a quasi-steady-state frequency deviation of -200 mHz or more. Likewise, in response to a frequency deviation of 200 mHz or more, power generation must be reduced by the value of the entire primary control reserve. In order to restrict the calling up of the primary control reserve to unscheduled power unbalances, the system frequency should not exceed or fall below a range of ± 20 mHz for long periods under undisturbed conditions [11].

3.5.1.5. Deployment Time of Primary Control Reserve

The deployment time of the primary control reserves of the various control areas should be as similar as possible, in order to minimize dynamic interaction between control areas. The primary control reserve of each control area i (determined in accordance with the corresponding contribution coefficient C_i) must be fully activated within 15 seconds in response to disturbances ΔP of less than 1500 MW, or within a linear time limit of 15 to 30 seconds in response to a ΔP of 1500 to 3000 MW. These contribution coefficients are calculated annually for each area or interconnection partner using the following formula:

$$C_i = E_i / E_u \quad (3.3)$$

where E_i is the electricity generated in control area i , E_u is the total electricity production in all control areas N on the interconnected network. As a minimum requirement, the deployment of the primary control reserve must be consistent with the curves plotted (see Fig. 3-4) which represent the overall behaviour of the system.

The activated power will lie on or above the plotted curves (see Fig. 3-4), until the balance between power generation and consumption has been restored. For each control area i , the figures for power indicated in figure 3-4 are multiplied by the relevant contribution coefficient C_i .

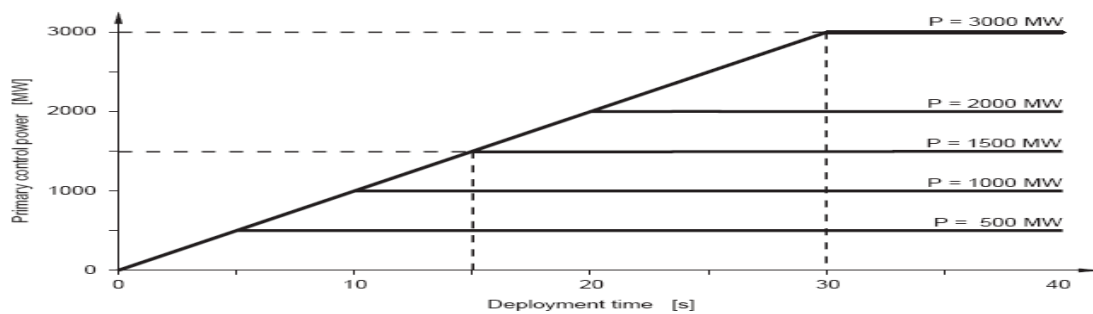


Fig. 3-4: Overall behaviour of the system [11].

3.5.2. Secondary Control

Secondary control maintains a balance between generation and consumption (demand) within each control area, taking into account the exchange program, without impairing the primary control that is acting on the synchronous level. Secondary control makes use of a centralised automatic control modifying the active power set points of generation sets in the time frame of tens of seconds to typically 15 minutes after an incident. Secondary control is based on secondary control reserves that are under automatic control [10].

3.5.2.1. Principle of the Network Characteristic Method

In order to determine, whether power interchange deviations are associated with an imbalance in the control area / block concerned or with the activation of primary control power, the network characteristic method needs to be applied for secondary control of all control areas / blocks in the synchronous area.

According to this method, each control area / block is equipped with one secondary controller to minimise the area control area (ACE) G in real-time:

$$G = (P_{\text{measure}} - P_{\text{program}}) + K_{ri} (f_{\text{measure}} - f_0) \quad (3.4)$$

where P_{measure} is the sum of the instantaneous measured active power transfers on the tie lines; P_{program} is

the resulting programmed exchange with all the neighboring control areas; K_{ri} , the system factor, is a constant in MW/Hz set on the secondary controller; $f_{measure}$ is the measured instantaneous value of system frequency; and f_0 is the set-point (nominal) frequency[10,11 and 49]..

The ACE is the control area's unbalance ($P_{measure} - P_{program}$) minus its contribution to the primary control, if K_{ri} is equal to the control area's power system frequency characteristic. The power transits are considered positive for export and negative for import.

3.5.2.2. Secondary Controller

The desired behaviour of the secondary controller over time will be obtained by assigning a proportional-integral characteristic (PI) to control circuits, in accordance with the following equation [11, 49]:

$$\Delta P_{di} = -\beta_i * G_i - \frac{1}{T_i} \int G_i * dt \quad (3.5)$$

where:

- ΔP_{di} the correcting variable of the secondary controller governing control generators in the control area i ;
- β_i the proportional gain of the secondary controller in control area i;
- T_i the integration time constant of the secondary controller in control area i;
- G_i the area control error(ACE) in control area i.

As system frequency and power deviations are to return to their set point values within the required time (without additional control needed), an appropriate integral term needs to be applied. An excessively large proportional term may have a detrimental effect upon the stability of interconnected operation. In particular, where hydroelectric plants are used for secondary control, there is a risk that an increase in the proportional term will initiate network oscillations. This natural period of oscillation may range from 3 to 5 seconds and may be subject to change as the synchronous area is extended.

In case of a persisting positive or negative ACE, leading to a saturation of the secondary control reserves, the integral term should be limited. The non-windup character of the secondary controller allows recovering control as soon as the ACE returns to zero. Parameter settings for secondary controllers of all control areas need to follow a common guideline to ensure co-operative secondary control within the synchronous area.

3.5.2.3. Secondary Control Reserve

Secondary control reserve is the amount of generation that the secondary controller may call upon in addition to the power that it has already put into service in control actions. Secondary control reserve should always be available to cover load variations as well as the loss of a generating unit. Secondary

control reserve depends upon the availability of generators within the transmission system operator (TSO) and must always be sufficient to eliminate ACE [50].

3.5.2.4. Recommended Secondary Control Reserve

An empirically determined curve is used to estimate the minimum secondary control reserve required for the UCTE system [13, 50].

$$R = \sqrt{aL_{\max} + b^2} - b \quad (3.6)$$

where:

- R The recommendation for secondary control reserve in MW;
- L_{\max} Maximum anticipated consumer load in MW for the Control Area;
- a, b Have empirically values of 10 MW and 150 MW respectively.

The following curve is established with the following values: $a = 10$ and $b = 150$

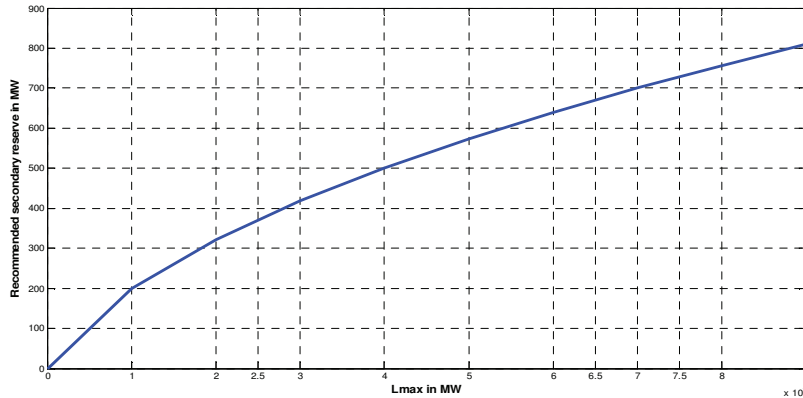


Fig. 3-5: Recommended secondary control reserve in MW.

3.5.2.5. Quality of Secondary Control during Major Disturbance

The quality of secondary control during major disturbance (generator shutdown or loss of load) must be monitored by measuring and analysing the reaction or response of the synchronously interconnected network.

In order to assess the quality of secondary control in control areas or blocks, trumpet-shaped curves of the type $H(t) = f_0 \pm A * e^{-t/T}$ have been defined on the basis of values obtained from experience and the monitoring of the network frequency over a period of years [11, 49 and 51]. When the network frequency is maintained within the trumpet during the secondary control process, the completion of the latter is deemed to be satisfactory, in terms of technical control.

The trumpet curve for a given incident will be plotted using the following values (see Fig. 3-6):

- The set-point frequency f_0

- The actual frequency f_1 before the incident
- The maximum frequency deviation Δf_2 after the incident, with respect to the set-point f_0

The following relationship will apply to the trumpet curve (envelope curve) [43];

$$H(t) = f_0 \pm A * e^{-t/T} \quad (3.7)$$

The value A is established on the basis of frequency monitoring over a period of years for

$$A = 1.2 * \Delta f_2 \quad (3.8)$$

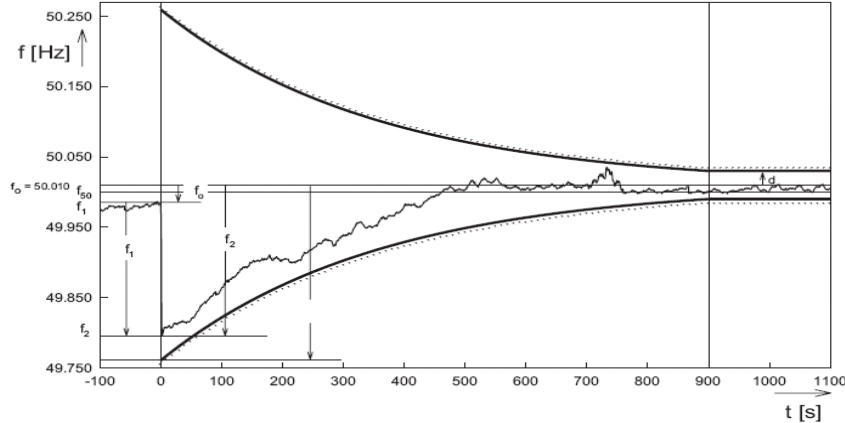


Fig. 3-6: Trumpet curve [11].

The network frequency must be restored to a margin of $d = \pm 20$ mHz of the set point frequency 900 seconds (15 minutes) after the start of an incident. Hence, the time constant T of the trumpet curve is determined by the following formula:

$$T = 900 / \ln(A/d) \quad (3.9)$$

for $T \leq 900s$ and $|d| = 20$ mHz

3.5.3. Tertiary Control

Tertiary control is any automatic or manual change in the working points of generators or loads participating, in order to [11]:

- guarantee the provision of an adequate secondary control reserve at the right time,
- distribute the secondary control power to the various generators in the best possible way, in terms of economic considerations.

Changes may be achieved by:

- connection and tripping of power (gas turbines, reservoir and pumped storage power stations, increasing or reducing the output of generators in service);
- redistributing the output from generators participating in secondary control;
- changing the power interchange program between interconnected undertakings;
- load control (e.g. centralized telecontrol or controlled load-shedding).

CHAPTER 4

Power Plant Model Description and Model Validation

4.1. Dynamic Model of Ataturk Hydro Power Plant

4.1.1. Introduction

The hydroelectric power plant (HEPP) of the Ataturk Dam (see Fig. 4-1) is the biggest of a series of 19 power plants of the South-eastern Anatolia Project. It is located at 24 kilometers to Bozova town of Sanliurfa. It consists of eight Francis turbine and generator groups of 300 MW each, supplied by Sulzer Escher Wyss and ABB Asea Brown Boveri respectively [67]. The power plant's first two power units came on line in 1992 [68], and it became fully operational in December 1993. The HEPP can generate 8,900 GWh of electricity annually [69]. Its capacity makes up around one third of the total capacity of the South-eastern Anatolia Project [70].



Fig. 4-1: The Ataturk dam.

During the periods of low demand for electricity, only one of the eight units of the hydroelectric power plant is in operation while in times of high demand, all the eight units are in operation. Hence, depending upon the energy demand and the state of the interconnected system, the amount of water to be released from the HEPP might vary between 200 and 2000 m³/sec in one day [70].

The unit of Ataturk hydro power plant (HPP) has two operating modes: speed control (SC) and power control (PC). SC is used for start-up in island operation. PC mode is used for primary frequency control while the unit is supplying power to 380 kV Turkish networks. Speed-droop is the change in active power output of the unit proportional to the frequency deviation (open-loop control) as illustrated in the following equation [54, 71]:

$$R = \frac{\Delta f / f_n}{\Delta P / P_n} \times 100 \quad (4.1)$$

where;

R Speed-droop;

Δf Steady-state frequency deviation;

ΔP Change of active power generation caused by turbine governor as a result of the frequency deviation Δf ;

f_n Rated frequency;

P_n Unit rated power.

4.1.2. Model of the Power Plant

The model of the power plant was made in SIMULINK / MATLAB software and consists of the following dynamic sub-models:

- Hydraulic and mechanical system (Turbine and Penstock Modelling)
- Power and speed Control
- Governor

The block scheme of the complete model with its sub-models is presented in figure 4-2.

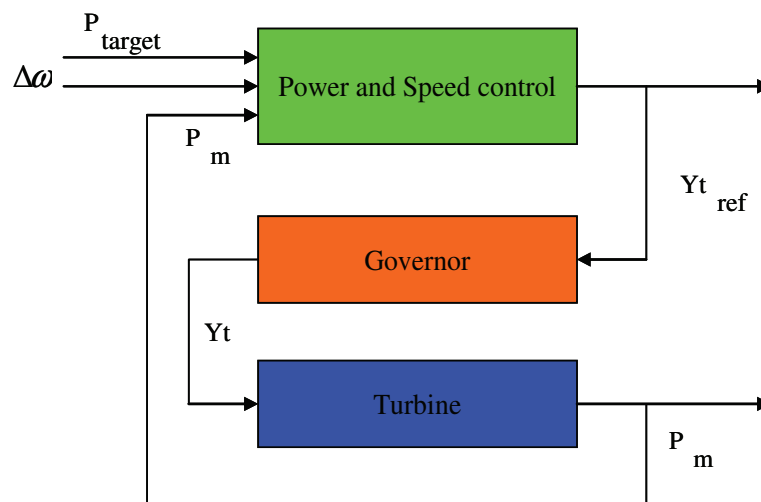


Fig. 4-2: General representation of sub-models.

where;

P_{target} Power setpoint

$\Delta\omega$ Deviation of frequency

Y_{t_ref} Setpoint position governor guide vane

Y_t Position governor guide vane

P_m Power of the turbine

Every signal is given in per units (p.u.). This simplifies the interface between the parts and makes the algorithm for modelling easier. The main data of the Ataturk HPP Unit 1:

Type of turbine	: Francis
Rated power	: 300 (MW)
Rated flow	: 218.5 (m^3 / s)
Rated head	: 151.2 (m)

4.1.2.1. Hydraulic and Mechanical system

▪ Turbine and Penstock Modelling

Hydraulic turbines may be defined as prime movers that transform the kinetic energy of falling water into mechanical energy of rotation and whose primary function is to drive a electric generator. Hydroelectric plants utilise the energy of water falling through a head that may vary between a few meters and 1500 or even 2000 meters [66].

All HPPs in priority list are equipped with a certain type of reaction turbines which is Francis turbine, illustrated in figure 4-3. The water enters a spiral casing (volute) which surrounds the runner, who's cross sectional area decreases along the water path in such a way to keep the water velocity constant in magnitude. Departing the volute the water is directed on the runner by the guide vanes mounted all around the periphery of the runner. Each vane is pivoted and all will be turned in synchronism to alter the flow rate throughout the turbine, and hence the power output as required by governor action. The runner blades deflect the water so that its angular momentum is changed. From the centre of the runner, the water is turned into the axial direction and flows to the tailrace via the draft tube. In order to ensure the hydraulic turbine is full of water, the lower end of the draft tube is always submerged below the water level in tailrace [35, 71 and 72].

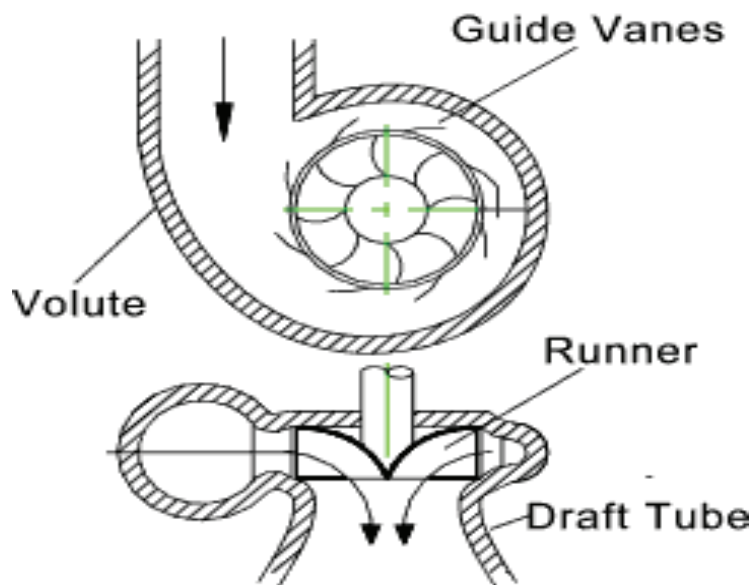


Fig. 4-3: Francis Turbine [72]

The turbine and penstock characteristics are determined by four basic relations between the turbine mechanical power, velocity of water in the penstock and turbine inlet (in per unit notation velocity also corresponds to flow rate) and the acceleration of the water column [6].

The mechanical power (P_m) that can be transferred to the generator shaft from the Francis Turbine is a nonlinear function related to the flow rate (q) and hydraulic pressure which is strongly dependent on hydraulic head available (h). The nonlinear relationship is expressed via an efficiency term as a function of head and flow rate and the mechanical power of a turbine is expressed as in equation (4.2) [6, 74 and 75]

$$P_m(q, h) = \eta(q, h) \times q \times \rho \times g_a \times h \quad (4.2)$$

where,

- P_m the mechanical power of the turbine (W)
- η the efficiency factor
- q the flow rate (m^3/sec)
- ρ the density of water (kg/m^3)
- g_a the gravitational acceleration constant (m/s^2)
- h the hydraulic head (m).

The output power of the Francis turbine is adjusted by changing the opening of wicket gates, hence the amount of water flowing into the runner blades. As the opening of the wicket gate changes, the effective flow area of the water changes; therefore, the inlet water velocity in the penstock, hence the inlet water flow to the turbine runner changes. This relationship in per unit is as expressed in equation (4.3).

$$q = A\sqrt{h}(p.u.) \quad (4.3)$$

There are two dominant nonlinearities in the hydraulic turbine model proposed in [76], which is utilized throughout this study. The remaining equations regarding the hydraulic turbine model are nothing but a restatement of the well known HYGOV model [63, 77].

The first nonlinearity (see Fig. 4-8) in the model is the relationship between the actual gate opening and effective flow area. The no load losses of the turbine is included in the modelling process via subtracting the gate opening corresponding to no load flow from the actual gate opening and also the nonlinear relationship between gate opening and effective flow area due to geometry of the turbine is included in the nonlinear function expressed in (4.4).

$$A = f(Y_t) \quad (4.4)$$

where

- A the effective flow area (per unit)

- f the nonlinear function relating gate opening and effective flow area
 Y_i the wicket gate opening (per unit)

A sample graph representing the nonlinear relationship between gate opening and effective flow area is illustrated in Fig. 4-4.

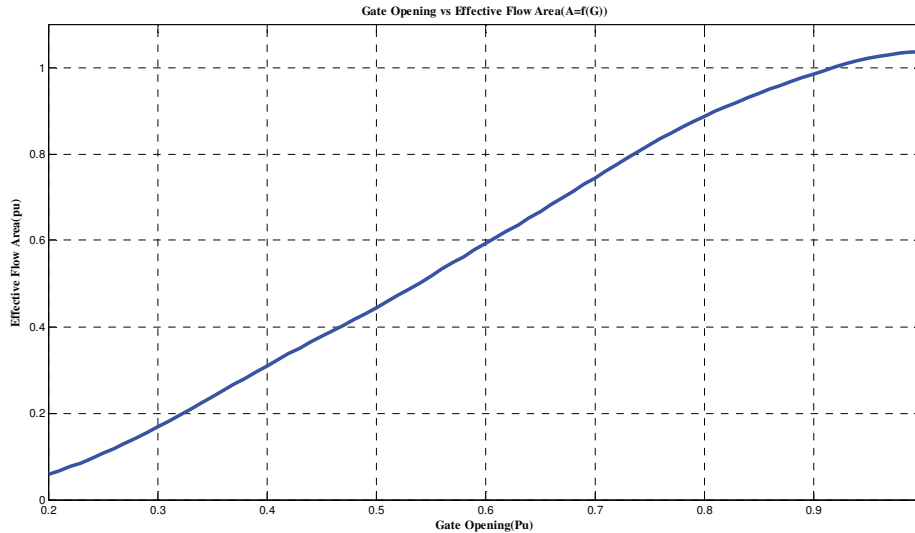


Fig. 4-4: A Sample Gate Opening and Effective Flow Area Relationship for Ataturk HPP.

The second nonlinearity (see Fig. 4-8) in the turbine model is the nonlinear relationship between the mechanical power, the water flow and the hydraulic head. This nonlinearity is expressed by using the "Shell Curve" (a.k.a. Hill Chart, Performance Chart or Efficiency Curve), which expresses the output mechanical power of the turbine as a function of the head and the water flow as illustrated in figure 4-5. Shell curves are obtained in the model prototype tests of hydraulic turbines in specific laboratories. In the shell curve, the solid lines correspond to the loci of operating points with equivalent efficiency, whereas the dashed lines correspond to the loci of operating points corresponding to equivalent mechanical power. The operational limits of the hydraulic turbine are also illustrated in the shell curves.

In this study, the shell curve will be utilized to represent the nonlinear relation between output power, hydraulic head and water flow rate. Specific points will be selected from different regions of the shell curve and the relation for the remaining operating points will be found by piecewise linear interpolation between the selected points. Hence the accuracy of the nonlinear surface in representing the nonlinear relation between output power, hydraulic head and water flow rate is strongly dependent on the number and spectrum of the selected operation points from the shell curve.

The nonlinear relationship relating mechanical power output with water flow and hydraulic head is as expressed in equation (4.5)

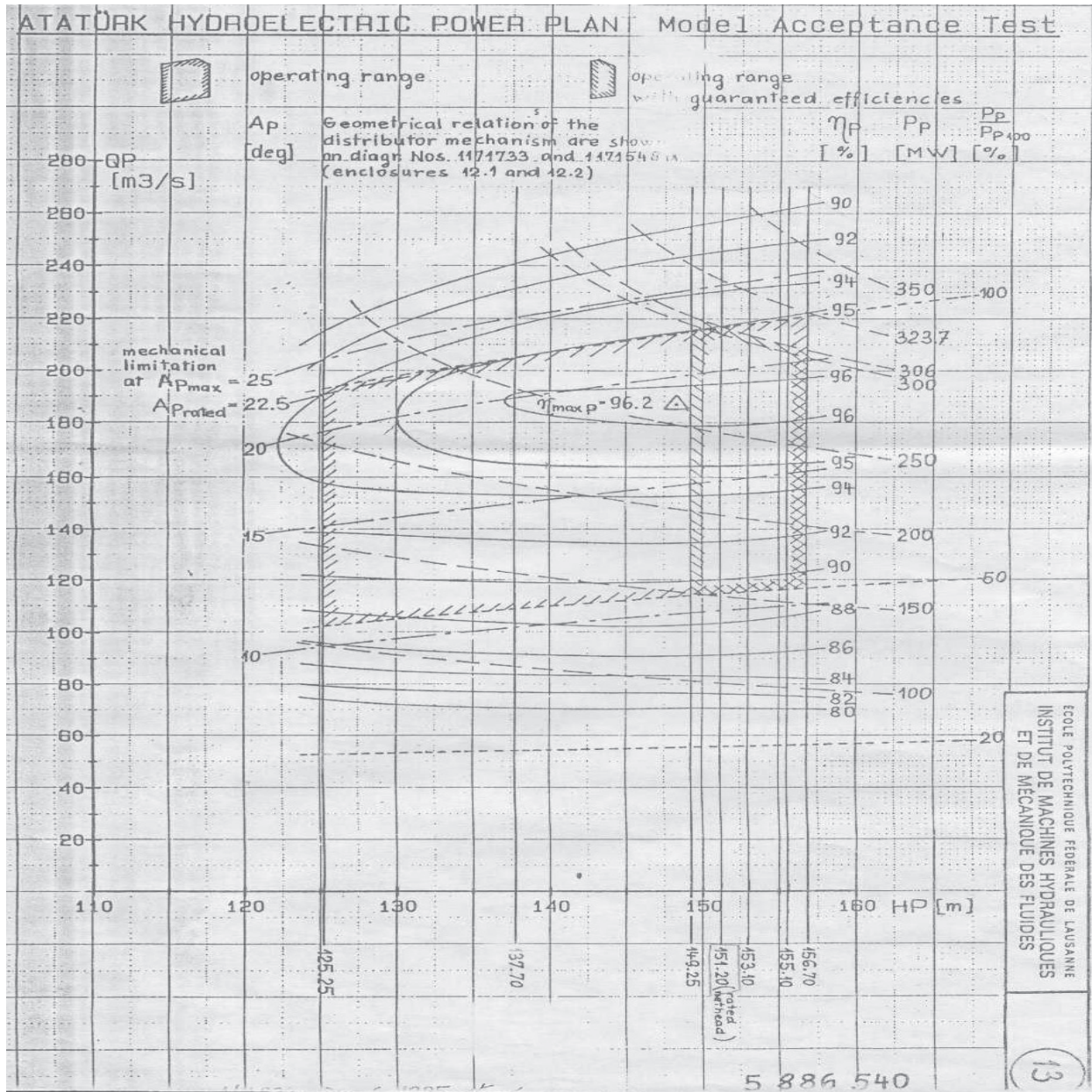


Fig. 4-5: The shell curve of Ataturk HPP.

$$P_m = g(q, h) \tag{4.5}$$

where

- P_m the mechanical power of the turbine (per unit)
- g the nonlinear function relating mechanical power to water flow and hydraulic head, as expressed in (4.2)
- h the hydraulic head (per unit)

A sample graph representing the nonlinear relationship relating mechanical power to water flow and hydraulic head obtained from the shell curve is illustrated in figure 4-6.

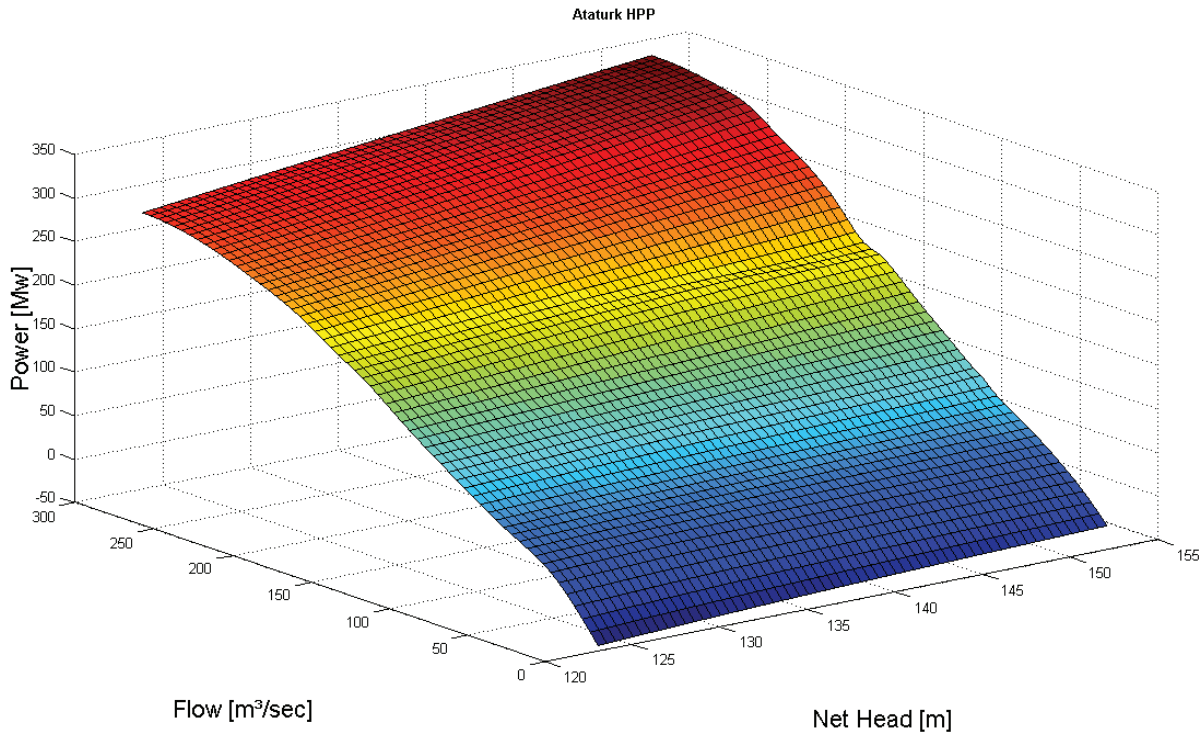


Fig. 4-6: Characteristics of the turbine, derived from the shell curve.

▪ Modelling the Water Column

The third equation regarding the nonlinear turbine model (see Fig. 4-8) is related to the acceleration of the water column. The characteristics of the water column in the penstock feeding the turbine carry great importance in representing the dynamical behaviour of the hydraulic turbine.

The most important parameter in representing the characteristics of the water column is the inertia of water in the penstock. This inertia causes a great amount of lag for changes in mechanical power against changes in wicket gate opening. In fact, the power has a transient response which is initially in the opposite sense to that intended by changing the guide vane position. Although the turbine guide vane opening may change rapidly, the water column inertia prevents the flow from changing as rapidly. Consequently, after a rapid increase in guide vane opening, and before the flow has had time to change appreciably, the velocity of water into the wheel drops because of the increased area of the guide vane opening. The power transfer to the wheel actually drops before it increases to its required steady state value. This is the most prominent factor, which makes a hydraulic turbine such an uncooperative component in a speed control system [35, 78].

The most basic water column model as expressed in [46-47] represents a single penstock with a very large or no surge tank so that no changes in reservoir head occur in response to flow changes. A hydraulic turbine model developed for a hydroelectric power plant containing a surge tank can be investigated from [79]. While developing the penstock model; it is assumed that the water acts as incompressible fluid so that here the water hammer effect may be neglected.

The penstock head losses due to the friction of water against the penstock wall are proportional to flow (q) squared as expressed in (4.6) [63].

$$h_f = h_0 - h = R_{fr} \times q^2 \text{ (p.u.)} \quad (4.6)$$

where,

h_f the head loss due to friction (per unit)

R_{fr} the friction coefficient

q the flow through the penstock (per unit)

Considering the water column in the penstock as a solid mass, the rate of change of flow in the penstock is related to the pressure, hence the hydraulic head available, using Newton's 2nd law of motion. The force on the water mass is

$$(h_0 - h - h_f) \rho \times g_a \times A_p = L \times A_p \times \rho \times \frac{dv}{dt} \quad (4.7)$$

where,

h_0 the gross head (m)

h the head at the turbine admission (m)

h_f the head loss due to friction (per unit)

ρ the density of water (kg/m³)

g_a the gravitational acceleration constant (m/s²)

A_p the cross sectional area of the penstock (m²)

L the length of the penstock (m)

v denotes the speed of the water column in the penstock (m/s)

Since the area of the penstock is constant and it is assumed that the flow of water is laminar (i.e., turbulence does not occur), the multiplication of the speed of the water column with the area of the penstock gives the rate of flow of water in the penstock.

Hence, (4.7) can also be expressed as in (4.8).

$$\frac{dq}{dt} = (h_0 - h - h_f) \frac{g_a \times A_p}{L} \quad (4.8)$$

In per unit notation, (4.8) is expressed as in (4.9) and in (4.10).

$$\frac{\bar{dq}}{dt} = (1 - \bar{h} - \bar{h}_f) \frac{h_{base} \times g_a \times A_p}{L \times q_{base}} \quad (4.9)$$

$$\frac{\bar{dq}}{dt} = \frac{(1 - \bar{h} - \bar{h}_f)}{T_w} \quad (4.10)$$

and

$$T_w = \frac{L \times q_{base}}{h_{base} \times g_a \times A_p} = \frac{L \times v_{base}}{h_{base} \times g_a} \quad (4.11)$$

where, T_w is the water starting time at rated load. It is important to note here that the water starting time varies with load. The water starting time represents the time required for a head h_{base} to accelerate the water in the penstock from standstill to the velocity v_{base} . This is calculated between turbine inlet and the forebay or the surge tank if a large one exists [63, 77].

For unit 1 of Ataturk hydro power plant the water starting time is calculated according to the equation (4.11) and equal 3 seconds [54].

The equation (4.10) constitutes an important characteristic of the mechanical power response of a hydroelectric power plant against wicket gate opening changes. If the wicket gate is closed for a certain amount, a back pressure will arise causing the water to decelerate. That is, if there is a positive pressure change, there will be a negative acceleration change. Similarly, a negative pressure change will cause a positive acceleration change.

Water starting time at any loading is related to the water starting time at rated load by the equation (4.12).

$$T_w = \frac{h_r \times q_0}{q_r \times h_0} T_{w_{rated}} \quad (4.12)$$

While developing the penstock model, it was assumed that the water acted as an incompressible fluid so that the water hammer effect could be neglected. However, for some power system studies, it may be necessary to express the dynamic relation between the hydraulic system and the power system. Considering the water compressibility and pipe elasticity, the water dynamics can be written in per unit notation as in (4.13) and in (4.14) for a hydroelectric power plant with a large reservoir or a very large surge tank as illustrated in figure 4-7. It is important to note here that the term "s" in (4.13) and in (4.14) correspond to the Laplacian operator. The equations (4.13) and (4.14) are utilized to analyze the effect of travelling waves with typical frequency range around 1 Hz in the penstock and hence very similar to the long transmission line equations used in analyzing wave phenomena in power systems.

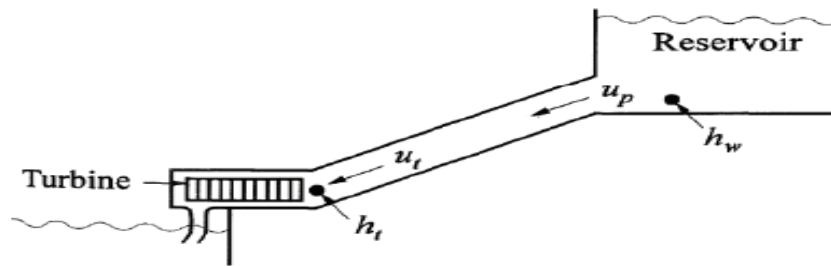


Fig. 4-7: The Schematic of a Hydroelectric Power Plant with a Reservoir.

$$\bar{h}_t = \bar{h}_w \operatorname{sech}(T_e s) - Z_n \bar{q}_t \tanh(T_e s) - r \bar{q}_t^2 \quad (4.13)$$

$$\bar{q}_p = \bar{q}_t \cosh(T_e s) + \frac{1}{Z_n} h_t \sinh(T_e s) \quad (4.14)$$

where,

h_t corresponds to the head at turbine admission (per unit)

h_w corresponds to the gross head (per unit)

T_e corresponds to the elastic time of water (s)

Z_n corresponds to the hydraulic impedance of the penstock (per unit)

q_t corresponds to the flow rate in the turbine inlet (per unit)

q_p corresponds to the flow rate in the penstock (per unit).

Also it should be noted that, $T_e = \frac{L}{\text{wave velocity}}$ and $Z_n = \frac{q_{\text{rated}}}{h_{\text{rated}}} \times \frac{\text{wave velocity}}{A_p g_a}$, where typical values

for wave velocity of water is 1220 m/s for steel penstocks and 1420 m/s for rock penstocks and L is the length of the penstock.

Taking the first two terms of the Taylor series expansion of the equations (4.13) and (4.14) ends up with the final equation regarding the penstock dynamics expressed in frequency domain as (4.15).

$$h_t = \frac{2T_w}{T_e^2 s} (q_p - q_t) \quad (4.15)$$

Hence, the combined model of turbine and penstock of Ataturk HPP is illustrated in figure 4-8.

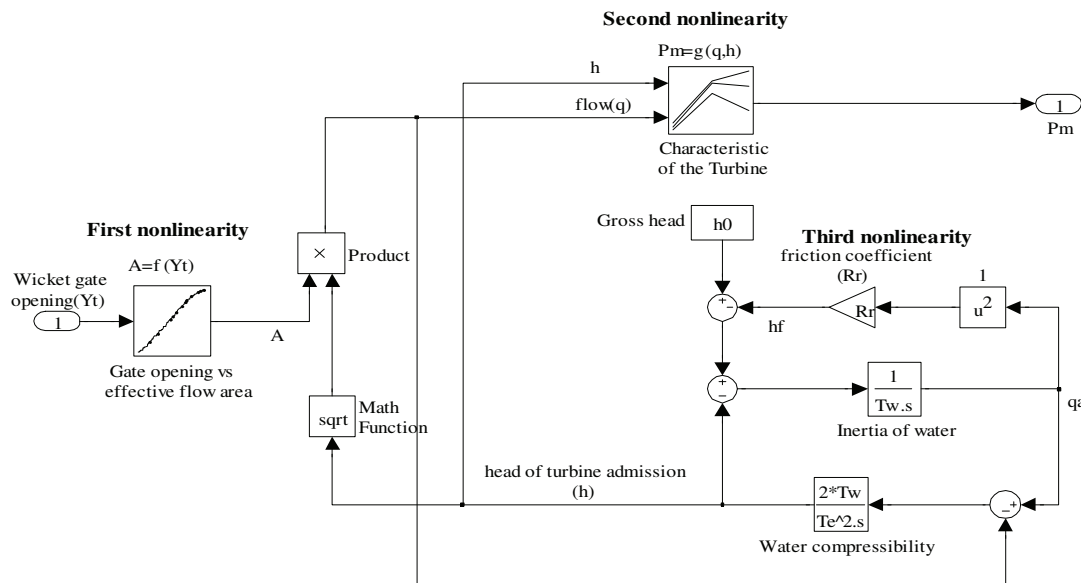


Fig. 4-8: The Combined Turbine and Penstock Dynamical Model of Ataturk HPP

4.1.2.2. Speed ,Power Control and Governor Model

Figure 4-9 shows detail the speed and power control model of the Ataturk power plant, consisting of power setpoint (P_{target}), mechanical power (P_m), generation power (P_G), rated frequency (n_G), frequency setpoint (n_{G0}), integral time constant (T_p), mechanical time constant (T_g), speed droop (Sigma), accelerating input gain (K_{acc}), acceleration time constant (T_{acc}), transient gain (r), transient time (T_n) and setpoint position governor guide vane ($Y_{t ref}$).

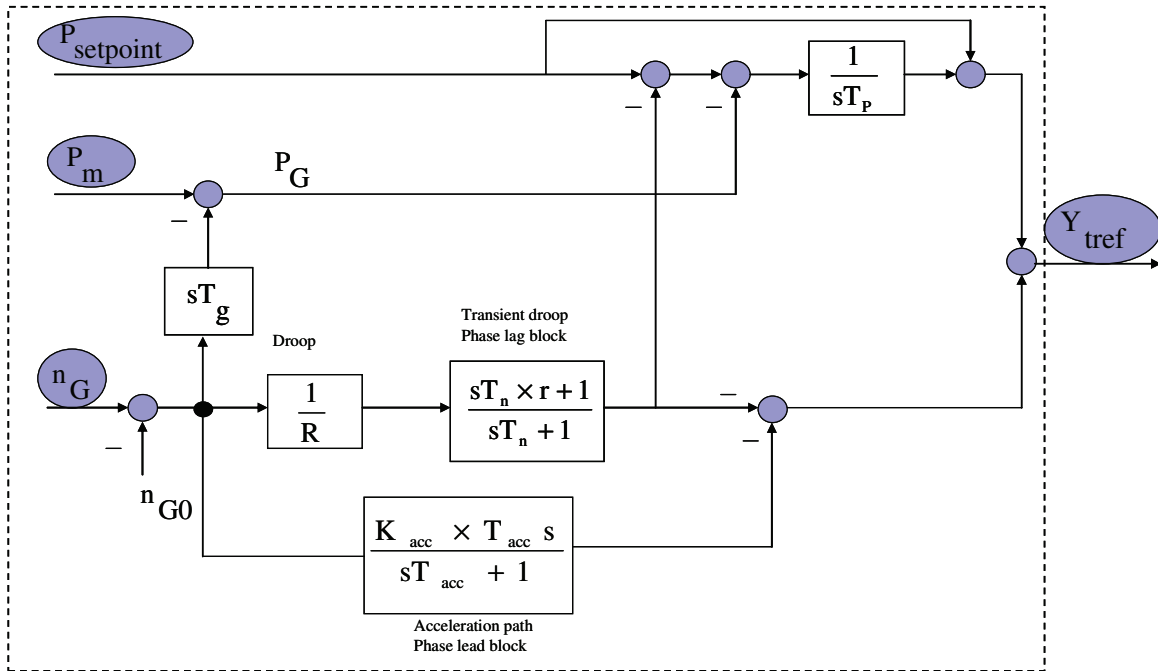


Fig. 4-9: Speed and power control structure.

Figure 4-10 shows detail of governor model consist of input of governor ($Y_{t ref}$), PID controller (P2, TI2 and D2), pilot servo (T_{pilot}), main servo (T_{main}) and the output of governor to the turbine system is Y_t

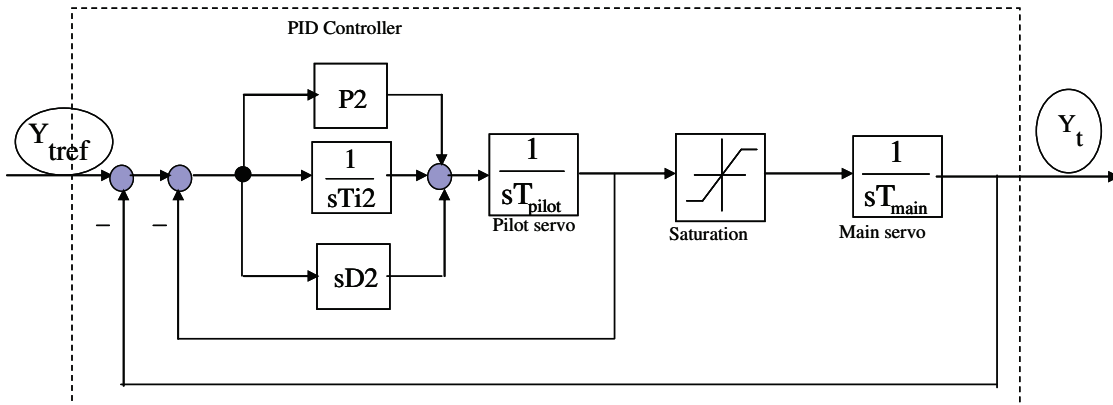


Fig. 4-10: Speed and power control structure.

4.1.3. Tests on Unit1 of Ataturk HPP

During the course of Turkey's ENTSO-E-CE (former UCTE) Interconnection Project, there have been several workshops and studies by Interconnection Working Group to determine the governor structure and control parameters of newly refurbished Ataturk Hydro Power Plant Unit Governors [80].

A site visit was realized by Turkey's ENTSO-E-CE (former UCTE) interconnection working group members to Ataturk hydro power plant (HPP) between dates 10-12 February 2009. The main purpose of this site visit was to analyze the performance of Ataturk Unit 1 governor that was implemented in the new control system, according to the advices of the workshops, during the control system rehabilitation project of Ataturk and Karakaya Hydro Power Plants' 14 Units, owned by EUAS. Of course the aim was to reach optimum speed and power control parameters (see Fig. 4-9) and define this unit as a model for the remaining units to be refurbished under this rehabilitation project.

Ataturk hydro power plant units are mainly operating between a minimum continuous operation point of 215 MW and maximum continuous operation point of 285 MW, during day hours, connected to AGC system for secondary control also with 5% of primary control reserve of 15 MW each (8% Permanent Droop)[54].

Tests carried out on Unit 1 Governor were realized, by directly simulating the frequency measurement signal of the governor on the control software. Simulated island mode test was realized per IEC-60308 [102] which was also programmed in the software prior. 200 mHz steps, 7 second period 100 mHz peak and 30 second period 100 mHz peak sinusoids were applied with "0" mHz dead band on frequency measurement and response of the unit to those inputs were recorded.

4.1.4. Simulation Results

The model made in described manner was verified after connection of the sub models in one complete power plant model. After fine tuning of the parameters some additional simulations can be made. Here, some comparisons of the simulations and measured signals are presented.

4.1.4.1. Test 1 (change on load set point with step 10% till 100% load), (interconnected mode)

In one of such measurement (the command is given in sense of increasing active power of the unit in small steps 10-20 MW and then decreasing active power of the unit in small steps 10-20 MW). Figure 4-11 shows the comparison between simulation and measured signals, for output power and wicket gate position.

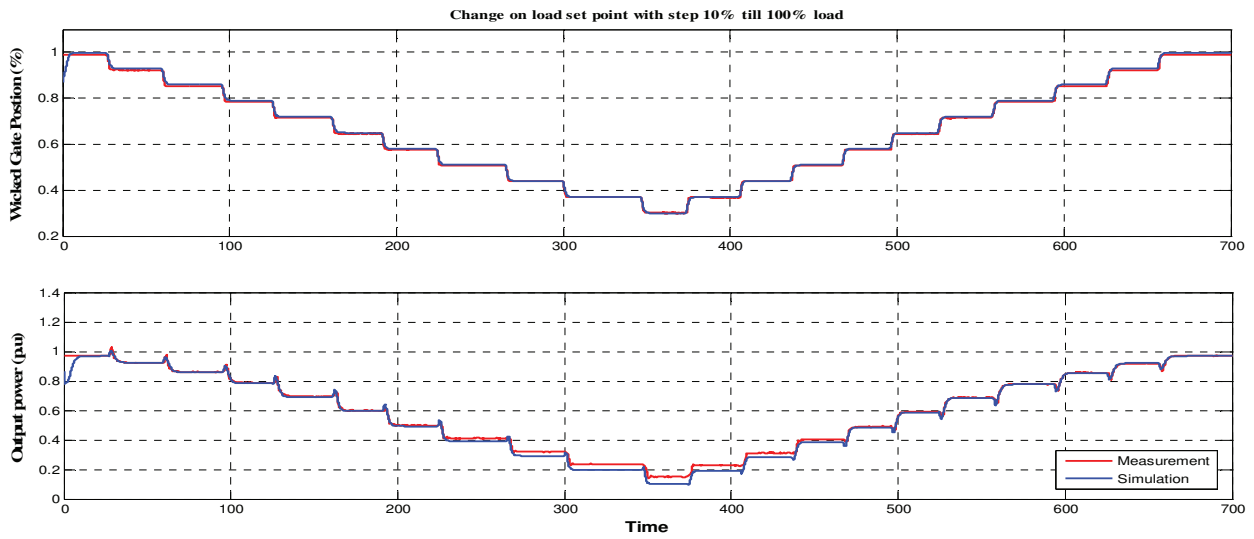


Fig. 4-11: Output power and wicket gate position.

4.1.4.2. Test 2 (Primary Control Response), (interconnected mode)

In this test, the parameters set on unit 1 of Ataturk HPP are listed in the following table:

Table 4-1: Parameters for the grid

P_n	P_0	T_w	T_p	r	T_n	T_{acc}	K_{acc}	Sigma
300	258	3 s	25s	0.12	100s	0.3s	4	0.08

Figure 4-12 illustrates the response of Unit 1 to - 200 mHz step in frequency ~ 4 % changes (~90% of expected response in 30 seconds) and response of Unit to + 200 mHz change in frequency 4.2% change (back to initial operating point). The figure shows the comparison between simulation and measured signals for wicket gate position and output power.

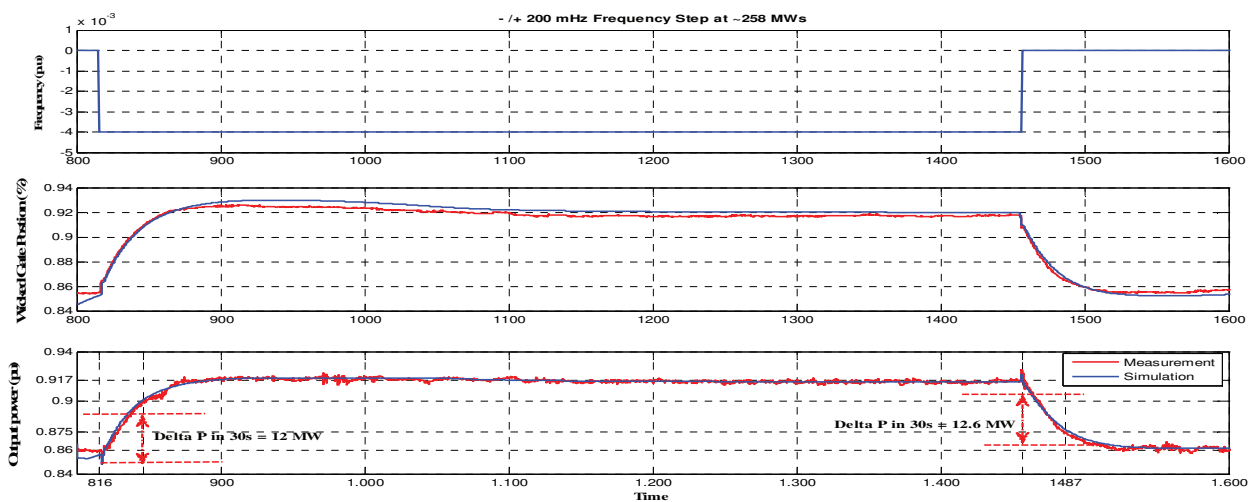


Fig. 4-12: Response of Unit to \mp 200 mHz step change in frequency.

4.1.4.3. Test 3 (30 and 7 sec. periods, 100 mHz peak), (interconnected mode)

In this test, the parameters set on unit 1 of Ataturk HPP are listed in the following table:

Table 4-2: Parameters for the grid

P_n	P_0	T_w	T_p	r	T_n	T_{acc}	K_{acc}	Sigma
300	250	3 s	25s	0.5	30s	1s	30	0.08

Figure 4-13 illustrates the response of Unit 1 to 30 and 7 second period sinusoidal changes in frequency. For 30 seconds period observed peak to peak power demand dictated by permanent droop is 15 MW (5%) and no observable response of the unit 1 to these changes for 7 seconds period (due to 100 sec. transient gain time constant and backlashes in the mechanical system). The figure shows the comparison between simulation and measured signals, for output power and wicket gate position.

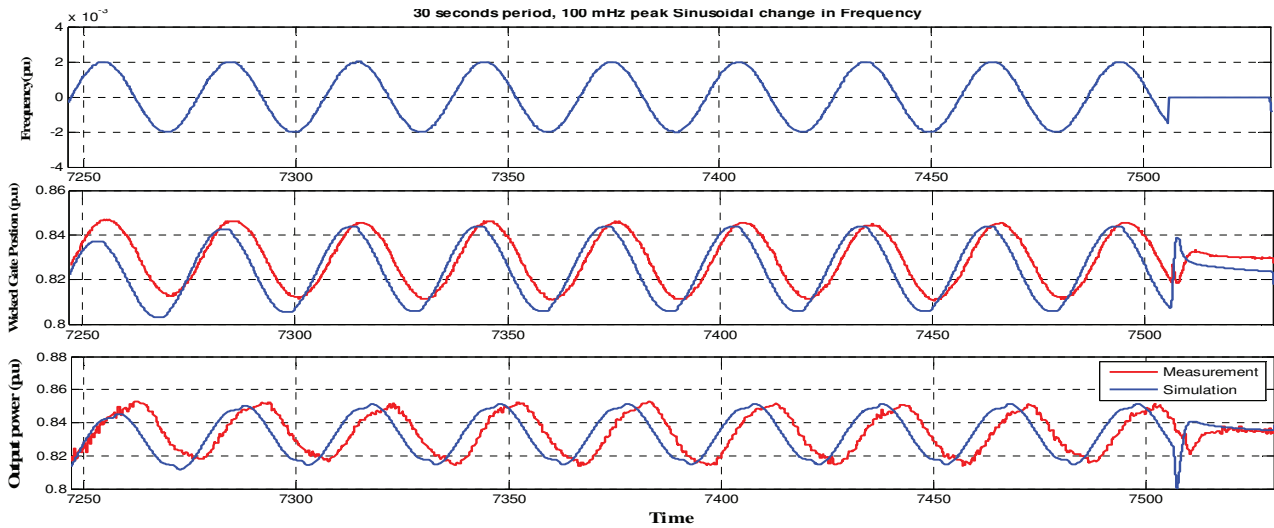


Fig. 4-13: Response of Unit 1 to 30 seconds period sinusoidal change in frequency.

Figure 4-14 illustrates the phasor diagram for 30 seconds period sinusoidal frequency and the overall response in the positive damping region.

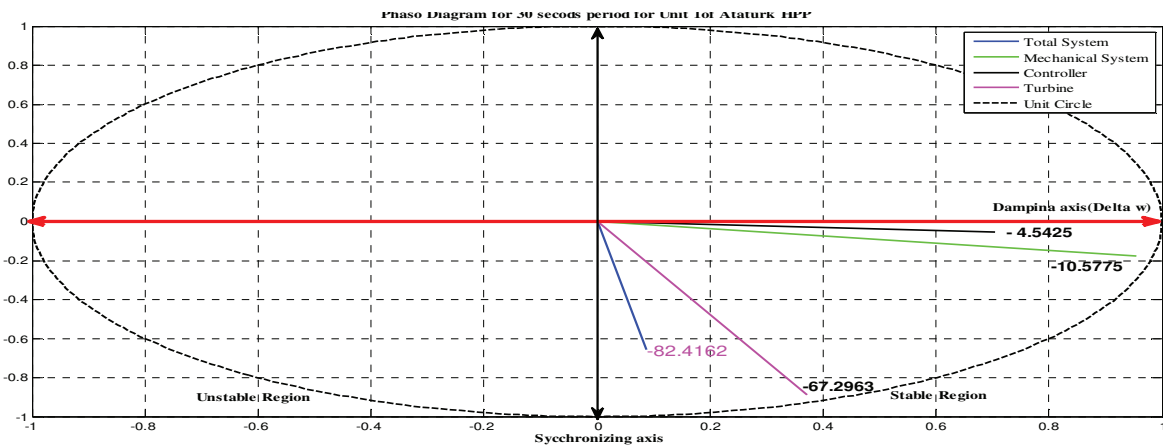


Fig. 4-14: Phasor diagram for 30 seconds period.

As seen in the above figures 4-14, the governor activates nearly all (~90%) of its reserve power in 30 seconds and the phase shift between $\Delta\omega$ and ΔP is less than 90 degrees (the phasor of total system is in the stable region) for frequency oscillations with 30 seconds period. Hence, it is concluded that the response of the unit is satisfactory.

4.1.4.4. Test 4 (island mode test)

The simulated island mode test was realized per IEC-60308 which was also programmed in the software prior [81]. Figure 4-15 shows the comparison between simulation and measured signals for frequency, wicket gate position and output power. The figure illustrates the frequency behaviour in an island mode. The initial load 261 MW (0.87 p.u. on the MVA base) an additional load of 0.044 p.u. is applied at time 4487.8 seconds. In this test the power controller off and the parameters set on Unit 1 of Ataturk HPP for island operation are listed in the following table:

Table 4-3: Parameters for Island Operation

P_n	P_0	T_w	T_p	r	T_n	T_{acc}	K_{acc}	Sigma	ΔPL
300	261	3 s	25s	0.12	60s	0.3s	4	0.08	0.044

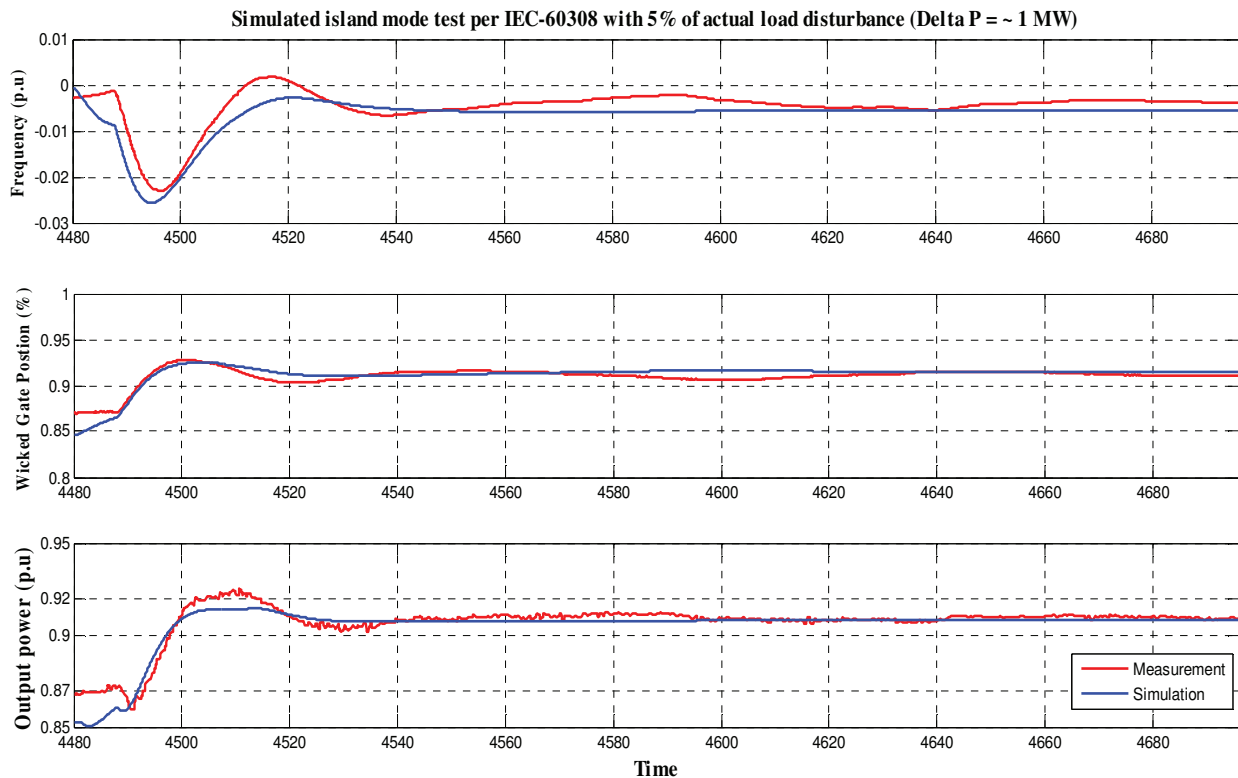


Fig. 4-15: Response of Unit 1 to island mode test per IEC-60308.

The test was carried out on the newly refurbished Unit 1 governor of Ataturk hydro power plant. The developed model of Ataturk HPP fits with the measurements and is reliable for all operating working points of the system from zero to full operation.

The set of control parameters was reached taking into account:

- The requirements for ENTSO-E-CE system;
- The requirements peculiar to the Turkish power system before and after interconnection;
- Extents of the physical realities of Ataturk hydro power plant.

For interconnected grid:

- The step of - 200 mHz should result in 15 MW within 30 seconds;
- For 30 sec period of grid frequency the simulation was stable (small than 90 degrees);
- For 7 sec period of grid frequency the unit did not respond.

The set of parameters was obtained giving the priority to the island operation stability which is a main requirement of Turkey's ENTSO-E-CE interconnection working group from hydro power plants to improve system stability. So as long as those parameters are used on the unit a single set valid both for grid operation and island mode operation is under concern.

In the end, the performance of the governor implemented in this control system rehabilitation project is capable of satisfying the ENTSO-E-CE requirements for the realization of Turkey's ENTSO-E-CE interconnection.

4.2. Dynamic Model of Oymapinar Hydro Power Plant

4.2.1. Introduction

Oymapinar Dam is an arch dam built on the Manavgat River in Turkey in 1984. It is an arch dam in design, 185 m in height, built to generate hydroelectric power [82].

Oymapinar Dam is located 12 km north of Manavgat Waterfall. It is an artificial, freshwater dam with a capacity of 300 million cubic meters [83]. It is 23 km upstream of Manavgat town 40 km east of city of Antalya in southern Turkey and located on the Manavgat River which runs into the Mediterranean.

Oymapinar Dam in Antalya province has been built with the aim of flood and electrical energy production between the years 1977-1983 and opened in operation in 1984. Annual mean flow is 3816 milion m³. Oymapinar Dam has four underground turbines (4x135 MWs) with a total capacity of 540 megawatts and has produced 1620 GWh energy [84]. As more dams have been built, it is the fifth largest.



Fig. 4-16: The Oymapinar dam.

The main data of the Oymapinar HPP Unit 2:

Type of turbine	: Francis
Rated power	: 135 (MW)
Rated flow	: 106.2 (m ³ /s)
Rated head	: 143 (m)

4.2.2. Test of Oymapinar Power Plant

The Oymapinar HPP is one of the considerable size HPPs in Turkey, will be one of the border plants of ENTSO-E-CE after interconnection and unit speed control, it was decided that a site visit in order to finalize the settings of governor in Oymapinar HPP is necessary. The site visit, attended by representatives of ETİ Alüminyum A.S., Ministry of Energy, TEIAS, ENTSO-E-CE Interconnection Project Group, TÜBİTAK and VATECH, was realized between dates 1-5 December 2008 [85].

During the field tests, studies were focused on, implementation and performance of governor. Regarding the governor, the parameters that are set by VA TECH were tested, new set of parameters were calculated and tested in order to satisfy the expectations. Although the tests were performed for all units, the results of unit 2 will be presented here as an example.

4.2.2.1. Governor Structure

According to the discussions with ENTSO-E-CE Interconnection Project Group, the main requirement in a governor structure is the direct effect of speed deviation on controller output. Further, it is necessary to have an accelerating path (derivative of speed) in order to reduce the delay (or phase shift) between the speed deviation and power output deviation. As seen in the block diagram (see Fig. 4-17), both are available in the new governors of Oymapinar HPP.

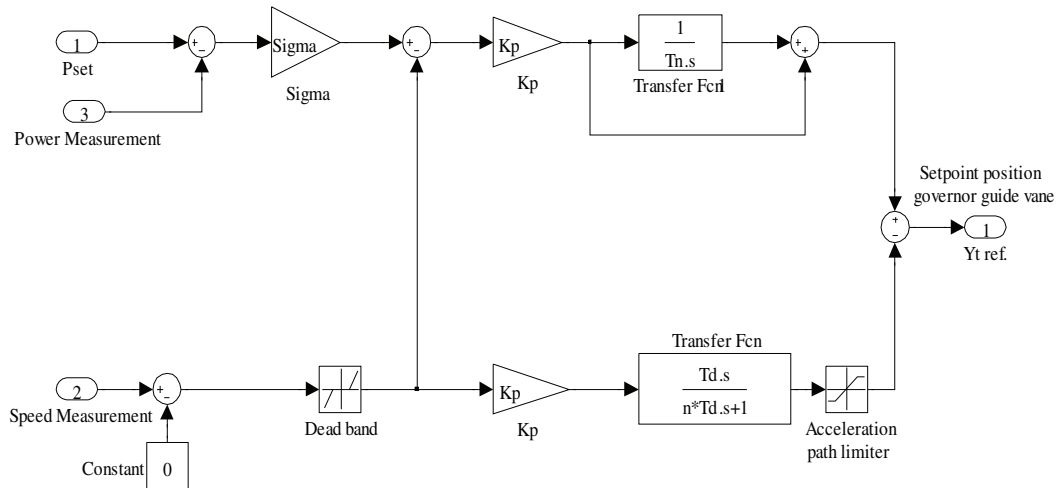


Fig. 4-17: The block diagram of governor of Oymapinar HPP.

4.2.2.2. Expectations and Tests

The studies on governor are focused on the tuning of parameters in order to satisfy the expectations defined by ENTSO-E-CE Interconnection Project Group, which can be summarized as;

- The phase shift between the power output and the frequency deviation for oscillations with 30 seconds period should be less than 90 degrees.
- The phase shift between the power output and the frequency deviation for oscillations with 7 seconds period should be less than 90 degrees.
- The primary frequency control response (for 200 mHz frequency deviation) should be completed in a time period comparable with 30 seconds.
- The Unit (with grid operation settings) should be stable in island operation.

In order to prove that the unit primary frequency control performance satisfies the criteria above, following tests were performed on the field with the help of VA TECH representatives:

4.2.3. Simulation Results

4.2.3.1. Step Response Test, (interconnected mode)

The speed measurement of the controller was disabled and an artificial frequency measurement signal was generated. Using the artificial signal a 200 mHz frequency deviation was simulated as a step when the accelerating path is not active and with a ramp of 200 mHz/sec. when the accelerating path is active.

4.2.3.2. Sinus Test, (interconnected mode)

The speed measurement of the controller was disabled and an artificial frequency measurement signal was generated. Using the artificial signal sinusoidal frequency deviations were simulated with periods of 7 and 30 seconds and amplitude of 200 mHz.

In these tests the parameters set are implemented by VA TECH are given in Table 4-4.

Table 4-4: The setting of governor of unit 2 of Oymapinar HPP

P_n	P_0	T_n	K_p	T_d	n	Acc. Lim-up	Sigma	Acc. Lim-down
138.5	10	3	9	2.43	0.165	5	0.04	5

Figure 4-18 shows the step response of unit 2 of Oymapinar HPP to ∓ 200 mHz step in frequency. The governor activates nearly all (~90% of expected response in 30 seconds). The figure shows the comparison between simulation and measured signals, for output power, wicket gate position and wicket gate setpoint.

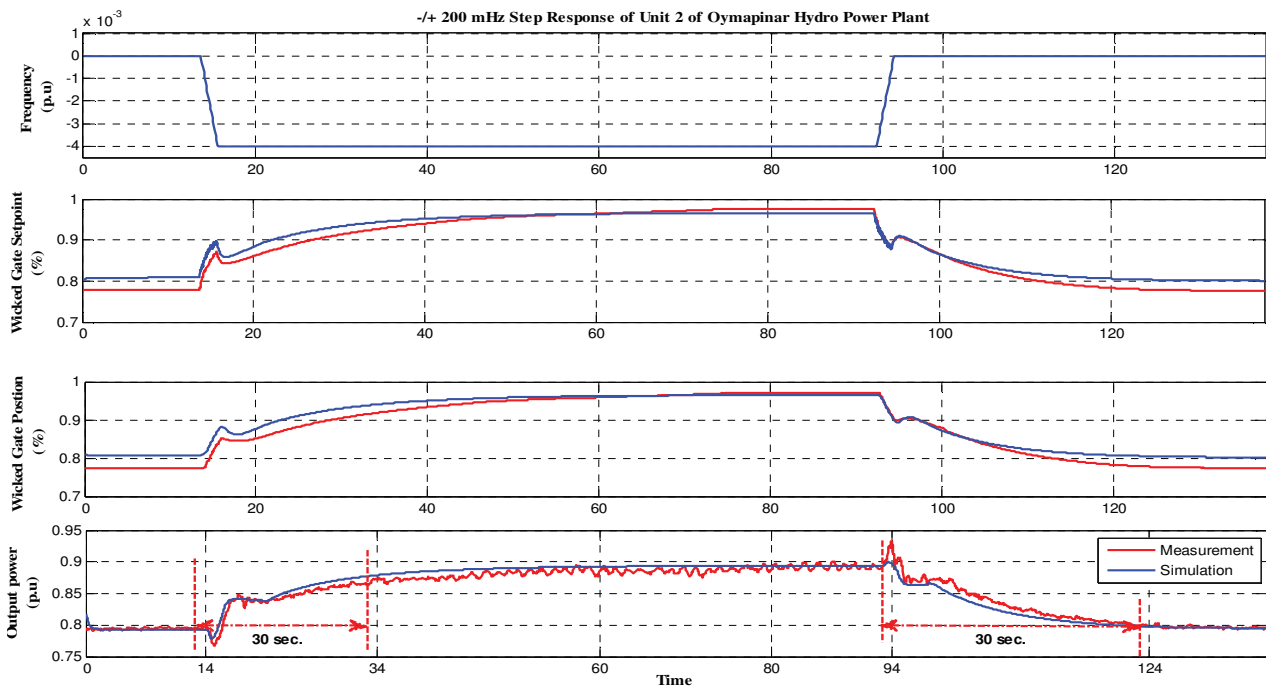


Fig. 4-18: Response of Unit to ∓ 200 mHz step.

Figure 4-19 illustrates the response of unit 2 to 7 and 30 seconds period sinusoidal changes in frequency. Figure 4-20 and 4-21 show the phase diagrams of sinus tests of unit 2. The phase shift between $\Delta\omega$ and ΔP is less than 90 degrees for frequency oscillations with both 7 and 30 seconds period.

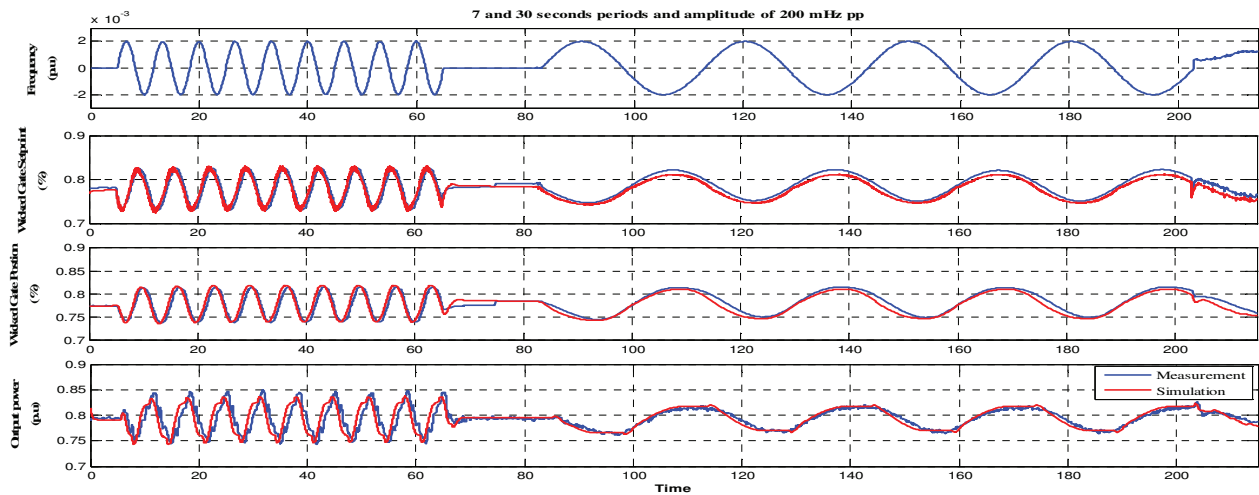


Fig. 4-19: Response of Unit 1 to 7 and 30 seconds periods.

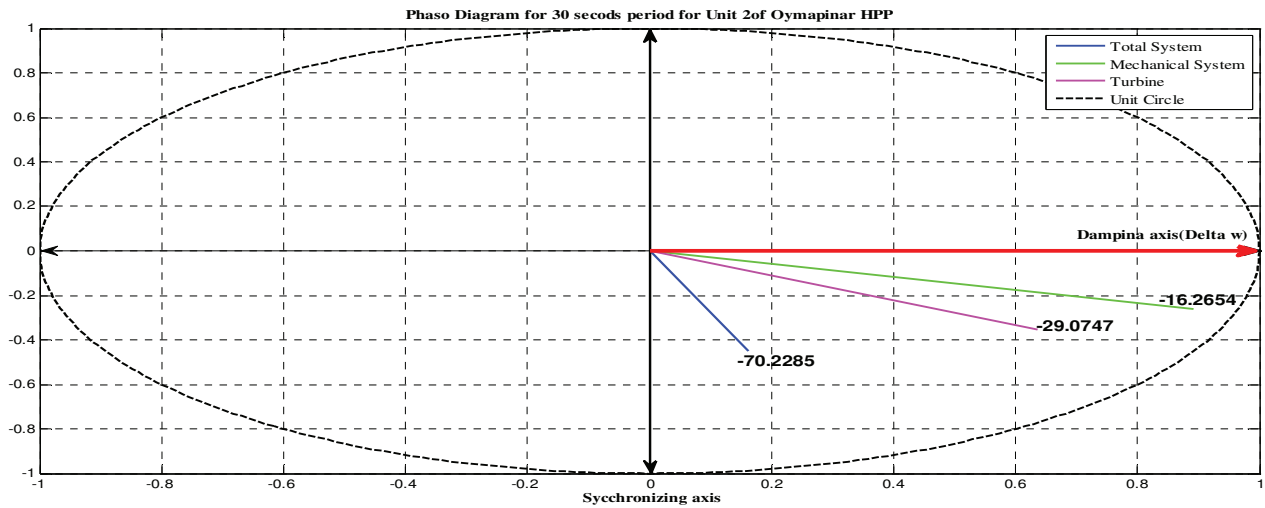


Fig. 4-20: Phasor diagram for 30 second's sinus test.

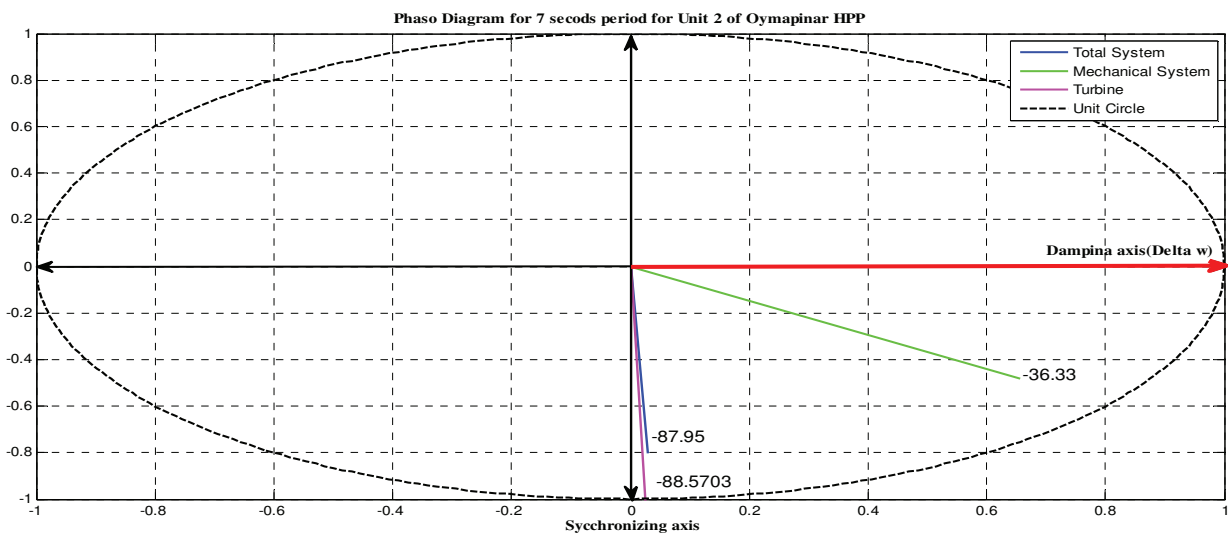


Fig. 4-21: Phasor diagram for 7 seconds sinus test.

As seen in the above figures 4-20 and 4-21, the governor activates nearly all ($\sim 90\%$) of its reserve power in 30 seconds and the phase shift between $\Delta\omega$ and ΔP is less than 90 degrees (the phasor of total system is in the stable region) for frequency oscillations with both 7 and 30 seconds period. Hence, it is concluded that the response of the unit is satisfactory.

4.3. Dynamic Model of the Turkish Power System

There are three different groups of plants in the Turkish power system based on the source of energy; Natural Gas Combined Cycle Power Plants (NGCCPPs), Thermal Power Plants (TPPs) and Hydro Power Plants (HPPs) as shown in figure 4-21a. Their installed capacity ratio is almost equal (i.e. $\approx 30\%$). In figure 4-21a the HPPs are represented by blue blocks mostly located in the East, while the TPPs and NGCCPPs are represented by red blocks mostly located in the West.

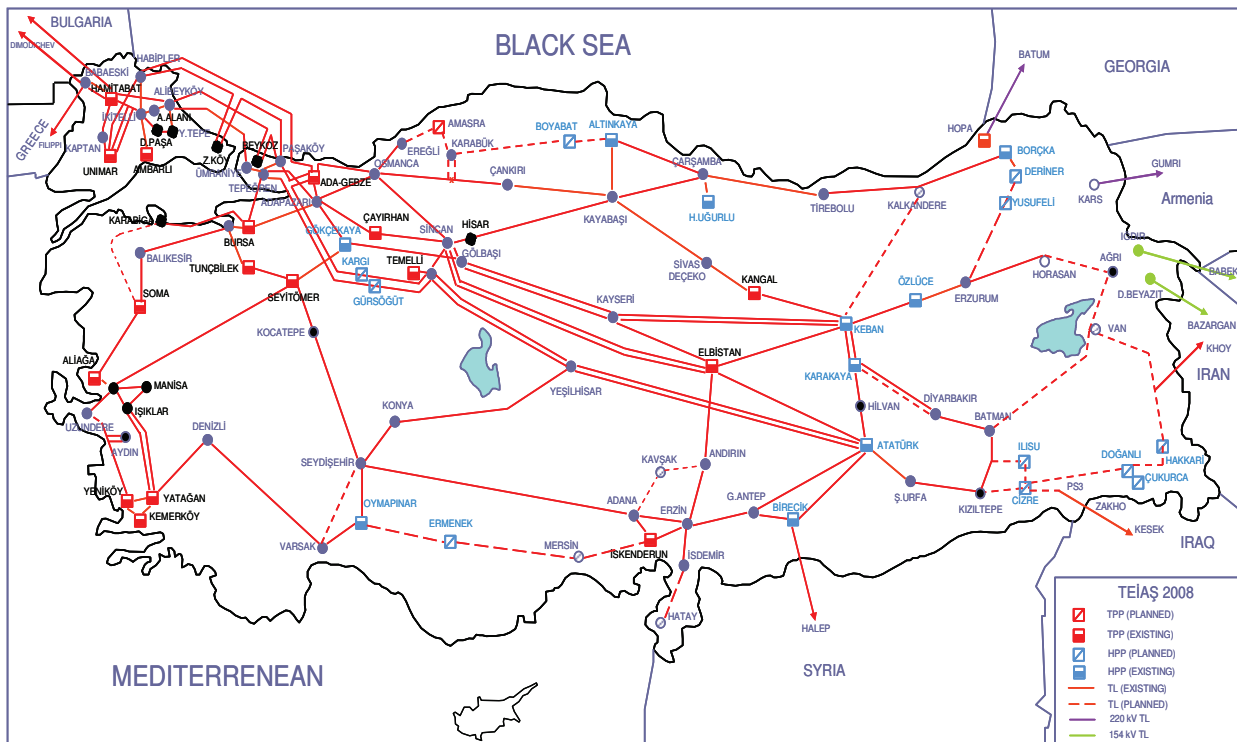


Fig. 4-22a: Turkish Network.

The NGCCPPs usually consist of three generators; two gas turbines that burn the natural gas, and one steam turbine that run on the steam generated by high temperature exhaust gases of single or both gas turbines. The TPPs consist of boilers that burn coal or other fuel to generate high pressure steam before steam turbine. Finally the HPPs use the kinetic energy of water as a source for generation [35].

The hydro plant unit controller models are prepared in detail covering the dynamics and friction of penstock and detailed actual controller models which are determined by site visits and field tests. The control philosophy is resolved for each HPP in the priority list via manufacturer documentation. The documentations of major TPPs and NGCCPPs provided by TEIAS are utilized to model their unit controllers. Also the secondary control model consists of the real controller as in operation in Ankara

(see Chapter 6, Section 6.6). Any model consists of separate models for power controller, governor and turbine regulator. After determining the unit controller models of individual plants in the priority list, the system model is built by combining them (see Fig. 4-22b). Details of the speed & power control structure and parameters of the models of the hydro, thermal and gas power plants can be found in the Appendix A, Appendix B and Appendix C.

MATLAB/SIMULINK software [59] is utilized for modelling and simulation studies performed in this thesis.

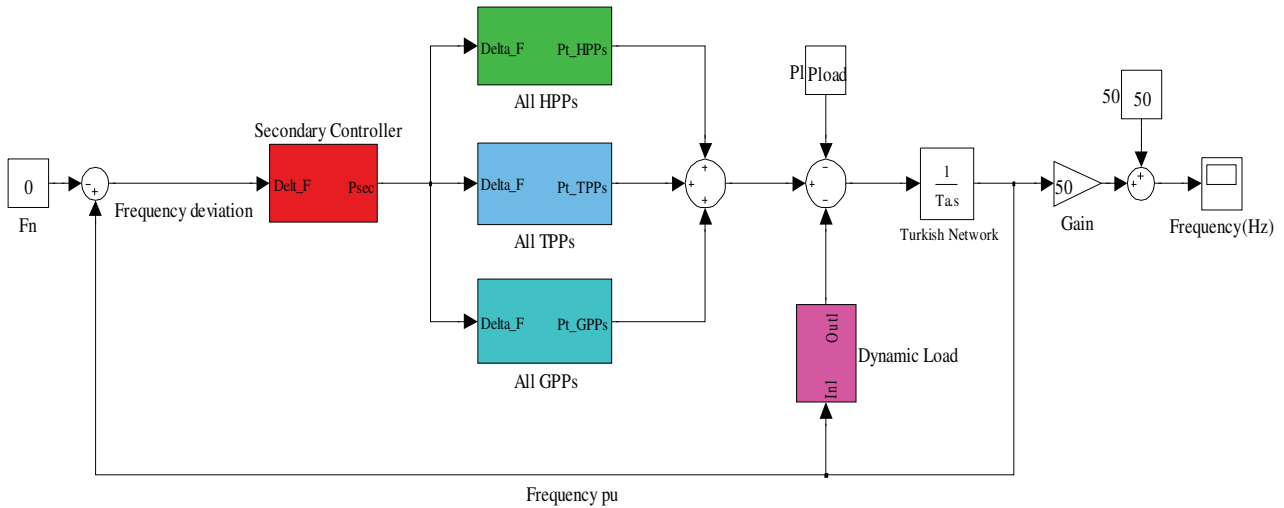


Fig. 4-22b: The overall model of the whole Turkish system with primary and secondary control.

4.3.1. Test 1 (High Load 25 GW)

This Test was carried out by Turkish Electricity Transmission Company (TEIAS) and Electricity Generation Company (EUAS). The incidence under consideration has happened in the Turkish power system during isolated operation with high load condition on 13 January 2010. In particular, it is analyzed the consequences of an outage in the Turkish power system where 2 units of Karakaya hydro power plant has tripped on 13.01.2010 at 15:04:50 pm with 600 MW generation loss.

4.3.2. Simulation Results

4.3.2.1. Island Operation with Primary Control

Figure 4-23 shows the frequency of overall performance in Hz and shows the comparison between simulations and measured signals with 600 MW generation loss in the Turkish power system with high load condition (25 GW) and the primary control reserve is 725 MW.

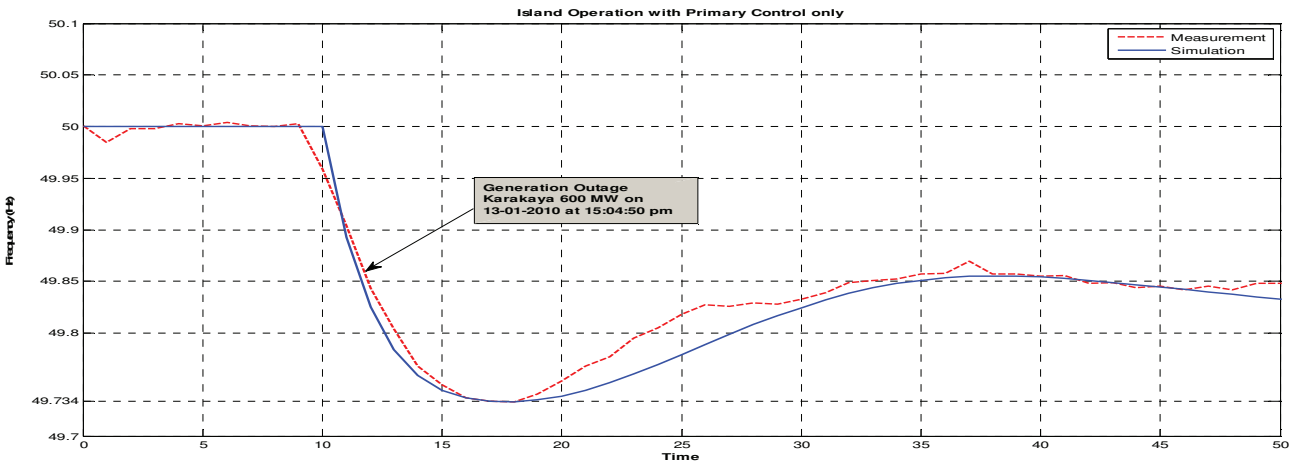


Fig. 4-23: The frequency behaviour in island operation with primary control.

4.3.2.2. Island Operation with Secondary Control

Figure 4-24 shows the trumpet curve, frequency of overall performance and shows the comparison between simulations and measured signals with 600 MW generation loss in the Turkish power system with high load condition (25 GW), the primary control reserve is 725 MW and class 1 (Ataturk, Karakaya, Altinkaya and Hasan Ugurlu hydro power plants) and class 2 (Adapazari, Gebze, Temelli, Aligia, Bursa, Keban power plants) have contributed to the secondary control. The K-factor of Turkey is 1480 MW/Hz and the parameters of integration time constant (T_{CR}) and the normal signal gain (G_A) are 70 seconds and 0.5 respectively.

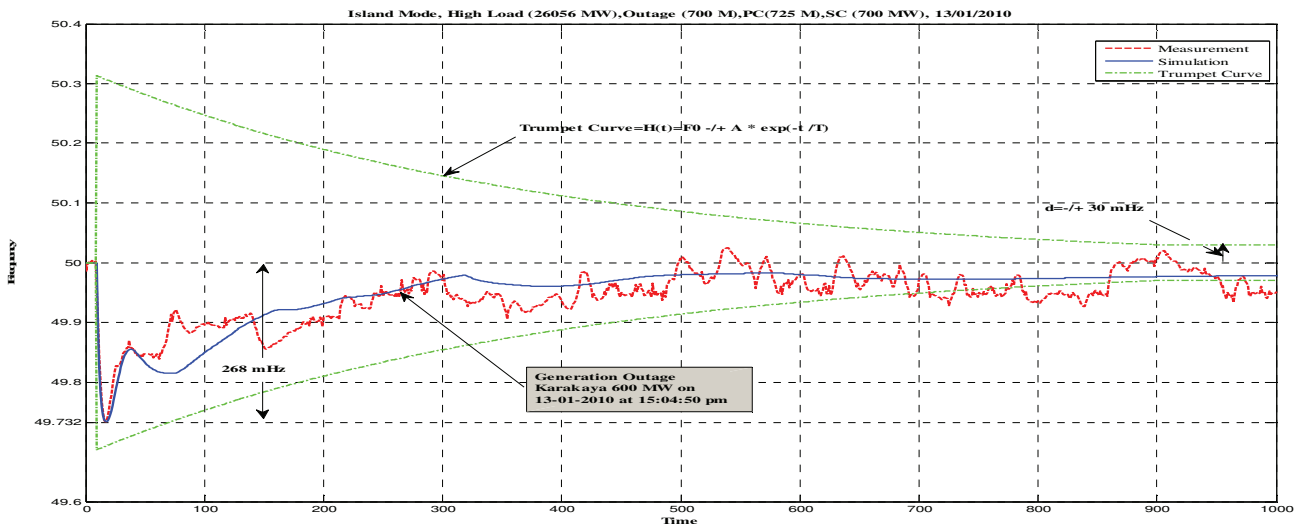


Fig. 4-24: The frequency behaviour in island operation with primary and secondary control.

As seen in the above figures 4-23 and 4-24, the maximum frequency deviation is reached at -268 mHz.

4.3.3. Test 2 (Low Load 18 GW)

This Test was carried out by Turkish Electricity Transmission Company (TEIAS) and Electricity

Generation Company (EUAS). The incidence under consideration has happened in the Turkish power system during isolated operation in low load condition on 22.02.2010. In particular, it is analyzed the consequences of an outage in the Turkish power system where unit 1 of Iskenderun thermal power plant has tripped on 22.02.2010 at 07:01:18am with 450 MW generation loss.

4.3.4. Simulation Results

4.3.4.1. Island Operation with Primary Control

Figure 4-25 shows the frequency of overall performance in Hz and shows the comparison between simulations and measured signals with 450 MW generation loss in the Turkish power system in low load condition (18 GW) and the primary control reserve is 520 MW.

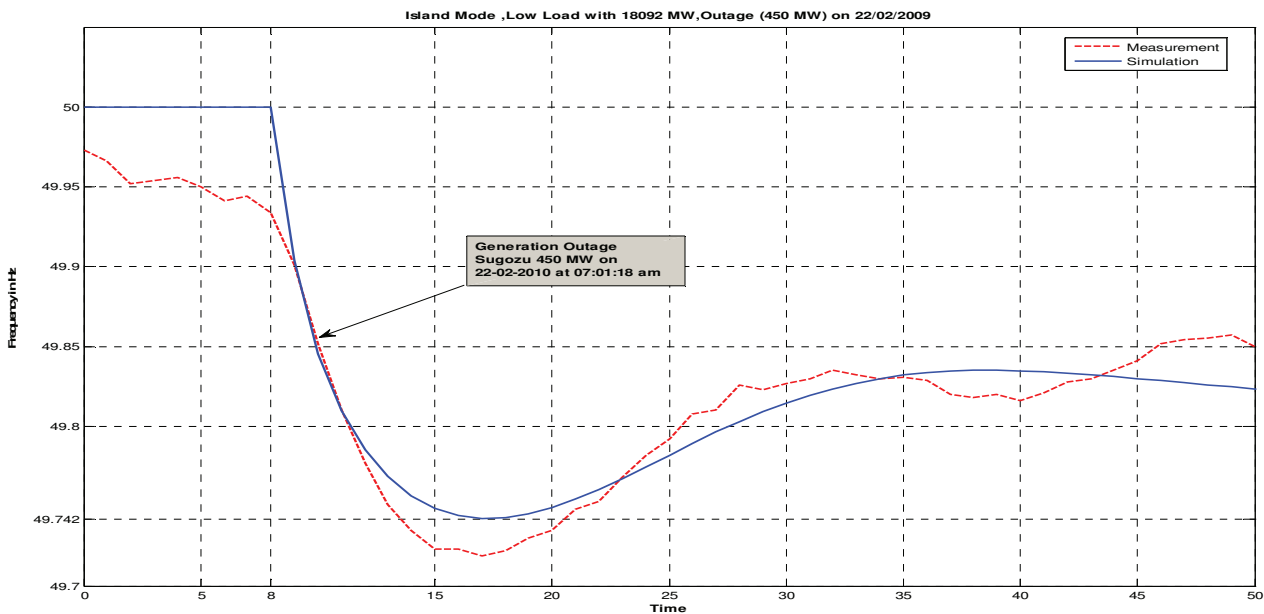


Fig. 4-25: The frequency behaviour in island operation with primary control.

4.3.4.2. Island Operation with Primary and Secondary Control

Figure 4-26 shows the trumpet curve, frequency of overall performance and shows the comparison between simulations and measured signals with 450 MW generation loss in the Turkish power system in low load condition (18 GW) and the primary control reserve is 520 MW. Class 2 (Adapazari, Gebze, Temelli, Aligia, Bursa, Keban power plants) and class 3 (Iskenderun TPP) have contributed to the secondary control. The K-factor of Turkey is 1480 MW/Hz and the parameters of integration time constant (T_{CR}) and the normal signal gain (G_A) are 70 seconds and 0.5 respectively.

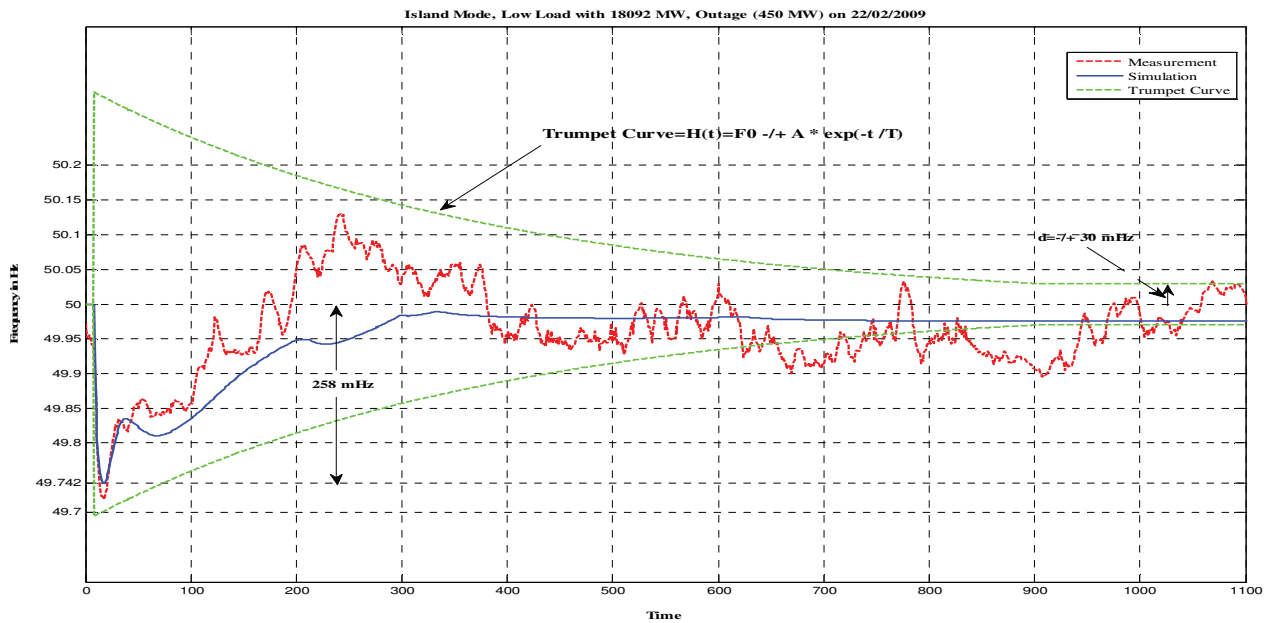


Fig. 4-26: The frequency behaviour in island operation with primary and secondary control.

It can be seen from figures 4-25 and 4-26, that the maximum frequency deviation is reached at -258 mHz.

4.3.5. Test 3 (High Load 25 GW)

This Test was carried out by Turkish Electricity Transmission Company (TEIAS). The incidence under consideration has happened in the Turkish power system during isolated operation with high load condition (25 GW) on 17.05.2010. In particular, it is analyzed the consequences of an outage in the Turkish power system where unit 1 of Iskenderun thermal power plant has tripped on 17.05.2010 at 12:03:30 pm with 580 MW generation loss [55].

4.3.6. Simulation Results

4.3.6.1. Island Operation with Primary and Secondary Control

Figure 4-27 shows the trumpet curve, frequency of overall performance and shows the comparison between simulations and measured signals with 580 MW generation loss in the Turkish power system with high load condition (25 GW) and the primary control reserve is 675 MW. The primary control allocations (675 MW) in the isolated Turkish system were as follows: 317 MW allocated to the hydro power plants (HPPs) and 358 MW allocated to the (TPPs +NGCCPP). Class 1(Ataturk, Karakaya, Altinkaya and Hasanugurlu hydro power plants) and class 2 (Adapazari, Gebze, Temelli, Aligia, Bursa, Keban power plants) are contributed in secondary control reserve. The K-factor of Turkey is 1824 MW/Hz and the parameters of integration time constant (T_{CR}) and the normal signal gain (G_A) are 70 seconds and 0.5 respectively.

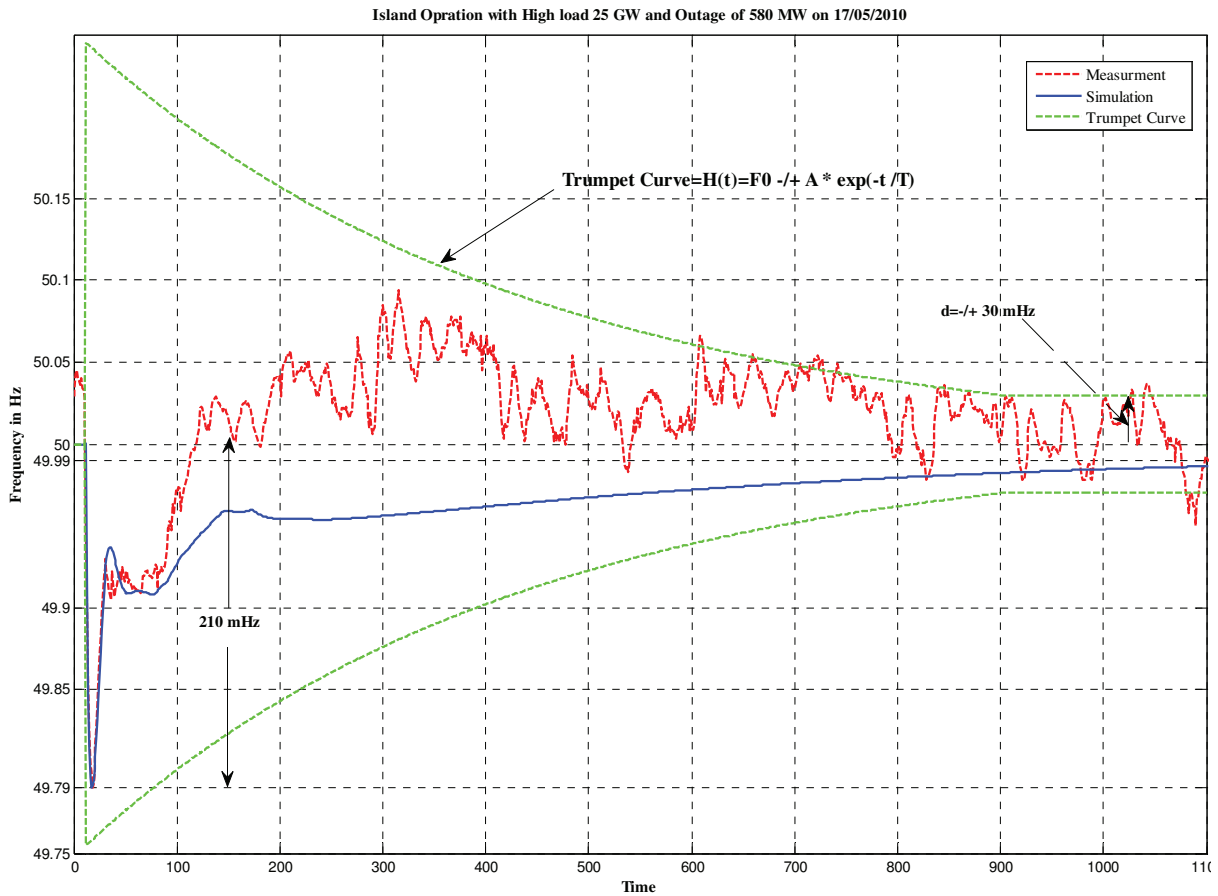


Fig. 4-27: The frequency behaviour in island operation with primary and secondary control.

As seen in the above figures 6-24 the maximum frequency deviation is - 210 mHz . During the first 100 seconds the simulation and measurements are approximately fitting and after that the simulation lowers than the measurement and this could be due to a load change in the Turkish power system.

4.4. Conclusion

As the simulation results, it can be seen that the models of the individual power plants and the overall model of the whole Turkish power system fits well with the measurements done in reality. This is true for the individual controllers of the plants (Ataturk and Oymapinar hydro power plants) and for the overall behaviour of the primary and secondary control of the whole Turkish power system. This holds in high and low load conditions. Finally, the model of the Turkish power system is validated regarding the allocation of primary and secondary control.

CHAPTER 5

Design of Governor Control and Parameter Optimization

5.1. Background

The study "Complementary technical studies for the synchronization of the Turkish power system with the UCTE power system" identified previously that unsuitable control structures and control parameter settings of hydraulic units are the main causes for an existing frequency control problem in the Turkish power system. The individual behaviour of generating units is usually optimised with respect to operational unit requirements and local grid requirements, but does not take into account all effects on the overall dynamic performance and stability of the entire power system [7, 53].

In large interconnected power systems like in the ENTSO-E-CE (former UCTE) power system possible negative effects of single units or certain generation technologies (e.g. of hydraulic units) on the overall system performance are less observable and may therefore be tolerated. This approach is not admissible for the Turkish power system as the Turkish power system is significantly different in

- Size (about 1/12 of installed capacity in comparison with ENTSO-E-CE)
- Structure of supply (about 1/3 of the total load is supplied by hydraulic units during peak hours, whereas the power supply within ENTSO-E-CE is dominated by thermal power plants)
- Longitudinal structure of the system in East-West direction with long transmission lines – the operation of themselves could be managed only by the help of permanent serial compensation.

Under these conditions it has to be ensured that each individual generation unit taking into account its specific dynamic characteristics contributes to the stability of the overall system frequency by means of suitable control structures and parameters.

A further aspect related with turbine governors concerns the inter-area oscillations after synchronisation of the Turkish power system with ENTSO-E-CE system. Due to the very low oscillation mode, which is expected at about 0.15 Hz (7 seconds period), the turbine governor control system might have an impact on the damping of the oscillations. Especially hydraulic units have to be taken into account in this respect because of their specific dynamic characteristic.

5.2. Stability Criteria for Power and Frequency Control in the Turkish System

The frequency performance (stability) of a power system results from the summary effect of its individual units, i.e. in the ideal case each individual unit should have a positive contribution to the frequency stability [42]. This leads to the following design philosophy:

- The controller dynamics have to ensure a stable operation in island conditions (*i.e.* a unit feeding a load of its own size). As it concerns feedback control systems, techniques used

within classical control theory (*e.g.* Phasor Study Method, Bode plot, Phase-Margin Criterion, Nyquist Criterion, etc.) can be applied to assess the stability around selected operating points

- The same controller dynamics utilized in parallel grid operation ensure a positive contribution to the overall frequency performance and stability. Thereby the adaptations related to the changeover between parallel grid operation and island operation do not effect these conditions provided that the decisive controller dynamics remain the same

5.2.1. Basic Requirements for all Generating Technologies

Active power imbalances in the power system are reflected throughout the system by a change in frequency. For satisfactory operation of a power system, the frequency must remain in the admissible ranges. Therefore generating units have to be equipped with speed governors providing the primary speed control action. The relationship between speed and load (generating unit output for a given frequency) can be adjusted by changing the load reference set-point of the speed controller or through a power controller. The latter is more convenient for the power plant operators but has significant drawbacks on the overall system performance (frequency stability, inter-area oscillations) unless the following criteria are fulfilled:

- The speed control loop must determine the dynamic behaviour
- The power control loop must solely adapt the steady state operating point. To this aim the proportional part of the PI-Controller needs to be sufficiently low (ideally zero) and the time constant of the power controller needs to be sufficiently high (depending on the dynamic characteristics of the speed controller)

Figure 5.1 shows a solution where the output signals of the speed controller and the power controller are added (parallel solution) and form the control signal for the actuator. Another solution would be a power controller that adapts the speed reference set-point of the speed controller. In fact the actual realization is part of the individual design of manufactures as long as there is a real speed control loop determining the dynamic behaviour of the unit. Against this background it has to be underlined that the implementation of speed control functionality via frequency bias and an adapted proportional part of the PI-controller (*e.g.* set to 1) is not equivalent to a real speed control loop and always leads to a adverse transient false control response [see Fig. 5-2 and Fig. 5-3].

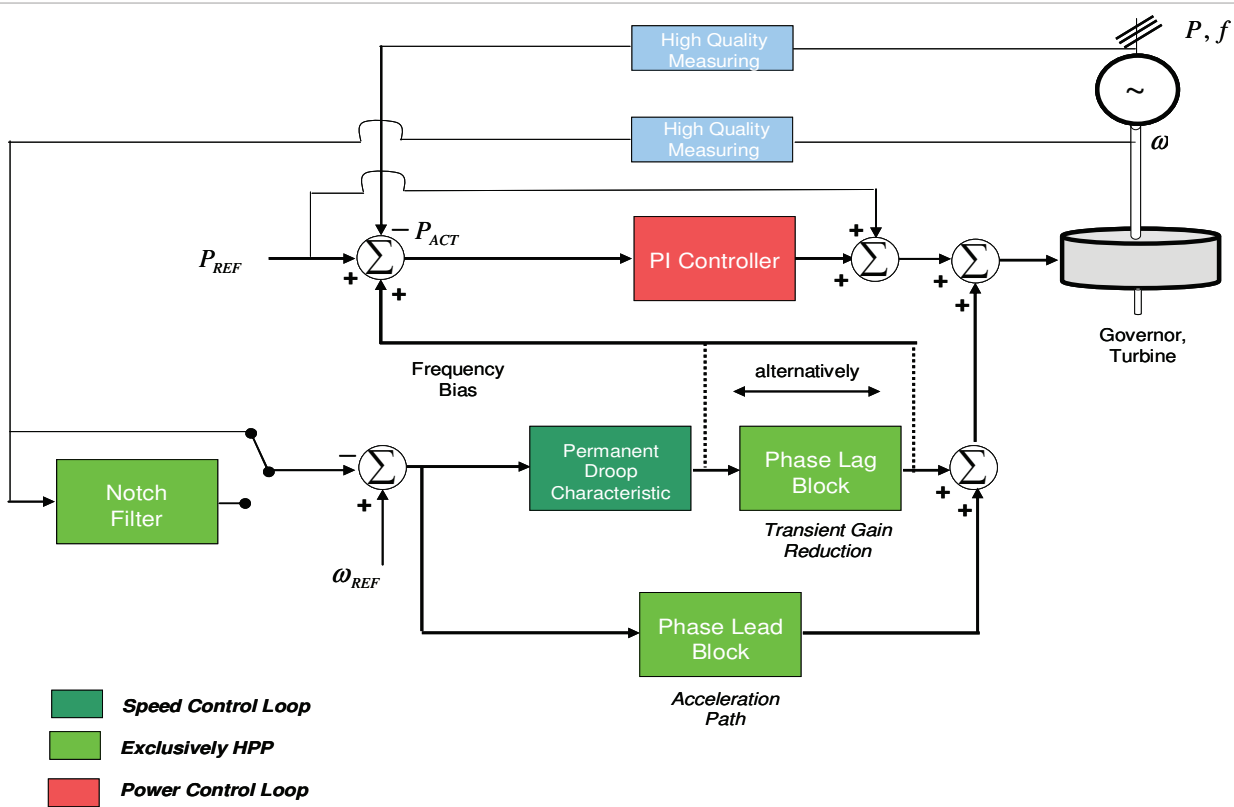


Fig. 5-1: Required controller functionality (different designs possible).

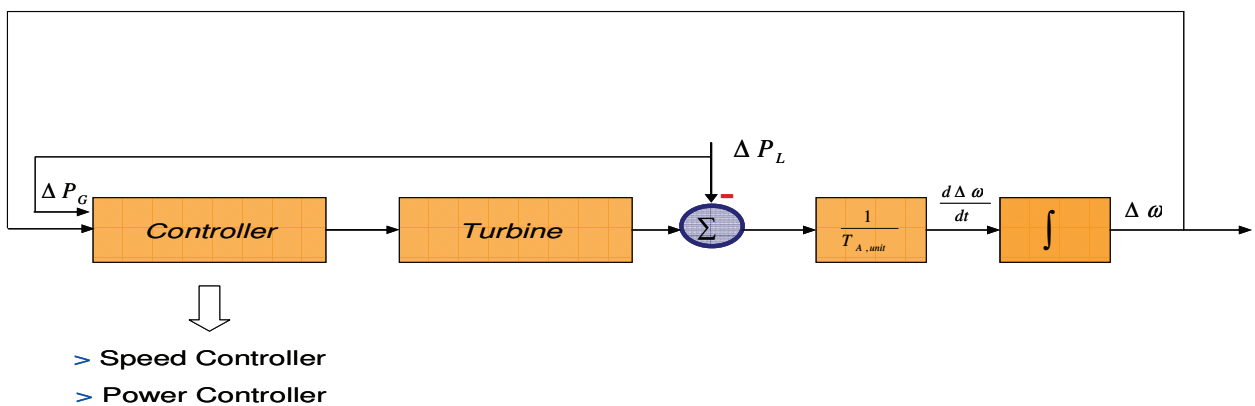


Fig. 5-2: Mid-term model.

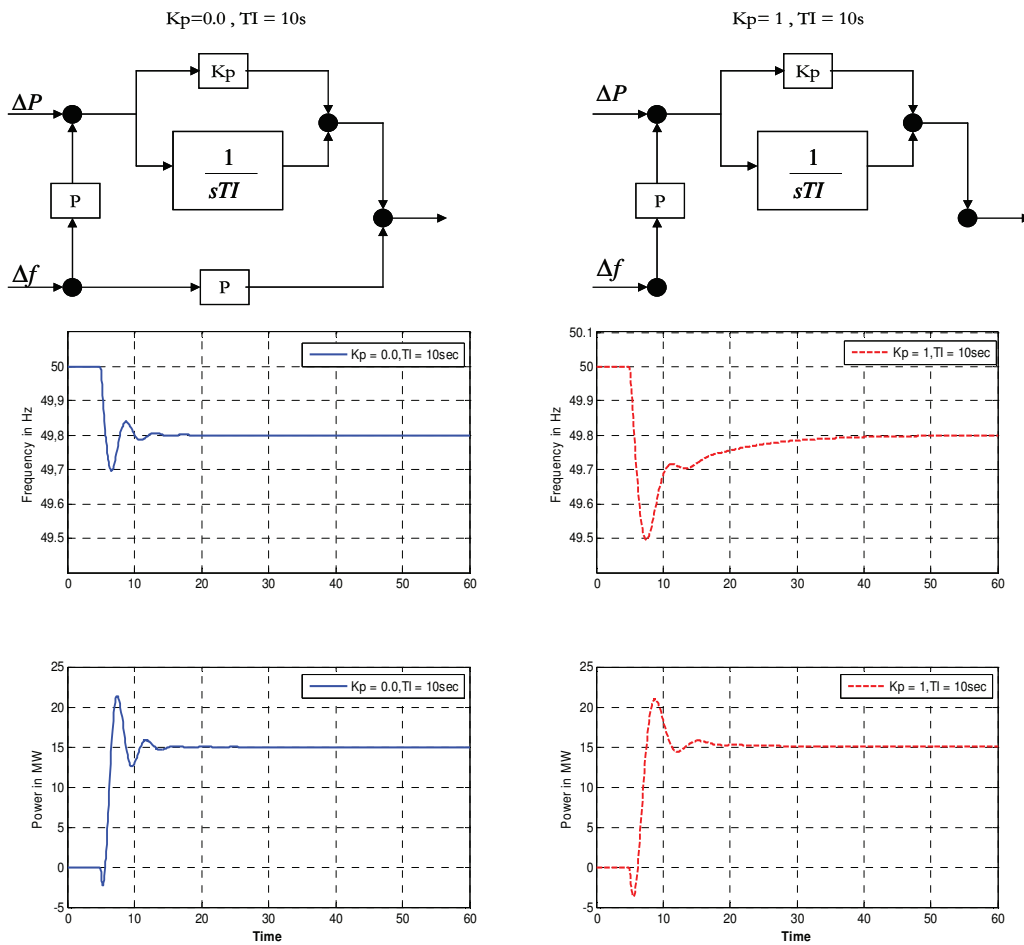


Fig. 5-3: Demonstration of transient false control response.

5.2.2. Special Requirements HPP

5.2.2.1. Requirement for A transient Droop

Hydraulic turbines have a peculiar response due to water inertia: a change in gate position produces an initial turbine power change which is opposite to that sought (non-minimum phase system). For stable control performance, a large transient (temporary) droop R_T with a long resetting time T_R is therefore required. This is accomplished by the provision of a rate feedback or transient gain reduction compensation as shown in figure 5-4a [47].

This can be achieved by including lead-lag compensators in the speed controller (see Fig. 5-1). Again these functions can be realized and arranged in different ways and are part of the individual design of manufacturers.

5.2.2.2. Tuning of Speed-Governing Systems

For the determination of the optimum governor parameters, the stability of the generating unit when supplying an isolated non-synchronous load must be considered. This represents the most severe condition from the viewpoint of frequency control and the corresponding settings ensure stable

operation for all situations involving system islanding. Moreover the negative effects of HPP on inter-area oscillations are suppressed as due to the more sluggish behaviour the unit can not follow the oscillation.

For stable operation under islanding conditions, the optimum choice of the transient (temporary) droop R_T and reset time T_R is related to the water starting time T_W and mechanical starting time T_M as follows [47, 56]:

$$R_T = [2.3 - (T_W - 1.0)0.15]T_W/T_M \quad (5.1)$$

$$T_R = [5.0 - (T_W - 1.0)0.5]T_W \quad (5.2)$$

The requirement for stability of speed control under islanding conditions or other isolated modes of operation is in conflict with the governor settings required for fast loading and unloading under normal synchronous operation. Therefore the capability of HPP to contribute to primary frequency control is generally affected adversely in terms of MW/s that can be provided.

Figure 5-4 illustrates the effect of the transient droop compensation on the stability characteristics of the governing system.

Figure 5-4a shows the block diagram of the speed-governing system of a hydraulic unit supplying an isolated load. The speed governor representation includes permanent droop R_p of 0.05, transient droop compensation is given by [57] $G_c(s) = \frac{1 + T_R s}{1 + (R_T/R_p) * T_R s}$ and a governor time constant T_G of 0.5sec.

Turbine is represented by classical model with T_W of 2sec. The generator is represented by its equation of motion with a mechanical starting time T_M of 10sec. and a system-damping coefficient K_D of 1.0 per unit. The calculated values T_R and R_T according to the equations 5.1 and 5.2 are 9sec. and 0.43 respectively.

Figure 5-4b shows the bode plot for open-loop frequency response characteristics with and without transient droop compensation. Without transient gain the gain and phase margins are -12.4 dB and -104 degrees respectively. The uncompensated system is hence unstable (blue line). With transient gain the gain and phase margins are 5.3 dB and 42.3 degrees respectively. The compensated system is hence stable (green line).

Phase margin is just the difference between -180 degree and the actual phase angle of the frequency response function, measured at the frequency where the magnitude of the frequency response function, is equal to one. On a Bode plot that frequency is the zero db crossing frequency as shown in figure 5-4b.

Gain margin is just the amount of gain that you can add to move the zero db crossing to occur at the same frequency as the -180 degree crossing.

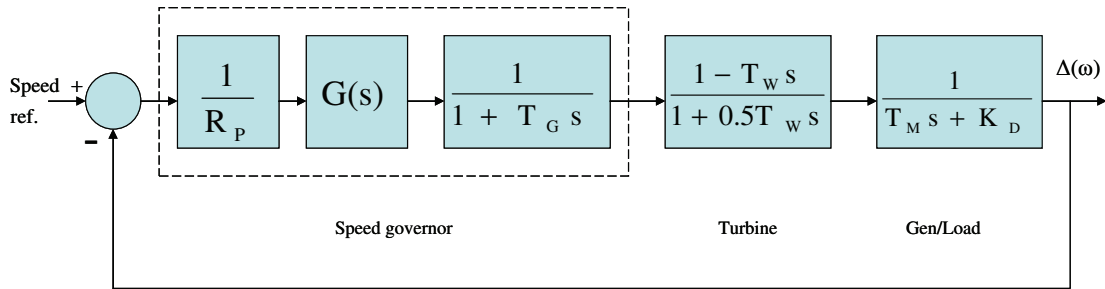


Fig. 5-4a: Block diagram of speed-governing system.

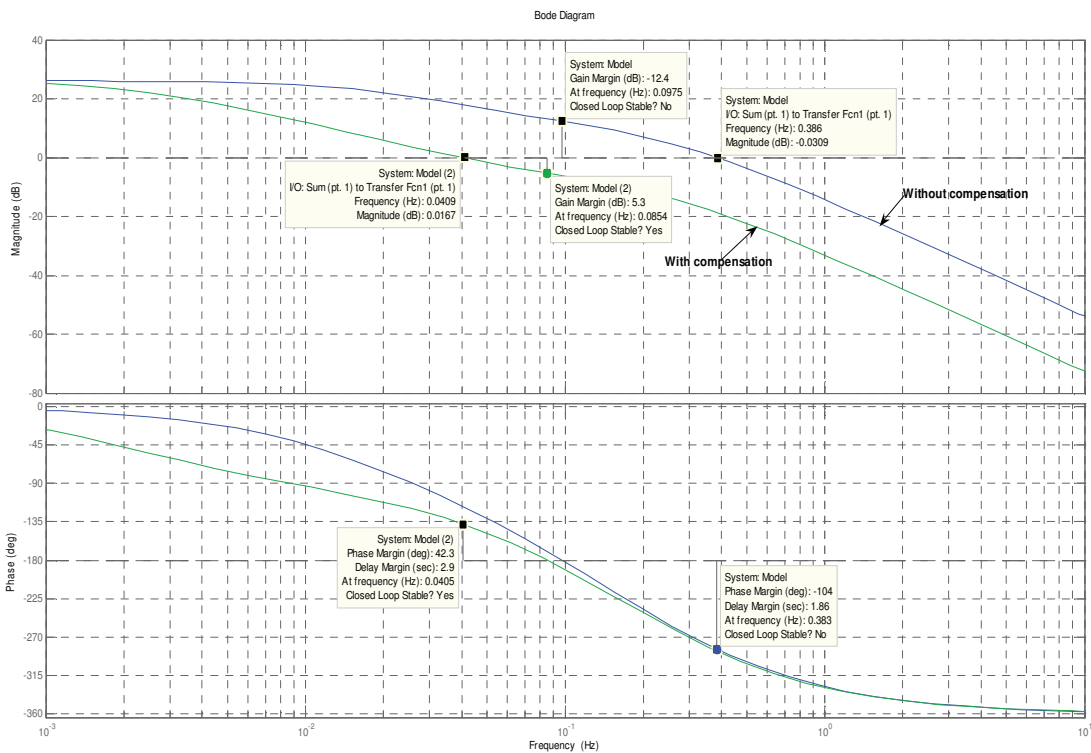


Fig. 5-4b: Bode plot with and without transient droop compensation.

5.2.3. Challenge for the Turkish Power System

The challenge in a predominantly hydroelectric power system such as the Turkish power system is to balance diverging requirements (see Fig. 5-5).

In order to prepare the presently isolated Turkish power system (see Chapter 6) for the interconnection to ENTSO-E-CE:

- A: the stability of frequency control has to be ensured ;

- B: sufficient primary control reserves and response rates have to be provided to handle the "normative" outage (approx. 700MW) by taking into account certain frequency performance criteria ;

After the interconnection to ENTSO-E-CE (see Chapter 7)

- C: the stability of frequency control in case of islanding from ENTSO-E-CE has to be ensured;
- D: the Turkish Power System as control area must be capable to activate primary control according to the ENTSO-E-CE requirements (approx. 300 MW-350 MW in 30sec in case of 200 mHz frequency drop). The primary control reserve should not exceed the necessary value (export of primary control power has negative effect on damping of inter area oscillations);
- E: no negative effects on the damping of inter-area oscillations.

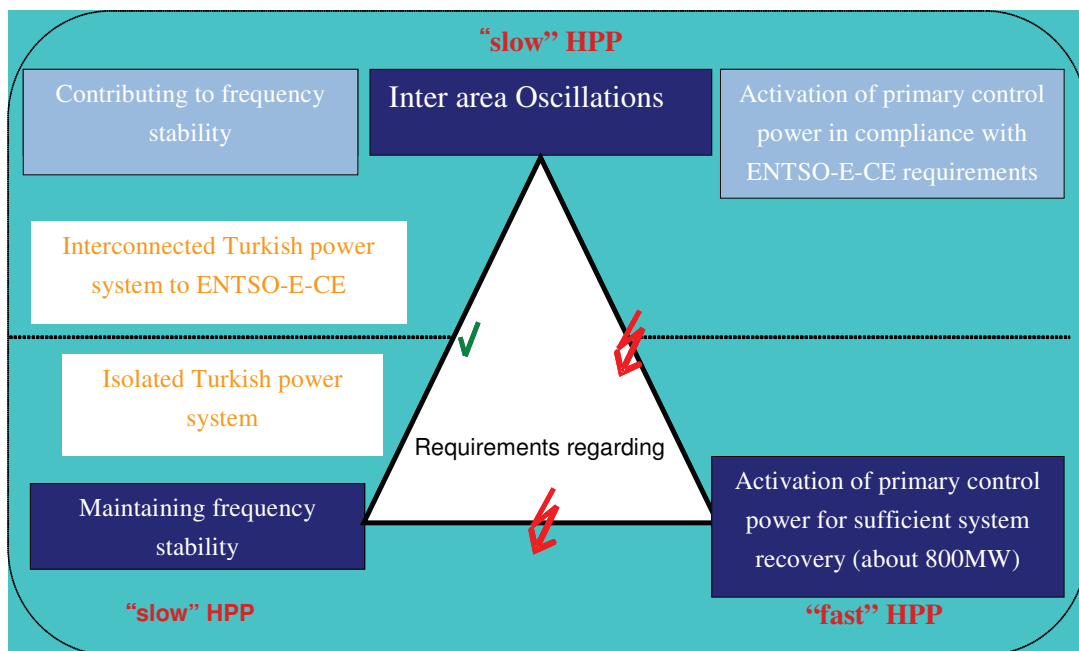


Fig. 5-5: The trade-off to be solved for the Turkish power system.

As illustrated in figure 5-5, the requirements on turbine controllers that lead to a stable frequency performance are also beneficial for the damping of inter-area oscillations, but diverge from the requirements that are desirable with respect to the activation of primary control power. This is the trade-off that has to be solved.

5.3. Strategy and Recommendations

To fulfil the above mentioned requirements the primary control concept of the Turkish power system has to be redesigned:

- 1) Primary control according to ENTSO-E-CE requirements should be provided exclusively by TPP and NGCCPP. To this aim the participation of TPP to primary frequency control should be expedited within the bounds of technological possibility and moreover reserve contracts with

respect to modern NGCCPP should reflect the technical possibilities. HPP in general should be tuned for "island mode" stability and primarily participate in secondary control.

One important precondition for the implementation of this strategy is to improve the secondary control performance at first in order to reduce (slow) frequency deviations and thus to minimize the mechanical stress for the units.

Taking into account that modifications within TPP have to be done in a deliberate way by considering the technological limitations and economical aspects the following measures should be aspired:

- The vast majority (preferably, all) of the steam turbine generators of TPPs with unit rated power ≥ 50 MW, should contribute to the primary frequency control, with fast response to speed/frequency derivations.
- In order to obtain a fast response, in keeping with many similar TPPs in service in the ENTSO-E-CE system, the speed control should give priority to turbine action, in turbine-boiler well coordinated mode or boiler follows mode. The turbine follows mode of lignite-coal fired TPPs cannot give a fast response.
- If there are justified concerns for damages of the boilers fired by low quality lignite, deemed incompatible with operation of boiler in automatic control mode, it is recommended to consider that boiler could continue to be operated in manual mode and steam turbine be called to contribute to primary fast speed control, by utilizing the thermal inertia of boiler (in evaporator, drum, superheaters, re-superheaters). With this option the steam pressure should be allowed to undergo a small variation, of course in a limited conservative range kept under control by reliable protections re-instating pressure to rated value if a preset limit is attained in (exceptional) cases. By rule, keeping in mind the continuous fluctuations up and down of frequency and the deviations elimination by the secondary frequency control, it is expected that the steam pressure limits could only very rarely be attained in synchronous operation with the ENTSO-E-CE.
- Application of condensate stopping (only usage of the stored energy)

Even though the control capabilities of different generating technologies (limited either by technical restrictions within the power plant itself or by requirements related to the overall system security) have to be taken into account for the efficient allocation of control reserve it is nevertheless desirable to maintain a high degree of market flexibility and not to exclude certain generating technologies.

Besides in case of the Turkish power system in order to fulfil requirement B additional participation of HPP according to the ENTSO-E-CE requirements might be necessary. This leads two the following recommendation:

- 2) Facilitate the participation of hydraulic units to primary frequency control as far as possible. The participation of hydraulic units to primary frequency control is in principle possible, but underlies certain restrictions:

- HPP with significant water starting time constant ($T_w > 1s$) have to be tuned taking into account the aforementioned stability criteria. This yields in limited response rates (30s-ramp can not be tracked) which is acceptable as according to the UCTE Operation handbook the 30s-ramp is not mandatory for individual units but for the entire control area.
- For units with low water starting time constant ($T_w \leq 1sec.$) the aforementioned stability criteria might be violated provided that the following criteria are met.
 - Not each individual unit, but the Turkish power system as a whole fulfils the required stability criteria for frequency control. Thereby it is conceded that selected individual units will be tuned with priority on primary control activation in terms of MW/s (30s-ramp). The effect on the overall frequency stability has to be assessed by simulation studies.
 - When relating the speed input to the power output of the turbine (open loop) it should be aspired to achieve a phase shift between the two phasors which is less than 90° for the time period $T=25s...30s$ (swinging period of the isolated Turkish power system) and the time period $T=7s$ (oscillation period after interconnection to ENTSO-E-CE). If the phasor cannot be shifted to the stabilizing area alternatively a notch filter can be foreseen to fade out the critical oscillation.

Figure 5-6 shows the criteria for hydro power plants to participate in primary control. Thereby the classification according to $T_w > 1sec.$ or $T_w \leq 1sec.$ should serve as orientation and is not absolute fix value.

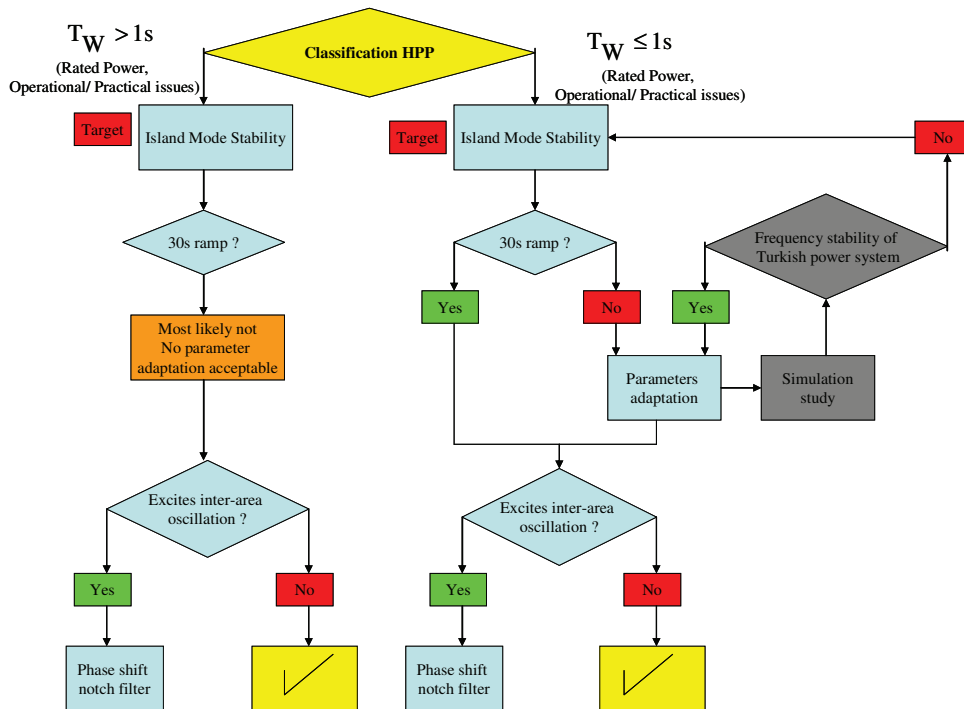


Fig. 5-6: Decision-tree for HPP for participating in primary control.

5.4. Consequences Regarding Assessment of Power and Frequency Control

5.4.1. Sudden Power Imbalance

When considering the isolated Turkish power system the frequency deviations depend both on the dynamic characteristic of primary control and secondary control, which are different in thermal and hydraulic systems. The required stability criteria lead generally to reduce response rates of HPP. This involves:

- possible difficulties to fulfill the trumpet curve which is originally designed for thermal systems in case of outages

5.4.2. Stationary Power Imbalance (load mismatch)

The quality of load matching during stationary operation (slow frequency deviations) depends on the secondary control performance.

During the parallel operation with ENTSO-E-CE unintended power exchange almost equals the power/load mismatch, which depends in the stationary operation on the secondary control performance. In case HPP are utilized for secondary control it is important that the stability criteria of secondary control reflect the dynamic characteristics of hydraulic units and that no inter-area oscillations are excited.

5.4.3. Random Power Imbalance (frequency fluctuations)

Random power imbalances lead to frequency fluctuations that correspond to the total gain of primary control, which in turn is the composite effect of the gains of thermal units and transient gains of HPP weighted with rated power. Due to the more sluggish behaviour of HPP

- higher but unavoidable frequency deviations / frequency noise due to load variations might be possible

These aspects have to be taken into account, when the expected unintended power exchange with ENTSO-E-CE is estimated from the frequency behaviour in isolated operation.

5.5. Strategy - Working Plan

According to the strategy the work comprises two basic tasks

- Theoretical and on-site analysis of individual units belonging to the decisive power plants with special consideration of the major hydraulic units.
- Analysis of the entire Turkish power system with an adequate simulation model in order to analyse the overall frequency performance and the possibilities to allocate primary control power among the different generating technologies.

5.5.1. Individual Units

The analysis of the individual units included the stocktaking and classification of existing controllers

(in terms of controller structures and control parameter settings), the set-up of simulation models in MATLAB and the theoretical analysis on the basis of adequate simulation models and test scenarios (stability of frequency control, provision of primary control power, impact on inter-area oscillations). Thereby the on-site analysis of the respective units is indispensable to adjust the simulation models to the reality and to investigate the real unit behaviour.

Both the theoretical and the on-site analysis concentrated on island mode conditions, step responses and the stimulation of the units by sinusoidal signals for the phasor study method.

Phasor study method is an appropriate means to reveal in particular the unit's contribution to the 7s - oscillation. This oscillation is an inter-area oscillation between coherent generator groups and as its period is determined by the distribution of inertia and the network topology (impedance) it is more or less fixed. Contrariwise the 30s- swinging period of the isolated Turkish power system is a coherent swinging (movement) of all generating units within Turkey and its period is impacted by the summary effect of all turbine control actions. Therefore modifications that are aspired in the turbine control system themselves have a feedback on the swinging period and necessitate investigating a wider frequency range.

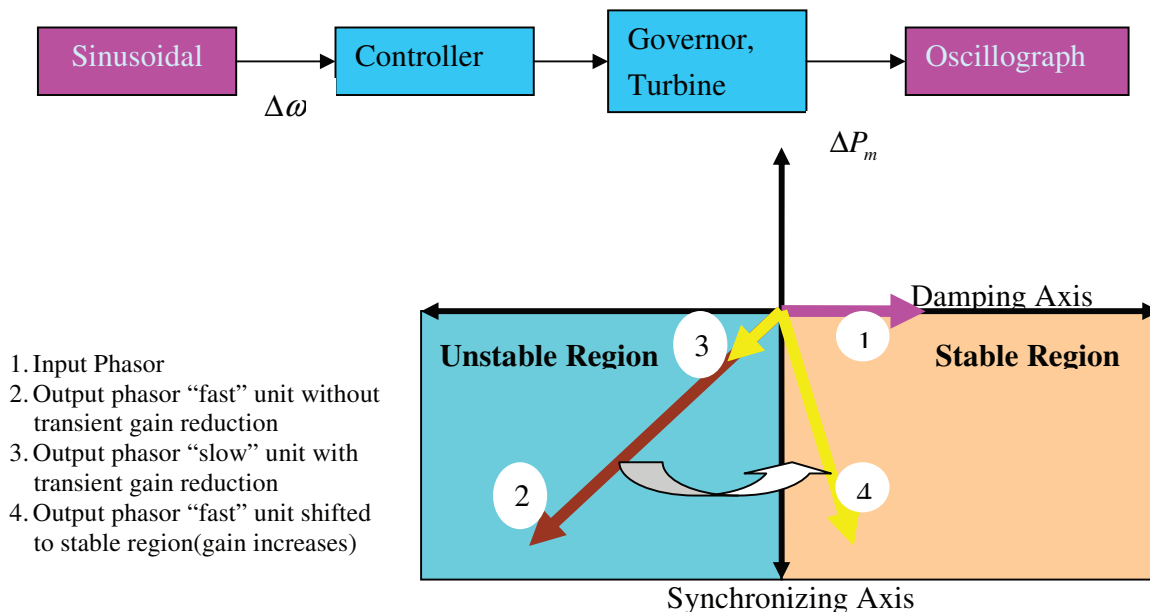


Fig. 5-7: Phasor study method principle.

Figure 5-7 illustrates the phasor study method principle. To provide damping the system consisting of the controller, the governor and the turbine must produce a component of electrical torque in phase with rotor speed deviations. Due to the inherent gain and phase characteristics of the system the phasor is shifted clockwise. The specific characteristics of HPP lead to a significant phase lag, especially for the 7s oscillation, so that the resulting phasor settles down in the destabilizing quadrant. Controller modifications can be utilized to mitigate this effect:

- By applying a sufficient transient gain reduction the unit response to the critical oscillation/swinging can be reduced or eliminated (reduction of phasor length). Due to its more sluggish behaviour the unit is not able to follow the oscillation/swinging and behaves more or less neutrally. As denoted before this approach yields also in operating stability for island mode conditions and contributes to the overall frequency stability of the Turkish Power System
- When a faster unit response is desired (i.e. operating of the unit without sufficient transient gain reduction) it can be sought to shift the phasor to the stabilizing area or to fade out the critical frequency by a notch filter. Phasor shifts are generally accompanied by additional mechanical stress on the valves. Moreover it has to be ensured that the stability criteria for the overall Turkish power system are not violated.

The final tuning of the unit has to be done on-site and could also be a compromise between "reducing the length of the phasor" and shifting it to some degree. Therefore it is of utmost importance that the controller structure exhibits all necessary features and that parameters can be changed easily.

The MATLAB models of all major power plants were created. Phasor study methodology has been performed for several of them and can be utilized for preliminary analysis and to investigate the effective set screws to achieve the desired control aim. However, the final tuning studies have to be performed on-site unless simulation model uncertainties are eliminated (e.g. by parameter identification etc). On-site studies are time-consuming and laborious so that currently only three HPP have been investigated in detail, namely Oymapinar, Atatürk and Birecik [85, 80 and 87].

5.5.2. Phasor Study Methodology

The main aim of the study is to determine the effects of governors of individual units on existing and expected power system frequency oscillations. The idea is to analyze units individually to observe whether its governor has a positive or negative effect on the stability of the power system frequency. The analysis is performed for two frequencies, which are the frequency oscillations of Turkish system with 30 seconds time period and the 7 seconds inter area oscillations expected to be observed after interconnection with the ENTSO-E-CE system.

The analysis is basically the phasor representation of frequency responses of power plants at certain frequencies. The approach is to apply a sinusoidal variation of frequency to the governor and to observe the output power variation with the assumption that this individual plant has negligible effect on the frequency oscillations. The phase shift and gain of the output power with respect to frequency deviations multiplied with droop is used to observe the damping coefficient of the output power.

At first the main characteristics of the Phasor study methodology is explained with a simplified model. Then we shall discuss the response of types of power plants (lignite/coal thermal power plants (TPPs), natural gas combined cycle power plants (GPPs), hydro power plants(HPPs) and all power plants together (PPs)).

5.5.2.1. Simplified Model

5.5.3. Open Loop

A sinusoidal frequency deviation is applied to the determined model and the mechanical output power of the unit is observed as shown in figure 5-8. The Turbine is represented by classical model (linear model) and the speed governor by pure gain $K_G = 1/R$.

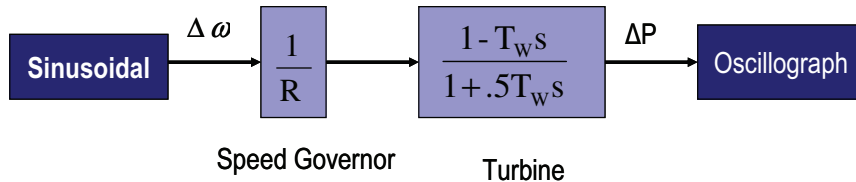


Fig. 5-8: Unit of simplified model with sinus.

Figure 5-9 illustrates the phasor study method for 30, 10 and 7 seconds period sinusoidal frequency. For $R = 0.4$ and $T_w = 2.0$ seconds the phase shift between $\Delta\omega$ and ΔP for frequency oscillations with both 30 and 10 seconds period is less than 90 degrees and for 7 seconds period is greater than 90. The time periods of the oscillations are $T_x = 30, 10$ and 7 seconds. Using the phasor study method with frequency $f_x = 1/T_x$ the angles are $-34.5, -85.12$ and -96.8 degrees respectively, this means the system is stable for 30 and 10 seconds period and unstable for 7 seconds period.

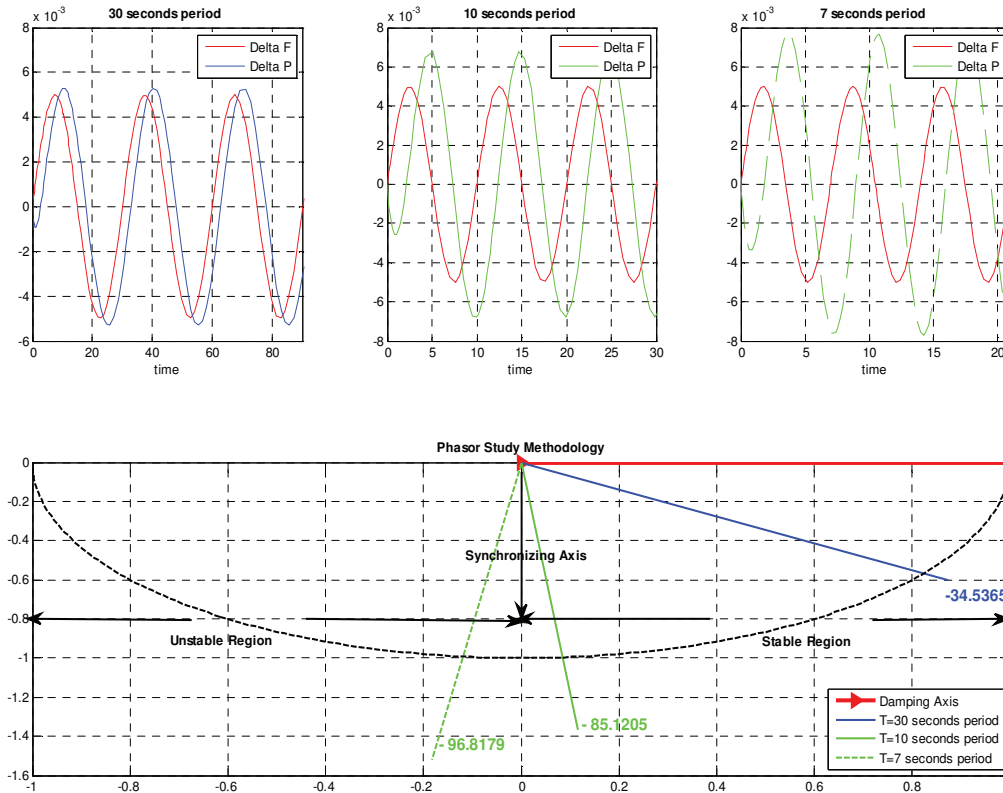


Fig. 5-9: Phasor study for linear model.

5.5.4. Closed Loop

A simplified block diagram representation of the speed control of a hydraulic generating unit feeding an isolated load is shown in figure 5-10. The Turbine is represented by classical model and the speed governor by pure gain $K_G = 1/R$. The generator is represented by its equation of motion with a mechanical starting time T_M of 10 seconds.

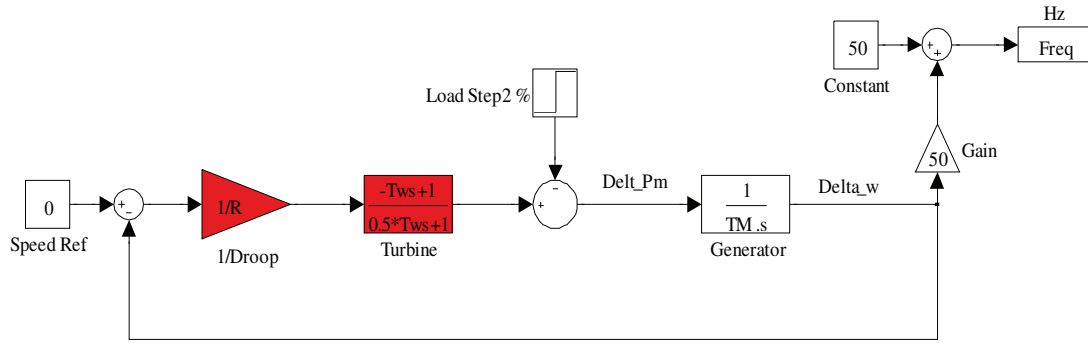


Fig. 5-10: Unit of simplified model.

Figure 5-11 shows the frequency behaviour of isolated load (closed loop) is stable for time period $T_x = 14$ seconds.

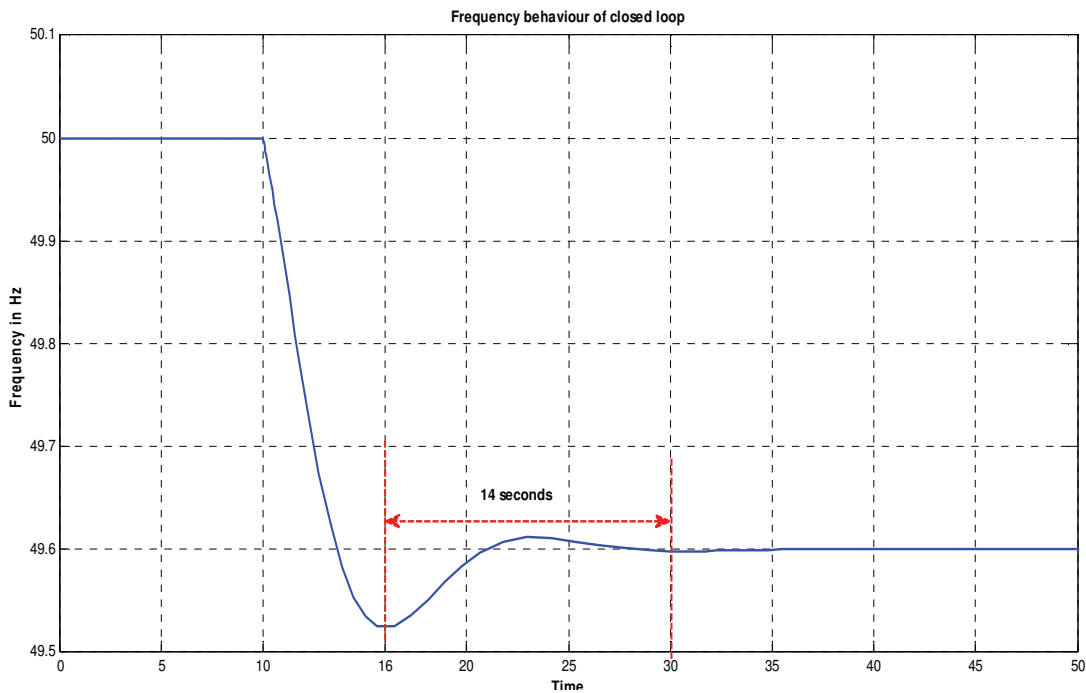


Fig. 5-11: The frequency behaviour of closed loop.

According to these results we can use this method to analyze the units individually to observe whether its governor has a positive effect (stable) or negative effect (unstable) on the stability of the power system frequency.

5.5.4.1. Model of the Turkish Power System

The overall model of the whole Turkish power system with the major power plants was made in SIMULINK / MATLAB software [59]. All power plants with their primary controllers and loads of Turkey are modelled completely in detail. Any model consists of separate models for power controller, governor and turbine regulator. The models made in the described manner were verified after connection of the sub models in one complete power plant model.

In order to investigate the contribution of the governors of the unit model of all power plants (GPPs, TPPs and HPPs) together to damping of oscillations with different periods. A sinusoidal frequency deviation is applied to the determined model and the mechanical output power (or mechanical torque) of the unit is observed as shown in figure 5-12.

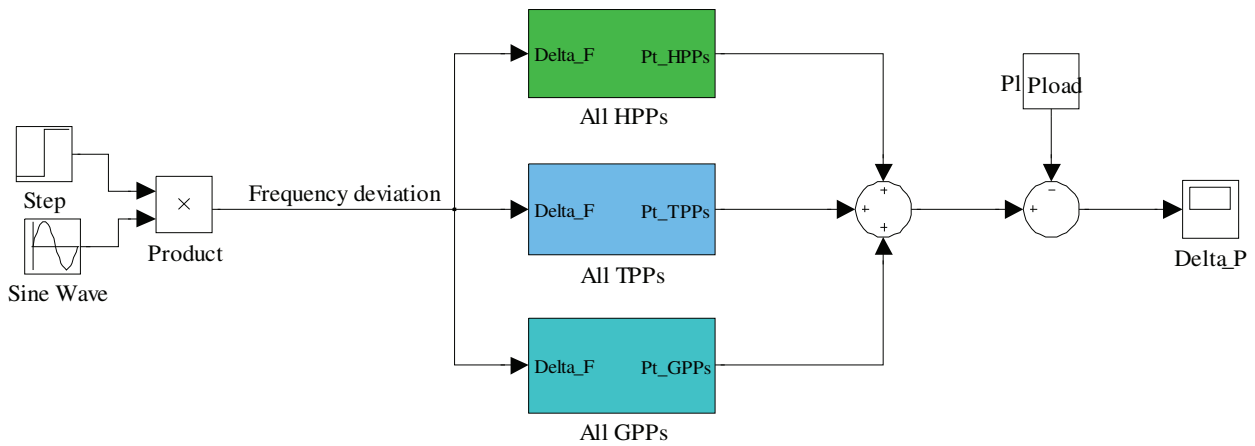


Fig. 5-12: Unit model of all power plants.

The resulting phasor is used to determine the damping and synchronizing components of the mechanical output power change which is the result of governor action. Note that the real phasor which is of interest is " $-\Delta P_m$ " due to the sign convention in the swing equation [57, 61 and 62];

$$\frac{2H}{\omega_n} \frac{d^2 \Delta \delta}{dt^2} + \Delta P_e - \Delta P_m = 0 \quad (5.3)$$

where;

P_m Mechanical power input, in pu

P_e Electrical power output, in pu

H Inertia constant, in MW.s/MVA

δ Rotor angle, in elec. rad

t Time, in second

ω_n Synchronous speed in electrical units

The analysis is performed for two frequencies, which are the frequency oscillations of Turkish system

with 30 seconds period and the 7 seconds inter area oscillations expected to be observed after interconnection with the ENTSO-E-CE.

For phasor study methodology I made a summary to see the difference directly between the cases as shown in figures 5-13 and 5-14.

- For all TPPs, GPPs, HPPs and all power plants together 4 cases are used as shown in Fig. 5-11
- For each power plant individually 2 cases are used as shown in Fig. 5-14
- For all cases the amplitude of the input signal and backlash of governor system values are 100 mHz and ± 50 mHz respectively. The dead band values are different between ± 20 mHz and ± 50 mHz

Where;

- Case 1 : The model without backlash (BL) and without dead band (DB)
- Case 2 : The model with backlash (BL) only
- Case 3 : The model with dead band (DB) only
- Case 4 : The model with backlash (BL) and dead band (DB)

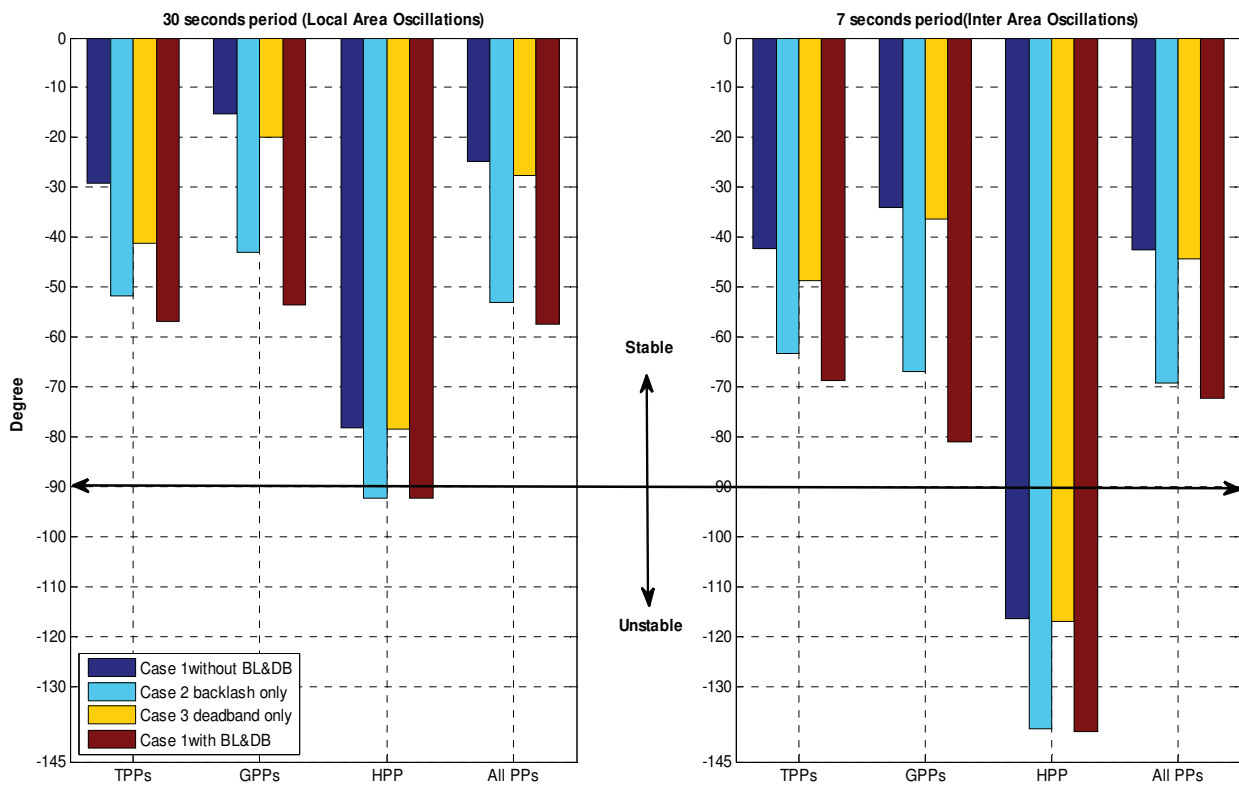


Fig. 5-13: Schematic diagram comparing all power plants.

Table 5-1: The angles summary for all cases

	30 second period					7 second period			
	TPPs	GPPs	HPPs	PPs		TPPs	GPPs	HPPs	PPs
Case1	-29.2	-15.23	-78.13	-24.65	Case1	-42.2	-34.13	-116.3	-42.44
Case2	-51.82	-42.93	-92.22	-53.1	Case2	-63.2	-66.85	-138.5	-69.2
Case3	-41.17	-19.77	-78.4	-27.68	Case3	-48.6	-36.26	-116.9	-44.25
Case4	-56.9	-53.51	-92.3	-57.4	Case4	-68.54	-80.91	-139	-72.2

As a result of Table 5-1;

- The output power phasor for all thermal power plants and all gas power plants for 30 and 7 seconds period have a positive damping component (less than 90 degrees).
- The output power phasor for all hydro power plants with backlash for 30 and 7 seconds period have a negative damping component (greater than 90 degrees).
- The output power phasor for all power plants together (TPPs, GPPs and HPPs) for 30 and 7 seconds period have a positive damping component.
- The all power plants together (TPPs, GPPs and HPPs) are stable (less than 90 degrees) for the frequency oscillations of Turkish system with 30 seconds period and the 7 seconds inter-area oscillations expected to be observed after interconnection with the ENTSO-E-CE. The Turkish system should be stable in island operation (chapter 5).

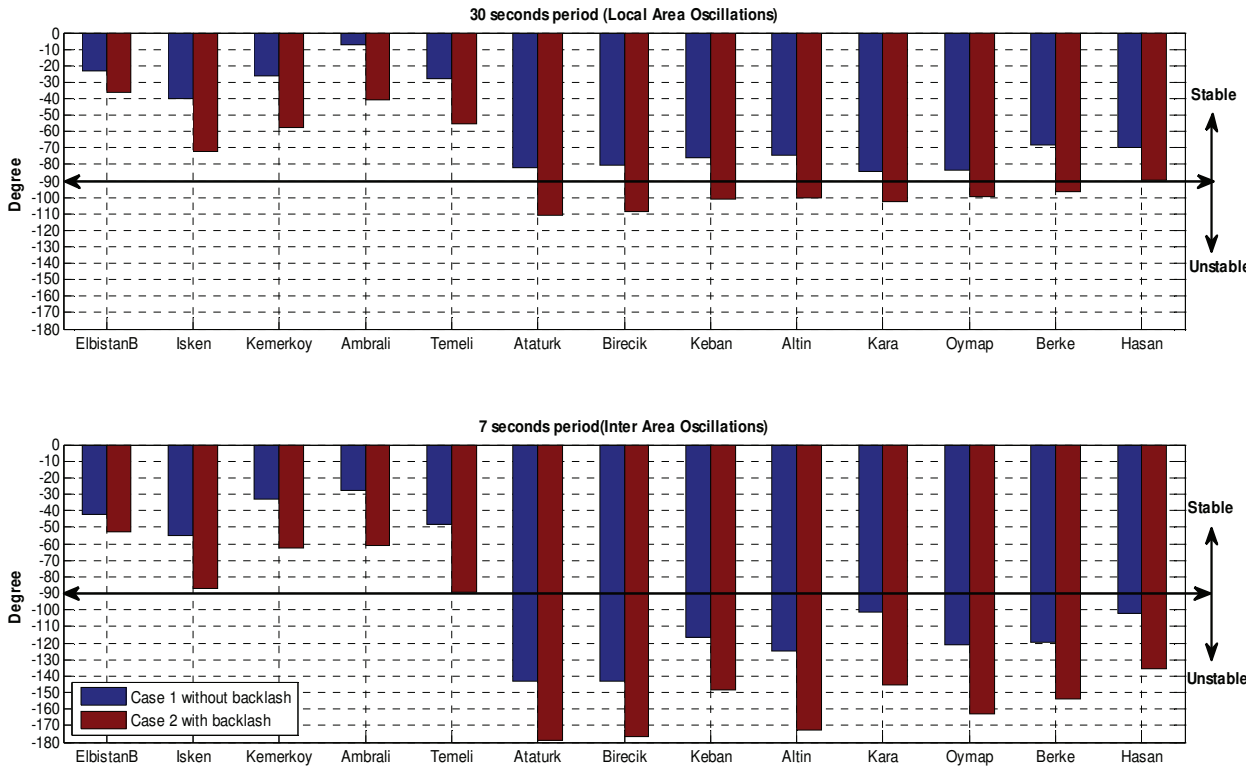


Fig. 5-14: Schematic diagram comparing all power plants individually.

Table 5-2: The angles summary for case1 and case 2

	Name of power plant	30 seconds period		7 seconds period	
		Case 1	Case2	Case 1	Case2
TPPs	Elbistan A, Elbistan B, Cayirhan and Kangal TPPs	-22. 91	-36. 41	-42.35	-52.48
	Iskenderun, Soma, Ambarlifo, Seyitomer and Can TPPs	-40. 34	-71. 96	-55.39	-87.21
	Kemer koy, Yatagan and Yenikoy TPPs	-26. 25	-57. 82	-32.97	-62.38
GPPs	Ambarli, Bursa, Hamitbat and Unimar GPPs	-7. 24	-40. 94	-27.88	-61.12
	Gebze, Adapazari, Aliaga and Temelli GPPs	-27. 59	-55. 3	-48.3	-89.23
HPPs	Ataturk HPP	-81. 8	-111.33	-143.22	-178.5
	Birecik HPP	-80. 73	-108.64	-143.12	-176.6
	Keban HPP	-75. 8	-101.19	-116.57	-148.7
	Altinkaya HPP	-74. 23	-100.41	-125.1	-173.1
	Karakaya HPP	-84. 37	-102.64	-101.65	-145.32
	Oymapinar HPP	-83. 37	-99.69	-120.8	-162.99
	Berke HPP	-68.48	-96.15	-119.9	-153.5
	Hasanugurlu HPP	-69.55	-89.37	-102.3	-135.3

As a result of Table 5-2;

- The output power phasor for each power plant individually for thermal power plant and gas power plant for 30 and 7 seconds period have a positive damping component(less than 90 degrees).
- The output power phasor for each power plant individually for hydro power plants with backlash for 30 and 7 seconds period have a negative damping component.

5.5.4.2. Example: The Phasor Study Methodology for Case 4

The phasor study methodology for case 4, 100 mHz frequency amplitude is shown in detail as following figures:

Figure 5-15 shows the output power phasor for both local area oscillations (30 seconds period) and inter-area oscillations (7 seconds period) have a positive damping component -24.6 and -44.44 degree respectively which indicates positive contribution governor of all power plants to the damping of both oscillations.

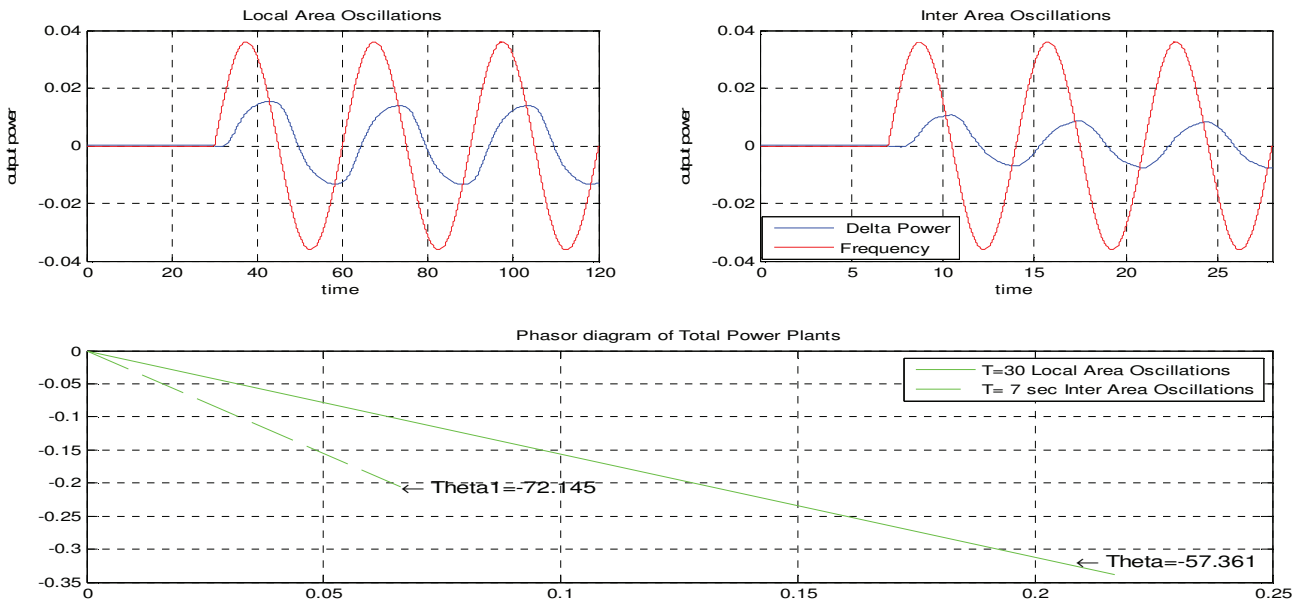


Fig. 5-15: Phasor study for all power plants.

Figures 5-16 and 5-17 show the phasor study for both local area oscillations (30 seconds) and inter area oscillations (7 seconds period) for each power plant individually.

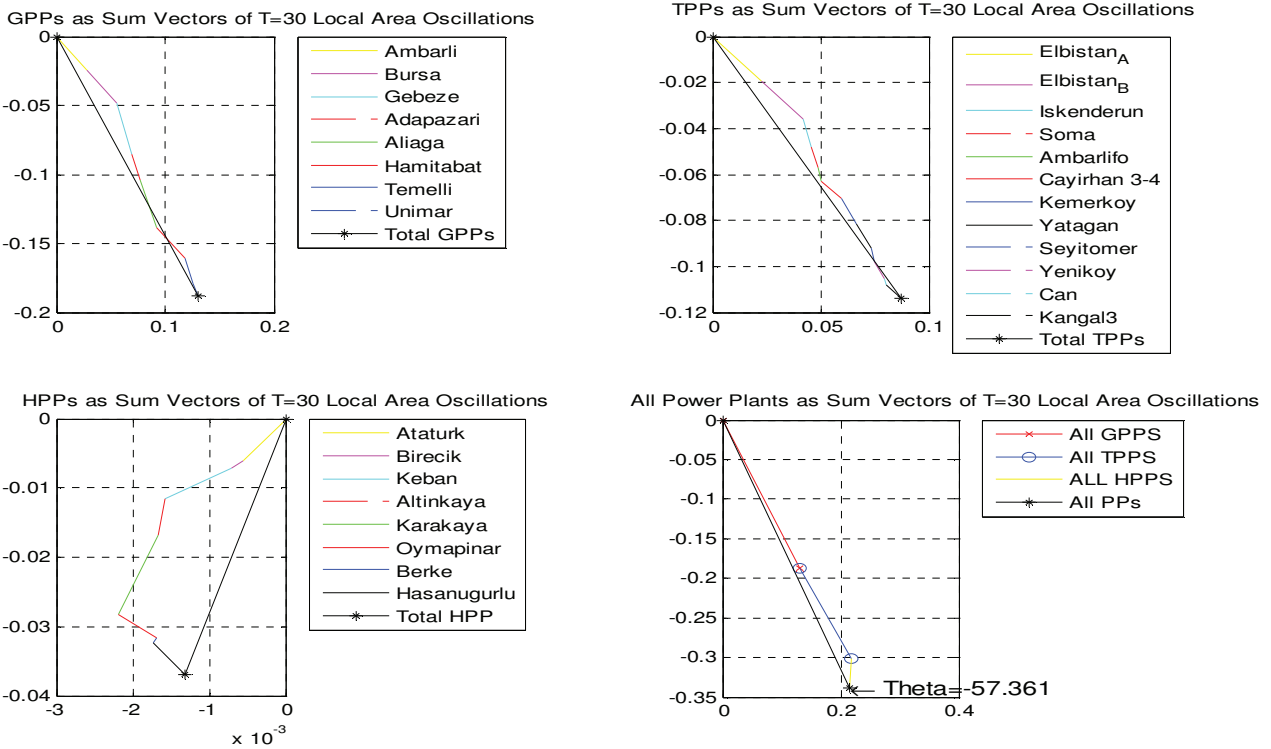


Fig. 5-16: Responses of individual all power plants as sum of vectors.

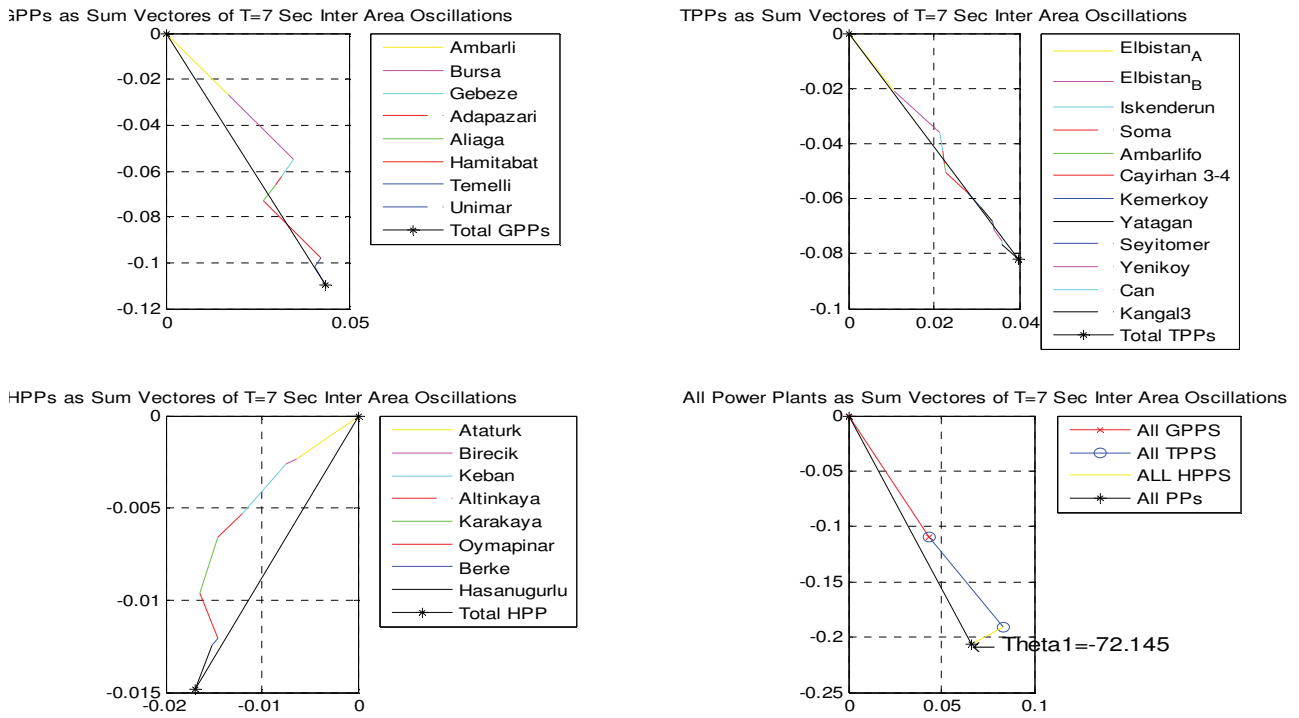


Fig. 5-17: Responses of individual all power plants as sum of vectors.

5.5.4.3. The Phasor Study Methodology with Different Amplitudes

The phasor study methodology for the Turkish power system with all power plants together with backlash value (± 50 mHz) and different amplitudes (see Fig. 5-18).

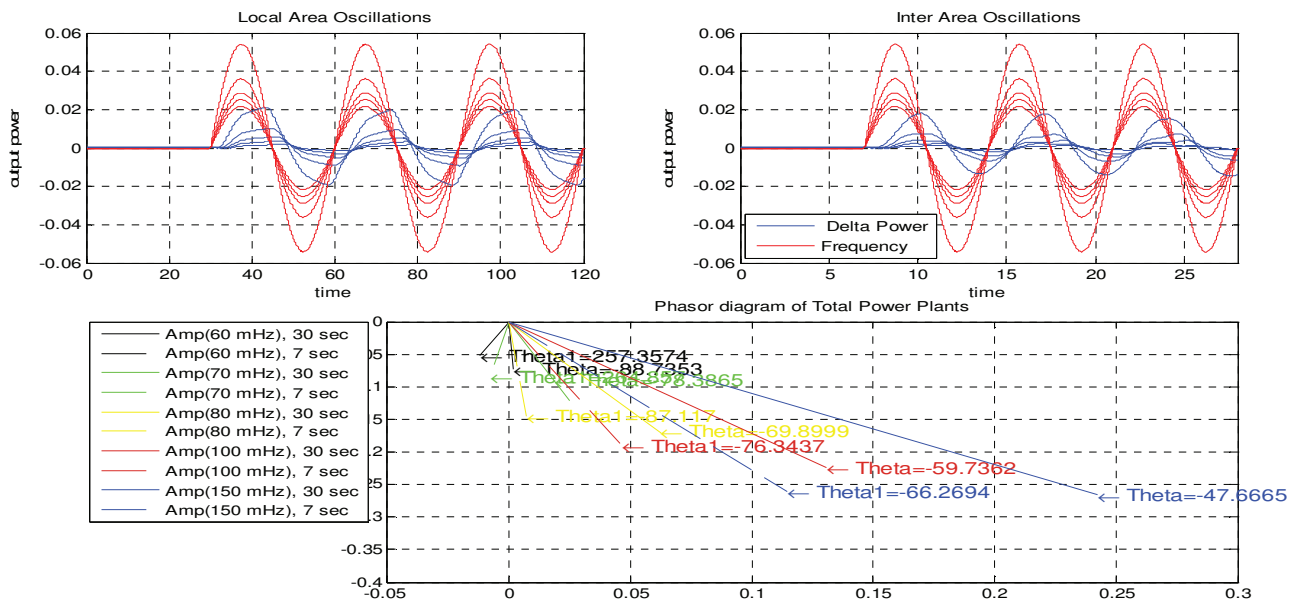


Fig. 5-18: Phasor study for all power plants with different amplitudes.

As seen in the above figure 5-18 the output power phasor for both local area oscillations (30 seconds) and inter-area oscillations (7 seconds period) have angles as shown in Table 3-3.

Table 5-3: The angles summary for all power plants with different amplitudes

Amplitude	Backlash	30 seconds period	7 seconds period
60 mHz	-/+ 50 mHz	-88.73	-102.6
70 mHz	-/+ 50 mHz	-78.38	-95.2
80 mHz	-/+ 50 mHz	-69.89	-87.12
100 mHz	-/+ 50 mHz	-59.73	-76.3
150 mHz	-/+ 50 mHz	-47.6	-66.26

As a result for different amplitudes:

- If the oscillation amplitude is within backlash (≤ 50 mHz) there is no positive but also no negative effect.
- If the oscillation amplitude is "around" backlash width (e.g. 60 mHz, 70 mHz and 100 mHz) there should be a significant phase shift.
- If the oscillation amplitude is much higher the backlash effects become more neglectable

CHAPTER 6

Isolated Turkish Power System

6.1. Frequency Control in Power Systems

The electric frequency f in the network (the system frequency) is the only parameter that is common for synchronously interconnected systems. It is a power quality parameter whose steady-state value is identical at every point of the interconnected power system [49].

The system frequency is determined by the rotational speed of synchronized generators. In the steady state all connected generators are synchronized, i.e. the rotors of all generators have the same rotational speed and rotate in the same direction. According to Newton's second law for rotational motion, the rotors' motion can be expressed by the following equations [55, 49]:

$$M \frac{d^2\delta}{dt^2} + D \frac{d\delta}{dt} = P_m - P_e \quad (6.1)$$

$$\Delta\omega = \frac{d\delta}{dt} \quad (6.2)$$

where;

M Inertia coefficient

D The damping factor

P_m Mechanical power delivered by the turbine

P_e The generator electric power

δ The rotor angle w.r.t. the synchronously rotating axis

$\Delta\omega = \omega - \omega_s$ The change in the rotor angular speed w.r.t. synchronous speed ω_s

If the power system is balanced (the frequency is constant), then $\Delta\omega = \omega - \omega_s = 0$, i.e. $P_m = P_e$. That means the generated power is balanced by the power of loads and active power losses in the network. Unbalance of power in the system results in an increase or decrease of the system frequency (the rotational speed of rotors). The rate of frequency changes depends on the power unbalance and the inertia of rotating masses of generators' rotors.

6.2. Composite Load

A large number of various loads are being connected to electric power systems. In terms of the power system analysis it is impracticable to follow the behaviour of each load. Therefore, for practical reasons, the notion of composite load has been introduced. It represents the resultant behaviour of a large group of diverse loads connected to a node of a high-voltage network. Variation of system parameters (including the frequency f) results in a change of the active power consumption of composite loads. The dependence of consumed active power P_L on the frequency f is expressed by the

static power–frequency characteristic for the consumed active power $P_L=P(f)$. The static characteristics are usually unitized with respect to the nominal frequency f_n , nominal power P_n [49].

In the neighborhood of the nominal frequency value the static power–frequency characteristic for consumed active power can be expressed by a linear relationship. This relationship is numerically expressed by the frequency susceptibility of a load K_{pf} defined as the quotient of the relative power deviation and the relative frequency deviation:

$$k_{pf} = \frac{\Delta P_{pu}}{\Delta f_{pu}} = \frac{P_{npu} - P_{pu}}{f_{npu} - f_{pu}} = \frac{(P_n - P)/P_n}{(f_n - f)/f_n} \quad (6.3)$$

Figure 6-1 shows power–frequency static characteristics for active power consumption of various types of loads.

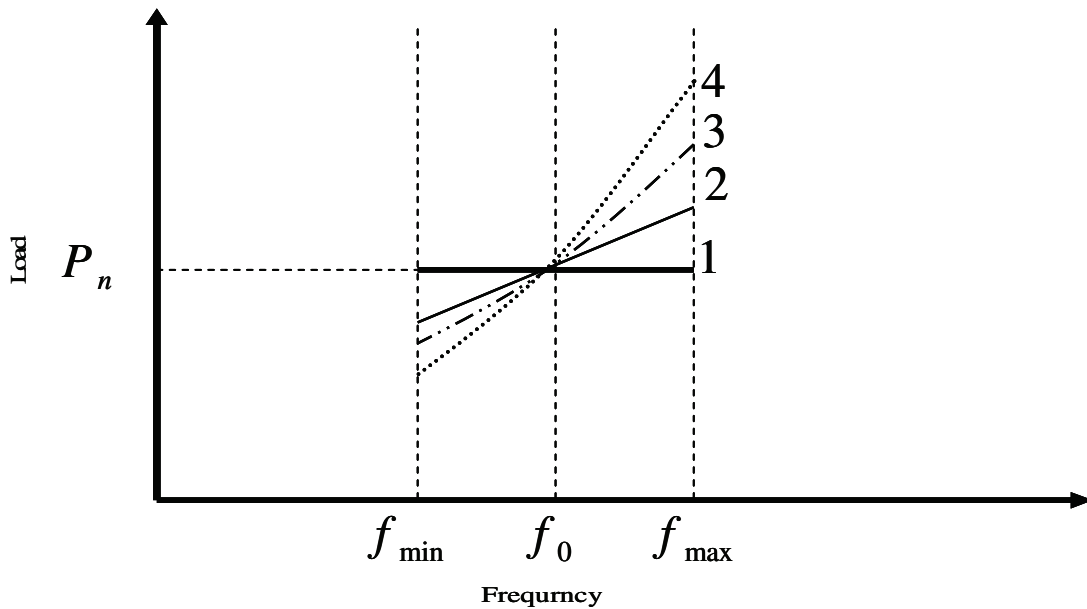


Fig. 6-1: Power consumption of various types of receivers versus frequency variation.

The value of susceptibility factor K_{pf} depends on the structure of a composite load, i.e. on the contribution of a given load group. In theory (assuming all loads are connected in parallel at a common node) the resultant frequency susceptibility factor K_{pf} can be determined from the formula

$$k_{pf} = \frac{\sum_i^n k_{pf} * P_{Li}}{P_L} \quad (6.4)$$

where;

k_{pf} The frequency susceptibility factor for the i^{th} group of loads;

P_{Li} The power of the i^{th} group of loads;

P_L The total power of loads.

Analytical calculations are difficult because the contribution P_{Li}/P_L of a given load group to the composite load cannot be determined. The values of K_{pf} are usually obtained by measuring $P_L=P(f)$ characteristics for typical groups of loads.

For the convenience of practical calculations the frequency susceptibility factor c_f expressed as a percent of power deviation per 1 Hz is used. Converting the relationship (6.3), it is possible to obtain

$$k_{pf} = \frac{\Delta P_{pu}}{\Delta f_{pu}} = \frac{\Delta P / P_n}{\Delta f / f_n} \rightarrow \frac{\Delta P}{P_n} = k_{pf} * \frac{\Delta f}{f_n} \quad (6.5)$$

That is,

$$\Delta P\% = \frac{\Delta P}{P_n} * 100 = k_{pf} * 100 * \frac{\Delta f}{f_n} = c_f * \Delta f \quad (6.6)$$

For a typical composite load, comprising industrial, commercial and residential loads, the c_f factor values are of the order of 1–6% per 1 Hz.

6.3. The Generation Characteristic

The rotational speed of generators in the power system is proportionally related to the system frequency:

$$\frac{\Delta f}{f_n} = \frac{\Delta \omega}{\omega_n} \quad (6.7)$$

from relationship (6.7) it is possible to formulate an equation for a single generating unit:

$$\frac{\Delta f}{f_n} = -R_i * \frac{\Delta P_{mi}}{P_{ni}} \rightarrow \frac{\Delta P_{mi}}{P_{ni}} = -K_i * \frac{\Delta f}{f_n} \rightarrow \Delta P_{mi} = -K_i * P_{ni} * \frac{\Delta f}{f_n} \quad (6.8)$$

and

$$R = \frac{\Delta f^*}{\Delta P^*} = \frac{(f_{smin} - f_{smax})/f_0}{(P_{max} - P_{min})/P_0} \quad (6.9)$$

where;

- ΔP_m the change in mechanical power of the i^{th} generating unit;
- P_{ni} the nominal power of the i th generating unit;
- R_i the droop of the i th generating unit;
- Δf^* the relative frequency variation;
- f_{smin}, f_{smax} the frequencies corresponding to minimum unit and maximum load;
- P_{max}, P_{min} the powers under unit maximum and minimum load condition;
- P_0 unit reference power (currently rated power).

The overall power change ΔP_G for N generators in service will be:

$$\Delta P_G = \sum_{i=1}^N \Delta P_{mi} = -\frac{\Delta f}{f_n} \sum_{i=1}^N K_i P_i \quad (6.10)$$

At steady state the equilibrium between the power generation P_G and the system load P_L (i.e. total power consumed, including the system losses) occurs:

$$P_G = \sum_{i=1}^N P_{mi} = P_L \quad (6.11)$$

Dividing Equation (6.10) by P_L , the system static characteristics are obtained which express the dependence of the change of generated power and frequency variation for N operating generators:

$$\frac{\Delta P_G}{P_L} = -\frac{\Delta f}{f_n} \frac{\sum_{i=1}^N K_i P_i}{P_L} = -\frac{\Delta f}{f_n} * K_G \rightarrow \frac{\Delta f}{f_n} = -R_G * \frac{\Delta P_G}{P_L} \quad (6.12)$$

where $R_G = 1/K_G$ is referred to as the system droop.

Figure 6-2 shows a summation of characteristics of generating units which yields a resultant generation characteristic of the system.

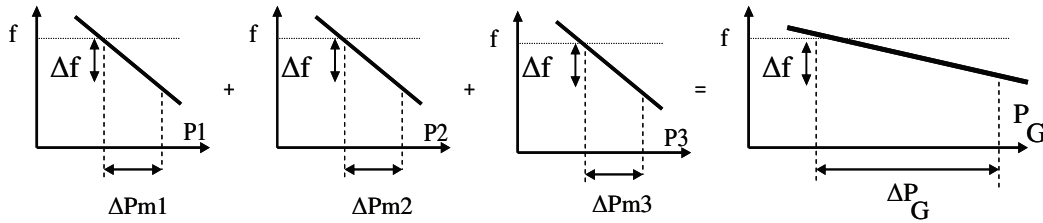


Fig. 6-2: Summation of characteristics of generating units.

6.4. Frequency Control in an Islanding System

A power system can be referred to as an islanding system when it is disconnected from other systems and does not exchange power through tie-lines. Due to the fact that frequency is the same within the entire system, frequency control in an islanding system can be achieved in a relatively simple way.

After a load change, the frequency reaches a new steady-state level, different from the initial value. The frequency (or rotational speed) error causes an additional integral term to generate a signal which modifies the value of the power setting of a generating unit. With a sufficiently large number of generating units supplied with control systems of this type, the power system yields such a change in the generated power that frequency returns to its initial value. This concept of frequency control can be referred to as decentralized since it is performed by regulators in power stations situated at various locations within the system [49].

6.5. Primary Control

Primary control consists of changing a generating unit's power versus the frequency, according to its static generation characteristic as determined by the speed governor settings. The objective of primary control is to re-establish a balance between generation and demand within the synchronous area at a frequency different from the nominal value.

The primary control action time is 0 to 30 s after disturbance of the balance between generation and demand. Under normal conditions the system operates at nominal frequency, maintaining the condition of equality of generated power and demand. Each disturbance of this balance, due to, for example, disconnection of a large generating unit or connection of a large load, causes a change in frequency. At first, the frequency varies rapidly, practically linearly, and attains the maximum deviation from the nominal value, referred to as the dynamic frequency deviation (see Fig. 6-3).

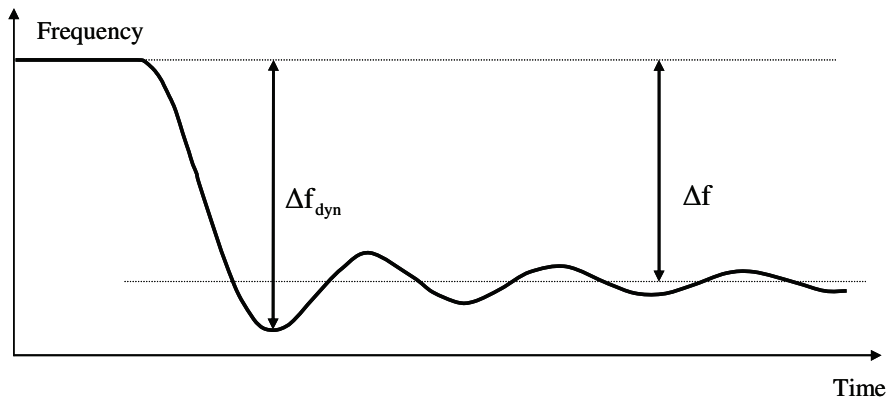


Fig. 6-3: Definition of the dynamic (Δf_{dyn}) and quasi-steady-state frequency (Δf) deviation.

This deviation in the system frequency will cause the primary controllers of all generators subject to primary control to respond within a few seconds. The controllers alter the power delivered by the generators until a balance between the power output and consumption is re-established. At the moment when the balance is re-established, the system frequency stabilizes and remains at a quasi-steady-state value, but differs from the frequency set point because of the generators droop.

The magnitude of the dynamic frequency deviation depends on: the amplitude and development over time of the disturbance affecting the balance between power output and consumption, the kinetic energy of rotating machines in the system, the number of generators subject to primary control, the dynamic characteristics of the machines (including controllers) and the dynamic characteristics of loads. The quasi-steady-state frequency deviation is governed by the amplitude of the disturbance and the system stiffness.

The contribution of a generator to primary control depends upon the droop of the generator and the primary control reserve of the generator concerned. Figure 6-4 shows the characteristics of two generators a and b and of different droops under equilibrium conditions, but with identical primary

control reserves. In the case of a minor disturbance, for which the frequency offset is smaller than Δf_a , the contribution of generator a (with the smaller droop) will be greater than that of generator b (the one with the greater droop).

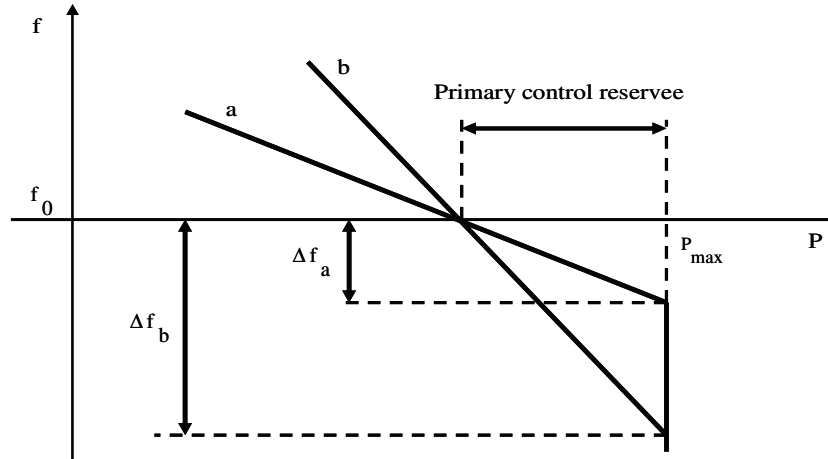


Fig. 6-4: The contribution of two generators, with different droops, to primary control

The primary control reserve of generator a is exhausted (i.e. where the power generating output reaches its maximum value) earlier (at the frequency offset Δf_a) than that of generator b (which will be exhausted at the frequency offset Δf_b), even when both generators have identical primary control reserves. For an adequate operation of frequency control it is crucial that the system has a proper level of primary control reserve at any instant of time allocated in a possibly large number of generating units and activated within a few seconds of detecting the frequency deviating from its nominal value.

6.6. Secondary Control

Secondary control makes use of a central regulator, modifying the active power set points of generating sets subject to secondary control, in order to restore power interchanges with adjacent control areas to their programmed values and to restore the system frequency to its set-point value at the same time. By altering the operating points of individual generating units, secondary control ensures that the full reserve of primary control power activated will be made available again[49].

Secondary control operates slower than primary control, in a timeframe of minutes. Its action becomes evident about 30s after a disturbance/event, and ends within 15 min. Since under normal operating conditions of a power system the power demand varies continuously, secondary control takes place continually in such way as not to impair the action of primary control.

Secondary control is based on secondary control reserves that are under automatic control. The secondary control model consists of the real controller as in operation in Ankara and also the individual controllers in the involved power plants [12].

The secondary control is a part of the Project Group "Rehabilitation of the frequency control

Performance of the Turkish Power System for synchronous Operation with ENTSO-E-CE-CE" and to provide advice to TEIAS for the tuning of AGC system parameters in order to perform according to the ENTSO-E-CE requirements.

6.6.1. Strategy - Working Plan

The scope of the work has been planned to be executed with the implementation of the following:

- Evaluation of the performance of the existing secondary control ;
- Analysis of findings, identification of problems, proposal of corrective measures and testing of the performance;
- Projection of performance in parallel mode.

6.6.2. Characteristics of the Secondary Control in the Turkish Power System

6.6.2.1. Presentation of Power Plant Parameters for Secondary Frequency Control

As a first step, data collection about the AGC main operational principles and the characteristics of the units under secondary control (dead bands, secondary control range, ramp up and ramp down rates, restricted zones, unit droop, unit control error, time delay, joint controller function) has been accomplished via Turkish Electricity Transmission Company (TEIAS). The initially collected data for the unit's characteristics have been updated in order to reflect the improvements that have been implemented in the plants equipment during the work duration and their current values are presented in the following Table 6-1.

Table 6-1: The power plant parameters for secondary frequency control

Power Plant	Type	Class	Regulating Range	Type of AGC Interface at Power Plant	Number of Units and Unit Capacity (MW)	Unit AGC Ranges (MW)	Total Capacity (MW)	Min. AGC Cap. (MW)	Max. AGC Cap. (MW)	Secondary Reserve (MW)	Integration Time (sec.)	Delay (sec)	Ramp Down Rate per Unit (MW/min)	Ramp Up Rate per Unit. (MW/min)	Average Turbine Time Constant
Ataturk	Hydro	1	±25	Plant	8x300	220-280	2400	1760	2240	±240	20	20	60	60	10
Karakaya	Hydro	1	±30	Plant	6x300	210-280	1800	1260	1680	±210	25	15	60	60	10
Altinkaya	Hydro	1	±30	Plant	4x175	90-170	700	340	660	±160	25	25	30	30	10
H. Ugurlu	Hydro	1	±10	Plant	4x125	90-120	500	340	460	±60	10	25	20	20	10
Adapazari	CCGT	2	0	Block	(2GT+1ST)		798	685	745	±30	40	35	15	15	40
Gebze Block-A	CCGT	2	0	Block	(2GT+1ST)		797	690	750	±30	40	45	15	15	40
Gebze Block-B	CCGT	2	0	Block	(2GT+1ST)		797	690	750	±30	40	45	15	15	40
Ankara	CCGT	2	0	Block	(2GT+1ST)		797	710	780	±35	40	30	15	15	40
Izmir Block-A	CCGT	2	0	Block	(2GT+1ST)		795	700	770	±35	40	45	15	15	40
Izmir Block-B	CCGT	2	0	Block	(2GT+1ST)		795	700	770	±35	40	45	15	15	40
Bursa Block-A	CCGT	2	0	Block	(2GT+1ST)		716	605	620	±7,5	60	20	12	12	60
Bursa Block-B	CCGT	2	0	Block	(2GT+1ST)		716	605	620	±7,5	60	20	12	12	60
Keban	Hydro	2	0	Plant	8x165	150-160	1320	1200	1280	±40	40	20	30	30	40
Sugozu Unit-1	Thermal	3	0	Unit	1x660	600-660	660	600	660	±30	40	120	20	20	40
Sugozu Unit-2	Thermal	3	0	Unit	1x660	600-660	660	600	660	±30	40	120	20	20	40
Cayirhan Unit-3	Thermal	4	0	Unit	1x160	145-160	160	145	155	±5	60	210	5	8	60
Cayirhan Unit-4	Thermal	4	0	Unit	1x160	145-160	160	145	155	±5	60	170	5	8	60
Birecik	Hydro	4	0	Plant	6x112	100-112	672	600	660	±30	35	60	10	10	35

6.6.2.2. Presentation of AGC Main Characteristics

TEIAS has since 2004 put in operation a modern National Control Center (NCC) in Ankara made by Siemens. The version of the Automatic Generation Control (AGC) used is SINAUT SPECTRUM release 4.3. The control cycle of the AGC is 4 seconds control and takes frequency measurements every 1 second and MW measurements every 2 seconds. TEIAS has Load Frequency Control/Automatic Generation Control (LFC/AGC) program at National Control Center and necessary systems at most of the major power plants for participation to secondary frequency control. Automatic Generation Control program is used in the Turkish Electricity Network since about 20 years [7].

The overall goal of the Load Frequency Control (LFC) is to:

- Keep the frequency in the interconnected power system close to the nominal value.
- Restore the scheduled interchanges between different areas, e.g. countries, in an interconnected system.

Another purpose of the secondary control done by means of set-point values from National Control Center is to release the used primary reserves and make them ready for use during the next disturbances to be occurred in the system. Load Frequency Control (LFC) function calculates Area Control Error (ACE) periodically every 4 seconds. Accurate frequency measurement which is measured at NCC every second and the tie-line flow values telemetered every 2 seconds are used in this calculation.

$$ACE = \Delta P + K \times \Delta f \quad (6.13)$$

where;

- ΔP Deviation in tie-lines power flows;
- Δf Deviation in system frequency;
- K k-factor of the control area of Turkey (MW/Hz).

Controls are based on set-points. Each set point is the sum of a base-point and a regulation component. ACE is distributed to the power plants under the control of AGC based on the capabilities as defined by the unit characteristics (i.e. unit limits, unit response rates, unit control modes and unit regulating ranges)

The Load Frequency Control (LFC) function of the AGC currently is concerned with regulating the active power output of the generating units and with maintaining the desired system frequency since the Turkish Transmission System is not interconnected with other systems (the Constant Frequency mode is selected, i.e. $ACE = K_r \times \Delta f$). The economic dispatch function is not used at the Turkish AGC system.

The Area Control Signal is processed by a PI controller (see Fig. 6-5), where the correcting total desired generation (P_{sec}), in most of the cases, is calculated as:

$$P_{\text{sec}} = -(G_A \times \text{ACE} + \frac{G_A}{T_{\text{CR}}} \int \text{ACE} \times dt) \quad (6.14)$$

while when the ACE is within a defined deadband then P_{sec} is calculated as:

$$P_{\text{sec}} = -(G_S \times \frac{G_A}{T_{\text{CR}}} \int \text{ACE} \times dt) \quad (6.15)$$

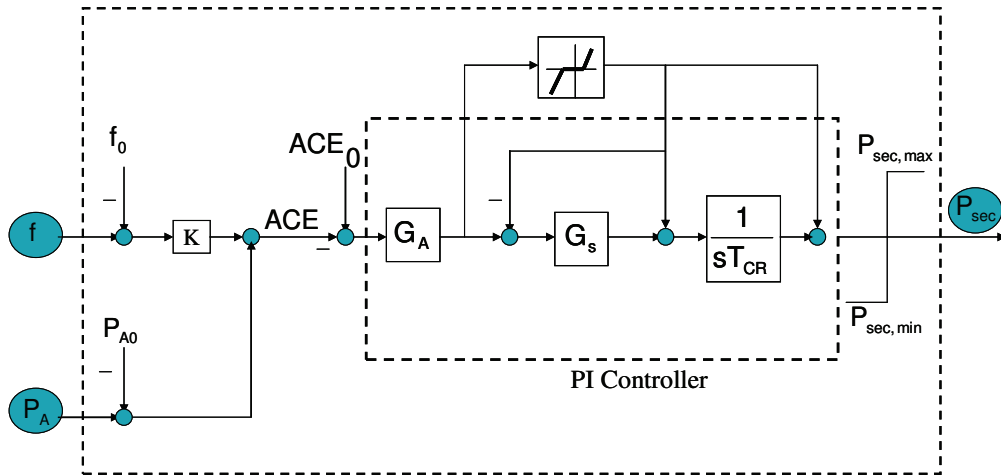


Fig. 6-5: The structure of secondary controller of Turkish power system.

where;

- f Actual system frequency
- f_0 Set-point frequency
- K k-factor of the control area of Turkey
- G_A Normal gain
- G_S Small gain
- T_{CR} Time constant of the secondary controller
- ACE The area control error (ACE)

According to SIEMENS the LFC function uses three classes of generating units when calling up secondary reserves as shown in figure 6-6;

- The first class is called *flexible units with regulating range*. In this class there should be fast units that are able to give a part of their operating range for secondary reserve. Following a change of the Area Control Error (ACE) these units are the first to respond.

If their regulating range is exhausted then the units at the second class;

- Second class is called *flexible without regulating range*, are used to reduce the ACE to zero along with all the secondary range of the first class units.
- Finally when the regulating capacity of all Flexible units is inadequate then regulation is assigned to *Supportive units*.

- There is also another class of units called Inflexible. Regulation is never assigned to the units in this class and they do not contribute to the secondary reserve capacity.

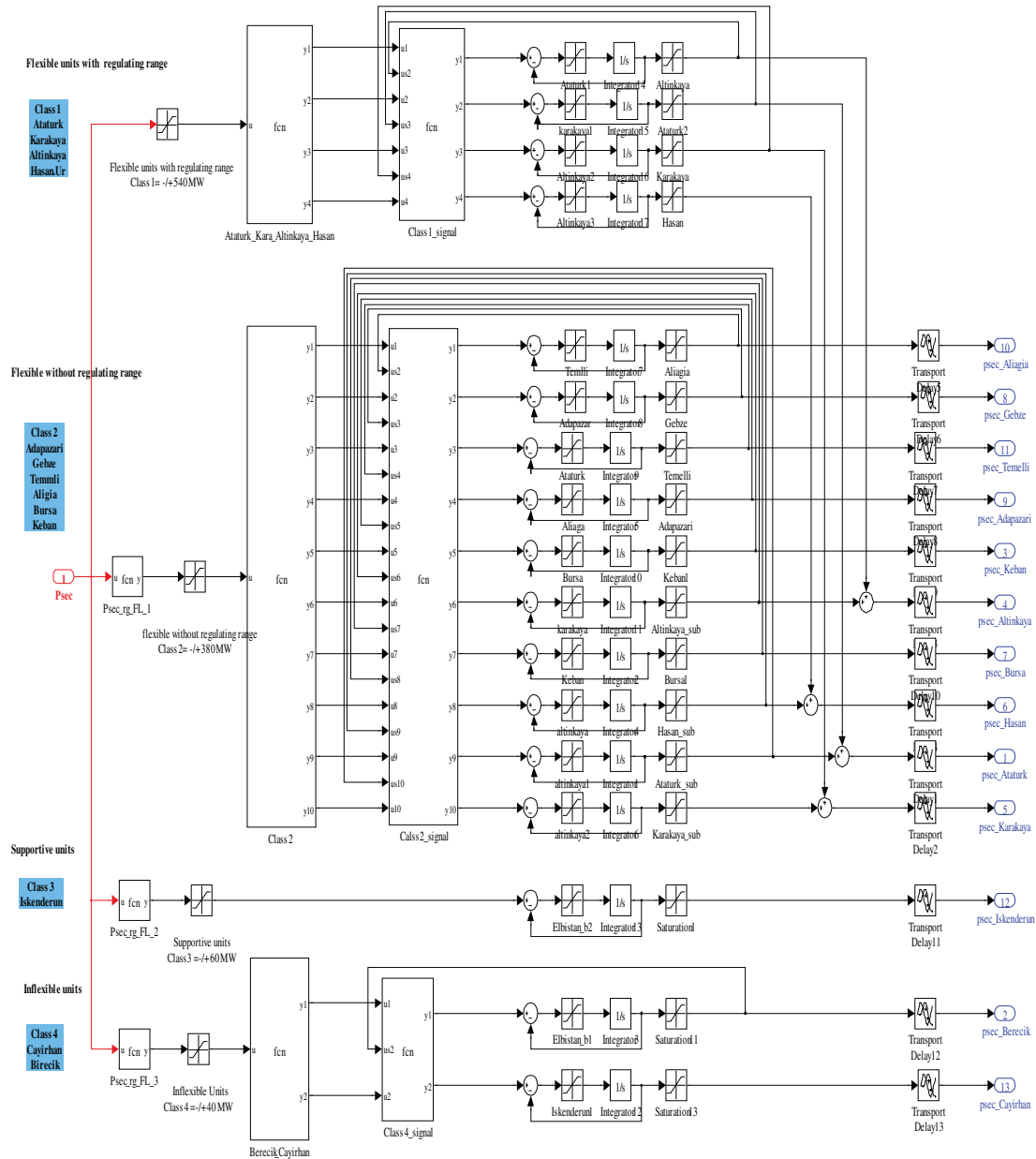


Fig. 6-6: The structure of distribution unit.

It became clear that it is very important to assign units with similar response rate in each class because otherwise the overall response will be dictated by the slower units. Also it is important to have the correct ramp rates of the plants in the controller and also within the plants of each class. Especially for the units within the first class the regulating range of the units should be proportional to the ramp rate. This means faster units should have bigger regulating range so that the full ramp rate of the unit is used and all units of the same class must reach the limits of their regulating ranges at the same time (see Fig. 6-7).

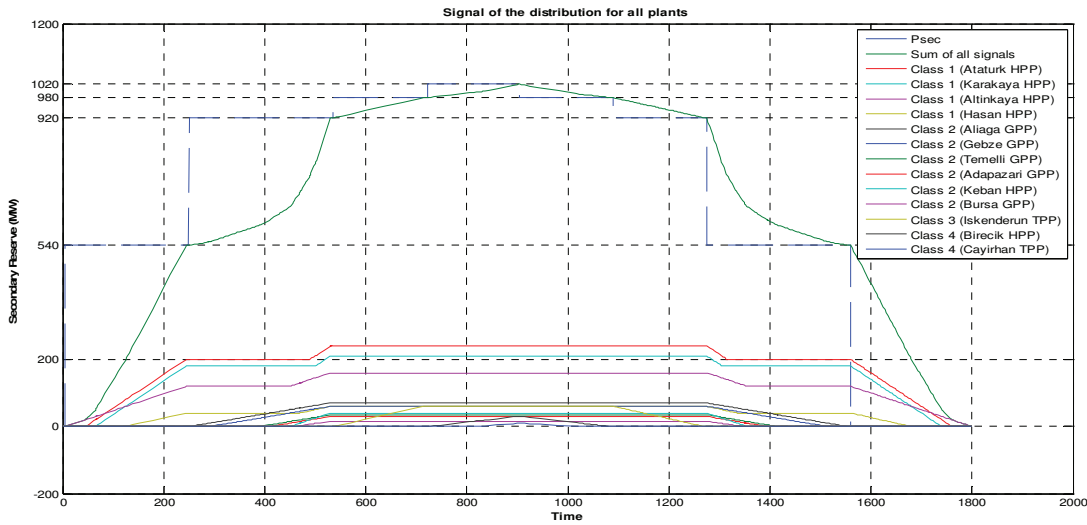


Fig. 6-7: Signal of the distribution unit.

Figure 6-7 shows the signal of the distribution unit for all classes as following;

- If the signal from National Control Center (NCC) in Ankara increase till ± 540 MW that means that class 1 only work for secondary control;
- If the signal from NCC increase than ± 540 MW till ± 920 MW that means the class 1 and class 2 are working for secondary control;
- If the signal from NCC increase than ± 920 MW till ± 1020 MW that means the class 1, class 2, class3 and class 4 are working for secondary control.

6.6.2.3. AGC Tuning of Power Plants

As it was mentioned above it is very important to assign units with similar response rate in each class and it is also important to have the correct ramp rates of the plants in the controller and also within the plants of each class. It was agreed to use fast hydro units in the first class and a combination of other units in the other classes. In order to do that, tests were carried out to a selection of units to check the actual response of the units to a step change, to define accordingly the tuning parameters in the controller and place them in the appropriate class. It is noticed that the definition of tuning parameters is facilitated in the AGC software by a simulation modelling tool.

The tests were carried out by EMS, HTSO, ESO, Rostock University, and SIEMENS between dates 6-9 of May 2008 at TEIAS National Control Center (Ankara) to various generating units in order to check their performance under secondary control.

According to the tests carried out with the plants for each class was prepared is given below.

Class 1 (flexible units with regulating range)

- Altinkaya HPP (max 4 units) each unit with ± 20 MW regulating range
- Ataturk HPP (max 8 units) each unit with ± 25 MW regulating range

- Karakaya HPP (max 6 units) each unit with ± 30 MW regulating range

Class 2 (flexible units without regulating range)

- Adapazari CCGT
- Ankara CCGT
- Bursa CCGT Block-A and Block-B
- Gebze CCGT Block-A and Block-B
- Izmir CCGT Block-A and Block-B
- Keban HPP (max 8 units)
- Ozluce HPP (max 2 units)

Class 3 (supportive)

- Elbistan – B TPP (4 units)
- Iskenderun TPP unit-1 and unit-2

Class 4 (inflexible)

- Cayirhan TPP unit-3 and unit-4
- H. Ugurlu HPP (max 4 units)
- Birecik HPP (max 6 units)

6.6.2.4. Tuning of AGC Controller

Several parameters of the main AGC controller were checked in order to identify areas for improvement. According to the ENTSO-E-CE formula (see Chapter 3, Section 3.5.2.1) the controller integration time T_i should be between 50 and 200 seconds and the normal gain should be between 0.1 and 0.5. Also there is no reference to a small signal gain to be used.

According to these requirements the normal signal gain in the Turkish AGC was set to 0.5 from the previous value of 0.75. It was also noted that there is a difference between the SIEMENS formula (equation 6.13) and the ENTSO-E-CE formula regarding the definition of the integral term: the integration time T_i of the ENTSO-E-CE formula corresponds to T_{CR} / Gain of the SIEMENS formula where Gain the normal gain and T_{CR} the desired common unit response time according to SIEMENS terminology. The value of T_{CR} was set to 50 seconds from the previous value of 40 seconds which corresponds to $T_i = 50/0.5 = 100$ seconds according to the ENTSO-E-CE formula (while with the previous parameter values of Gain and T_{CR} the equivalent T_i was $40/0.75 = 53$ seconds).

The small signal gain was active at the Turkish AGC controller with a small signal gain of 0.5 and a dead band of 5 MW. The dead band value was changed to zero (0) MW in order to deactivate the effect of small signal gain.

The frequency bias at the AGC controller was 1100 MW/Hz. It has been suggested that a better value would be 1480 MW/Hz according to calculations that have been presented and approved in a previous

Meeting of ENTSO-E-CE Project Group "Connection of Turkey". This value replaced the old one to the AGC main controller.

6.6.2.5. Analysis of Findings, Identification of Problems and Proposal of Corrective Measures

Several tests were carried out and various parameters were checked and subsequently changed. Several of the main controller's parameters were changed to correspond to the ENTSO-E-CE requirements.

In order to enhance the performance of AGC by exploiting as much as possible the contribution of the fast units in the secondary control, the response of "indicative" units was tested. According to the results, classes for the secondary control were defined in order to categorise the plants according to their rate of reaction and appropriate regulating ranges have been selected.

Initially big ramp rates were defined for the hydro plants of 80 MW/min but from the tests it was clear that the response of said units was not that fast. These rates have an effect on the way that the participation factors of the AGC controller are calculated and therefore more realistic values ranging from 30 MW/min to 40 MW/min were selected. It is recommended that if the response of the hydro units is improved these ramp rates shall be increased and in general if any changes are taking place in the power plants, that can affect their performance in secondary control, the respective modelling parameters in AGC shall be updated accordingly.

The unusual time delays, for hydro plants, for starting to respond in secondary control commands in Ataturk and Karakaya power plants should be reduced (these delays probably caused by problems in the operation of the existed LFC interface in the power plants or in the joint controllers of the plants). A "set point feedback" is recommended to be implemented in the SCADA function for all power plants, in order to help to trouble shooting and pin point communication problems. Moreover, the problems with the secondary control in the hydro plants Birecik and H. Ugurlu should be investigated and when solved then these units should be re-classified and upgraded from the inflexible class.

It is recommended that the performance of the system frequency should be monitored at least for a week before any changes to the controller parameters are made and the response be compared to the previous one and the best value that improves the system frequency is kept. The parameters to be checked initially by trial and error is the integration time of the controller (e.g. $T_{CR} = 60$ or 70 sec).

Finally, it has been noticed that the performance of the major hydro plants that are suitable for participating in secondary control (e.g. Ataturk and Karakaya) is influenced by their sensitive contribution in primary control.

In general it is recommended to be applied in the Turkish power system the practice in which the secondary control shall be provided mainly by the hydro units and the primary control shall be provided mainly by the thermal units. The combined cycle plants can contribute to both primary and secondary control with co-ordinated ranges.

6.6.3. Presentation of Measures that have been Implemented and their Results on the Performance of the Secondary Control of the System

6.6.3.1. Tuning of AGC Controller

According to the comments of the colleagues from TEIAS the tuning that has been done in the AGC software of NCC at Ankara, during the tests (6-9 May 2008), has been proved quite successful in practice after implementation and testing for a long period. In particular, the setting of the value 1480 MW/Hz as the frequency bias at the AGC controller has been proved to reflect better the actual network characteristic of the Turkish power system than the previous used value of 1100 MW/Hz. In order to comply with ENTSO-E-CE requirements the normal signal gain in the Turkish AGC was set to 0.5 from the previous value of 0.75 while the desired common unit response time was set to 50 seconds from the previous value of 40 seconds. The use of these parameters changed the central AGC controller to send slightly less aggressive regulation commands than before. On the other hand, in the new tuning it has been done an assignment of units with similar response rate in three classes of generating units when calling up secondary reserves. This should result in to that the overall response will not be dictated by the slower units while also the control commands to a lot of units will be minimized. It has been reported that the secondary control co-operates well with the improved primary control that is performed by the units of Turkish power system since the ancillary services contract with TEIAS came into force. Afterwards, when the control systems of Ataturk and Karakaya power stations have been renewed successfully the relevant parameters of AGC for the modelling of these two plants have been modified accordingly, in order to reflect their new improved operational behaviour.

The isolated tests in Turkish power system in maximum load conditions were carried out successfully by TEIAS on 11-24 of January 2010, with the above described AGC tuning. Similarly, the isolated tests in Turkish power system in minimum load conditions were carried out successfully by TEIAS on 22 of March - 04 April 2010, with the same values in the main AGC parameters except of a change in the value of desired common unit response time that was set to 60 seconds from the previous value of 50 seconds, as it has been suggested as a better value after monitoring of the overall performance of the secondary control system.

After the isolated tests were carried out successfully and in view of the trial parallel operation it was suggested to compute the K-factor of Turkish AGC according to the ENTSO-E-CE relevant procedures. In particular, the ENTSO-E-CE subgroup system Frequency (former TSO FORUM) has a method to determine the coefficients $C_i-P_{pi}-K_{ri}$ of each member country of ENTSO-E-CE, for every year by considering the net generations during the previous year.

According to the latest calculation of the coefficients $C_i-P_{pi}-K_{ri}$ for the year 2010 and using net generation in the ENTSO-E-CE system is 2688 TWh and net generation in the Turkey is 198.4 TWh the K for the Turkish AGC is calculated as:

$$K = (198.4/2886) \times 26530 = 1824 \text{ MW/Hz}$$

It is suggested that ENTSO-E-CE system frequency will calculate for the year 2011 the coefficients C_i - P_{pi} - K_{ri} for all member countries without taking into consideration the interconnection of Turkey for the parallel operation. The primary reserve of Turkey (P_p) will be assigned to 300 MW and the K will be assigned to 1824 MW/Hz from September 2010 to the end of 2011. Starting from 2012 Turkey will be integrated normally in the table of ENTSO-E-CE network.

In order to test the performance of secondary control system in the Turkish power system with values appropriate for the parallel operation (in line with the methodology of ENTSO-E-CE frequency) it has been decided to change, from 6th April 2010 the main parameters of AGC as follows: $K=1800$ MW/Hz and integration time constant $T_{CR}=70$ seconds and it has been proved that the AGC performance remains quite good during the island operation.

6.6.3.2. Allocation of Secondary Reserve to Units

The allocation of secondary reserve to the units should be done taking into account that the use of hydro units for secondary control and of thermal units for primary control has more effective results for ensuring sufficient quality of power balance in the Turkish power system. The combined cycle plants can contribute to both primary and secondary control with co-ordinated ranges. The power plants that were assessed as capable for secondary control during the isolated tests for maximum load and minimum load conditions are presented in the following Table 6-2.

Table 6-2: Units for secondary control

Name of Power Plant	Unit Number	Number of Units	Unit Rated Active Power [MW]	Secondary Control Range min per unit [MW]	Secondary Control Range max per unit [MW]	Secondary Control Range per power plant [MW]
Adapazari NGCC	Block (2G+1S)	1	798	685	765	80
Ankara NGCC	Block (2G+1S)	1	797	685	765	80
Gebze NGCC-A	Block-A (2G+1S)	1	797	685	765	80
Gebze NGCC-B	Block-B (2G+1S)	1	797	685	765	80
Izmir NGCC-A	Block-A (2G+1S)	1	795	690	765	75
Izmir NGCC-B	Block-B (2G+1S)	1	795	685	765	80
Bursa NGCC-A	Block-A (2G+1S)	1	716	656	716	60

Bursa NGCC-B	Block-B (2G+1S)	1	716	656	716	60
Isken TPP	1	1	660	600	660	60
Isken TPP	2	1	660	600	660	60
Elbistan-B TPP	1,2,3,4	4	360	280	350	280
Cayirhan TPP	3	1	160	145	160	15
Cayirhan TPP	4	1	160	145	160	15
Can TPP	1,2	2	160	140	150	20
Ataturk HPP	1,2,3,4,5,6,7,8	8	300	200	300	800
Karakaya HPP	1,2,3,4,5,6	6	300	200	300	600
Keban HPP	1,2,3,4,5,6,7,8	8	160	150	160	80
Birecik HPP	1,2,3,4,5,6	6	112	100	112	72
Altinkaya HPP	1,2,3,4	4	175	100	175	300
TOTAL	TOTAL		16,963	13,677	16,694	3,017

It can be seen from this table that the total nominal secondary control range of generating units in Turkish power system, is currently 3017 MW. The ENTSO-E-CE requirement for secondary control reserve under automatic control is calculated with the implementation of the "empiric" sizing approach i.e. the total secondary control reserve in operation should not be less than $R = \sqrt{10L_{\max} + 22500} - 150$ (see Chapter 3, Section 3.5.2.4), where L_{\max} being the maximum anticipated consumer load in MW for the control area over the period considered (e.g. the peak load according to the schedule in the day-ahead). Assuming the load ranging from 18 to 29 GW the formula results in a requirement the minimum secondary control reserve are 300 to 409 MW respectively i.e. the minimum required secondary control range is between 600 and 818 MW (range is calculated as twice the reserve for upwards and downwards regulation). This is in line with the requirements for primary control allocation. For the island mode of operation of Turkish power system it is required to have 700 MW of primary reserve and 300-400 MW secondary reserve under automatic control while during the parallel mode of operation it is required to have 300 MW of primary reserve, 300-400 MW secondary reserve under automatic control and about 400 MW of secondary reserve that can be activated manually within 15 minutes.

Therefore, about 1/4 of the current nominal secondary regulation capacity is needed to be actually on line and under automatic control. This target can be achieved with a proper unit commitment schedule that ensures the correct reserve allocation to the units. This allocation should be done on a daily basis taking into account the actual current capabilities of the units (e.g. current maximum production of the hydro units according to the water level of the reservoir) and that the ranges for primary and secondary control must be co-ordinated in units that are planned to be used for both controls (i.e. if a unit is planned to provide primary and secondary control then the planned primary reserve reduces accordingly the planned secondary reserve). Furthermore, it is recommended to consider in the planning of secondary reserve allocation that some hydro units should be available at any time on-line

and under automatic control in order to ensure that sufficient system ramp rate is available for secondary regulation in order to comply with "trumpet curve" requirements when large outages occur.

6.6.4. Model of Primary and Secondary control of the Turkish Power System

The model of the Turkish power system with all power plants was made in SIMULINK / MATLAB software. All power plants with their primary controllers and loads of Turkey are modelled completely in detail. Also the secondary control model consists of the real controller as in operation in Ankara and also the individual controllers in the involved power plants. Any model consists of separate models for power controller, governor and turbine regulator. The models made in the described manner were verified after connection of the sub models in one complete power plant model (see Fig. 6-8).

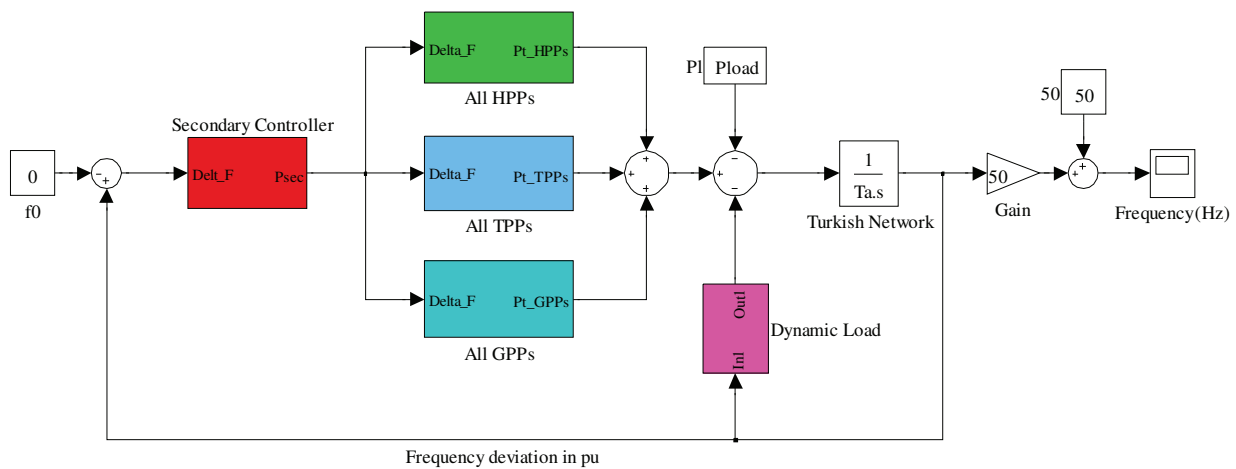


Fig. 6-8: The overall model of the whole Turkish system with primary and secondary control.

6.6.5. Simulation Study of Target Solution for Primary and Secondary Control Allocation

In order to manage an outage of the largest unit (approx. 700 MW) and to prepare the Turkish Power System to fulfil ENTSO-E-CE criteria (approx. 300 MW within 30s for Turkey as control area) primary control power shall be allocated as follows:

Taking into account a total amount of primary control power of approx. 700 MW

- 300 MW shall be allocated to thermal units (TPP and NGCCPP) in order to prepare the Turkish power system to fulfil ENTSO-E-CE requirements
- 400 MW shall be allocated to thermal units (TPP and NGCCPP) or to rehabilitated hydro units (see Table 6-3)

Remark: This concept of allocation is referred to as basis solution. In principle it is possible to provide a part of the 300 MW by rehabilitated hydro units provided that their water starting time constant is small ($T_w \leq 1 \text{ sec.}$) and that the impact on the frequency stability is acceptable.

The objective of the investigation is to show that with the proposed primary control concept the outage in Turkish power system (approx. 700 MW) in different system conditions can be managed without

violation of operational constraints. These constraints are

- $\Delta f_{\max} \leq 800\text{mHz}$ (in order to avoid load shedding);
- $\Delta f_{\text{stat}} \leq 200\text{mHz}$ Frequency performance (stable with sufficient damping)

The following parameter variations shall be considered and clarified:

- Regarding the 300 MW primary control power (PC) that has to be provided according to ENTSO-E-CE requirements it has to be determined to which extent rehabilitated hydro units with small water starting time constant ($T_w \leq 1\text{sec.}$) can contribute
- Regarding the 400 MW primary control power either thermal or rehabilitated hydro units can be utilized. This part of primary control power is not necessarily subject to ENTSO-E-CE requirements but necessary for the safety of the Turkish power system. From this follows that the participation of rehabilitated hydro units is not restricted to units with small T_w . However, rehabilitated hydro units with significant T_w have a more sluggish response and it has to be ensured that the operational constraints are not violated. A worst case scenario (400 MW allocated to 100% to rehabilitated hydro units (see Table 6-3)).

The total amount of secondary control reserve has to equal approximately 700 MW and must be activated within 15min. thereof

- 300-400 MW must operate under automatic control
- The remaining part can be activated manually within 15min

6.6.5.1. Calculation of primary control power for rehabilitated hydro units

Primary control of the power unit is described by the following equation:

$$\frac{\Delta P}{P_{\text{nom}}} = -\frac{100}{R} \frac{\Delta f}{f_{\text{nom}}} \quad (6.16)$$

in which Δf is the change in frequency in Hz, f_{nom} the nominal frequency (50 Hz), ΔP the change in power in MW and R the droop or statism in % [90]. Table 6-3 shows the calculated primary control power for the rehabilitated hydro power plants within the Turkish power system.

Table 6-3: Primary control power of the rehabilitated hydro power plants

Name of Power Plant	Rated Active Power	Contractual Reserve	Contractual Reserve	Physical Reserve	Droop	Working point	Real Primary Reserve
	[MW]	[% of rated power]	[MW]	[MW]	[%]		[MW]
Ataturk	2400	5	120	120	8	8x250	120
Karakaya	6x300	10	180	180	4	5x250	150
Birecik	6x112	5	34	34	5	4x100	22

Berke	3x170	5	26	51	4	2x150	34
Altinkaya	4x175	5	35	56	5	150	15
Hasan Ugurlu	500	5	25	50	4	220	25
Oymapinar	540	5	27	54	4	220	27
Total			447				393

6.6.5.2. Calculation of the T_w for Hydro power generation units

The water starting time T_w represents the acceleration time of water in the penstock between the turbine and the fore bay (or surge tank) and T_w is defined as follows [63-66]:

$$T_w = \frac{Q * L}{g * H * A} \quad (6.17)$$

where:

T_w : water starting time [s]

Q: water flow rate [m^3/s]

L: equivalent length of penstock [m]

g: gravitational acceleration [$9.81 m/s^2$]

H: hydraulic head at gate [m]

A: equivalent area of penstock [m^2]

Table 6-4 shows the calculated water starting time (T_w) for the most important hydraulic units within the Turkish power system.

Table 6-4: Calculation of water starting time constant

Power Plant	Q [m^3/s]	L [m]	H [m]	A [m^2]	T_w [s]
ATATURK	218	577	151	34.2	2.48
KARAKAYA	233	170	144	28.3	1.00
KEBAN	135	520	145	19.6	2.52
ALTINKAYA	170	246	116	38.48	0.96
BIRECIK	316.7	62	42	37.4	1.27
OYMAPINAR	106.2	220	143	21.24	0.79
BERKE	300	126	188	16.62	1.23
HASAN UGURLU	127	125	111	9.62	1.52

6.6.5.3. 700 MW Generation Loss

A generation loss of about 700 MW in the Turkish power system, secondary control reserve is 700 MW

operate under automatic control and the primary control allocations (700 MW) in the Turkish power system two cases were investigated:

- Case 1: PC = 700 MW [HPPs ($T_w \leq 1$ sec.) + (TPPs +GPPs)]
- Case 2: PC= 700 MW [HPPs ($T_w \leq 1$ sec. and $T_w \gg 1$ sec.) + (TPPs)]

6.6.5.4. Simulation Results

The simulation results for various study cases have been derived. The parameters of the central AGC controller are that the normal signal gain in the Turkish AGC is 0.5 while the desired common unit response time 70 seconds and the K is 1428 MW/Hz. In the following sections are described the principles that are used for this simulation and the results of sensitivity studies considering various cases of island operation of the Turkish power system results.

Case 1 and case 2 were investigated in high load conditions (24.5 GW). At time 5 seconds, 700 MW of generation is lost (increase of $\sim 2.5\%$ occurs in the load on the system) while the Turkish power system has a total generation of 27 GW. It is important to note that the size of the largest generation unit on the Turkish power system is 660 MW (Iskenderun thermal power plant), so this is the worst case scenario. Fig. 6-9 shows the frequency response of the overall model of the whole Turkish power system for primary control only and for primary and secondary control.

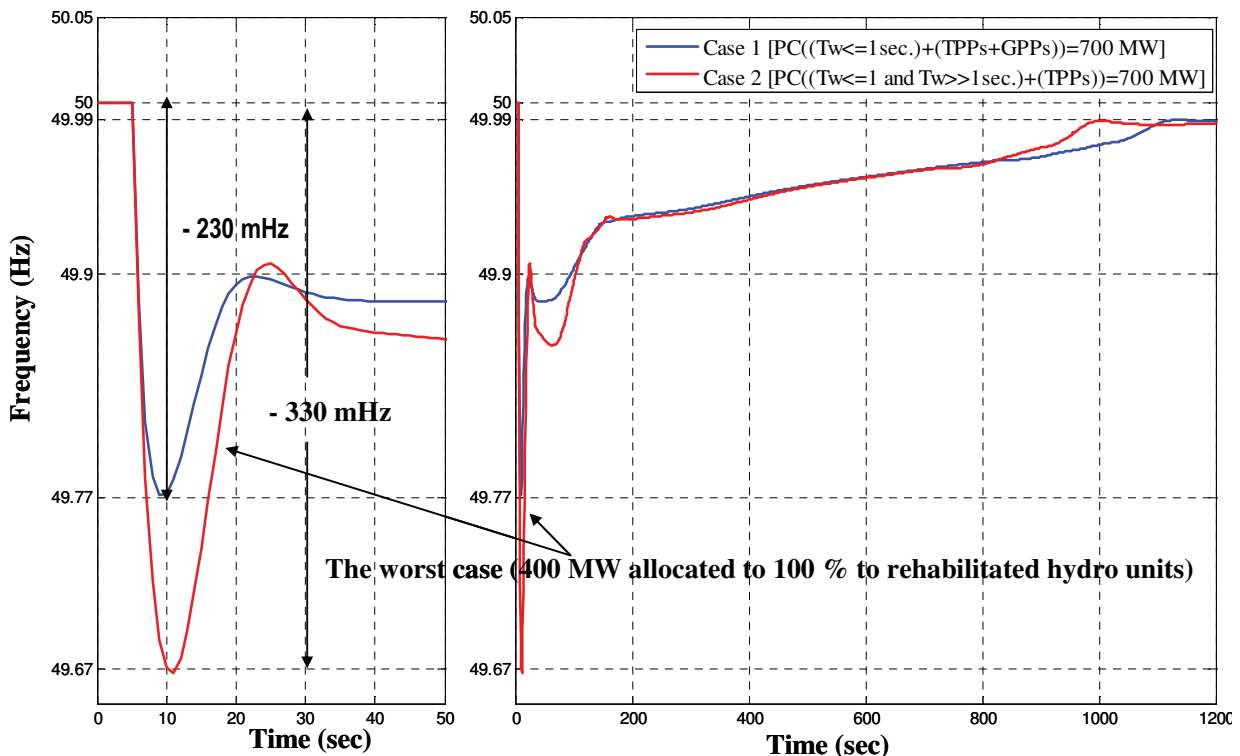


Fig. 6-9: Frequency response in island operation with primary and secondary control.

As seen in the above figure 6-9 the frequency deviation is reached for case 1 at -230 mHz and for case 2 at -363 mHz (400 MW allocated to 100% to rehabilitated hydro units).

Figure 6-10 shows the signal of secondary control reserve in MW and the area control error in the Turkish power system is calculated at the maximum deviation according to equation (6.13). ACE for case 1 and case 2 are -340 and -540 MW respectively.

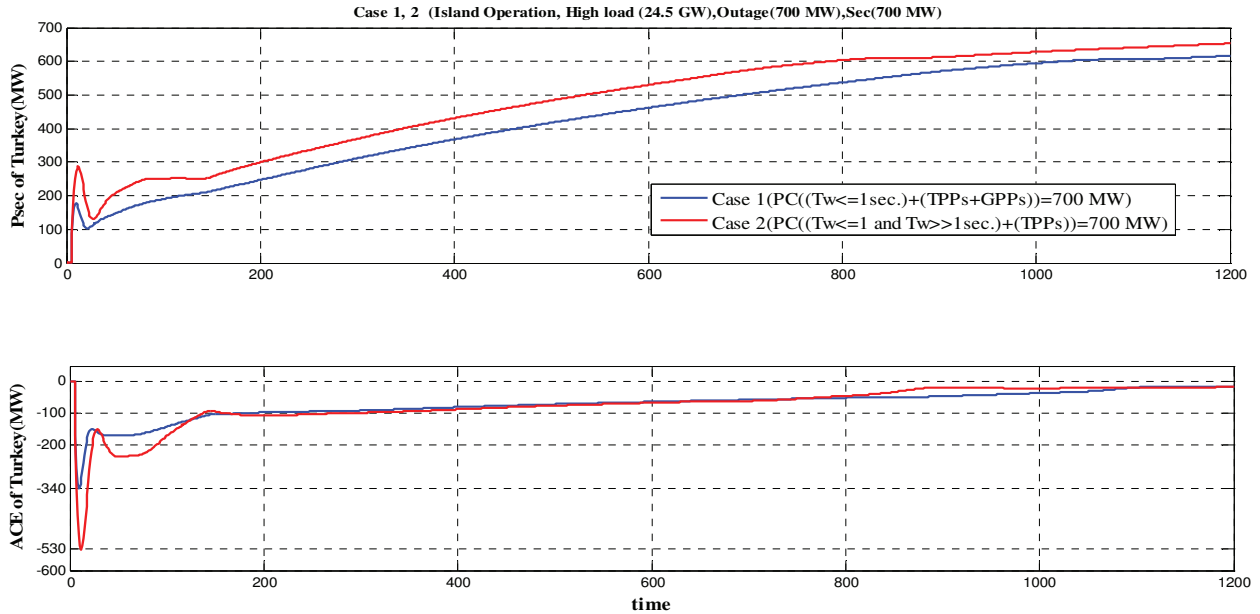


Fig. 6-10: Signal of secondary reserve and area control error.

According to case 1, figure 6-11 shows the deviation in power output (ΔP) of the overall model of the whole Turkish power system and the individual power plants (hydro power plants, gas power plants and thermal power plants) for primary control only and for primary and secondary control.

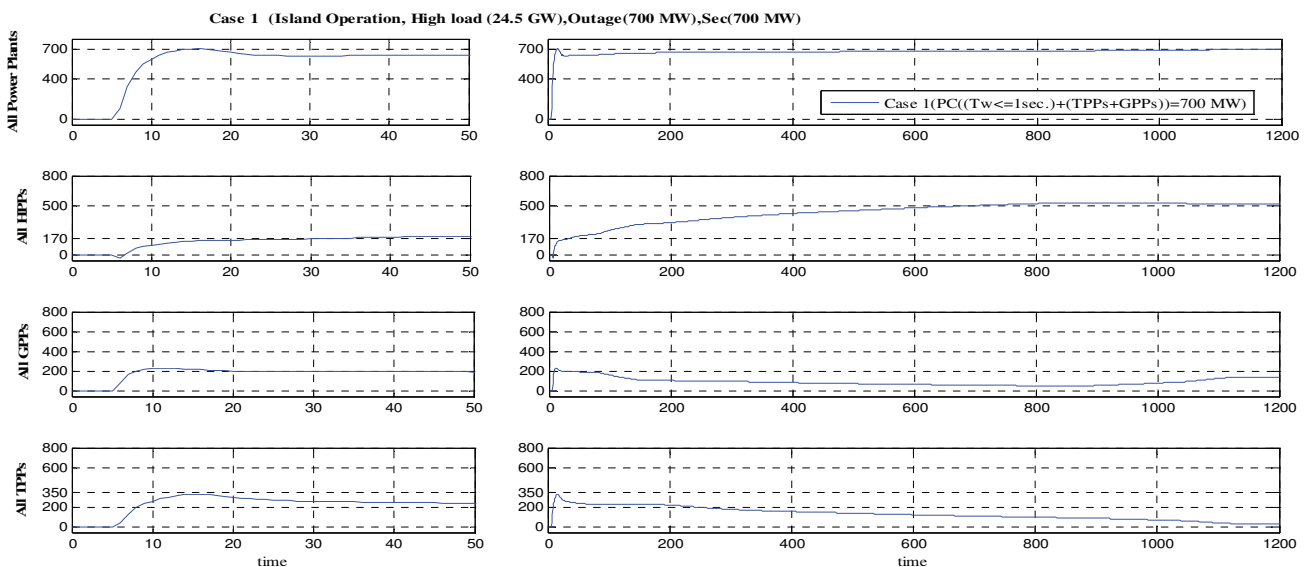


Fig. 6-11: The ΔP in island operation of all PPs, HPPs, GPPs and TPPs.

Figures 6-12, 6-13 and 6-14 show the power output of the individual hydro power plants, individual gas power plants and individual thermal power plants.

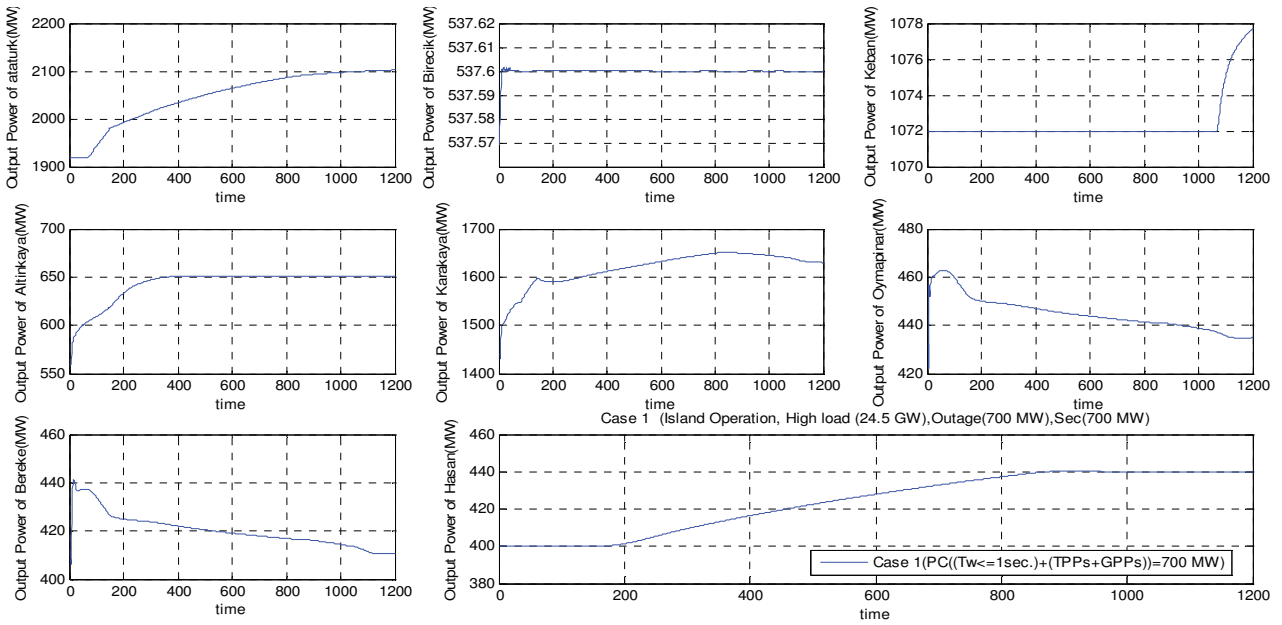


Fig. 6-12: The power output of individual hydro power plants.

As seen in the above figure 6-12 the rehabilitated hydro units with small water starting time constant $T_w \leq 1\text{sec.}$ (Altinkaya, Karakaya, Oymapinar and Berke hydro power plant) have contributed to the primary control power.

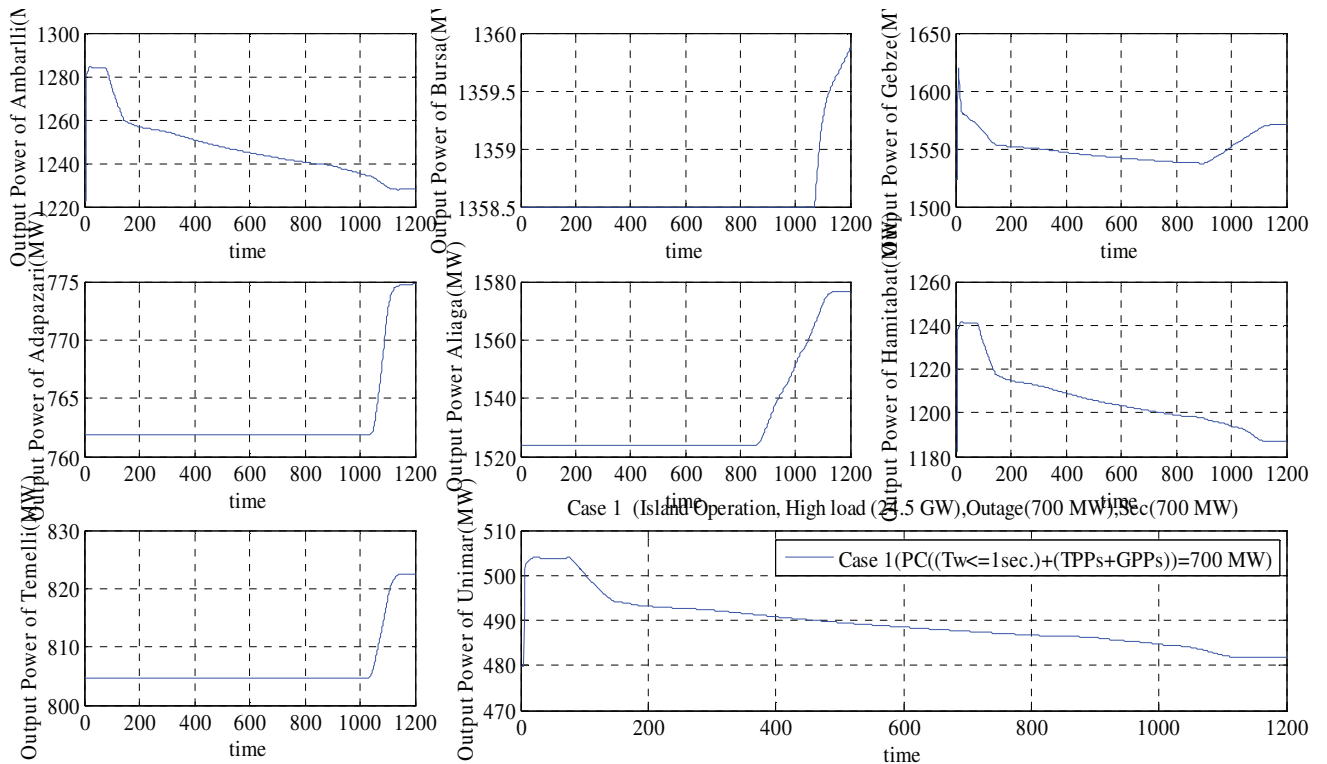


Fig. 6-13: The power output of individual gas power plants.

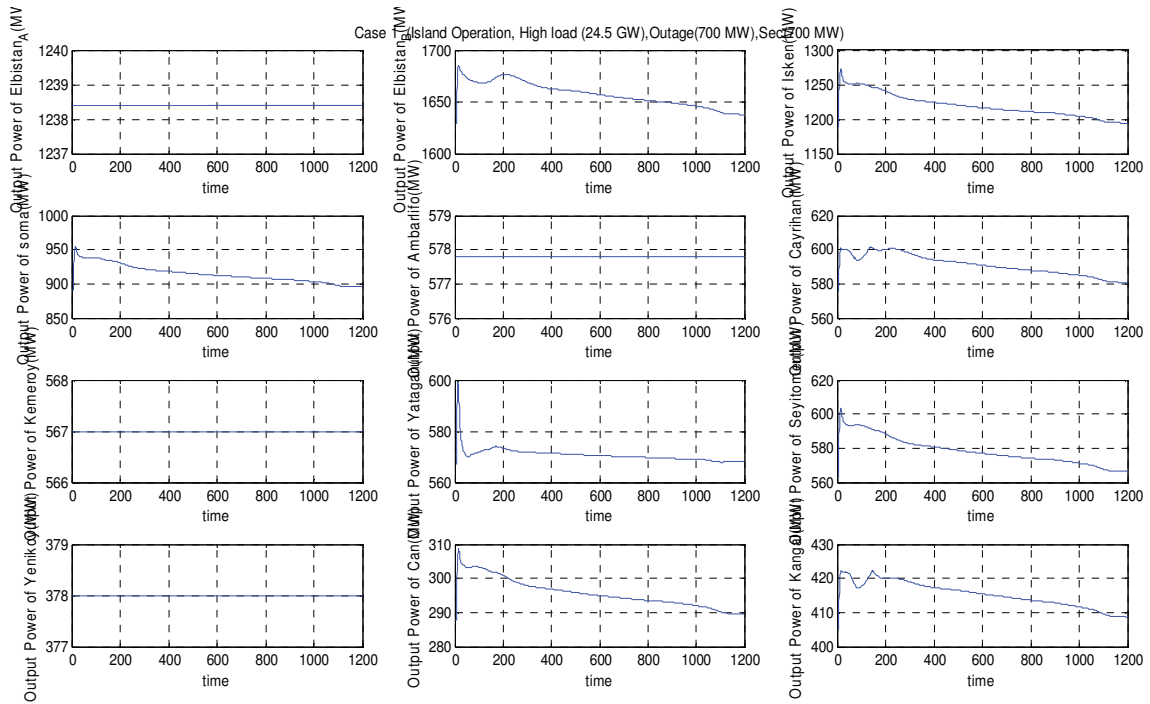


Fig. 6-14: The power output of individual thermal power plants.

It can be seen from figures 6-12, 6-13 and 6-14, that the class 1 (Ataturk, Karakaya, Altinkaya, and Hasan Ugurlu hydro power plant) and class 2 (Adapazari, Gebze, Temelli, Aligia, Bursa and Keban power plant) have contributed to the secondary control power.

According to case 2, figure 6-15 shows the deviation in power output (ΔP) of the overall model of the whole Turkish power system and the individual power plants (hydro power plants, gas power plants and thermal power plants).

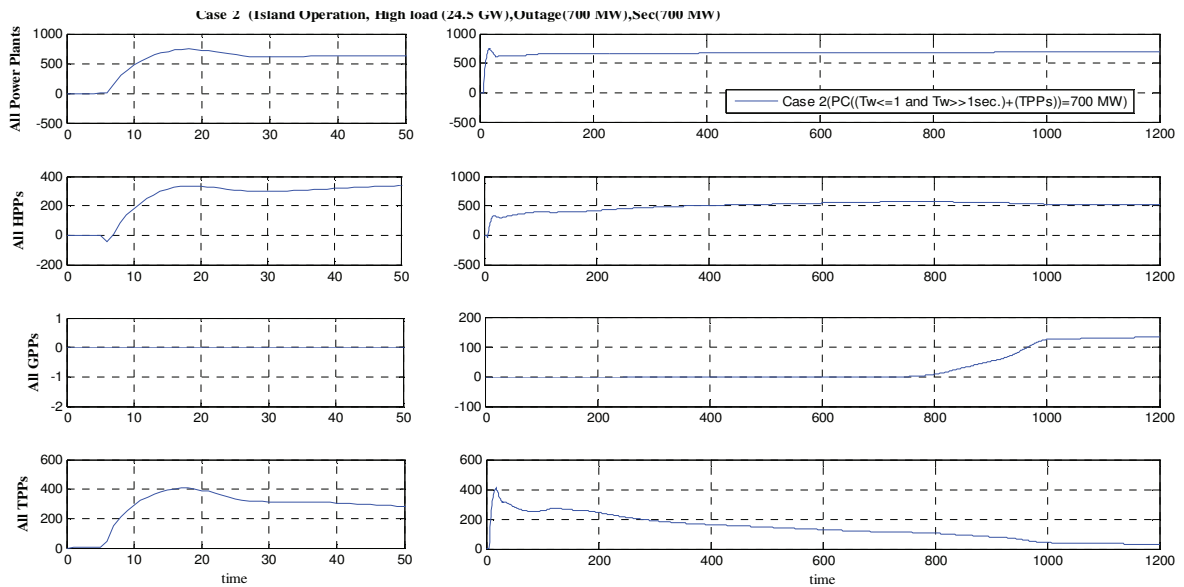


Fig. 6-15: The ΔP in island operation of all PPs, HPPs, GPPs and TPPs.

Figures 6-16, 6-17 and 6-18 show the power output of the individual hydro power plants, individual gas power plants and individual thermal power plants.

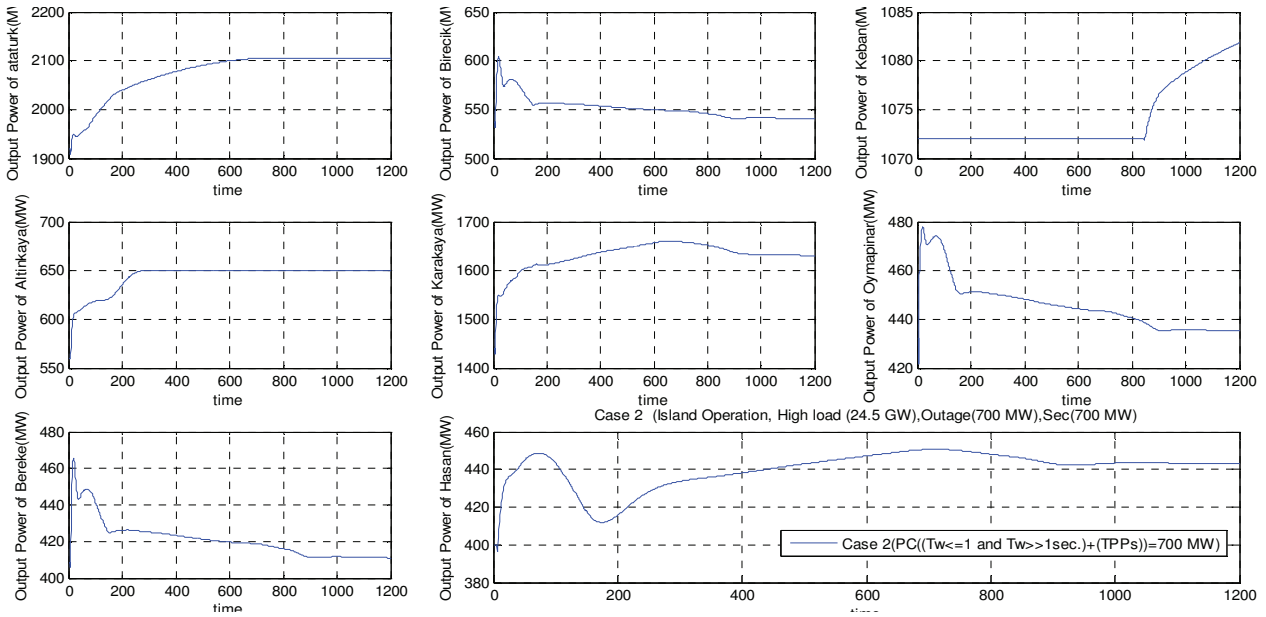


Fig. 6-16: The power output of individual hydro power plants.

As seen in the above figure 6-16 the rehabilitated hydro units (see Table 6-3) with water starting time constant $T_w \leq 1\text{sec.}$ and $T_w \gg 1\text{sec.}$ have contributed to the primary control power.

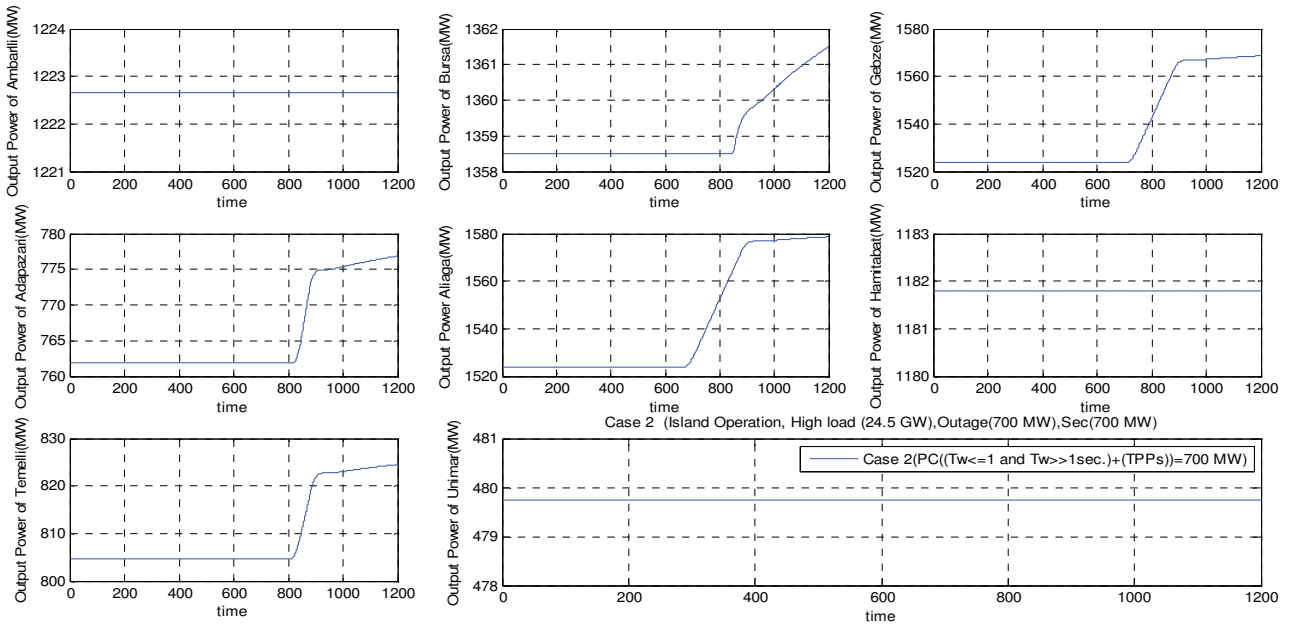


Fig. 6-17: The power output of individual gas power plants.

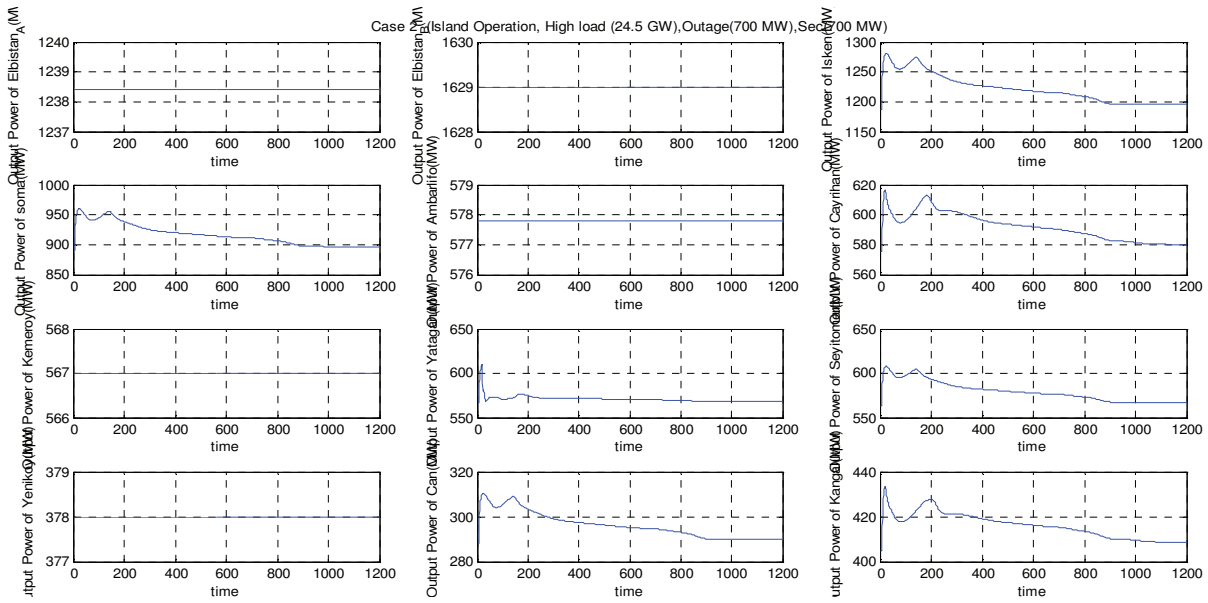


Fig. 6-18: The power output of individual thermal power plants.

It can be seen from figures 6-16, 6-17 and 6-18, that the class 1 (Ataturk, Karakaya, Altinkaya, and Hasan Ugurlu hydro power plant) and class 2 (Adapazari, Gebze, Temelli, Aligia, Bursa and Keban power plant) have contributed to the secondary control power.

As the result of island operation with 700 MW generation loss in the Turkish power system, primary control reserve (700 MW) and secondary control reserve (700 MW);

- Stability of overall frequency in island operation;
- The maximum frequency deviation $\Delta f_{\max} < 800\text{mHz}$;
- $\Delta f_{\max} < 200\text{mHz}$.

6.6.6. Parameter Optimization of Secondary Controller

The parameters optimization have been done in order to test the Turkish power system performance in view of the trial parallel operation because in the future the K-factor of Turkey, after its parallel connection to ENTSO-E-CE, will be calculated by a responsible technical ENTSO-E-CE group and the respective value of around 1800 MW/Hz. The T_{CR} also has got an increased value (comparing to the past) to reduce the impact of integral part of ACE in order to react correctly in the cases of certain disturbances. May be T_{CR} should have even bigger value (around 80 seconds or more – max is 100 seconds according to Policy 1 recommendations) after the connection of Turkey to the European grid.

Figure 6-19 shows the overall frequency performance with 700 MW generation loss and with different parameters of secondary controller (G_A and T_{CR}) in the Turkish power system with high load condition (26 GW), primary control reserve is 725 MW and the secondary control reserve is 700 MW (class 1 and class 2 have contributed).

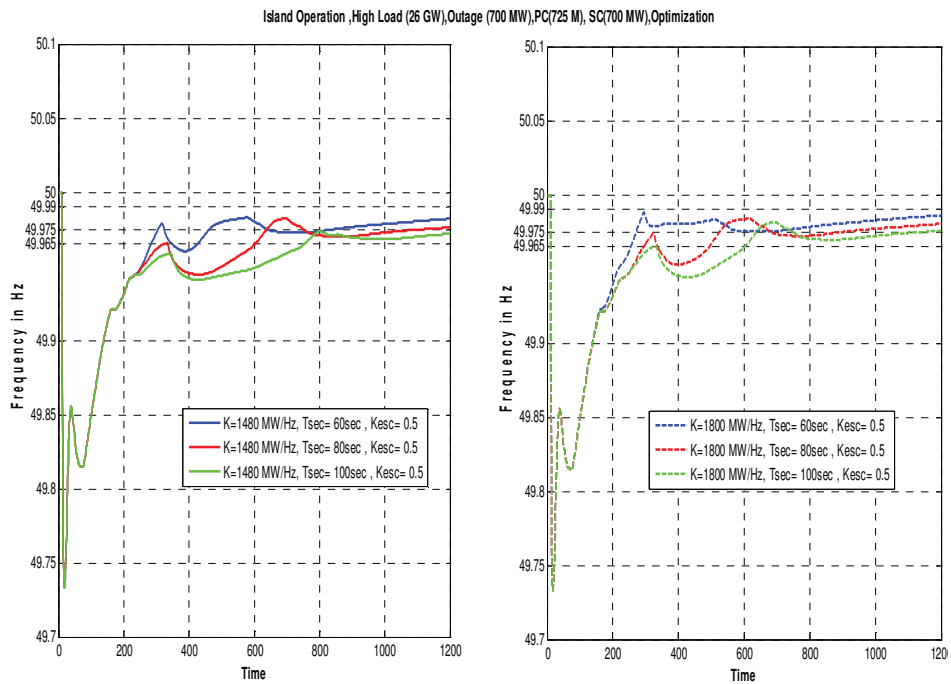


Fig. 6-19: Frequency performance in island operation.

Figure 6-20 shows the area control error in the Turkish power system due to the changing parameters of the secondary controller.

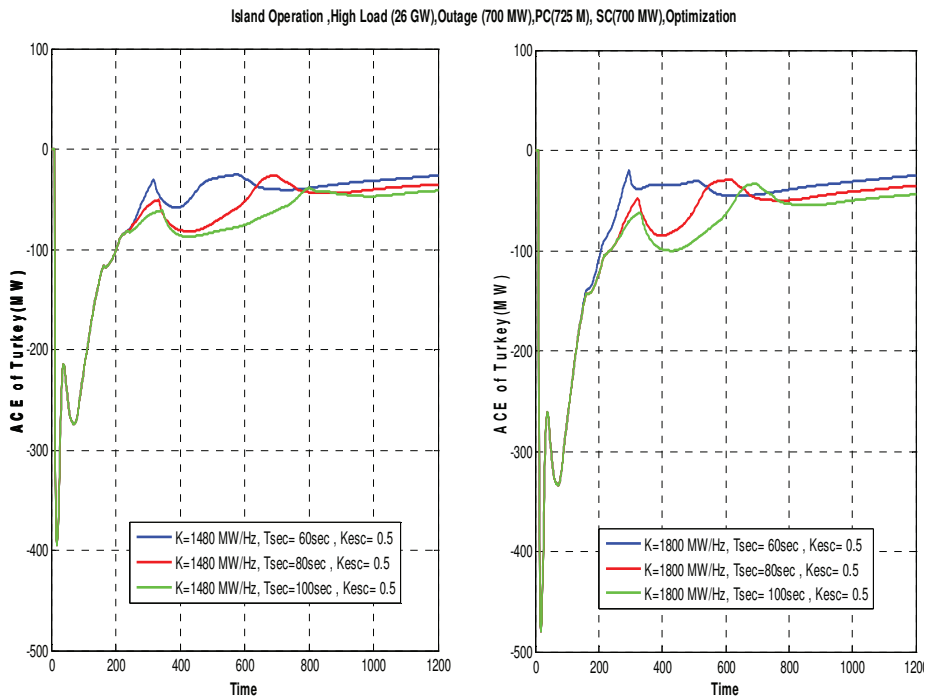


Fig. 6-20: The area control error of the Turkish power system.

As seen in the above figures 6-19 and 6-20, changing the parameters of the secondary controller has a small effect on the frequency and the area control error of the Turkish power system.

CHAPTER 7

Interconnected Operation with the ENTSO-E-CE System

7.1. Introduction

In such cases a joint reaction of primary control of all interconnected systems is foreseen in order to re-establish the balance between generation and demand. The result will be achieved at a frequency differing from its set-point value by Δf , and the power interchanges on tie lines will be different from the scheduled values. Whereas during primary control all systems provide mutual support, only the system in which the unbalance occurred is required to undertake secondary control action. The controller of this system activates appropriate secondary control power restoring the nominal frequency and scheduled power exchanges [49].

This concept of control in the interconnected systems will be discussed in the example of two systems A (i.e. ENTSO-E-CE system) and B (i.e. Turkish system), connected with a tie-line. The disturbance will be disconnection of generator B with generated power P_X (see Fig. 7-1).

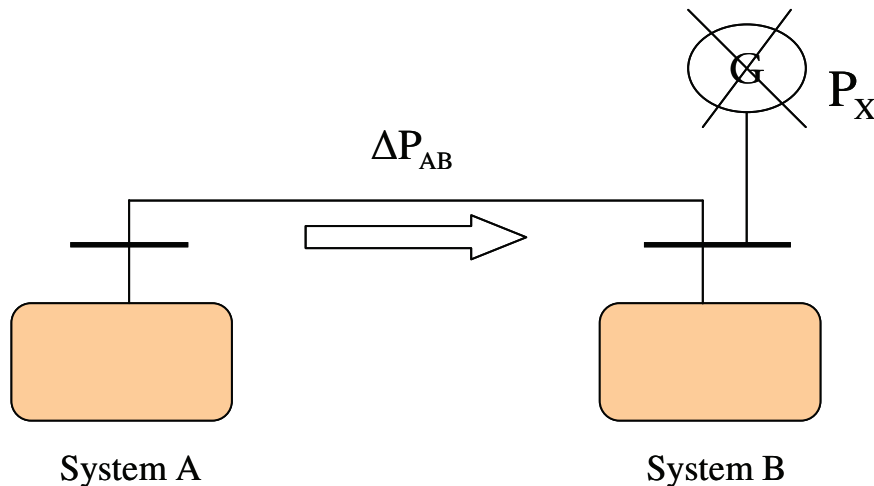


Fig. 7-1: Two power systems interconnected with a tie-line.

- **Before a disturbance**

The systems are assumed to operate at nominal frequency f_n , and the actual power exchange is assumed to be equal to the scheduled exchange before the disturbance, thus the deviation of power exchange $\Delta P_{AB} = 0$. The systems A and B are characterized by stiffness factors K_A and K_B , respectively.

- **Disturbance and Primary Control**

Due to a sudden loss of generated power, the frequency begins to change (decrease) and the frequency deviation Δf can be determined from the relationship.

$$\Delta f = \frac{P_X}{K_A + K_B} \quad (7.1)$$

Since generating capacity is lost, P_X will have a negative value. Hence, Δf will also be negative.

In response to the frequency deviation Δf , and on the basis of the network power frequency characteristics K_A and K_B , of the two separate networks, the following power values will be activated by primary control [48-49]:

$$\begin{aligned} \Delta P_A &= -K_A * \Delta f \\ \Delta P_B &= -K_B * \Delta f \end{aligned} \quad (7.2)$$

The loss of power P_X will be offset by the power values ΔP_A and ΔP_B in such a manner that the sum $\Delta P_A + \Delta P_B$ will be equal to the disconnected generating capacity P_X . The frequency will be stabilized at the lower level, equal to the nominal value reduced by Δf . At this point the action of primary control comes to the end.

▪ Behaviour of Secondary Control

The power exchange P between systems A and B will no longer correspond to the programmed value therefore ΔP_{AB} will not equal zero but will assume the value $\Delta P_{AB} = \Delta P_A$ of primary control power activated in system A and transferred to system B in order to bring the situation under control. In terms of system A the transferred power is exported power, hence its value is considered positive. In terms of system B it is imported power, thus $\Delta P_{BA} = -\Delta P_{AB}$.

If the value of $K = K_A$ is set on the secondary controller of system A, then the area control error for this system is

$$ACE_A = \Delta P_{AB} + K_A \Delta f = \Delta P_A + (-\Delta P_A) = 0 \quad (7.3)$$

That means the central regulator of system A does not react and no secondary control will be activated in system A. Primary control in system A will be maintained as long as the frequency deviation from the nominal value persists in the interconnected systems.

If the value of $K = K_B$ is set on the secondary controller of system B, then the area control error for this system is

$$ACE_B = \Delta P_{BA} + K_B \Delta f = -\Delta P_A + (-\Delta P_B) = P_X, \text{ while } P_X < 0 \quad (7.4)$$

It is self-evident that the control error determined by the central regulator of system B will be negative and its value equal to the power P_X , lost due to the tripping of the generating unit. The secondary control in system B is activated. The loss of generating capacity, due to the disturbance, will be offset by the action of the secondary control in system B, the frequency in the systems will be restored to the

nominal value, and power exchange will be re-established at its scheduled value (i.e. before the disturbance). The action of primary control in system B will decline when the frequency deviation Δf approaches zero. In order to provide effective secondary control, the generating units that contribute to this control process must have sufficient power reserve to be able to respond to the regulator signal with both the required change in generated power and the required rate of change.

The rate of change in the power output at the generator terminals significantly depends on the generation technique. Typically, for oil- or gas-fired power stations this rate is about 8% per min, for lignite-fired and hard-coal-fired power stations it is up to 2% and 5% per min, respectively, and for nuclear power stations this rate is up to 5% per min. Even in the case of reservoir power stations the rate is 2.5% of the rated plant output per second.

The secondary control range is the range of adjustment of the secondary control power, within which the central regulator can operate automatically, in both directions (positive and negative) from the working point of the secondary control power. The secondary control power is the portion of the secondary control range already activated at the working point. The secondary control reserve is the positive part of the secondary control range between the working point and the maximum value [49].

7.2. Simulation of Interconnection with ENTSO-E-CE System

After interconnection to the ENTSO-E-CE System the activation of primary control power according to the ENTSO-E-CE requirements is necessary. Secondary control has to restore the frequency to its nominal value and to maintain the required power frequency characteristic.

At first the main characteristics of parallel operation are discussed with a simplified mid term model. In this model there is no detailed representation of power plants and both the Turkish power and ENTSO-E-CE systems are represented mainly by their power frequency characteristics. Subsequent detailed models of power plants and their controllers are included in the model and the overall system behaviour is discussed in detail.

7.2.1. Simplified Mid Term Model

The Simulations are performed using a two area network consisting of the ENTSO-E-CE system with 300 GW and the Turkish power system with 30 GW, the principle block diagram is shown in figure 7-2. The model consists of the following parts:

- Red blocks: primary control part of the part networks (power plants) taking into account the required power frequency characteristics of the Turkish power system and ENTSO-E-CE
- Blue blocks: load of the part networks
- Green blocks: time constant and transfer ratio of the total network
- Orange blocks: secondary control of the part networks
- Yellow Blocks: signal measurements

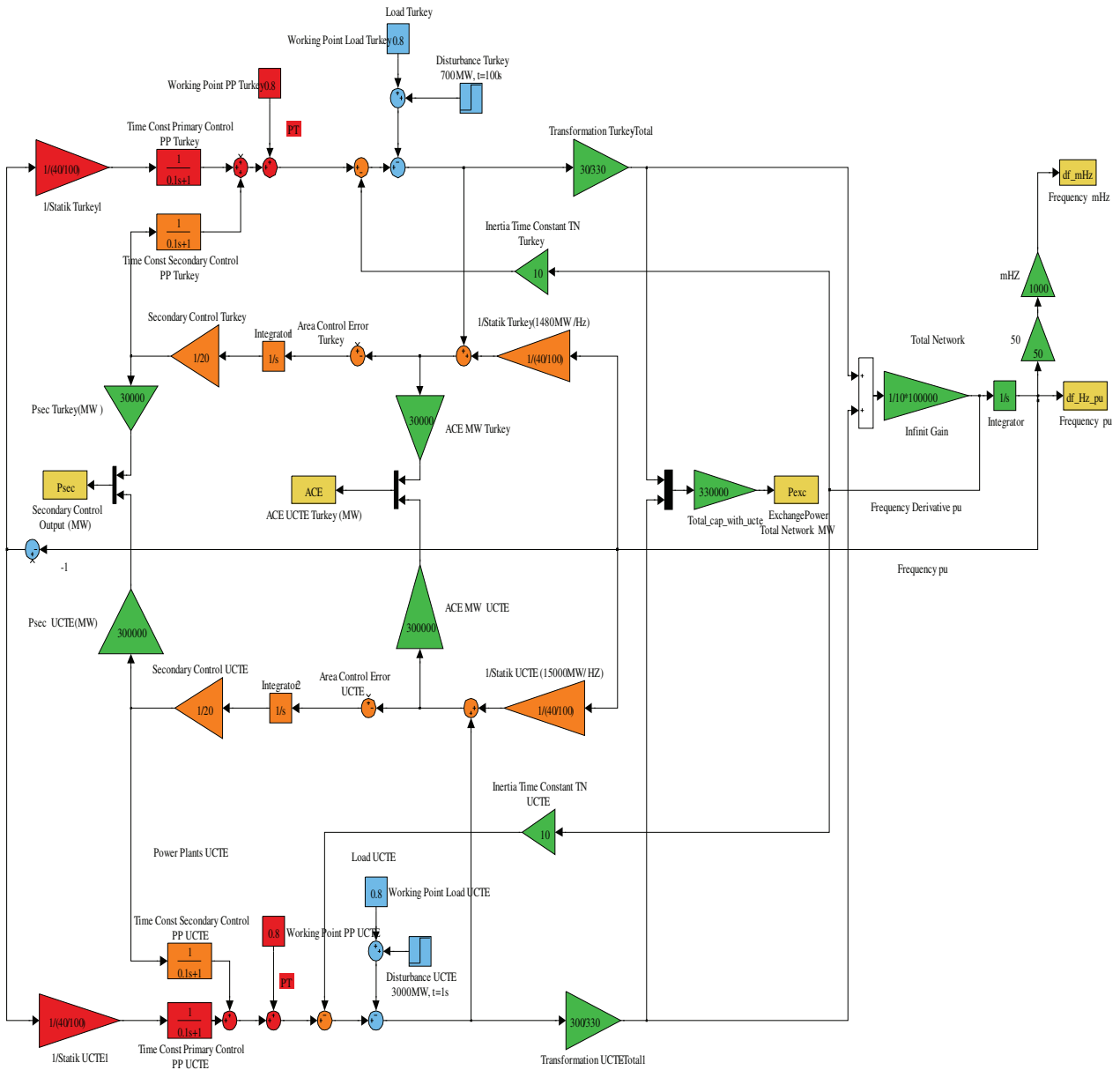


Fig. 7-2: Simplified mid-term Model of the Turkish and ENTSO-E-CE systems.

7.2.1.1. Test Simulations

For explaining the function of the model the following disturbances are performed:

- Generation loss of 700 MW in Turkey after 5 seconds
- Generation loss of 3 GW in ENTSO-E-CE system after 100 second

Figure 7-3 shows the frequency deviation in mHz without and with the secondary control

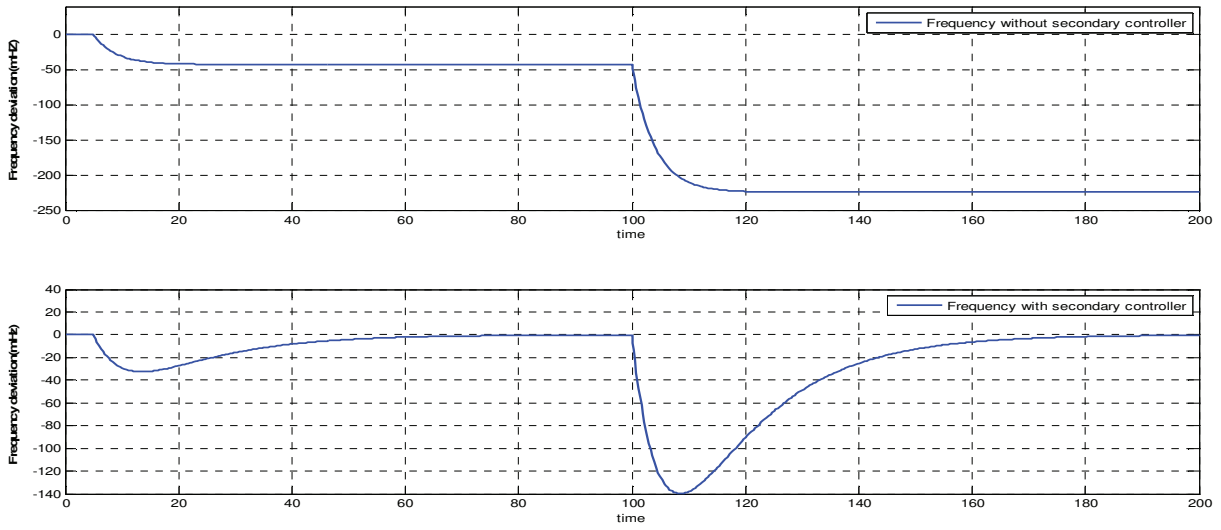


Fig.7-3: The frequency with and without secondary control.

Figure 7-4 shows the area control error (ACE) in MW for primary control only and for primary and secondary control. The ACE always shows the power surplus or deficit in a part network.

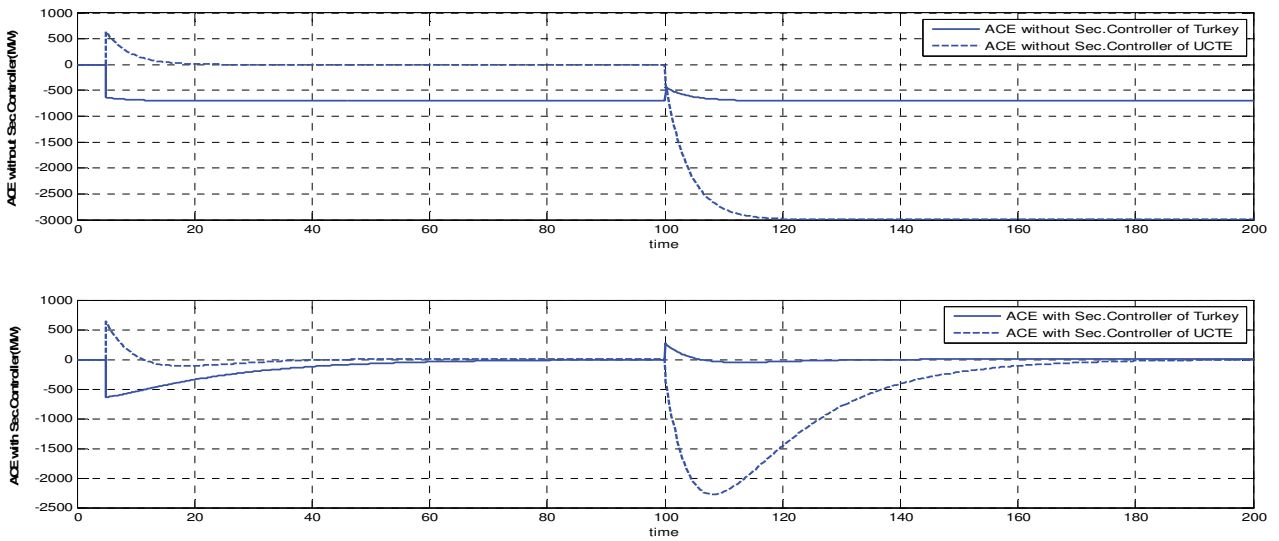


Fig. 7-4: The area control error with and without secondary control.

Figure 7-5 shows the exchange power in MW for both disturbances and for primary control only and for primary and secondary control together. Exported power is always positive.

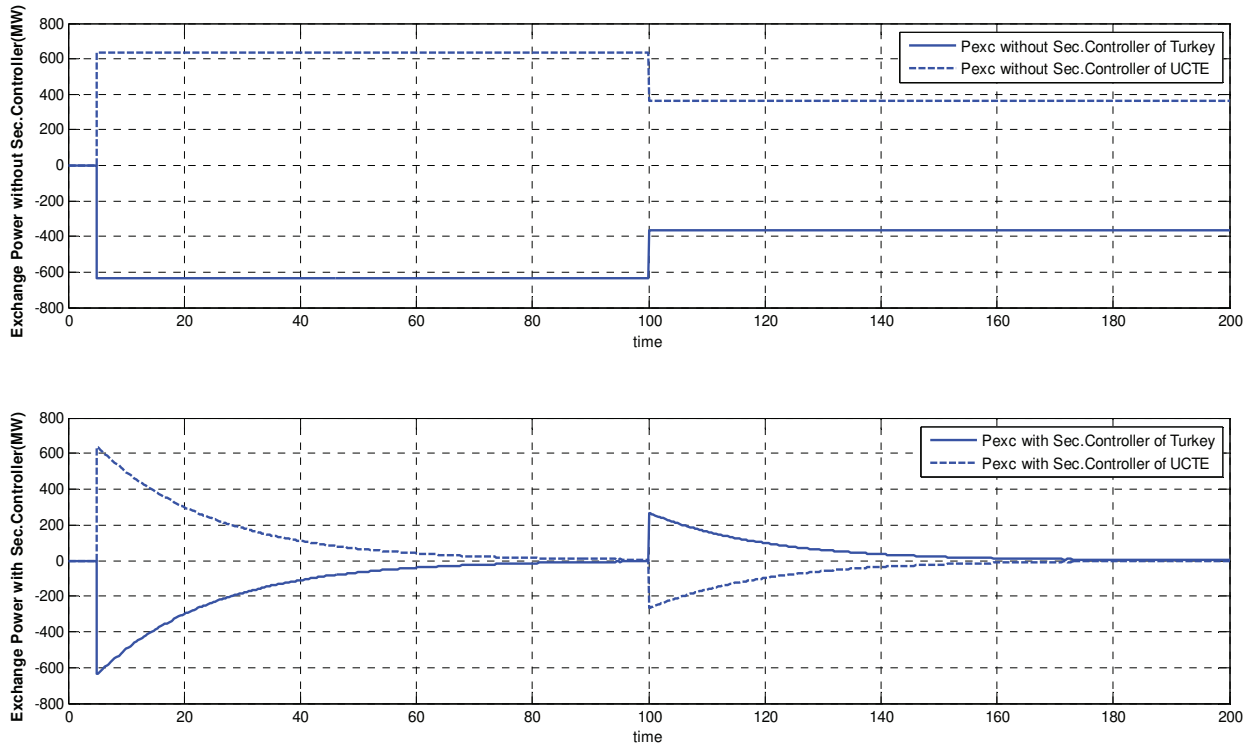


Fig. 7-5: The exchange power with and without secondary control.

7.2.2. Detailed Mid Term Model of the Turkish System with ENTSO-E-CE System

In order to fulfil ENTSO-E-CE (former UCTE) requirements, the Turkish power system as control area has to provide approximately 300 MW primary control power within 30 seconds. This amount has to be allocated to thermal units (TPP and NGCCPP).

The total amount of secondary control reserve has to equal approximately 700 MW and must be activated within 15 minutes .Thereof;

- 300-400 MW must operate under automatic control
- The remaining part can be activated manually within 15 minutes

The simulations are performed using a two area network consisting of the ENTSO-E-CE system with 300 GW and the Turkish power system with 25 GW (see Fig. 7-6). In the MATLAB model really used for the investigations of all power plants with their primary controllers and loads of Turkey are modelled completely in detail. Also the secondary control model consists of the real controller as in operation in Ankara and also the individual controllers in the involved power plants.

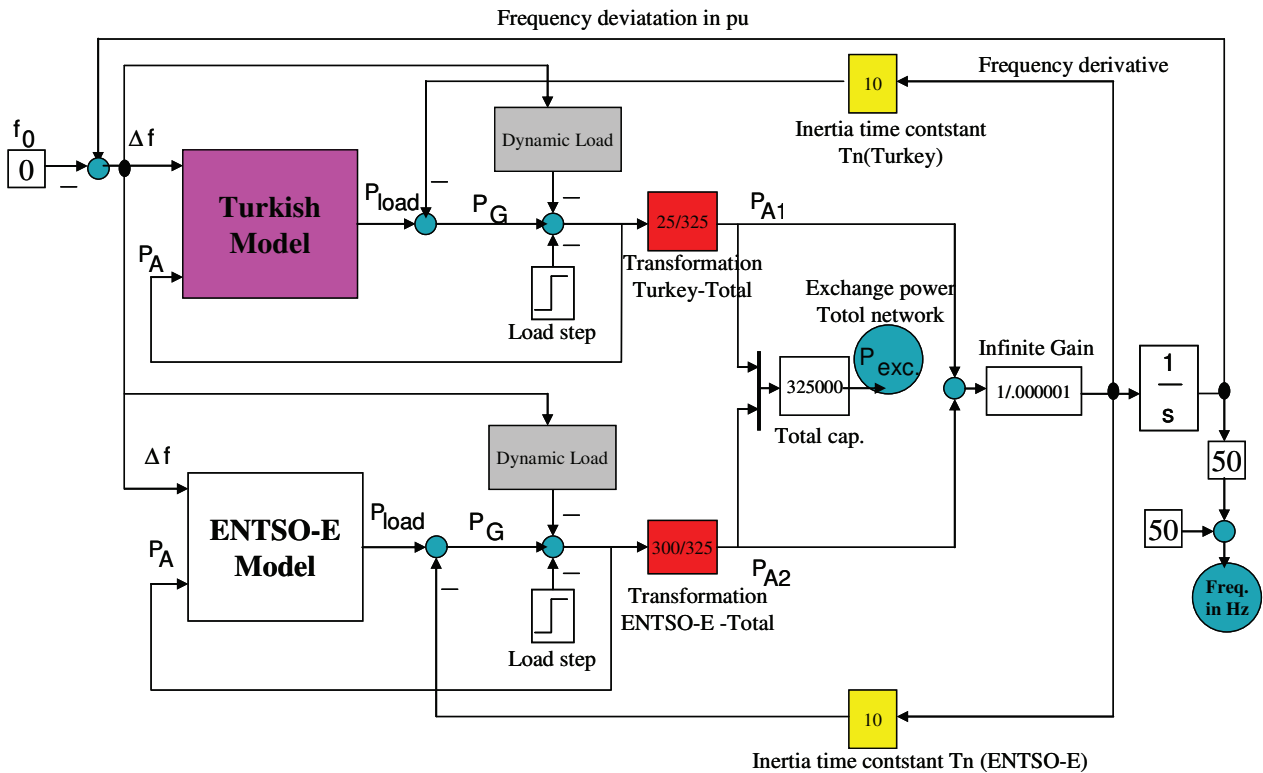


Fig. 7-6: Detailed mid-term model of the Turkish system with ENTSO-E-CE system.

7.2.3. Simulation Study of Interconnected Operation

For explaining the function of the model the following disturbances are analyzed:

- 700 MW generation loss in the Turkish power system
- Parameters optimization with 580 MW generation loss in the Turkish power system
- 1200 MW generation loss in the ENTSO-E-CE system
- 3GW generation loss in the ENTSO-E-CE system
- Existing load variation measured on 16/06/2009
- Existing load variation measured on 17/05/2010

In the following sections are described the principles that are used for this simulation and the results of sensitivity studies considering various cases of operation of the Turkish power system results with interconnection. Moreover, this tool will be provided to TEIAS in order to perform more studies, with actual system data, for other future cases from the operation of the Turkish power system.

7.2.3.1. 700 MW Generation Loss in the Turkish Power System

At time 5 seconds, 700 MW of generation is lost in the Turkish power system with high load condition (25 GW), secondary control reserve is 700 MW and primary control reserve is 300 MW (have contributed to TPP and NGCCPP).

Figure 7-7 shows the overall frequency performance in Hz and the exchange power in MW of the

Turkish and ENTSO-E-CE systems. The ENTSO-E-CE system will deliver nearly 630 MW to the Turkish power system and the frequency deviation is reached at -35 mHz .

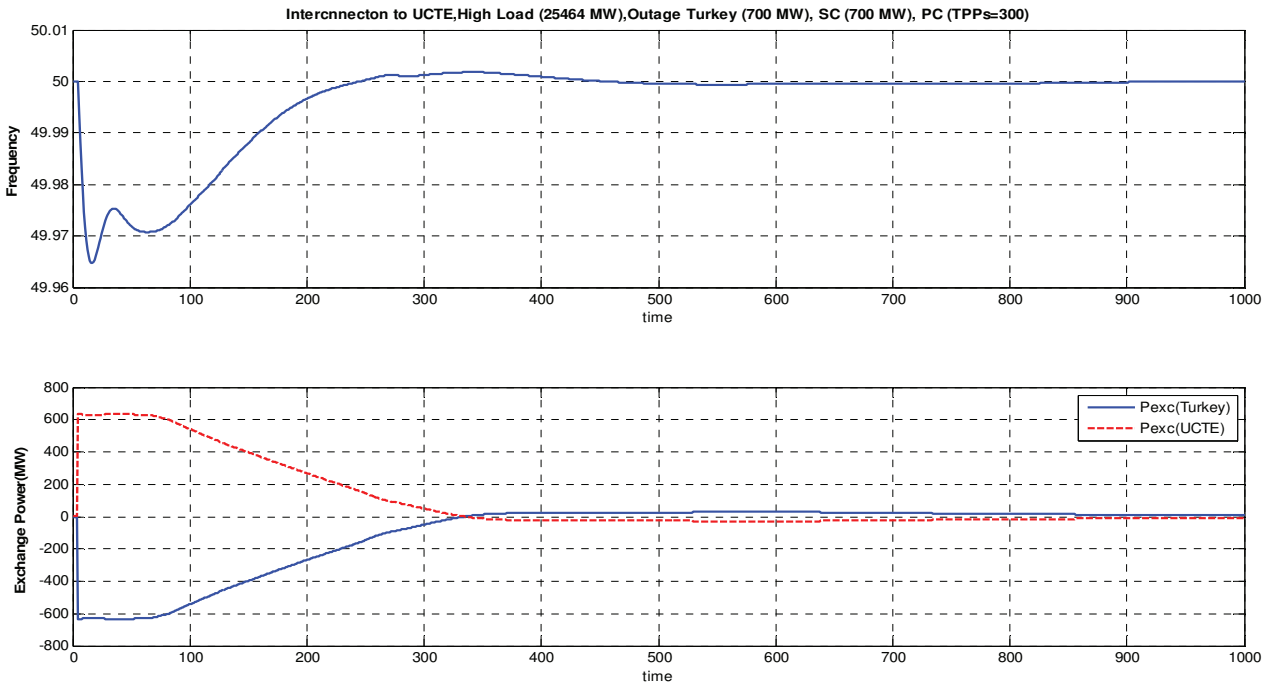


Fig. 7-7: The frequency and exchange power of the Turkish and ENTSO-E-CE systems.

Figure 7-8 shows the signal of secondary control power in MW and the area control error (ACE) in MW for the Turkish power system.

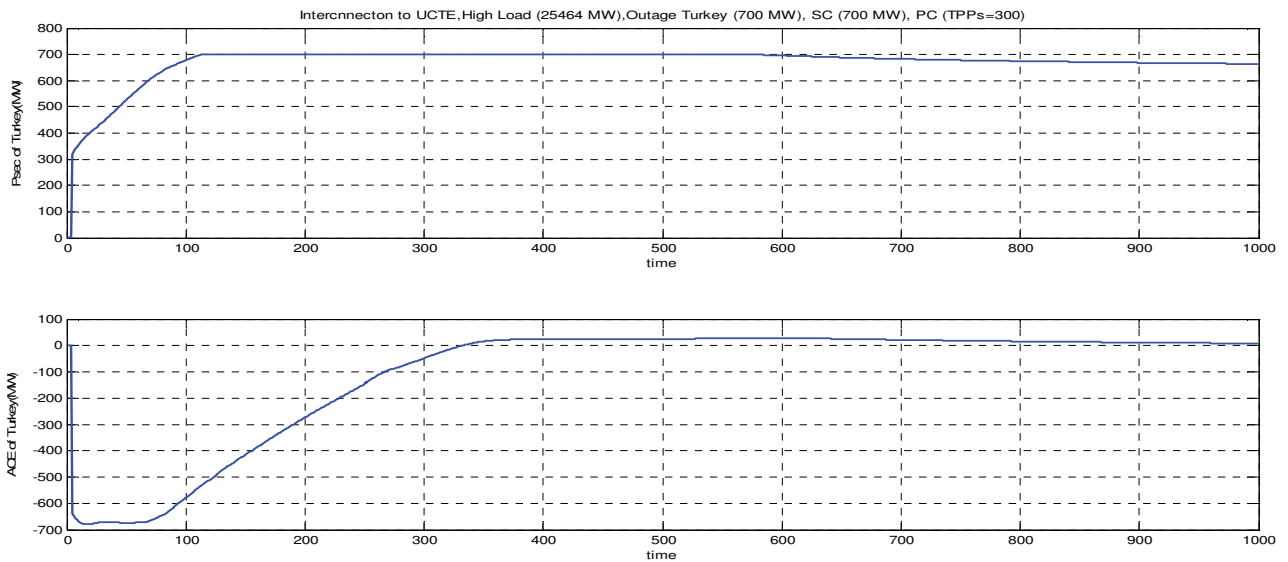


Fig. 7-8: The signal of secondary control and area control error of the Turkish system.

7.2.3.2. Parameters Optimization of the Secondary Controller

With the MATLAB model, the simulation tool in order to be used for a rough estimation of AGC performance of the Turkish power system in parallel operation with the ENTSO-E-CE system and for an advisory tuning of basic AGC parameters. Results, for various study cases have been derived. These study cases assume that the K-factor of Turkey will be set 1824 MW/Hz as concluded using the methodology of ENTSO-E-CE frequency, as described in Chapter 6, Section 6.6.3.1. The suggestion for the parameters of the central AGC controller for the period of parallel operation is that the normal signal gain in the Turkish AGC should be set to 0.5 while the desired common unit response time should be set to 80 seconds.

At time 10 seconds, 580 MW of generation is lost in the Turkish power system with high load condition (25 GW), secondary control reserve is 700 MW and primary control reserve is 300 MW (have contributed to TPP and NGCCPP). Figure 7-9 shows the overall frequency performance of the Turkish and ENTSO-E-CE systems in Hz and the exchange power of the ENTSO-E-CE system in MW and with different parameters of the secondary controller (G_A and T_{CR}) in the Turkish power system.

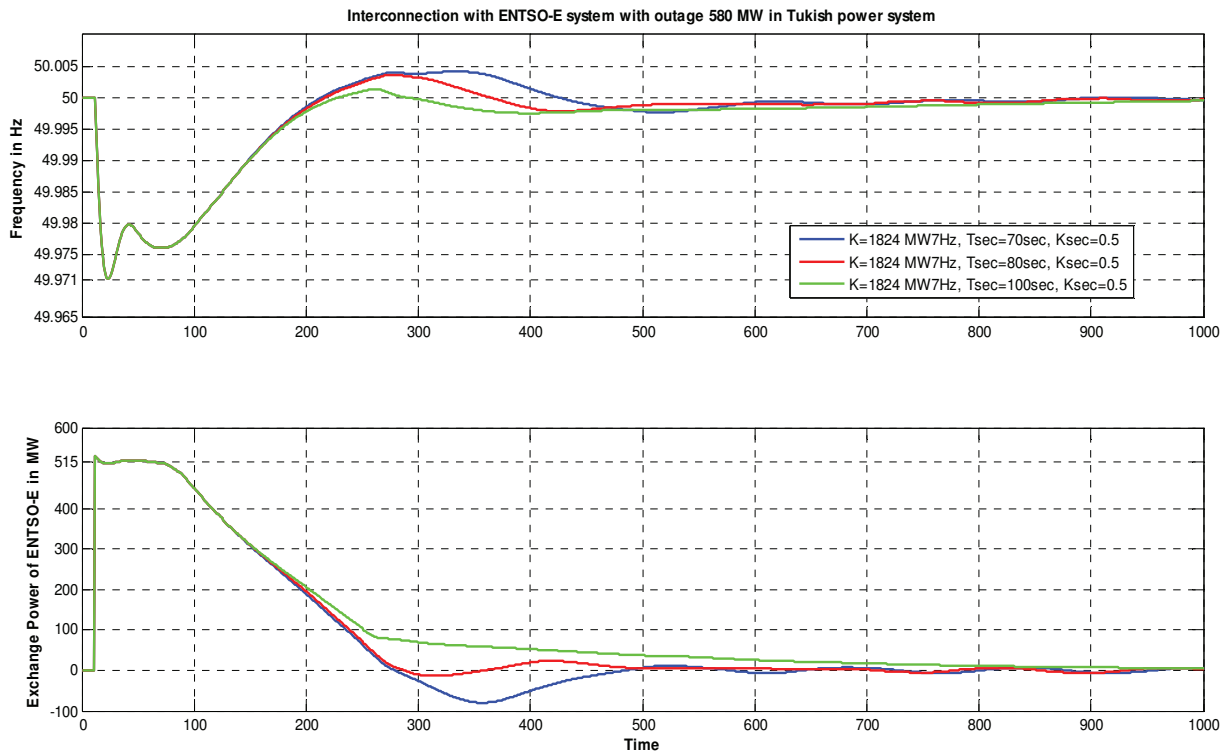


Fig. 7-9: The frequency and exchange power of Turkish and ENTSO-E-CE systems.

It can be seen from figure 7-9 that the ENTSO-E-CE system will deliver nearly 515 MW to the Turkish power system and the frequency deviations is reached at -30 mHz.

Figure 7-10 shows the area control error (ACE) for primary and secondary control of the Turkish power system in MW and the signal of secondary control power in MW.

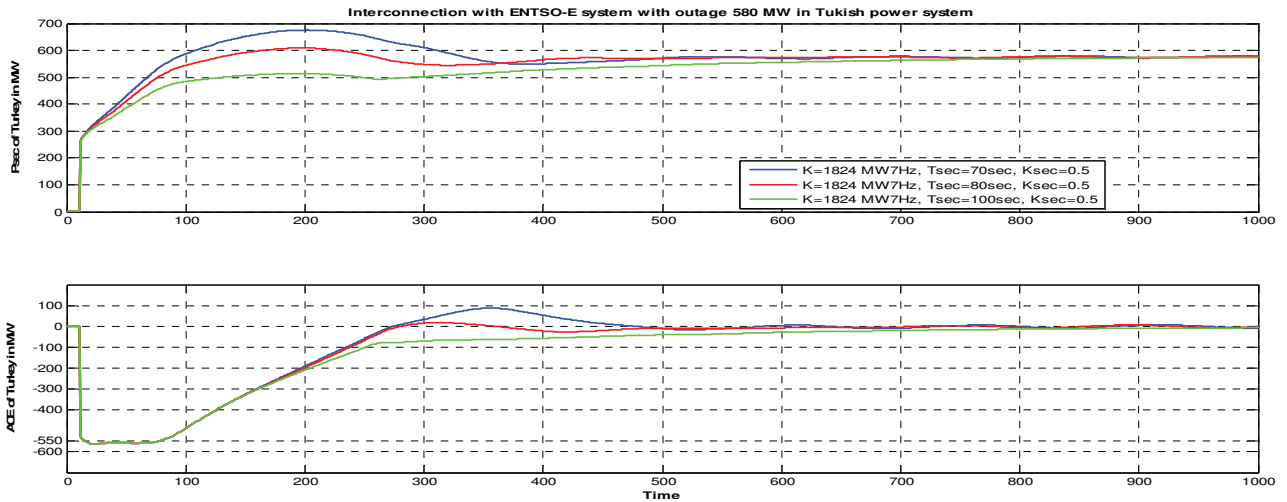


Fig. 7-10: The signal of secondary control and area control error of Turkish power system.

As seen in the above figures 7-9 and 7-10, changing the parameters of the secondary controller has a big effect on the frequency and the area control error of the Turkish power system. The best value for the time constant of integrator (T_{CR}) should be 80 seconds.

7.2.3.3. 1200 MW Generation loss in the ENTSO-E-CE System

At 5 seconds time, 1200 MW generation is lost in ENTSO-E-CE system with high load condition (25 GW) in the Turkish power system, secondary control reserve is 700 MW and primary control reserve is 300 MW in Turkey (have contributed to TPP and NGCCPP).

Figure 7-11 shows the overall frequency performance in Hz and the exchange power of the Turkish and ENTSO-E-CE systems in MW.

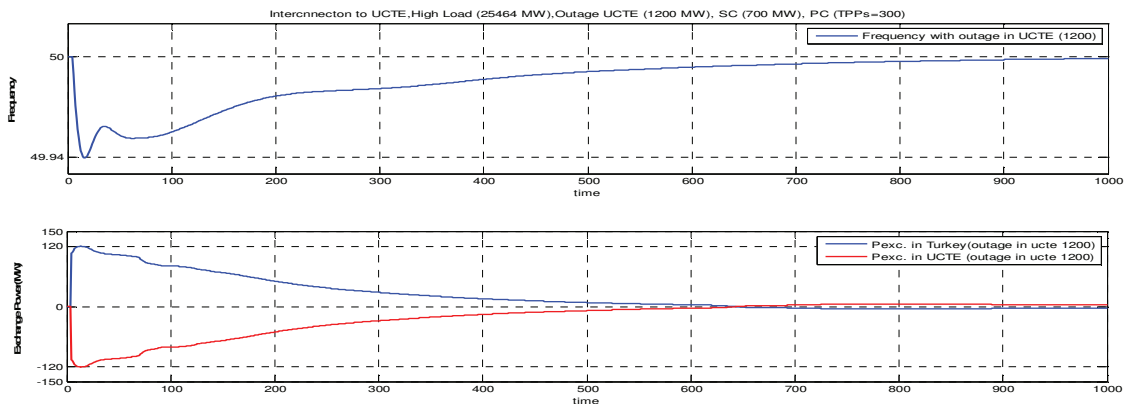


Fig. 7-11: The frequency and exchange power in Turkish and ENTSO-E-CE systems.

It can be seen from figure 7-11 that the Turkish power system will deliver nearly 120 MW to ENTSO-E-CE system and the frequency deviation is reached at - 60 mHz.

Figure 7-12 shows the area control error (ACE) of the ENTSO-E-CE and Turkish power systems in MW.

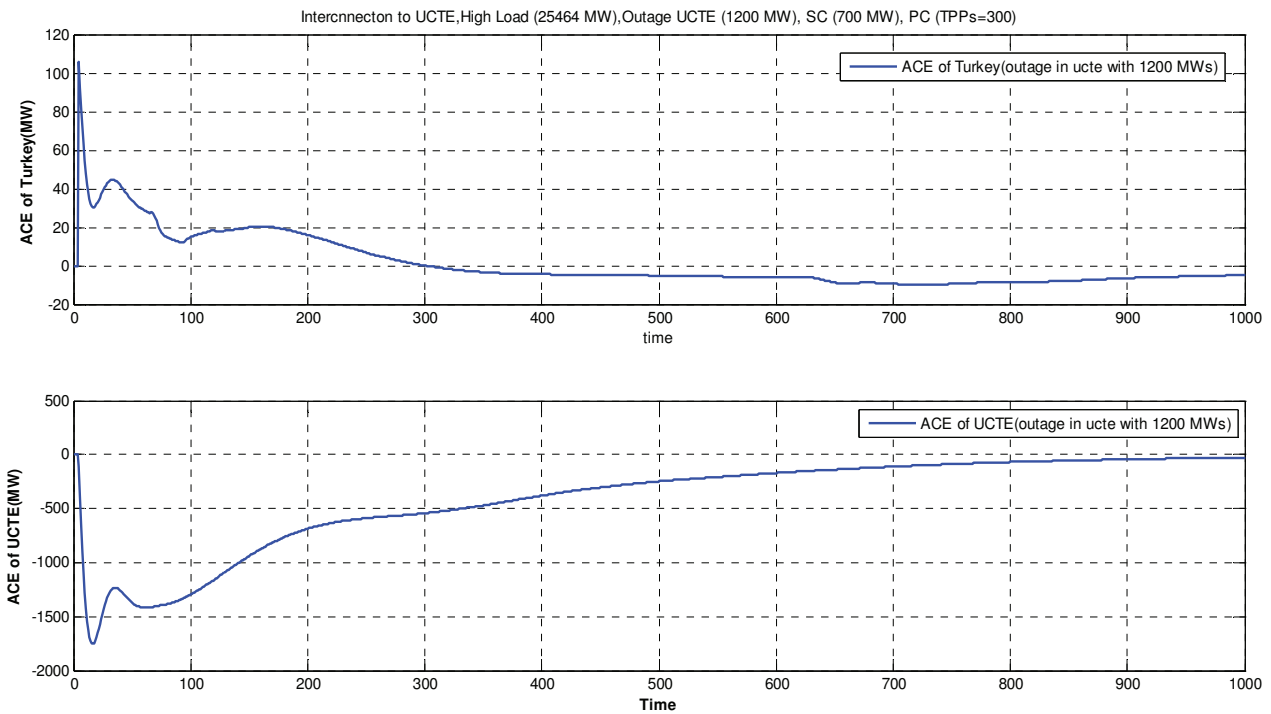


Fig. 7-12: The area control error in ENTSO-E-CE and Turkish systems.

7.2.3.4. 3 GW Generation Loss in the ENTSO-E-CE System

In case of large generation outages in the ENTSO-E-CE system (e.g. 3000 MW, which is considered as the ‘normative’ outage in ENTSO-E-CE, corresponding to a 200 mHz frequency drop) Turkey is expected to provide approx. 300 MW of primary control power to comply with the ENTSO-E rules. This value is adjusted by the power frequency characteristics of both systems.

The project "Rehabilitation of the Frequency Control Performance of Turkish Power System for Synchronous Operation with UCTE" concluded that the primary control concept of the Turkish Power System has to be redesigned: In order to fulfil diverging requirements (the Turkish power system as control area must be capable to activate its primary control within 30 seconds while maintaining the overall frequency stability) primary control should be provided by thermal units (TPP and NGCCPP) exclusively.

However, the sole allocation of primary control power to thermal units could cause undesired side-effects:

Hydro units (HPP) operating under active speed control react on frequency deviations and thus contribute unintentionally to primary control. Though this contribution is delayed (the speed controller of HPP exhibits generally transient gain reduction to facilitate stable operation), the total primary control contribution of the Turkish power system could exceed significantly the expected 300 MW. This could lead to the following problems

- Overloading of transmission lines

- Violation of limits with respect to the foreseen System Protection Scheme which will be implemented on the border between the Turkish Power System and the ENTSO-E-CE System.
- Decreased damping of inter-area oscillations

From the viewpoint of the interface between Turkey and ENTSO-E-CE this effect is temporarily as the secondary controller tries to maintain the desired power frequency characteristic: The generation picked up by HPP will be recognized as a component of the Area Control Error (ACE) and be backed off by the secondary controller in the steady state, i.e. there might be counteracting control actions.

In order to avoid this effect, different mitigation measures are possible:

- Optimised and coordinated allocation of primary control power to both thermal units (TPP, NGCCPP) and HPP, so that Turkey as control area shows the expected behaviour (this investigation is out of the scope of this study)
- Implementation of dead bands to deactivate the undesired contribution of HPP to primary control power. However, this approach implies that the speed controller is put out of action and what remains is a pure power controller with possibly negative effects on the system stability

In the next section the before mentioned effects are analyzed in detail by simulation. The following questions will be answered:

- What is approximately the amount of unintentional primary control power resulting from HPP?
- How does the interaction between primary and secondary control look like? Which measures can be recommended to avoid unnecessary (and uneconomical) control actions? In this regard, are large dead bands on HPP - speed controller tolerable from the perspective of system stability? Lead such dead bands to requirements for the parameterization of the remaining power controller (integration time constant, gain)? Besides dead bands, what can be recommended further?

➤ **Simulation results**

In order to answer these questions two scenarios / cases were set up for the parallel operation of the Turkish power system with the ENTSO-E-CE power system:

- Case 1: 3 GW generation loss in the ENTSO-E-CE system with primary control contribution according to the desired power frequency characteristic (approx. 300 MW allocated to (TPP, NGCCPP), impact of HPP deactivated by large dead bands)
- Case 2: 3 GW generation loss in ENTSO-E-CE system with primary control exceeding the desired contribution (approx. 300 MW allocated to (TPP, NGCCPP), but impact of HPP not deactivated)

The value of the dead band for case 1 and case 2 in the hydro power plants are ± 200 mHz and ± 20 mHz respectively.

As seen in figure 7-13 the amount of unintentional primary control power resulting from HPP is approx. 100 MW.

Figure 7-14 illustrates the opposing control actions due to the secondary controller which tries to maintain the desired "power frequency characteristic". So this study recommended that the value of K-factor of Turkey should increase to 1824 MW /Hz to decrease the unintentional primary control power and the area control error as resulted in figure 7-14 (red line).

With large dead band (± 200 mHz) the impact of HPP is deactivated and the amount of unintentional primary control power does not exceed 300 MW as shown in figure 7-13 but there will be a problem if the interconnection switches off; where the frequency will exceed 50 Hz in isolated operation as shown in figure 7-14. This study recommended that besides the dead bands there should be an increase in the integration time constant within the power controller for the rehabilitated hydro power plants to slow the power controller and then decrease the overall frequency as resulted in figure 7-15 (red line).

For case 1 the generation lost is 3 GW in the ENTSO-E-CE with high load condition in Turkish power system (25GW), secondary control reserve is 700 MW and primary control reserve is 300 MW (have contributed to TPP and NGCCPP).

For case 2 the generation lost is 3 GW in the ENTSO-E-CE with high load condition in Turkish power system (25 GW), secondary control reserve is 700 MW and primary control reserve is 300 MW (have contributed to TPP and NGCCPP) and 400 MW allocated to 100% to rehabilitated hydro units (see Table 7-1).

Table 7-1: Primary control power of the rehabilitated hydro power plants

Name of Power Plant	Rated Active Power	Contractual Reserve	Contractual Reserve	Physical Reserve	Droop	Working point	Real Primary Reserve
	[MW]	[% of rated power]	[MW]	[MW]	[%]		
Ataturk	2400	5	120	120	8	8x250	120
Karakaya	6x300	10	180	180	4	5x250	150
Birecik	6x112	5	34	34	5	4x100	22
Berke	3x170	5	26	51	4	2x150	34
Altinkaya	4x175	5	35	56	5	150	15
Hasan Ugurlu	500	5	25	50	4	220	25
Oymapinar	540	5	27	54	4	220	27
Total			447				393

Figure 7-13 shows the overall frequency performance of the Turkish and ENTSO-E-CE systems in Hz and exchange power of the Turkey for case 1 (continuous blue line) and case 2 (dashed blue line). For case 1 and case 2 it can be seen that the Turkish power system will deliver nearly 285 MW and 415 MW to ENTSO-E-CE system respectively.

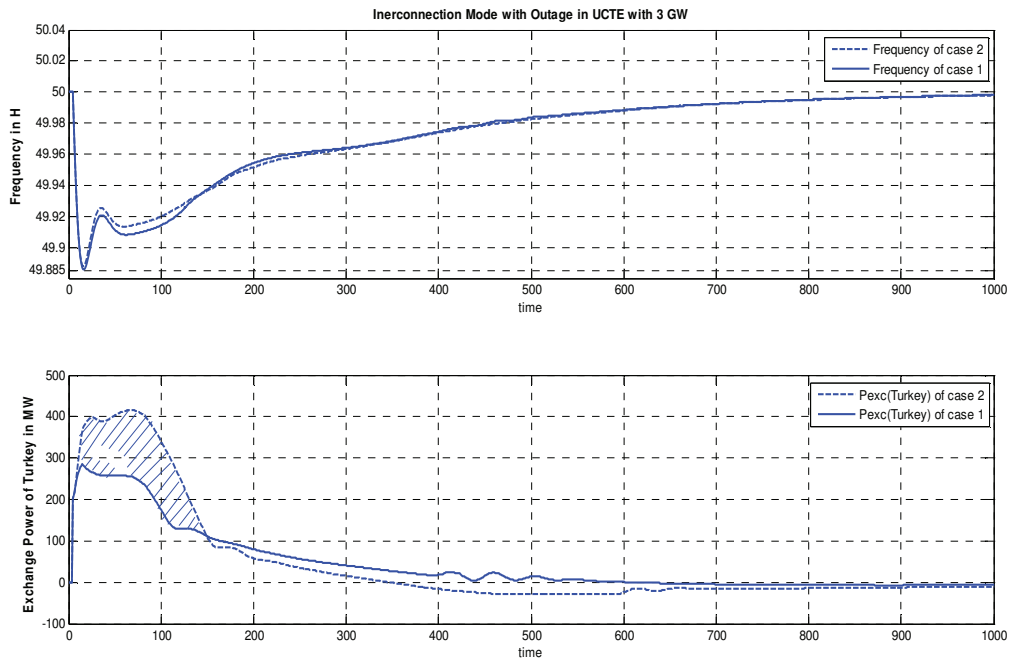


Fig. 7-13: The frequency and exchange power.

Figure 7-14 shows the signal of secondary control power in MW and the area control error (ACE) in MW for the Turkish power system.

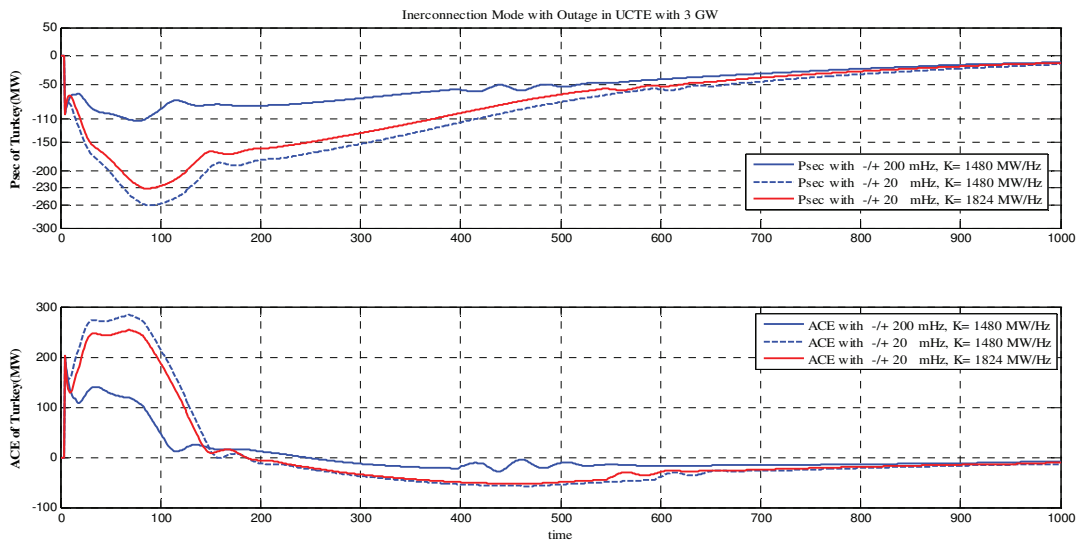


Fig. 7-14: The signal of secondary control and ACE for the Turkey system.

Figure 7-15 shows the overall frequency performance of the Turkish power system in island operation with 700 MW generation loss, secondary control reserve is 700 MW and the total amount of primary control reserve is 700 MW (300 MW have contributed to TPP ,NGCCPP and 400 MW allocated to 100% to rehabilitated hydro units). The simulations are performed using two cases for the 400 MW allocated to 100% to rehabilitated hydro units as resulted in figure 4-15.

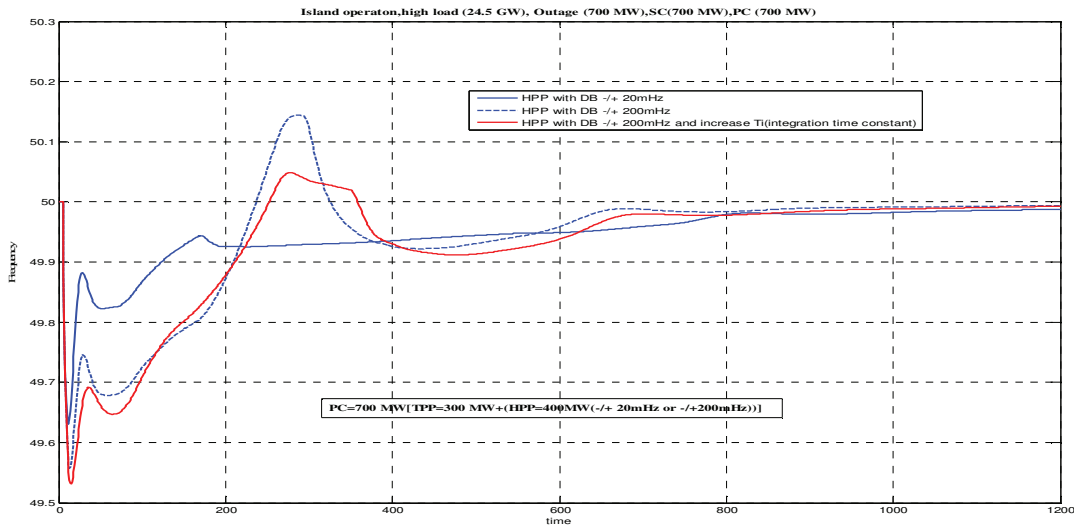


Fig. 7-15: The overall frequency performance in isolated Turkish power system.

7.2.3.5. Existing Load Variation of the Turkish Power System

- **Existing Load variation Measured on 16/06/2009**

The load variation was measured every 20 seconds on 16th of June 2009 and the working point with high load condition (24 GW). Figure 7-16 shows the load power in MW of the Turkish power system, the overall frequency performance in Hz and the exchange power in MW of the Turkish and ENTSO-E-CE systems.

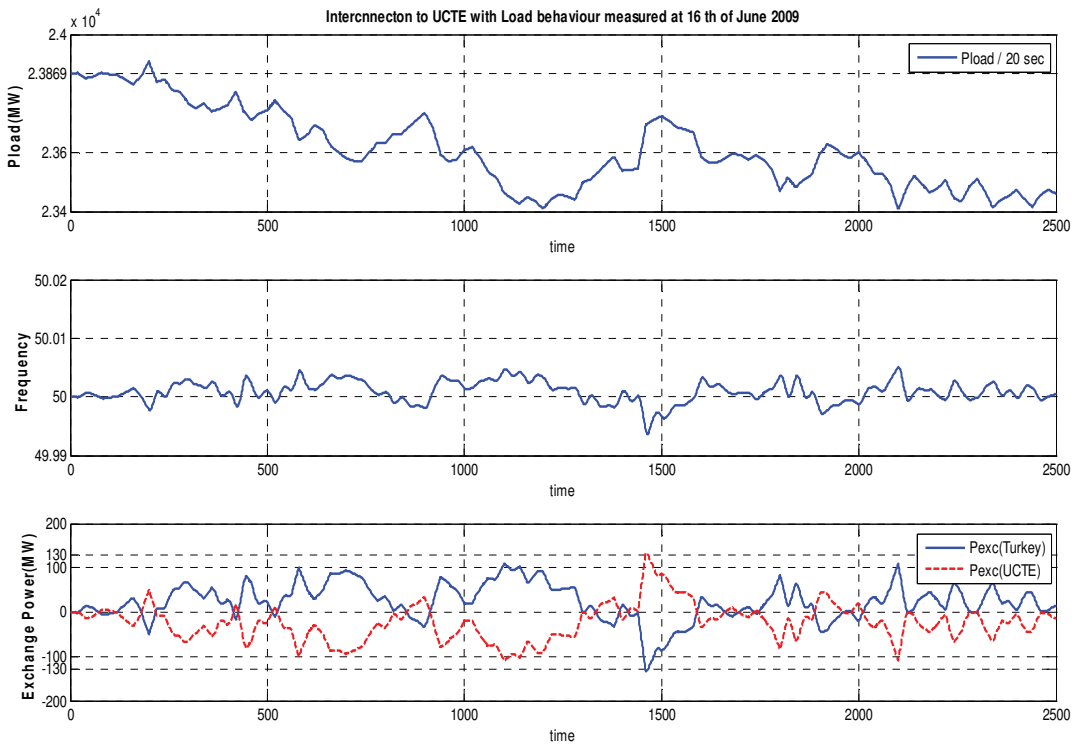


Fig. 7-16: The frequency and exchange power of the Turkish and ENTSO-E-CE systems.

- **Existing Load Variation Measured on 17/05/2010**

The load variation was measured every 10 seconds on 17th of May 2010 and the working point with high load condition (25 GW). Figure 7-17 shows the load power in MW of the Turkish power system, overall frequency performance in Hz and the exchange power in MW of the Turkish and ENTSO-E-CE systems.

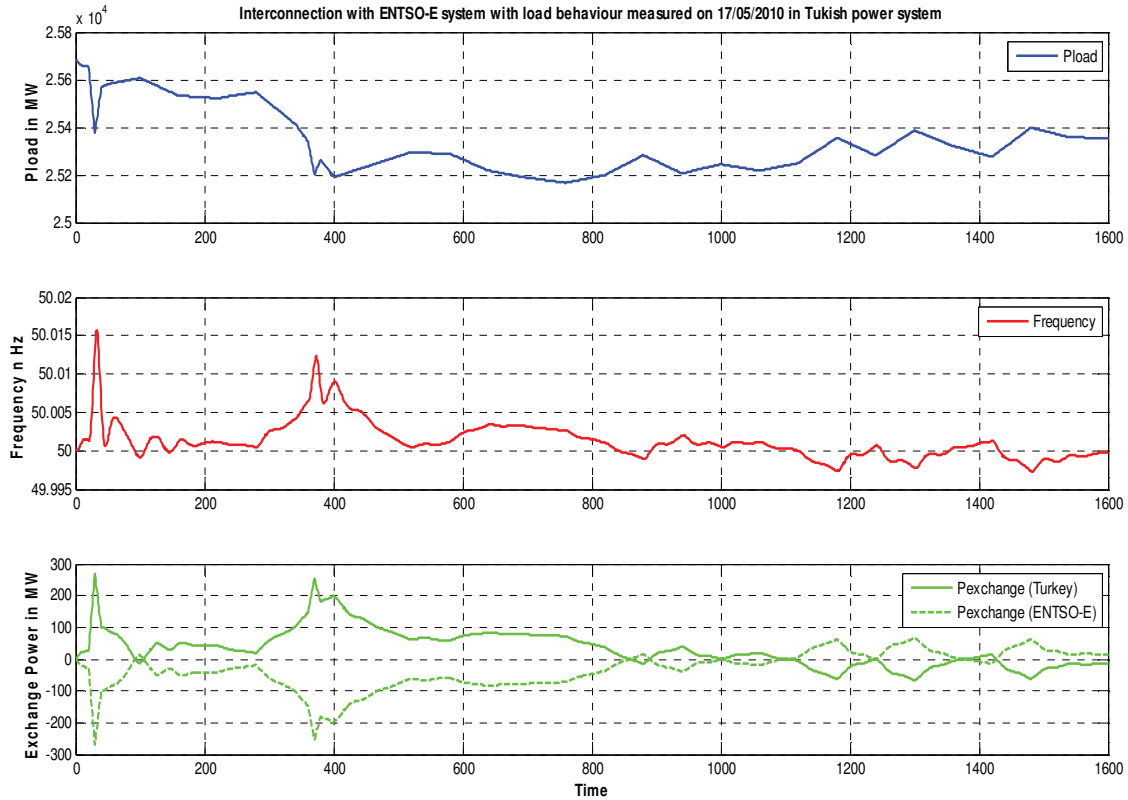


Fig. 7-17: The frequency and exchange power of the Turkish and ENTSO-E-CE systems.

As a result of the simulations (according to the existing load variations), it can be seen that the exchange power is between 0-250 MW and the frequency deviation is between $\pm(0 - 20$ mHz).

7.3. Current Status after Interconnection with ENTSO-E-CE System

On 18 September 2010 at 9h25 (CET) the Turkish power system was synchronized with the interconnected power systems of Continental Europe. In accordance with ENTSO-E procedures, during that period the security and performance of the interconnected systems will be monitored [94].

The trial parallel operation period will be divided into three phases:

1. Stabilization Period with no scheduled exchange of energy. This phase will last two weeks.
2. After the evaluation of the stabilization period, non-commercial energy exchange will be carried out between the Turkish system operator and respectively the Bulgarian and the Greek transmission system operators in both directions and at both borders. This phase will continue for two weeks.

3. Once these two phases are successfully accomplished, the trial operation period will proceed to Phase 3, in which limited capacity allocation for commercial electricity exchange between Turkey and ENTSO-E's Continental Europe Synchronous Area will be allowed.

7.3.1. The Stabilization Period

The parallel trial interconnected operation between the Turkish Power System and the ENTSO-E-CE system has started by 18th of September 2010.

The main objectives of the trial period are;

- Analyzing the stability of the interconnected network
- Observing, identifying and overcoming the possible practical problems regarding the equipment (both electrical and IT), software (fine tuning studies in the settings of the secondary controller, protection equipment etc.) and the personnel (operational routines and conventions).

The expected low frequency interarea modes between 0.1 Hz and 0.2 Hz are observed in the interconnected network. Although those oscillatory modes are damped out so as not to threat system security for the no exchange scenario, it is clear that enhancing the damping performance of the interconnected system against those modes are crucial for the reliability and the sustainability of the interconnection.

- a) 400MWs are inevitably wheeled (as expected) from Bulgaria to Greece over the Turkey interconnection due to the load flow scenario.
- b) Some inadvertent energy exchange has been observed throughout the first week of the parallel trial operation, which is well over the permitted value of 20MWHrs/hour. Figure 7-18 shows the amount of measured hourly inadvertent energy exchange between TPS and ENTSO-E CESA between 21.09.2010 and 24.09.2010. The most dominant factors that cause this phenomena can be listed as follows:
 - Settings of the secondary controller.
 - Mismatch between the forecasted demand and the realized demand, which causes imbalances in the market that can be overcome by enhanced demand forecast.
 - Significant instant demand changes (as much as 400MW) due to arc furnaces which can be overcome by coordinating the activity of the arc furnaces in the same facility in the first stage and throughout the system in the second stage.
 - Operational routines of the national load dispatch center personnel.

Hourly Unintended Energy Exchange

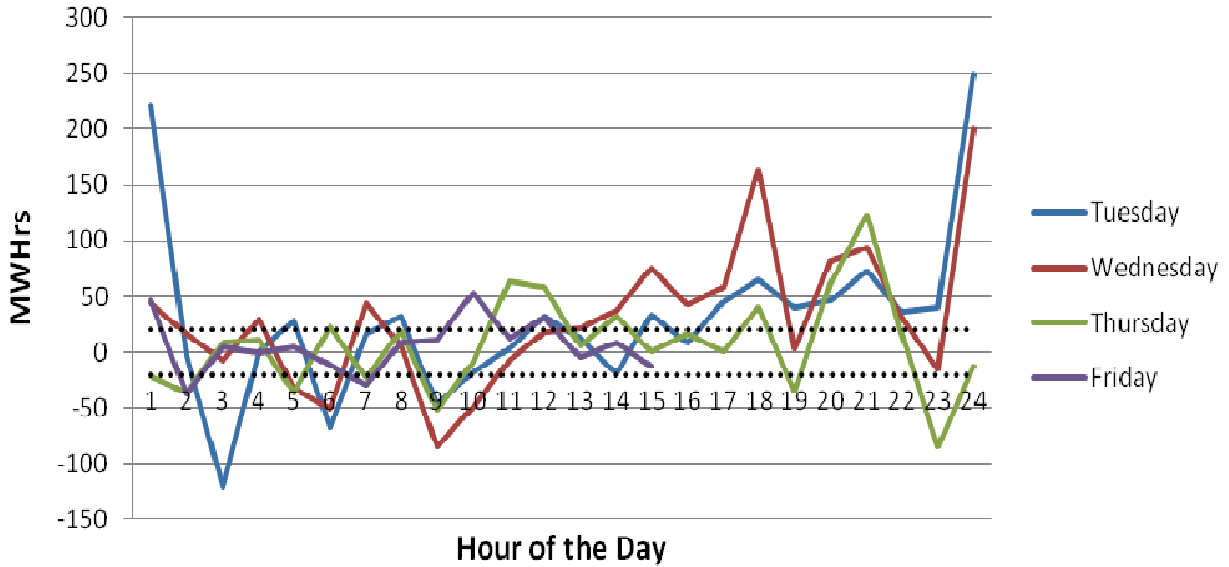


Fig. 7-18: Hourly Unintended Energy Exchange (21.09.2010 – 24.09.2010).

As can also be assessed from figure 7-19; the amount of hourly inadvertent energy exchange decreases at the end of the week with respect to the beginning of the week. The possible reasons of this phenomenon are analyzed as follows:

- The settings of the secondary controller are fine tuned in this period.
- The operators in the national dispatch center are better trained as their experience advance.

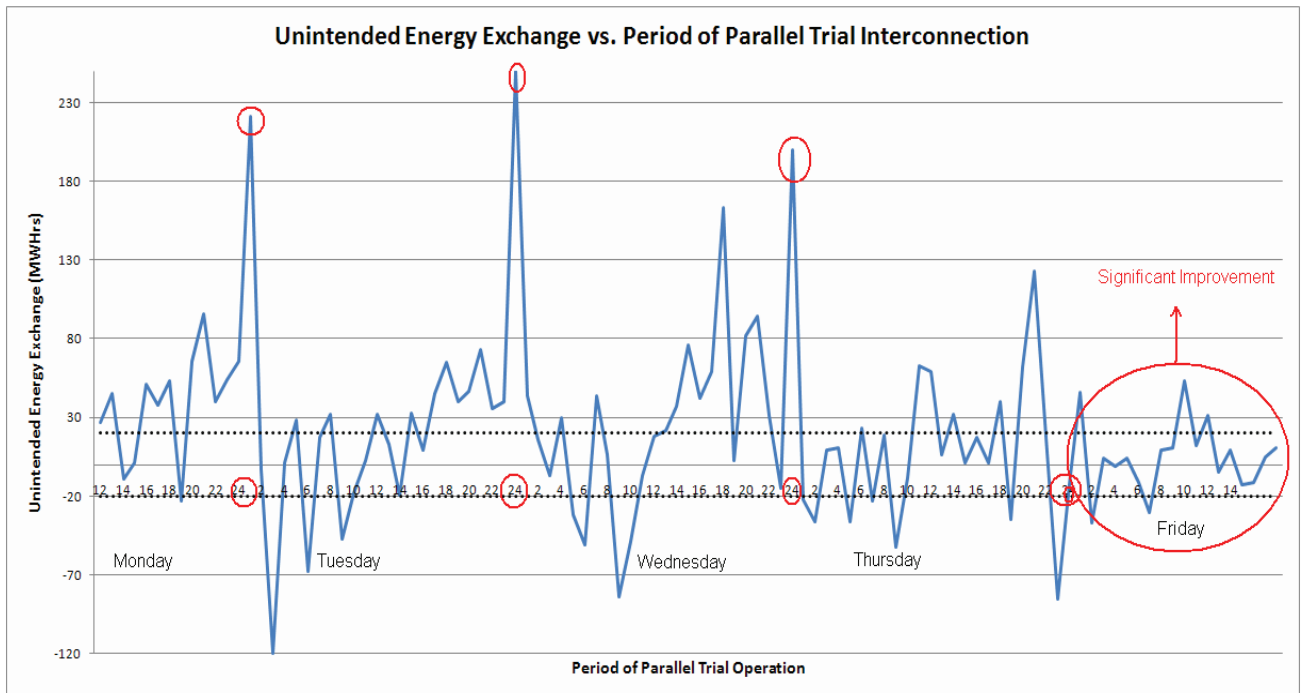


Fig. 7-19: Unintended Energy Exchange vs. Period of Parallel Trial.

CHAPTER 8

Conclusion

The connection of the Turkish power system with the ENTSO-E-CE (former UCTE), power system have been on the agenda of Turkey since 1975. In the past, tie lines were built with all neighbouring countries except Greece but the priority has always been given to the synchronous connection with the ENTSO-E-CE power system. None of these tie lines have been operated in synchronism and used only for energy exchanges with island supply and directed generation methods [29, 93].

The first feasibility study for investigation of the Turkish power system was successfully completed in 2007. Although according to the study results interconnection of the Turkish power system to ENTSO-E-CE system is found feasible but the necessity of the frequency control improvement in the Turkish power system and the sufficient damping performance of the generation units regarding low inter-area oscillations was emphasized as a precondition for reliable synchronous operation.

The process for investigation of the Turkish power system and the preparatory works for its synchronous interconnection to the ENTSO-E-CE network are progressing well under the coordination of the ENTSO-E-CE Project Group (Rehabilitation of Frequency Control Performance of Turkish Power System for Synchronous Operation with UCTE). A number of reports on the Turkish power system was finalized and approved. Besides the reporting activities, project group progressed with performing unit tests at the power plants. The unit tests of a hydro power plant type were finalized and approved. Unit tests of a conventional type thermal power plant were finalized and approved. Unit tests of a combined cycle natural gas type thermal power plant were finalized and approved [92].

The electric power system of Turkey as a candidate system for synchronization to ENTSO-E-CE should meet the requirements during island operation as well as following interconnection with the ENTSO-E-CE electricity transmission system [58]. For this purpose these work has evaluated the existing primary and secondary control on the Turkish power system through testing procedures and improvement the primary and secondary control of the Turkish power system for interconnected with the European system were performed. As a result, improvement of primary and secondary control of the Turkish power system concluded to the following:

- 1) The simulations results compared with the measurements, the models of the individual power plants (Ataturk and Oymapinar hydro power plants) and the overall model of the whole Turkish power system fits well with the measurements done in reality. This is true for the individual controllers of the plants and for the overall behaviour of the primary and secondary control of the whole Turkish power system. This holds in high and low load conditions. Finally, the model of Turkish power system is validated regarding the allocation of primary and secondary control. The oscillations of figure 1-3 for 20-30 seconds time period are reduced and the system can fulfil the requirements of the UCTE operational hand book.

- 2) From the phasor study method it can be concluded that the frequency performance of the Turkish Power System is sufficient and stable when all power plants (TPPs, GPPs and HPPs) are operating in parallel. Moreover there is no negative effect on the damping of the 7 seconds inter area oscillations expected to be observed after interconnection with the ENTSO-E-CE system: Negative effects of HPP are compensated by positive effects of TPP and NGCCPP.
- 3) The isolated tests in the Turkish power system in maximum load conditions were carried out successfully by TEIAS on 11-24 of January 2010. Similarly, the isolated tests in Turkish power system in minimum load conditions were carried out successfully by TEIAS on 22 of March - 04 April 2010
- 4) Due to the generation loss in the Turkish power system in isolated operation in high load conditions, the steady state frequency deviation (Δf_{state}) is less than 200 mHz, the maximum frequency deviation (Δf_{max}) is less than 800 mHz and stability of overall frequency.
- 5) For interconnection with ENTSO-E-CE system according to the outage in the Turkish power system with 700 MW and outage in ENTSO-E-CE with 1200 MW and 3 GW, the maximum frequency deviation (Δf_{max}) is less than 200 mHz and stability of overall frequency.
- 6) The allocation of secondary reserve to the units should be done taking into account that the use of hydro units for secondary control and of thermal units for primary control has more effective results for ensuring sufficient quality of power balance in the Turkish power system. The combined cycle plants can contribute to both primary and secondary control with coordinated ranges. During the island mode of operation of Turkish system it is required to have 700 MW of primary reserve and 300-400 MW secondary reserve under automatic control while during the parallel mode of operation it is required to have 300 MW of primary reserve, 300-400 MW secondary reserve under automatic control and about 400 MW of secondary reserve that can be activated manually within 15 minutes.
- 7) Findings of tests resulted in the conclusion that new control systems were required to be installed in specific hydro power plants (Ataturk, Karakaya), as appropriate interface equipment, for their active production remote control and to be supported by better SCADA communication links. It is noticed that these hydro plants have a very important contribution in the performance of secondary control in the Turkish power system.
- 8) It was needed to change the values of several parameters of the AGC in order to improve the secondary control performance and to comply with the ENTSOE-E-CE requirements. In particular, have been changed the values of frequency bias K for the calculation of ACE (current value 1800 MW/Hz instead of initial value 1100 MW/Hz), of all the parameters of the central PI controller: normal gain (current value 0.5 instead of initial 0.75), dead band for the use of small gain (current value zero instead of previous 5 MW), integration time constant (current value 70 sec instead of initial 40 sec) and the modelling parameters for a lot of power plants. Moreover, it has been done an assignment of units with similar response rate in three

classes of generating units when calling up secondary reserves. This had as a result that the overall response is not dictated by the slower units while also the control commands to a lot of units are minimized.

- 9) The secondary control performance has improved significantly with the above mentioned measures and it co-operates well with the improved primary control that is performed by the units of the Turkish power system after the rehabilitation works that have been done in a lot of units and the increased contribution of more power plants to frequency control after ancillary services contract with TEIAS came into force. The overall performance of the load frequency control of the Turkish power system has improved significantly, as it is proved by the associated statistical indices and most important by the successful isolated tests during maximum and minimum conditions according to the respective rules of the ENTSO-E-CE
- 10) In view of the parallel operation of the Turkish power system, after interconnection, it has been tested the functionality of AGC system under the appropriate mode ("Tie line Bias" mode) with fictitious values in interconnection line field measurements and also some fictitious interchange schedules. After the isolated tests were carried out successfully it was suggested to compute the K-factor of the Turkish AGC according to the ENTSO-E-CE relevant procedures. According to the latest calculation of the coefficients $C_i - P_{pi} - K_{ri}$ for the year 2010 and using net generation in the ENTSO-E-CE is 2688 TWh and net generation in Turkey 198.4 TWh the K-factor for the Turkish AGC is calculated as: $K = (198.4/2886) \times 26530 = 1824 \text{ MW/Hz}$.
- 11) It is suggested that ENTSO-E-CE system frequency will calculate for the year 2011 the coefficients $C_i - P_{pi} - K_{ri}$ for all member countries without taking into consideration the interconnection of the Turkey for the trial parallel operation. The primary reserve of Turkey (P_{pi}) will be assigned to 300 MW and the K_{ri} will assigned to 1824 MW/Hz from September 2010 to the end of 2011. Starting from 2012 Turkey will be integrated normally in the Table of ENTSO-E-CE.
- 12) With the MATLAB model, the simulation tool in order to be used for a rough estimation of AGC performance of the Turkish power system in parallel operation with the ENTSO-E-CE system and for an advisory tuning of basic AGC parameters. Results, for various study cases have been derived. These study cases assume that K-factor of the Turkey will be set 1824 MW/Hz as concluded using the methodology of ENTSO-E-CE Frequency. The suggestion for the parameters of the central AGC controller for the period of parallel operation is that the normal signal gain in the Turkish AGC should be set to 0.5 while the desired common unit response time should be set to 80 seconds.
- 13) The amount of unintentional primary control power resulting from HPP is approx. 100 MW and the opposing control actions due to the secondary controller tries to maintain the desired "power frequency characteristic". So this study recommended that the value of K-factor of Turkey increases to 1824 MW /Hz to decrease the unintentional primary control power and the area

control error.

- 14) With large dead band (± 200 mHz) the impact of HPP is deactivated and the amount of unintentional primary control power does not exceed 300 MW but there will be a problem if the interconnection switches off; where the frequency will exceed 50 Hz in island operation. So this study recommended that besides the dead bands there should be an increase in the integration time constant within the power controller for the rehabilitated hydro power plants to slow the power controller and then decrease the overall frequency.

On 18 September 2010 at 9h25 (CET) the Turkish power system was synchronized with the interconnected power systems of Continental Europe. The date thus marks the beginning of the parallel interconnection foreseen to last one year. In accordance with ENTSO-E procedures, during that period the security and performance of the interconnected systems will be monitored [94].

REFERENCES

1. The Energy Information Administration (EIA), International Energy Outlook, July 2010, www.eia.gov/oiaf/ieo/index.html.
2. Wikipedia, Power Station, 2010. [Online], Available: http://en.wikipedia.org/wiki/Power_station, 2010
3. British Electricity International, Modern Power Station Practice: incorporating modern power system practice (3rd Edition (12 volume set) ed.), 1991
4. Babcock & Wilcox Co, Steam: Its Generation and Use (41st edition ed.), (2005).
5. Thomas C. Elliott, Kao Chen, Robert Swanekamp (co-authors) (1997). Standard Handbook of Power plant Engineering (2nd edition ed.), McGraw-Hill Professional.
6. C. Gencoglu, Assessment of the effect of hydroelectric power plants governor settings on low frequency inter-area oscillations, Ms Thesis, Middle East Technical University, July. 2010.
7. Final Report Stability Study, Complementary technical studies for the synchronization of the Turkish power system with the UCTE Power System, 2007.
8. I. A. Nassar, H. Weber, Electrical Interconnection between Turkey and Europe: Problems and Solutions, 13th Middle East Power Systems Conference, Assuit University, Egypt, December 20-23, 2009, Pages 1-11.
9. Varadarajan Atur, David Kennedy, Review of electricity supply and demand in Southeast Europe, World Bank Working Paper, 2004.
10. UCTE Operation Handbook – Policy 1: Load-Frequency Control - Final Version (approved by Study Committee on 19 March 2009)
11. UCTE Operation Handbook–Appendix 1: Load-Frequency Control, (final 1.9 E, 16.06.2004)
12. Policy 1–Load-Frequency Control and Performance (Preliminary v. 1.2, draft, 03.10.2002)
13. UCTE Operation Handbook –Policy 1:Load-Frequency Control and Performance (final draft 1.9 E, 31.12.03)
14. UCTE Operation Handbook–Appendix 1- LF Control and Performance, (Preliminary v. 1.2, draft, 02.10.2002).
15. Adriano GUBERNALI, the Defence Plans against propagation of disturbances of vast interconnected power systems, PhD thesis, Rome, Italy, 2003
16. <http://www.worldatlas.com/webimage/countrys/asia/trlarge.htm>
17. Ministry of Environment and Forestry, First national communication of Turkey on climate change, (Eds. Apak, G., Ubay, B), MEF, Ankara, Turkey, 2007.

References

18. EIA International Petroleum Monthly, 2009, <http://www.eia.doe.gov/>,
19. Ministry of Energy and Natural Resources (ETKB), <http://www.enerji.gov.tr>
20. Kaygusuz K, Turker MF, Biomass energy potential in Turkey, *Renew Energy*, Volume 26, Issue 4, August 2002, Pages 661-678.
21. Fikret Akdeniz, Atila Çal and Doğan Güllü, Recent energy investigation on fossil and alternative nonfossil resources in Turkey, *Energy Conversion and Management*, Volume 43, Issue 4, March 2002, Pages 575-589.
22. Selçuk Bilgen, Sedat Keleş, Abdullah Kaygusuz, Ahmet Sarı, Kamil Kaygusuz, Global warming and renewable energy sources for sustainable development: A case study in Turkey, *Renewable and Sustainable Energy Reviews*, Volume 12, Issue 2, February 2008, Pages 372-396.
23. E. Toklu, M.S. Güney, M. Işık, O. Comaklı, K. Kaygusuz, Energy production, consumption, policies and recent developments in Turkey, *Renewable and Sustainable Energy Reviews*, Volume 11, Issue 6, August 2007, Pages 1312-1322; Volume 14, Issue 4, May 2010, Pages 1172-1186.
24. Arif Hepbasli, Development and restructuring of Turkey's electricity sector: a review, *Renewable and Sustainable Energy Reviews*, Volume 9, Issue 4, August 2005, Pages 311-343.
25. Tunc M, Camdali U, Liman T, Deger A., Electrical energy consumption and production of Turkey versus world, *Energy Policy*, Volume 34, Issue 17, November 2006, Pages 3284-3292.
26. Havva Balat, A renewable perspective for sustainable energy development in Turkey: The case of small hydropower plants, *Renew Sustain Energy Reviews*, Volume 11, Issue 9, December 2007, Pages 2152-2165.
27. Ibrahim Yüksel, Hydropower in Turkey for a clean and sustainable energy future, *Renewable and Sustainable Energy reviews*, Volume 12, Issue 6, August 2008, Pages 1622-1640.
28. Balat M, Balat H, Acici N, Thermal- electricity power plants in Turkey, *Energy Exploration Exploitation*, Volume 22, Number 2004, Pages 367-376.
29. Standard Summary Project Fiche IPA Decentralised National Programmes, Project number: TR 07 02 05, Frequency control performance, Jun 2006
30. Ibrahim Yüksel, Hydropower for sustainable water and energy development, *Renewable and Sustainable Energy Reviews*, Volume 14, Issue 1, January 2010, Pages 462-469.
31. Durmus Kaya, Renewable energy policies in Turkey, *Renewable and Sustainable Energy Reviews*, Volume 10, Issue 2, April 2006, Pages 152-163.
32. The Central Intelligence Agency (CIA), <https://www.cia.gov/>
33. World bank, <http://www.worldbank.org/tr>

References

34. Energy Market Regulatory Authority of Turkey (EMRA), Electricity market grid regulation, Ankara, 2003, www.epdk.gov.tr/english/regulations/electric/grid/grid.doc, August 2010
35. M. E. Cebeci, The Effects of Hydro Power Plants' governor Settings on the Turkish Power System Frequency, Ms Thesis, Middle East Technical University, Feb. 2008.
36. <http://www.euas.gov.tr/>
37. <http://www.enkapower.com/santraller.htm>
38. SAF 2009-2020: Report - System Adequacy Forecast 2009 – 2020, January 2009
39. UCTE, UCTE Operation Handbook – Introduction (final v2.5 E, 24.06.2004)
40. ENTSO, UCTE - Union for the Coordination of the Transmission of Electricity, 2009, <http://www.entsoe.eu/index.php?id=102>
41. UCTE, Statistical Yearbook UCTE, 2004
42. ENTSO, ENTSO-E Member Companies, 2009, <http://www.entsoe.eu/index.php?id=15>
43. UCTE, UCTE Transmission Development Plan, 2008
44. ENTSO, ENTSO-E Member Companies, 2009, <https://www.entsoe.eu/index.php?id=10>
45. ENTSO, 50 Hertz: a delicate balance, 2009, <http://www.entsoe.eu/index.php?id=108>
46. E.W. KIMBARK, Power System Stability, Vol I, II and III, John Wiley & Sons, Inc., New York, 1948.
47. P. KUNDUR, Power System Stability and Control, McGraw Hill (EPRI Power System Engineering Series), New York, 1994.
48. UCTE OH–Policy 1: Load-Frequency Control and Performance (final policy 2.2 E, 20.07.2004)
49. Angelo Baggini, Handbook of power quality, University of Bergamo, Italy, 2008.
50. Bogdan Lucus, Luís Filipe de Castro Ribeiro and Paul Brown, Load-Frequency Control, UCTE Operation Handbook, Porto, May 2005
51. Jan Machowski, Janusz W. Bialek, James R. Bumby, Power system dynamics: stability and control, 2008.
52. Evangelos Lekatsas, Energy cooperation among the SEE energy community treaty stats, 3rd SE Europe Energy Dialogue, Thessaloniki, June 18-19th, 2009.
53. Interim-Report Stability Study, Complementary Studies for the Synchronization of the Turkish Power System with UCTE System, 2006.
54. I. A. Nassar, H. Weber, Dynamic Model of Unit 1 of Ataturk Hydro Power Plant in Turkey, 13th Middle East Power Systems Conference, Assuit University, Egypt, December 2009,

References

55. Ibrahim A. Nassar , S. Al-Ali and Harald Weber, The Overall Frequency Behaviour of the Turkish Power System in Island Operation to Interconnection with European System, 13 Symposium Maritime, 2010, Rostock, Germany, pp.155-169
56. P.L. Dandeno, P. Kundur and J.P. Bayne, Hydraulic Unit Dynamic Performance under Normal and Islanding Conditions - Analysis and Validation, IEEE Transactions on Power Apparatus and Systems, Vol. PAS-97, No. 6, Nov/Dec 1978, Pages 2134-2143.
57. Nand Kishor, R.P. Saini and S.P. Singh, A review on hydropower plant models and control, Renewable and Sustainable Energy Reviews, Volume 11, Issue 5, June 2007, Pages 776-796.
58. MEDRING Update: Volume II- Analysis and Proposals of Solutions for the Closure of the Ring and North-South Electrical Corridors, Final draft, April 2010.
59. Mathworks Company, www.mathwork.com, 2010.
60. Nand Kishor, R.P. Saini and S.P. Singh, A review on hydropower plant models and control, Renewable and Sustainable Energy Reviews, Volume 11, Issue 5, June 2007, Pages 776-796.
61. S. C. TRIPATHY and V. BHARDWAJ, Automatic generation control of a small hydro-turbine driven generator, Energy Conversion, Mgmt Vol. 37, No. 11, pp. 1635--1645, 1996.
62. J.J. Grainger and W. D. Stevenson, Power System Analysis, New York: McGraw- Hill, 1994.
63. IEEE Working Group, Hydraulic turbine and turbine control models for system dynamic studies, IEEE Transactions on Power Systems, Vol. 7, No. 1, 167-179, Feb 1992.
64. İ. Eker, Governors for hydro-turbine speed control in power generation: a SIMO robust design approach, Energy Conversion, Mgmt 45 (2004), pp. 2207–2221.
65. Eker I, Tumay M., Robust multivariable-cascade governors for hydro turbine controls, Electrical Eng 2002, 84(4):229–37.
66. Quiroga, Oscar Daniel, Modelling and nonlinear control of voltage frequency of hydroelectric power plants, PhD Thesis, University of Catalonia , October 2000
67. Hydroelectric Power Plants in Southern Turkey, Retrieved on 2008-02-02. http://en.wikipedia.org/wiki/Atatürk_Dam
68. Helen Chapin Metz, ed. Turkey: A Country Study. Washington: GPO for the Library of Congress, 1995. <http://countrystudies.us/turkey/>
69. Tourism net, Retrieved on 2008-02-02. <http://countrystudies.us/turkey/>
70. The Tigris & Euphrates Basin, Vital Facts: Water Resources and Middle East. Retrieved on 2008-02-02. http://en.wikipedia.org/wiki/Atatürk_Dam
71. O. B. Tor, U. Karaagac, E. Benlier, Step-Response tests of a unit at Ataturk hydro power plant and

References

- investigation of the simple representation of unit control system, IEEE PES, 36th North American Power Symposium, University of Idaho, Moscow, USA, Aug. 2004.
72. Mansoor, S. P., Modelling and simulation of a hydro-power station, PhD Thesis, University of Wales, Bangor, 2000.
73. http://www.roymech.co.uk/Related/Fluids/Fluids_Machines.html
74. Issam Salhi, Said Doubabi, Fuzzy controller for frequency regulation and water energy save on micro-hydro electrical power plants, International Renewable Energy Congress, November 5-7, 2009 - Sousse Tunisia.
75. Edson C Bortoni; Guilherme S Bastos; Luiz E Souza, Optimal load distribution between units in a power plant, ISA transactions, Vol. 46, Oct. 2007, Pages 533-539.
76. E. De Jaeger N. Janssens B. Malfliet F. Van De Meulebroeke, Hydro turbine model for system dynamic studies, IEEE Transactions on Power Systems, Vol. 9, No. 4, November 1994.
77. IEEE Committee Report, Dynamic Models for Steam and Hydro Turbines in Power System Studies, IEEE Transactions on Power Apparatus and Systems, 1973.
78. F. R. Schleif AND A. B. Wilbor, The Coordination of Hydraulic Turbine Governors for Power System Operation, IEEE Transactions on Power Apparatus and Systems, vol. Pas-85, no.7, pp. 750–758, July 1966.
79. O. Yılmaz, M. E. Cebeci, C. Gençoglu, D. Gezer, EÜAS Berke Hydroelectric Power Plant: Study Report on Field Tests for Evaluating Primary Frequency Control Performance, TUBITAK Space Technologies Research Institute Power Systems Group, Ankara, Turkey, Aug. 2009.
80. O. Yılmaz, M. E. Cebeci and Müfit Altin, Atatürk Hydroelectric Power Plant: Tests on Unit 1 Governor, TUBITAK Space Technologies Research Institute Power Systems Group, Ankara, Turkey, February 2009.
81. IEC: 60308(1970): International Code for Testing of Speed of Governing Systems for Hydraulic Turbines.
82. Oymapinar Dam, Internet Database and Gallery of Structures, Retrieved 2006-11-19. http://en.wikipedia.org/wiki/Oymapinar_Dam
83. Oymapinar Dam, Turkey Odyessy, Retrieved 2006-11-19. http://en.wikipedia.org/wiki/Oymapinar_Dam
84. Kevser SENTURK, Funda ORUC KOCYIGIT, A Case Study: Evaporation Estimation at Oymapinar Dam, BALWOIS 2010 Conference, 25-29 May 2010, Ohrid, Republic of Macedonia
85. O. B. Tor, O. Yılmaz and Müfit Altin, Oymapinar Hydroelectric Power Plant: Tests on Unit Governor and PSS, TUBITAK Space Technologies Research Institute Power Systems Group,

References

- Ankara, Turkey, December 2008.
86. O. Yılmaz, M. E. Cebeci and Müfit Altın, Karakaya Hydroelectric Power Plant: Tests on Unit 1 Governor, TUBITAK Space Technologies Research Institute Power Systems Group, Ankara, Turkey, May 2009.
 87. O. Yılmaz, M. E. Cebeci, M. Altın and C. Gençoglu, Birecik Hydroelectric Power Plant: Study Report on Field Tests for Evaluating Primary Frequency Control Performance, TUBITAK Space Technologies Research Institute Power Systems Group, Ankara, Turkey, June. 2009.
 88. O. Yılmaz, M. E. Cebeci, C. Gençoglu, Altınkaya Hydroelectric Power Plant: Field Test Study Report, TUBITAK Space Technologies Research Institute Power Systems Group, Ankara, Turkey, Oct. 2009.
 89. O. Yılmaz, M. E. Cebeci, C. Gençoglu, Hasan Ugurlu Hydroelectric Power Plant: Field Test Study Report, TUBITAK Space Technologies Research Institute Power Systems Group, Ankara, Turkey, Oct. 2009.
 90. O. Tor, O. Yılmaz and M. E. Cebeci, Afsin Elbistan B Thermal Power Plant Governor Step Response Tests Report, TUBITAK Space Technologies Research Institute Power Systems Group, Ankara, Turkey, Oct. 2007.
 91. B Roffel, WW de Boer, Analysis of power and frequency control requirements in view of increased decentralized production and market liberalization, Control Engineering Practice, Volume 11, 2003, Pages 367–375.
 92. UCTE Annual Report , System Extension Studies and Projects, 2008
 93. Interim Evaluation Team Turkey, Infrastructure, Energy, Telecommunications, Transport, & Environment, November 2006
 94. ENTSO-E News, Brussels, 20.09.2010,
https://www.entsoe.eu/index.php?id=42&tx_ttnews%5Btt_news%5D=71&tx_ttnews%5BbackPid%5D=28&cHash=432e472e177cb2ccf47006e286712a0a
 95. A. Holst, M. Golubovic, H. Weber , Dynamic model of hydro power plant Djerdap I in serbia, International Youth Conference on Energetic (IYCE 2007), 31 May-2 June, 2007, Budapest, Hungary.
 96. Prillwitz, F., A. Holst, H. Weber, Reality oriented simulation models of the hydro power plants in Macedonia and Serbia / Montenegro, Annual scientific session with international participation, 07-09.10.2004, Varna, Bulgaria.
 97. Prillwitz, F., H. Weber, Simulation models of the hydro power plants in Macedonia and Yugoslavia, IEEE Power Tech, Bologna 2003, Italy

References

98. Prillwitz, F., S. Al-Ali, T. Haase, H. Weber, L. Saqe, Simulation model of the hydro power plant Shkopeti, 6th EUROSIM Congress on Modelling and Simulation, September 9-13, 2007, Ljubljana/Slovenia.
99. Weber, H., M. Hladky, T. Haase, S. Spreng and C. Moser, High quality modelling of hydro power plants for restoration studies, IFAC-Symposium on Power Plants and Power Systems Control, July 21-26, 2002, Barcelona, Spain.
100. Weber, H., V. Fustik, F. Prillwitz, A. Iliev, Practically oriented simulation model for the hydro power plant "Vrutok" in Macedonia, 2nd Balkan Power Conference, 19-21.06. 2002, Belgrade, Yugoslavia.
101. Weber, H., H.-P. Asal and E. Grebe, Characteristic numbers of primary control in the UCPTE power system and future requirements, ETG '97 summer meeting, July 21-22, 1997, Berlin, Germany.
102. Weber, H., D. Zimmermann, Investigation of the dynamic Behaviour of a high pressure hydro power plant in the Swiss Alps during the transition from inter-connected to isolated Operation, 12th Power Systems Computation Conference, 19-20. August 1996, Dresden.
103. Marc Soullière, Marc Langevin and Jean Bélanger, A Real-time regulator, turbine and alternator test bench for ensuring generators under test contribute to whole system stability, Planet-RT July 2009.

Table A-1: Parameters of Ataturk HPP Model

Parameters	Variable in Matlab	Definition	Ataturk Value
Mechanical			
	Tg_HPP	Mech. time con.	10
	ata_BLT	Backlash	± 50 mHz
Penstock			
	Tw	Water time con.	3
	Tl	Water wave travel time	0.38
	Rr	Friction con.	0.05
Power Control			
	Tp_HPP	Integral time con.	120
	Kacc	Acc. input gain	4
	Tacc	Acc. time	0.3
	Sigma_HPP_Pcon	Power control speed droop	0.08
	r	Transient Gain	0.12
	Tn	Transient time	100
Governor			
	deadband_HPP	Deadband (only in speed control)	0 mHz
	Sigma_HPP	Speed droop	0.08
Position Control			
	P2	Proportional gain	6
	Ti2	Integral time con.	1
	D2	Derivative gain	0
	Tpilot	Pilot Servo time con.	0.5
	Tmain	Main Servo time con.	1.1
	Rate	Opening time of wicket gate from 0 to 100%	28

■ Structure of Birecik HPP

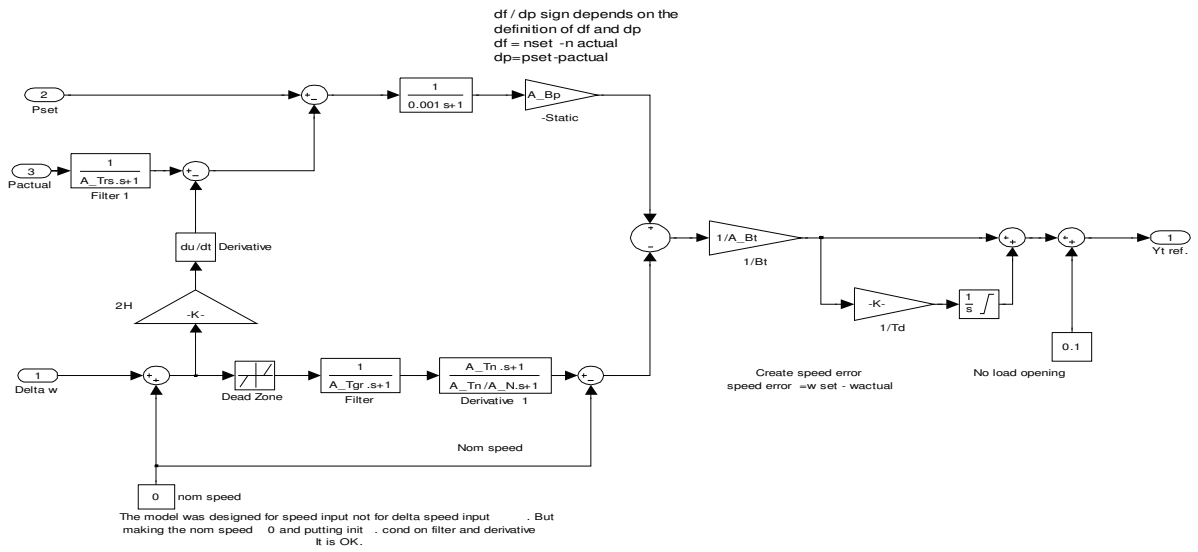


Fig. A-4: Power Control Model of Birecik HPP.

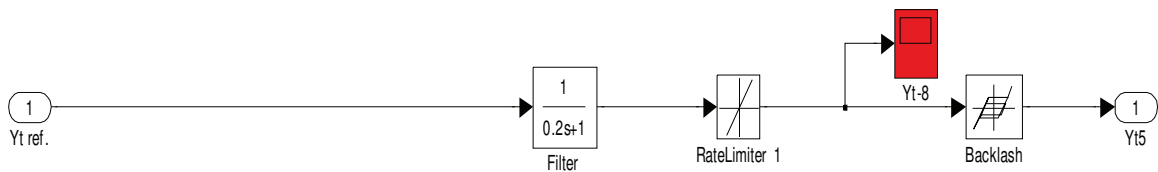


Fig. A-5: Governor Model of Birecik HPP.

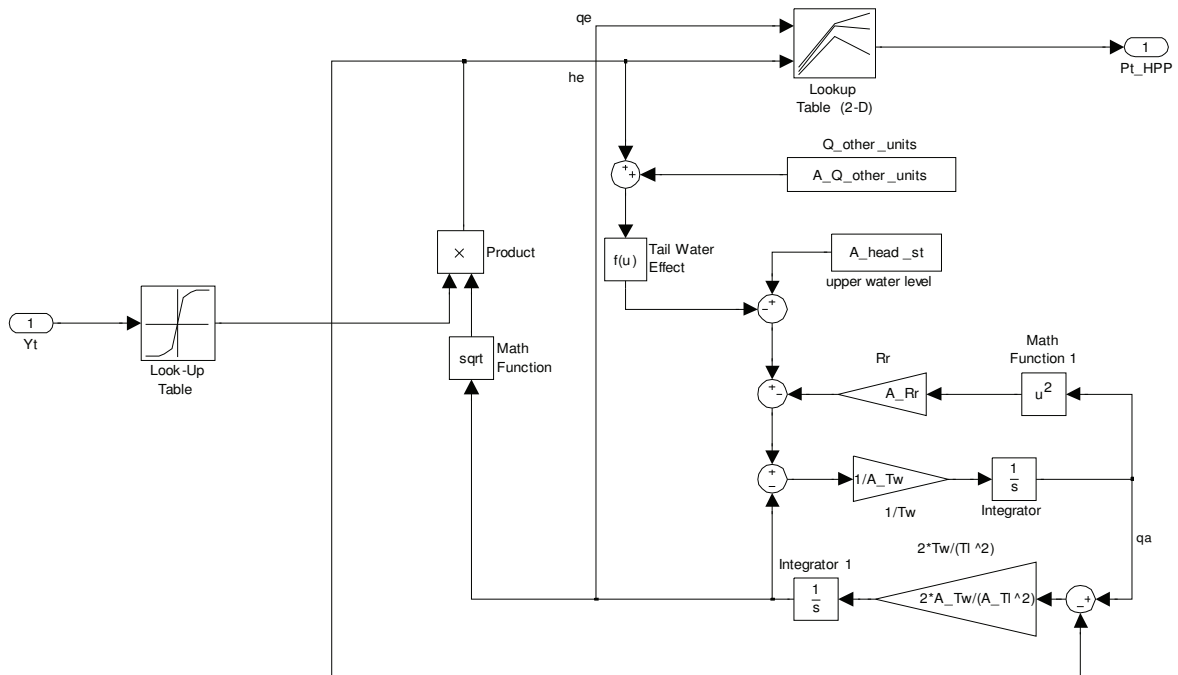


Fig. A-6: Turbine Model of Birecik HPP.

Appendix A

Table A-2: Parameters of Birecik HPP Model

Parameters	Variable in Matlab	Definition	Birecik Value
Mechanical			
	A_Tg_HPP	Mech. time con.	7
	A_BLT	Backlash	± 50 mHz
Penstock	A_Tw	Water time con.	2.17
	A_Tl	Water wave travel time	0.0573
	A_Rr	Friction con.	0.0143
Speed & Power Controller			
	A_Bp	Permanent Droop	0.05
	A_Bt	Transient Droop	0.45
	A_Td	Integration time constant	1
	A_N	Acceleration Gain	10
	A_Tn	Acceleration time constant	1
	A_Tgr	Time constant of the frequency filter	0.1
	A_TrS	Power measurement filter time constant	2
	deadband_HPP_A	Dead band	± 20 mHz
Governor			
	A_Topen		20
	A_Tclose		9
	A_Tmain	Main Servo time con.	0.1
	A_Tdist	Distribution valve time con.	0.2

▪ Structure of Keban HPP

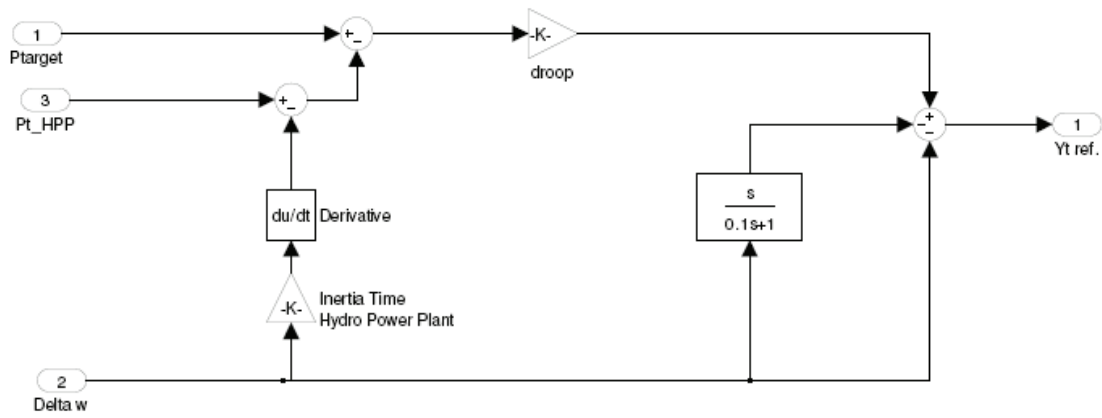


Fig. A-7: Power Control Model of Keban HPP.

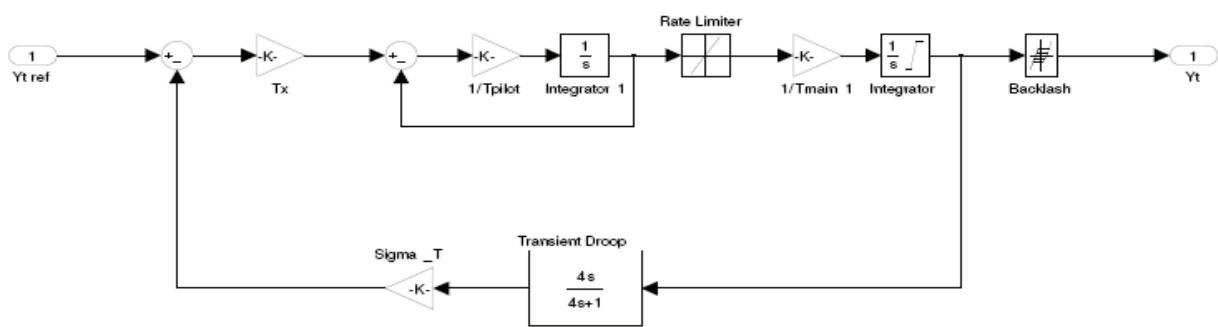


Fig. A-8: Governor Model of Keban HPP

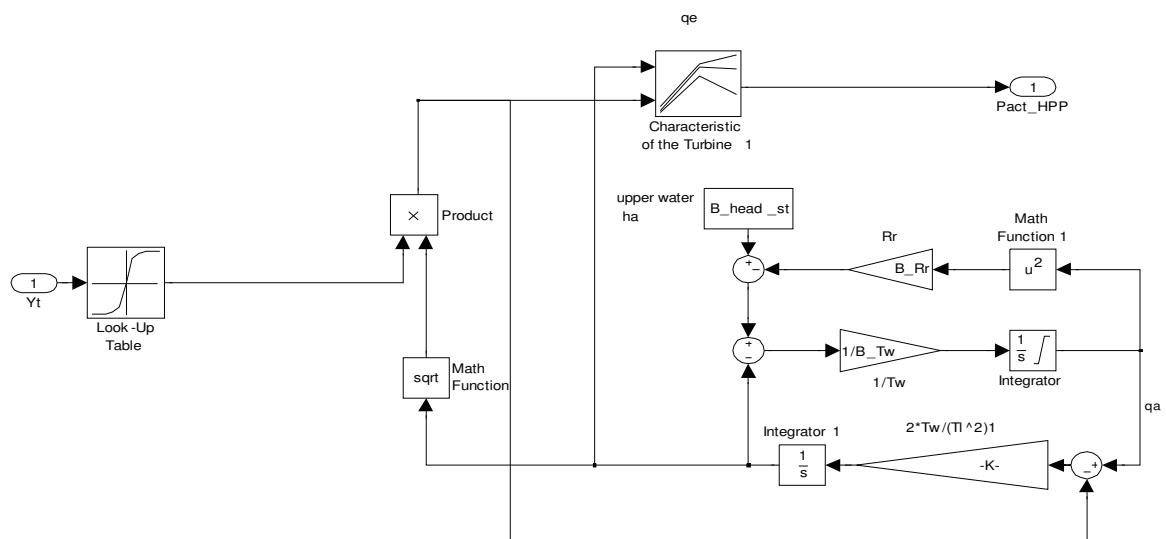


Fig. A-9: Turbine Model of Keban HPP.

Table A-3: Parameters of Keban HPP Model

Parameters	Variable in Matlab	Definition	Keban Value
Mechanical			
	B_Tg_HPP	Mech. time con.	5
	B_BLT	Backlash	± 50 mHz
Penstock	B_Tw	Water time con.	2.5
	B_Tl	Water wave travel time	0.7
	B_Rr	Friction con.	0.025
Power Control			
	B_Kacc_HPP	Acc. input gain	10
	B_Tacc_HPP	Acc. input time con.	1
	B_Sigma_HPP	Power control speed droop	.05
	deadband_HPP_B	Deadband	± 20 mHz
Governor			
	B_Sigma_T	Transient droop	.7
	B_Td	Transient time constant	4
	B_Tx		.52
	B_Tpilot_HPP	Pilot Servo time con.	0.1
	B_Tmain_HPP	Main Servo time con.	0.1
	B_Rate_HPP	Opening time of wicket gate from 0 to 100%	10

■ Structure of Altinkaya HPP

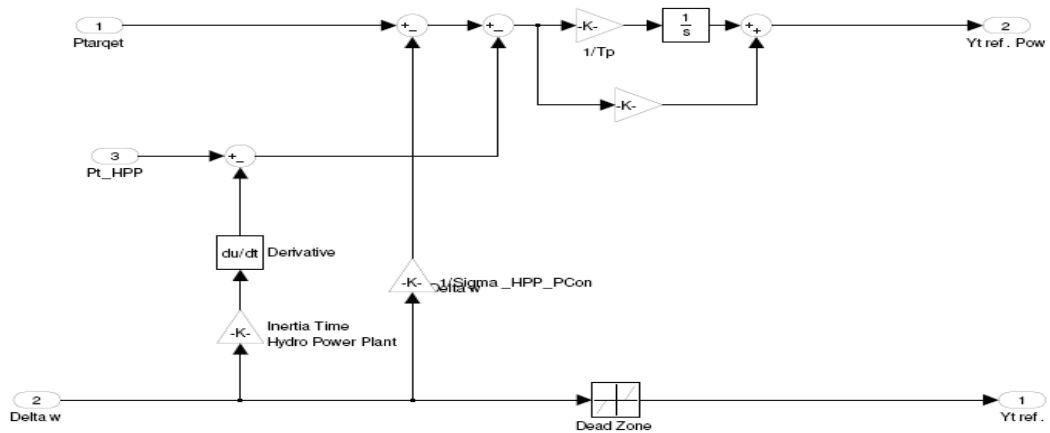


Fig. A-10: Power Control Model of Altinkaya HPP.

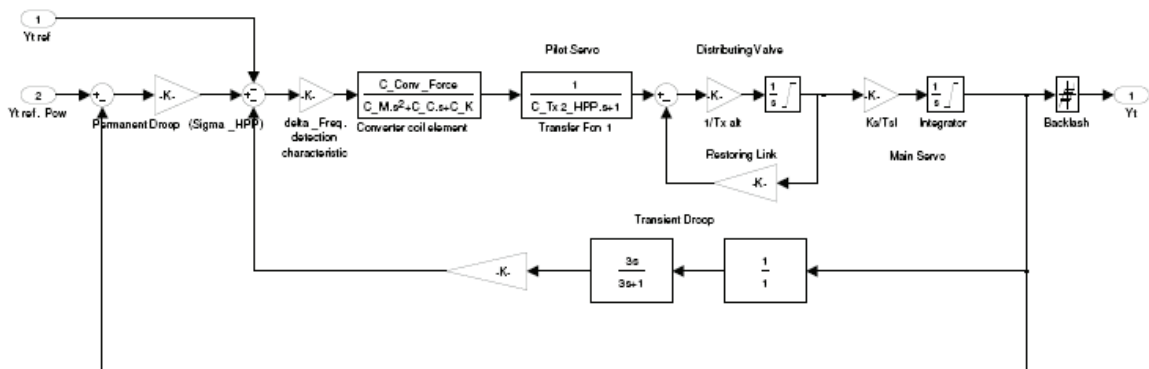


Fig. A-11: Governor Model of Altinkaya HPP.

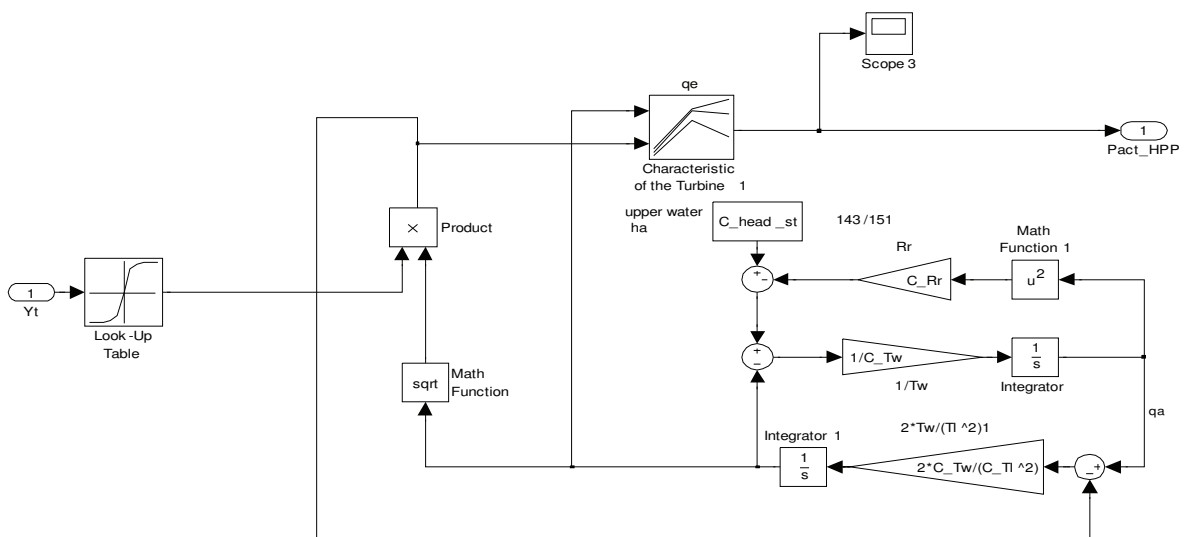


Fig. A-12: Turbine Model of Altinkaya HPP.

Table A-4: Parameters of Altinkaya HPP Model

Parameters	Variable in Matlab	Definition	Altinkaya Value
Mechanical			
	C_Tg_HPP	Mech. time con.	8.2
	C_BLT	Backlash	± 50 mHz
Penstock	C_Tw	Water time con.	.92
	C_Tl	Water wave travel time	0.164
	C_Rr	Friction con.	0.025
Power Control			
	C_Kp_HPP	Proportional gain	0.1
	C_Tp_HPP	Integral time con.	25
	C_Kacc_HPP	Acc. input gain	1
	C_Sigma_HPP_Pcon	Power control speed droop	0.05
	deadband_HPP_C	Deadband	± 20 mHz
Governor			
	C_df_det_gain	Frequency deviation detection gain	24.8
	C_Conv_Force	Converter force	0.42
	C_M	Mass of converter coil moving part	3.06e-04
	C_C	Viscosity coef. of pilot valve	0.0058
	C_K	Spring constant of converter	5
	C_Tx_HPP	Distributing valve time con.	0.02
	C_Tx2_HPP	Pilot servo time con.	0.405
	C_Kx_HPP	Restoring link gain	0.05
	C_Tsl	Main servo time con.	0.14
	C_Sigma_HPP	Speed (permanent) droop	0.05
	C_Sigma_T	Transient droop	0.3
	C_Td	Reset time con.	3
	C_Ks	cm to p.u. conversion	1 / 38
	C_Tlead	Lead time con.	0
	C_Tlag	Lag time con.	0

■ Structure of Karakaya HPP

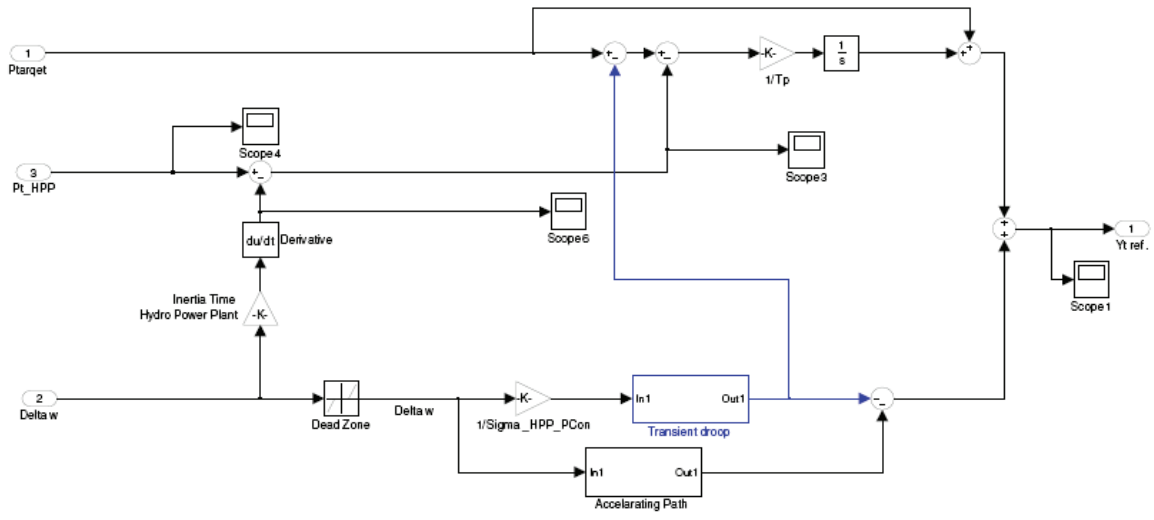


Fig. A-13: Power Control Model of Karakaya HPP.

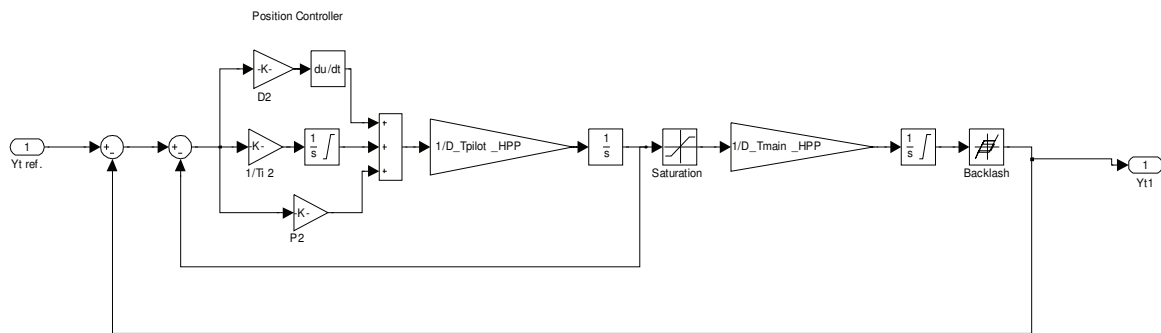


Fig. A-14: Governor Model of Karakaya HPP.

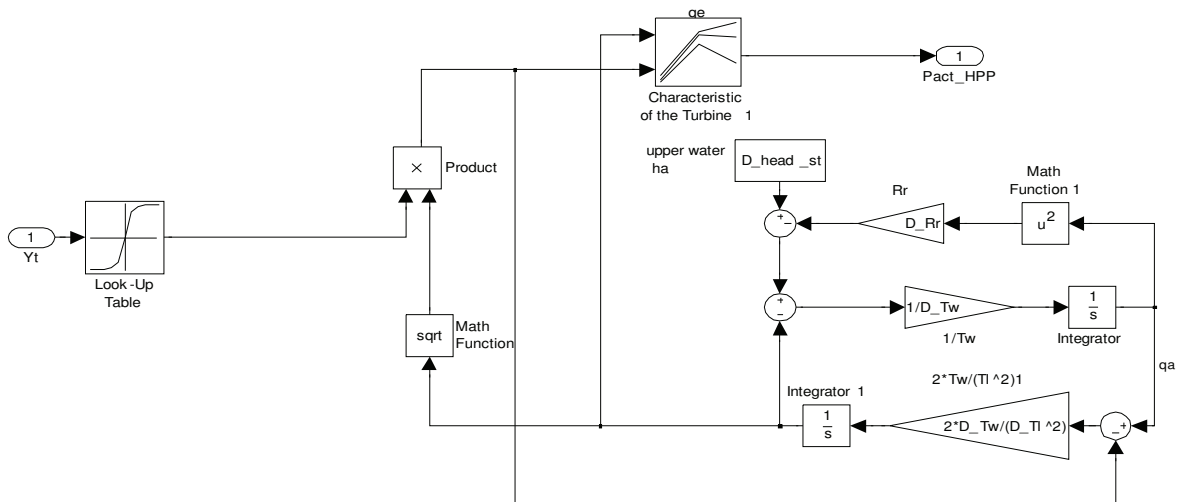


Fig. A-15: Turbine Model of Karakaya HPP.

Table A-5: Parameters of Karakaya HPP Model

Parameters	Variable in Matlab	Definition	Karakaya Value
Mechanical			
	D_Tg_HPP	Mech. time con.	10
	D_BLT	Backlash	± 50 mHz
Penstock	D_Tw	Water time con.	1.24
	D_Tl	Water wave travel time	0.133
	D_Rr	Friction con.	0.05
Power Control			
	D_Tp_HPP	Integral time con.	120
	D_Kacc	Acc. input gain	8.5
	D_Tacc	Acc. Time gain	0.5
	D_Sigma_HPP_Pcon	Power control speed droop	0.04
	D_r	Transient Gain	0.12
	D_Tn	Transient Time	47
	deadband_HPP_D	Deadband (only in speed control)	0 mHz
Governor			
	D_Sigma_HPP	Speed droop	0.08
Position Control			
	D_P2	Proportional gain	6
	D_Ti2	Integral time con.	1
	D_D2	Derivative gain	0
	D_Tpilot_HPP	Pilot Servo time con.	0.5
	D_Tmain_HPP	Main Servo time con.	1.1
	D_Rate_HPP	Opening time of wicket gate from 0 to 100%	20

■ Structure of Oymapinar HPP

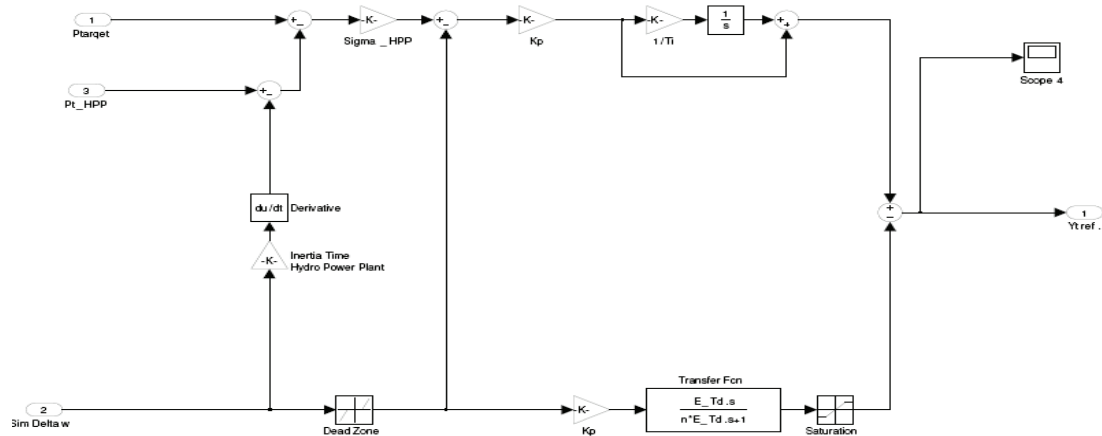


Fig. A-16: Power Control Model of Oymapinar HPP.

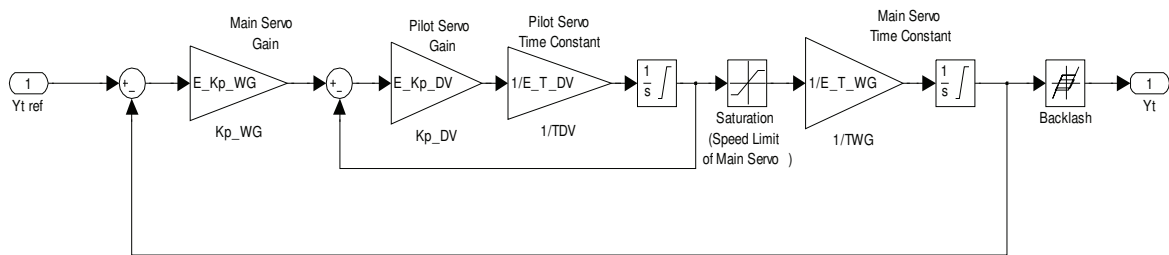


Fig. A-17: Governor Model of Oymapinar HPP.

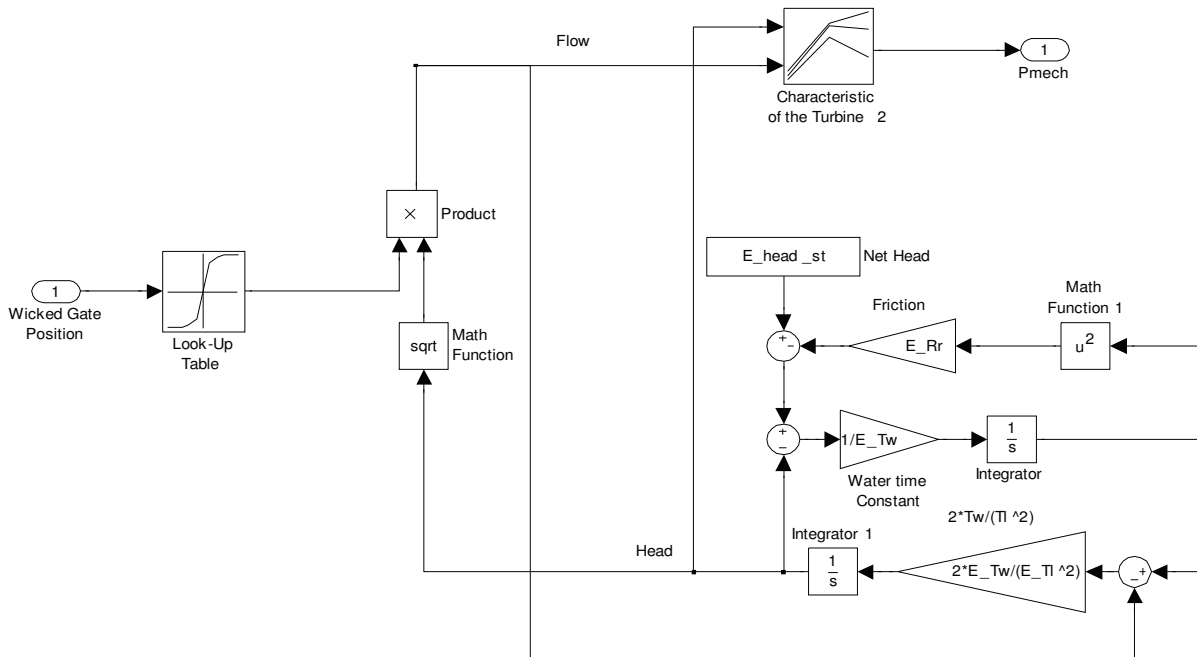


Fig. A-18: Turbine Model of Oymapinar HPP.

Table A-6: Parameters of Oymapinar HPP Model

Parameters	Variable in Matlab	Definition	Oymapinar Value
Mechanical			
	E_Tg_HPP	Mech. time con.	9
	E_BLT	Backlash	± 50 mHz
Penstock	E_Tw	Water time con.	0.79x1.25
	E_Tl	Water wave travel time	0.147
	E_Rr	Friction con.	0.053
Power Control			
	n	Transient Gain	0.165
	E_Td	Transient Time	2.43
	E_Kp	Proportional gain	8
	E_Ti	Integral time con.	3
	E_Sigma_HPP	Speed droop	0.04
	deadband_HPP_E	Deadband	± 20 mHz
Governor			
	E_Kp_DV	Distributing valve Gain	0.6
	E_T_DV	Distributing valve Time	0.1
	E_Kp_WG	Wicked Gate Gain	2.8
	E_T_WG	Wicked Gate Time	1.9
	E_Rate_up	Opening time of main servo from 0% to 100%	9
	E_Rate_down	Opening time of main servo from 0% to 100%	12

■ Structure of Berke HPP

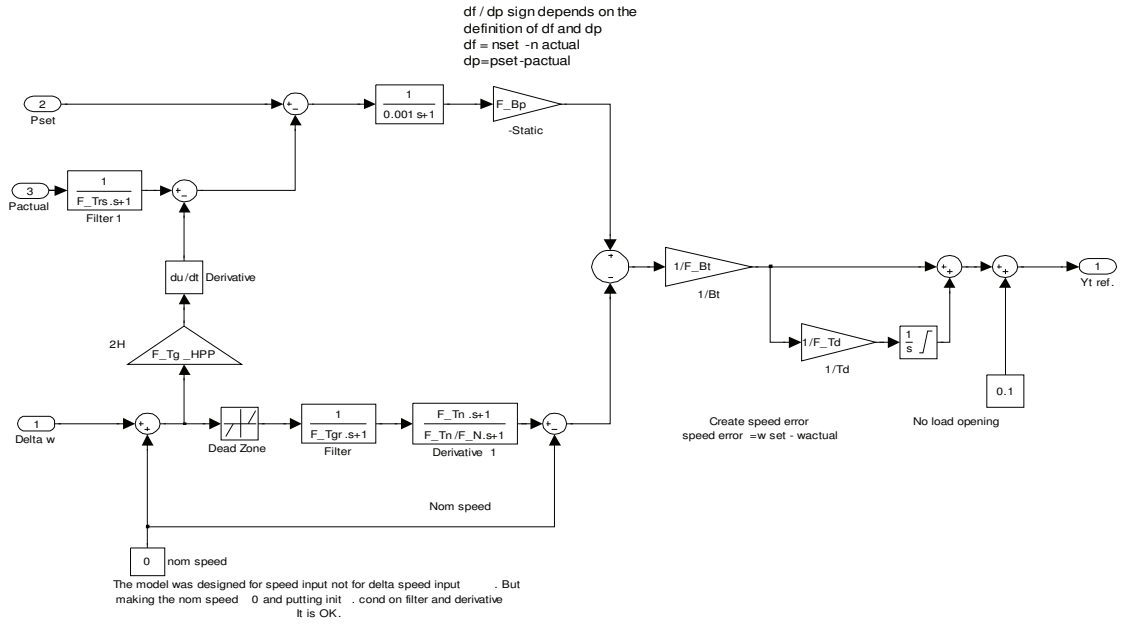


Fig. A-19: Power Control Model of Berke HPP.

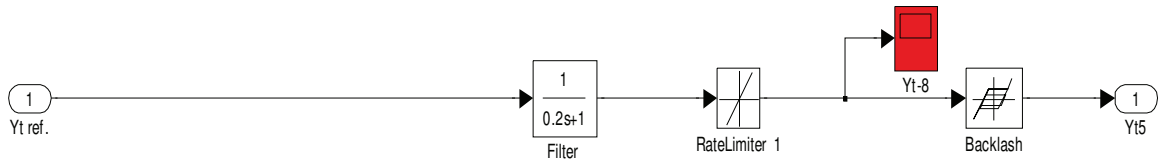


Fig. A-20: Governor Model of Berke HPP.

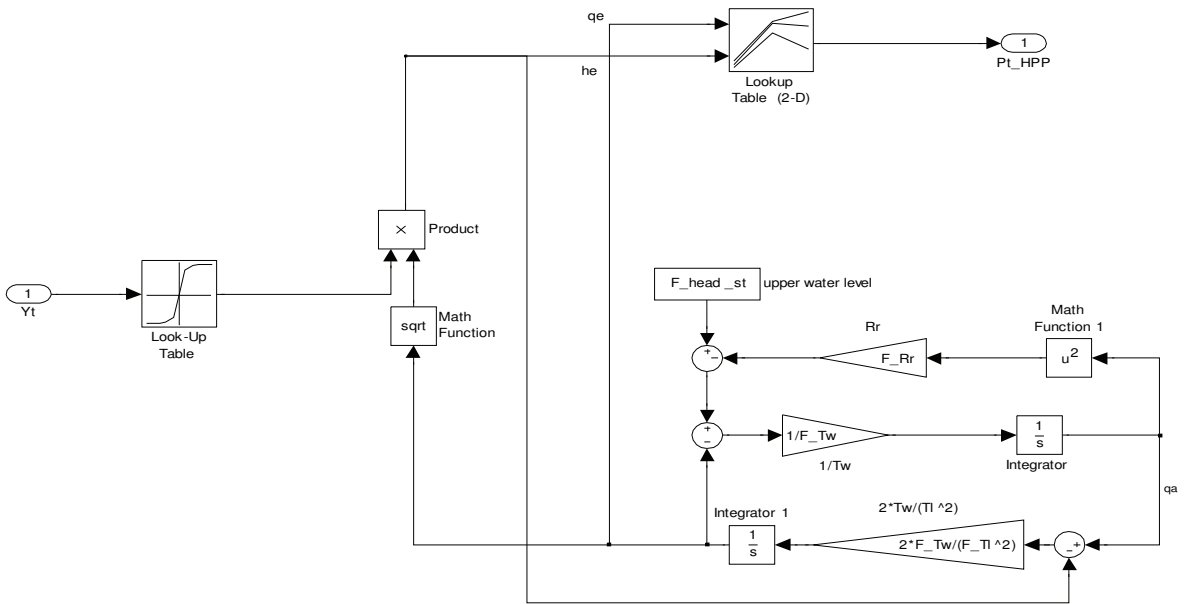


Fig. A-21: Turbine Model of Berke HPP.

Table A-7: Parameters of Berke HPP Model

Parameters	Variable in Matlab	Definition	Berke Value
Mechanical			
	F_Tg_HPP	Mech. time con.	7.6
	F_BLT	Backlash	± 50 mHz
Penstock	F_Tw	Water time con.	0.88
	F_Tl	Water wave travel time	0.084
	F_Rr	Friction con.	0.025
Speed & Power Controller			
	F_Bp	Permanent Droop	0.04
	F_Bt	Transient Droop	0.35
	F_Td	Integration time constant	1.25
	F_N	Acceleration Gain	10
	F_Tn	Acceleration time constant	0.35
	F_Tgr	Time constant of the frequency filter	0.1
	F_Trs	Power measurement filter time constant	1
	deadband_HPP_F	Dead band	± 20 mHz
Governor			
	F_Topen		20
	F_Tclose		15
	F_Tmain	Main Servo time con.	0.1
	F_Tdist	Distribution valve time con.	0.1
	F_Rate_HPP	Opening time of wicket gate from 0 to 100%	12

■ Structure of Hasanugurlu HPP

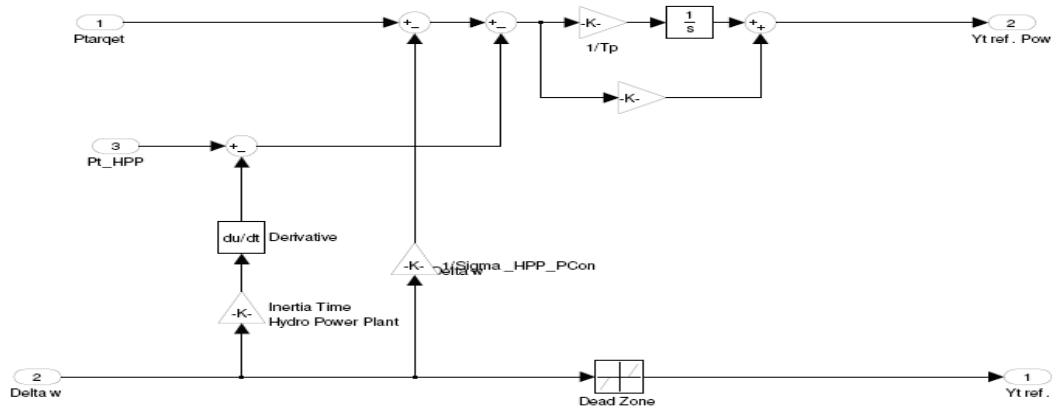


Fig. A-22: Power Control Model of Hasanugurlu HPP.

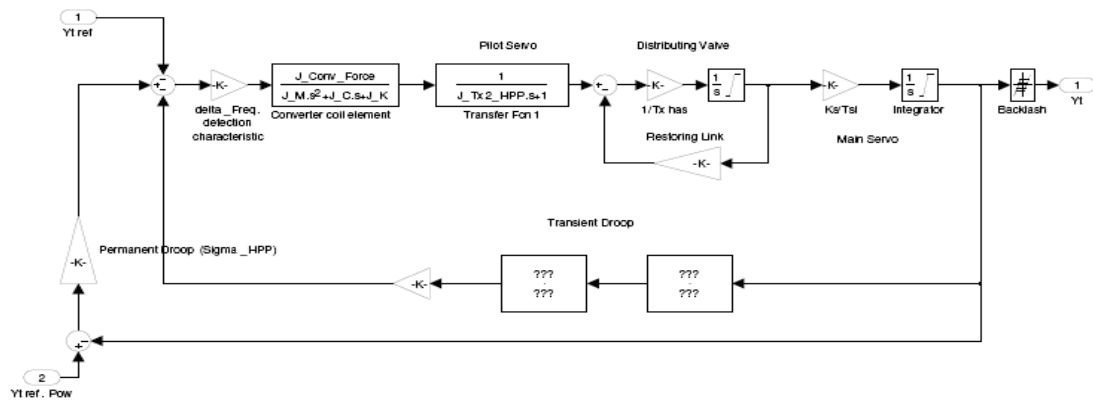


Fig. A-23: Governor Model of Hasanugurlu HPP

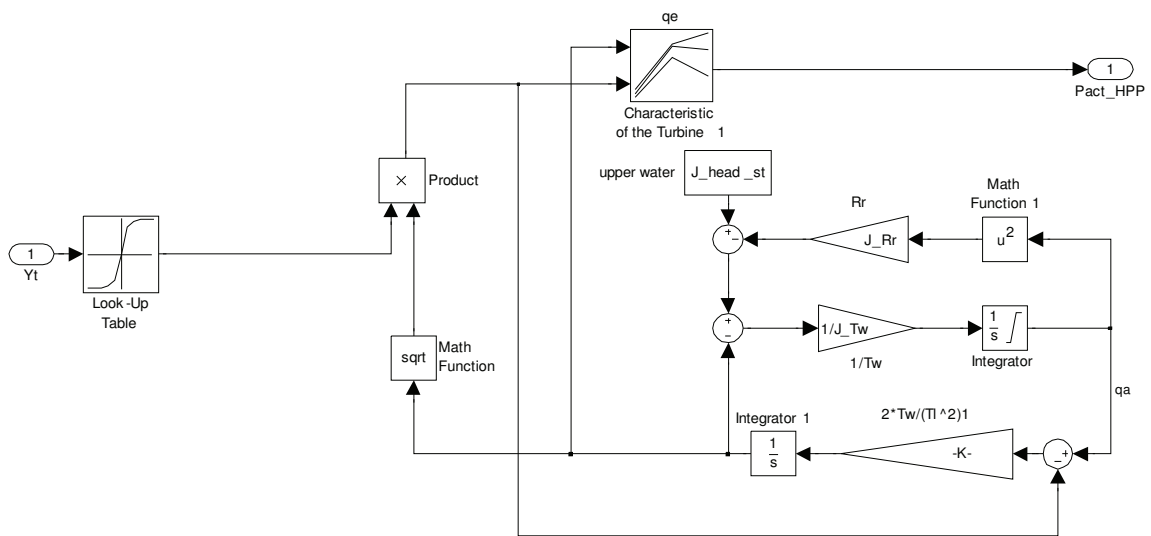


Fig. A-24: Turbine Model of Hasanugurlu HPP.

Table A-8: Parameters of Hasanugurlu HPP Model

Parameters	Variable in Matlab	Definition	Hasanugurlu Value
Mechanical			
	J_Tg_HPP	Mech. time con.	8
	J_BLT	Backlash	± 50 mHz
Penstock	J_Tw	Water time con.	1.52
	J_Tl	Water wave travel time	0.083
	J_Rr	Friction con.	0.025
Power Control			
	J_Kp_HPP	Proportional gain	0.1
	J_Tp_HPP	Integral time con.	25
	J_Kacc_HPP	Acc. input gain	1
	J_Sigma_HPP_Pcon	Power control speed droop	0.04
	deadband_HPP_J	Dead band	± 50 mHz
Governor			
	J_df_det_gain	Frequency deviation detection gain	24.8
	J_Conv_Force	Converter force	0.99
	J_M	Mass of converter coil moving part	6.22e-5
	J_C	Viscosity coef. of pilot valve	2.49e-3
	J_K	Spring constant of converter	0.5
	J_Tx_HPP	Distributing valve time con.	0.01
	J_Tx2_HPP	Pilot servo time con.	0.02
	J_Kx_HPP	Restoring link gain	0.1
	J_Tsl	Main servo time con.	0.37
	J_Sigma_HPP	Speed (permanent) droop	0.04
	J_Sigma_T	Transient droop	0.3
	J_Td	Reset time con.	4
	J_Ks	cm to p.u. conversion	.0241
	J_Tlead	Lead time con.	0
	J_Tlag	Lag time con.	0

Appendix B

Table B-9, B-10 and B-11 show the parameters of Elbistan_B, Cayirhan, Kangal TPP.

Table B-9: Parameters of Elbistan_B_TPP Model

Parameters	Variable in Matlab	Definition	Elbistan_B Value
Mechanical			
	Elbistan_B_Tg_TPP	Mech. time con.	6.8
	B_TPP_BLT	Backlash	± 50 mHz
Power Control			
	Elbistan_B_Ti_TPP	Power Control I	25
	Elbistan_B_Kp_TPP	Power Control P	0.1
	Elbistan_B_Sigma_TPP	Power Control droop	0.06
	Elbistan_B_SigmaTPP	Speed Control P	0.1
	Elbistan_B_Kpr	Pressure Deviation Bias	0.5
	deadband_TPP_ Elbistan_B	Dead band	± 20 mHz
Governor			
	Elbistan_B_Ty	Pilot Servo Delay	0.1
	Elbistan_B_Tmain	Main servo Delay	0.1
	Elbistan_B_Rate	Opening time of wicket gate from 0 to 100%	5
Turbine & Boiler			
	Elbistan_B_Thp	HP Delay	0.24
	Elbistan_B_Tmp	MP Delay	11
	Elbistan_B_Tlp	LP Delay	0.4
	Elbistan_B_HPgain	HP Gain	0.274
	Elbistan_B_MPgain	MP Gain	0.299
	Elbistan_B_LPgain	LP Gain	0.427
	Elbistan_B_Kb_TPP	Boiler P	1.35
	Elbistan_B_Tb_TPP	Boiler I	100
	Elbistan_B_Tk_TPP	Coal Delay	30
	Elbistan_B_TkTPP	Boiler Delay	20
	Elbistan_B_Ti_Ds	Steam Storage Con.	60

Table B-10: Parameters of Cayirhan 3-4 Model

Parameters			Cayirhan 3-4
	Variable in Matlab	Definition	Value
Mechanical			
	D_Tg_TPP	Mech. time con.	6.8
	D_TPP_BLT	Backlash	± 50 mHz
Power Control			
	D_Ti_TPP	Power Control I	25
	D_Kp_TPP	Power Control P	2
	D_Sigma_TPP	Power Control droop	0.06
	D_SigmaTPP	Speed Control P	0.1
	D_Kpr	Pressure Deviation Bias	0.5
	deadband_TPP_D	Dead band	± 20 mHz
Governor			
	D_Ty	Pilot Servo Delay	0.1
	D_Tmain	Main servo Delay	0.1
	D_Rate	Opening time of wicket gate from 0 to 100%	5
Turbine & Boiler			
	D_Thp	HP Delay	0.24
	D_Tmp	MP Delay	11
	D_Tlp	LP Delay	0.4
	D_HPgain	HP Gain	0.274
	D_MPgain	MP Gain	0.299
	D_LPgain	LP Gain	0.427
	D_Kb_TPP	Boiler P	1.35
	D_Tb_TPP	Boiler I	100
	D_Tk_TPP	Coal Delay	30
	D_TkTPP	Boiler Delay	20
	D_Ti_Ds	Steam Storage Con.	60

Table B-11: Parameters of Kangal 3 Model

Parameters			Kangal 3
	Variable in Matlab	Definition	Value
Mechanical			
	J_Tg_TPP	Mech. time con.	6.8
	J_TPP_BLT	Backlash	± 50 mHz
Power Control			
	J_Ti_TPP	Power Control I	25
	J_Kp_TPP	Power Control P	2
	J_Sigma_TPP	Power Control droop	0.06
	J_SigmaTPP	Speed Control P	0.1
	J_Kpr	Pressure Deviation Bias	0.5
	deadband_TPP_j	Dead band	± 20 mHz
Governor			
	J_Ty	Pilot Servo Delay	0.1
	J_Tmain	Main servo Delay	0.1
	J_Rate	Opening time of wicket gate from 0 to 100%	5
Turbine & Boiler			
	J_Thp	HP Delay	0.2
	J_Tmp	MP Delay	11
	J_Tlp	LP Delay	0.4
	J_HPgain	HP Gain	0.274
	J_MPgain	MP Gain	0.299
	J_LPgain	LP Gain	0.427
	J_Kb_TPP	Boiler P	1.35
	J_Tb_TPP	Boiler I	180
	J_Tk_TPP	Coal Delay	30
	J_TkTPP	Boiler Delay	20
	J_Ti_Ds	Steam Storage Con.	60

Structures of Iskenderun, Soma, Ambarlifo, Seyitomer, Can TPP

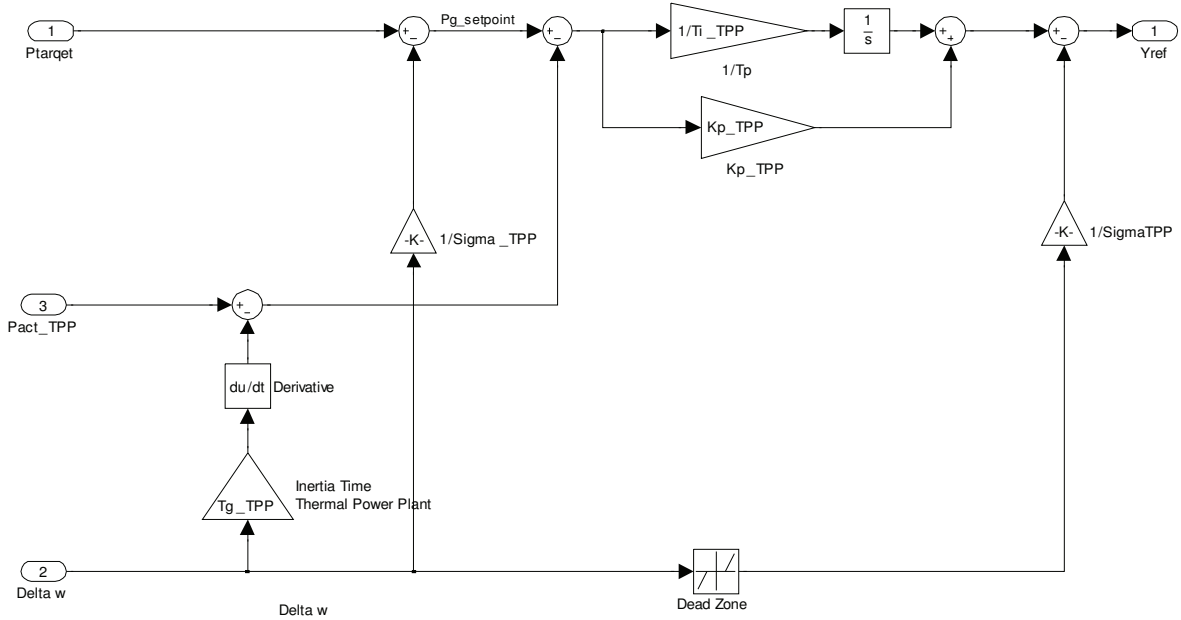


Fig. B-28: Power Control Model.

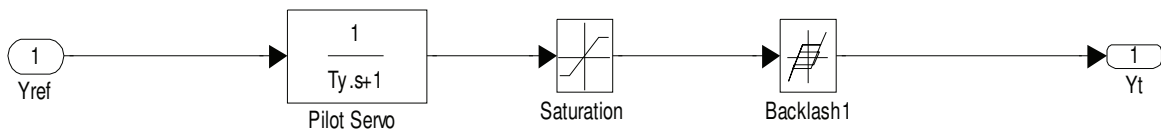


Fig. B-29: Governor Model.

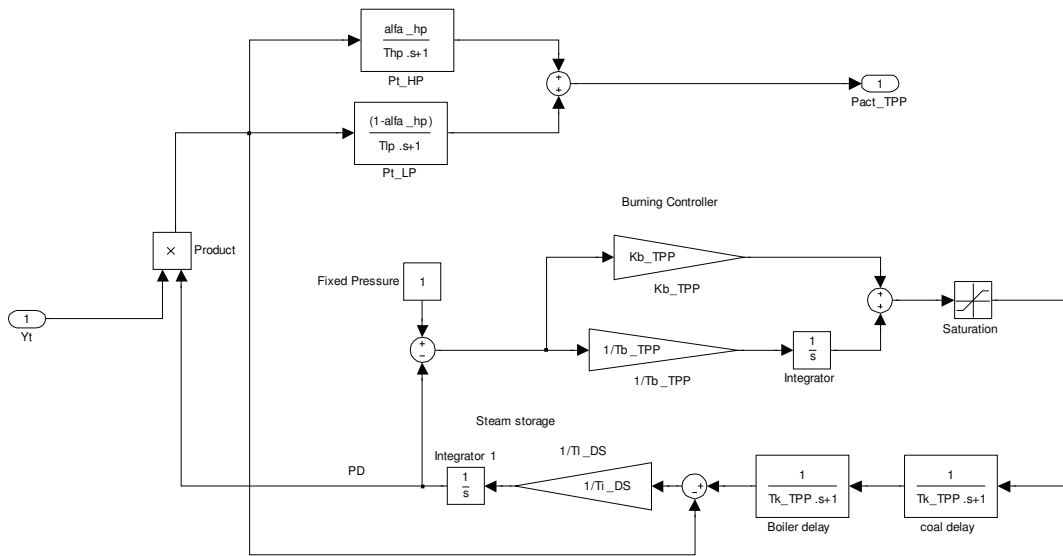


Fig. B-30: Turbine Model.

Appendix B

Tables B-12, B-13, B-14, B-15 and B-16 show the parameters of Iskenderun, Soma, Ambarlifo, Seyitomer and Can TPP.

Table B-12: Parameters of Iskenderun_TPP model

Parameters	Variable in Matlab	Definition	Iskenderun Value
Mechanical			
	A_Tg_TPP	Mech. time con.	14
	A_TPP_BLT	Backlash	± 50 mHz
Power Control			
	A_Ti_TPP	Power Control I	25
	A_Kp_TPP	Power Control P	0.1
	A_Sigma_TPP	Power Control droop	0.08
	deadband_TPP_A	Dead band	± 20 mHz
Governor			
	A_Ty	Pilot Servo Delay	0.3
Turbine & Boiler			
	A_Thp	HP Delay	0.5
	A_alfa_hp	Heat Transfer Coefficient	0.3
	A_Tlp	LP Delay	10
	A_Kb_TPP	Boiler P	1.5
	A_Tb_TPP	Boiler I	180
	A_Tk_TPP	Coal Delay	20
	A_Ti_Ds	Steam Storage Con.	60

Table B-13: Parameters of Soma_TPP model

Parameters	Variable in Matlab	Definition	Soma Value
Mechanical			
	B_Tg_TPP	Mech. time con.	14
	TPP_BLT	Backlash	± 50 mHz
Power Control			
	B_Ti_TPP	Power Control I	25
	B_Kp_TPP	Power Control P	
	B_Sigma_TPP	Power Control droop	0.08
	deadband_TPP_B	Dead band	± 20 mHz
Governor			
	B_Ty	Pilot Servo Delay	0.3
Turbine & Boiler			
	B_Thp	HP Delay	0.5
	B_alfa_hp	Heat Transfer Coefficient	0.3
	B_Tlp	LP Delay	10

Appendix B

	B_Kb_TPP	Boiler P	1.5
	B_Tb_TPP	Boiler I	180
	B_Tk_TPP	Coal Delay	20
	B_Ti_Ds	Steam Storage Con.	60

Table B-14: Parameters of Ambarlifo_TPP model

Parameters			Ambarlifo
	Variable in Matlab	Definition	Value
Mechanical			
	C_Tg_TPP	Mech. time con.	14
	C_TPP_BLT	Backlash	± 50 mHz
Power Control			
	C_Ti_TPP	Power Control I	25
	C_Kp_TPP	Power Control P	
	C_Sigma_TPP	Power Control droop	0.08
	deadband_TPP_C	Dead band	± 20 mHz
Governor			
	C_Ty	Pilot Servo Delay	0.5
Turbine & Boiler			
	C_Thp	HP Delay	0.5
	C_alfa_hp	Heat Transfer Coefficient	0.3
	C_Tlp	LP Delay	10
	C_Kb_TPP	Boiler P	1.5
	C_Tb_TPP	Boiler I	180
	C_Tk_TPP	Coal Delay	20
	C_Ti_Ds	Steam Storage Con.	60

Table B-15: Parameters of Seyitomer TPP Model

Parameters			Seyitomer
	Variable in Matlab	Definition	Value
Mechanical			
	G_Tg_TPP	Mech. time con.	14
Power Control			
	G_TPP_BLT	Backlash	± 50 mHz
	G_Ti_TPP	Power Control I	25
	G_Kp_TPP	Power Control P	0.1
	G_Sigma_TPP	Power Control droop	0.08
	deadband_TPP_G	Dead band	± 20 mHz
Governor			
	G_Ty	Pilot Servo Delay	0.5
Turbine & Boiler			
	G_Thp	HP Delay	0.5

Appendix B

	G_alfa_hp	Heat Transfer Coefficient	0.3
	G_Tlp	LP Delay	10
	G_Kb_TPP	Boiler P	1.5
	G_Tb_TPP	Boiler I	180
	G_Tk_TPP	Coal Delay	20
	G_Ti_Ds	Steam Storage Con.	60

Table B-16: Parameters of Can TPP Model

Parameters			Can
	Variable in Matlab	Definition	Value
Mechanical			
	I_Tg_TPP	Mech. time con.	14
Power Control	I_TPP_BLT	Backlash	± 50 mHz
	I_Ti_TPP	Power Control I	25
	I_Kp_TPP	Power Control P	0.1
	I_Sigma_TPP	Power Control droop	0.08
	deadband_TPP_I	Dead band	± 20 mHz
Governor			
	I_Ty	Pilot Servo Delay	0.3
Turbine & Boiler			
	I_Thp	HP Delay	0.5
	I_alfa_hp	Heat Transfer Coefficient	0.3
	I_Tlp	LP Delay	10
	I_Kb_TPP	Boiler P	1.5
	I_Tb_TPP	Boiler I	180
	I_Tk_TPP	Coal Delay	20
	I_Ti_Ds	Steam Storage Con.	60

Appendix B

Structures of Kemerkoj, Ytagan and Yenikoj TPP

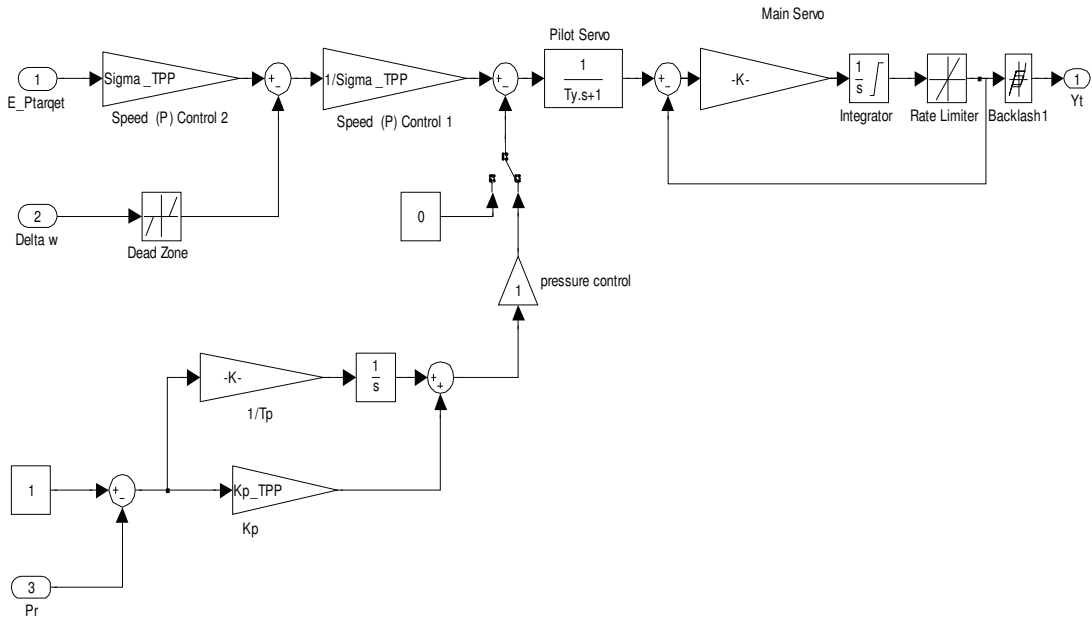


Fig. B-31: Governor Model.

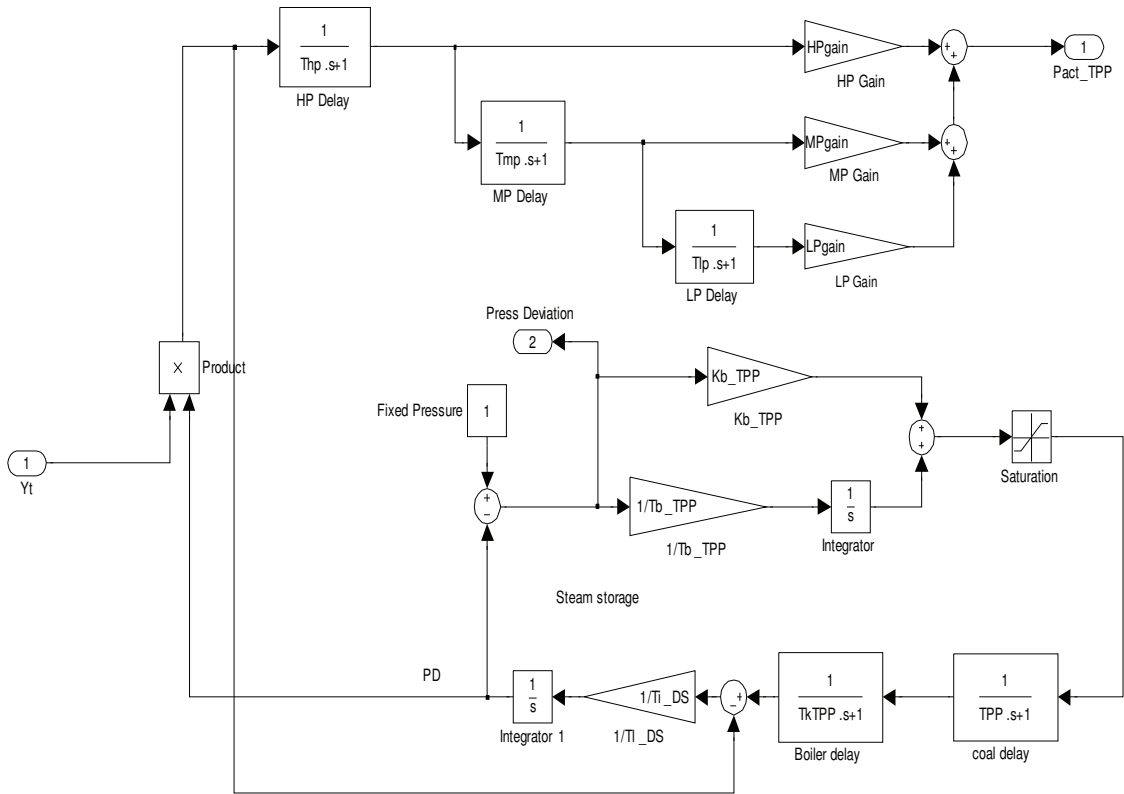


Fig. B-32: Turbine Model.

Appendix B

Table B-17, B-18 and B-19 show the parameters of Kemerkooy, Ytagan and Yenikoy TPP

Table B-17: Parameters of Kemerkooy Model

Parameters			Kemerkooy
	Variable in Matlab	Definition	Value
Power Control			
	E_Tp_TPP	Power Control I	50
	E_Kp_TPP	Power Control P	3
	E_Sigma_TPP	Power Control droop	0.035
	deadband_TPP_E	Dead band	± 20 mHz
Governor	E_TPP_BLT	Backlash	± 50 mHz
	E_Ty	Pilot Servo Delay	0.1
	E_Tmain_TPP	Main servo Delay	0.1
	E_Rate_TPP	Opening time of wicked gate from 0 to 100%	10
Turbine & Boiler			
	E_Thp	HP Delay	0.09
	E_Tmp	MP Delay	10
	E_Tlp	LP Delay	0.5
	E_HPgain	HP Gain	0.249
	E_MPgain	MP Gain	0.451
	E_LPgain	LP Gain	0.3
	E_Kb_TPP	Boiler P	1.35
	E_Tb_TPP	Boiler I	180
	E_Tk_TPP	Coal Delay	30
	E_TkTPP	Boiler Delay	20
	E_Ti_Ds	Steam Storage Con.	60

Table B-18: Parameters of Yatagan Model

Parameters			Yatagan
	Variable in Matlab	Definition	Value
Power Control			
	F_Tb_TPP	Power Control I	50
	F_Kp_TPP	Power Control P	3
	F_Sigma_TPP	Power Control droop	0.035
	deadband_TPP_F	Dead band	± 20 mHz
Governor	F_TPP_BLT	Backlash	± 50 mHz
	F_Ty	Pilot Servo Delay	0.1
	F_Tmain	Main servo Delay	0.1
	F_Rate	Opening time of wicked gate from 0 to 100%	10
Turbine & Boiler			
	F_Thp	HP Delay	0.09

Appendix B

	F_Tmp	MP Delay	10
	F_Tlp	LP Delay	0.5
	F_HPgain	HP Gain	0.249
	F_MPgain	MP Gain	0.451
	F_LPgain	LP Gain	0.3
	F_Kb_TPP	Boiler P	1.35
	F_Tb_TPP	Boiler I	180
	F_Tk_TPP	Coal Delay	30
	F_TkTPP	Boiler Delay	20
	F_Ti_Ds	Steam Storage Con.	80

Table B-19: Parameters of Yenikoy Model

Parameters	Variable in Matlab	Definition	Yenikoy Value
Power Control			
	H_Tb_TPP	Power Control I	50
	H_Kp_TPP	Power Control P	3
	H_Sigma_TPP	Power Control droop	0.035
	deadband_TPP_H	Dead band	± 20 mHz
Governor	H_TPP_BLT	Backlash	± 50 mHz
	H_Ty	Pilot Servo Delay	0.3
	H_Tmain	Main servo Delay	0.1
	H_Rate	Opening time of wicked gate from 0 to 100%	10
Turbine & Boiler			
	H_Thp	HP Delay	0.09
	H_Tmp	MP Delay	10
	H_Tlp	LP Delay	0.5
	H_HPgain	HP Gain	0.249
	H_MPgain	MP Gain	0.451
	H_LPgain	LP Gain	0.3
	H_Kb_TPP	Boiler P	1.35
	H_Tb_TPP	Boiler I	180
	H_Tk_TPP	Coal Delay	30
	H_TkTPP	Boiler Delay	20
	H_Ti_Ds	Steam Storage Con.	60

Appendix C

Natural Gas Combined Cycle Power Plants (NGCCPP)

- Structures of Ambarli, Bursa, Hamitbat and Unimar GPP

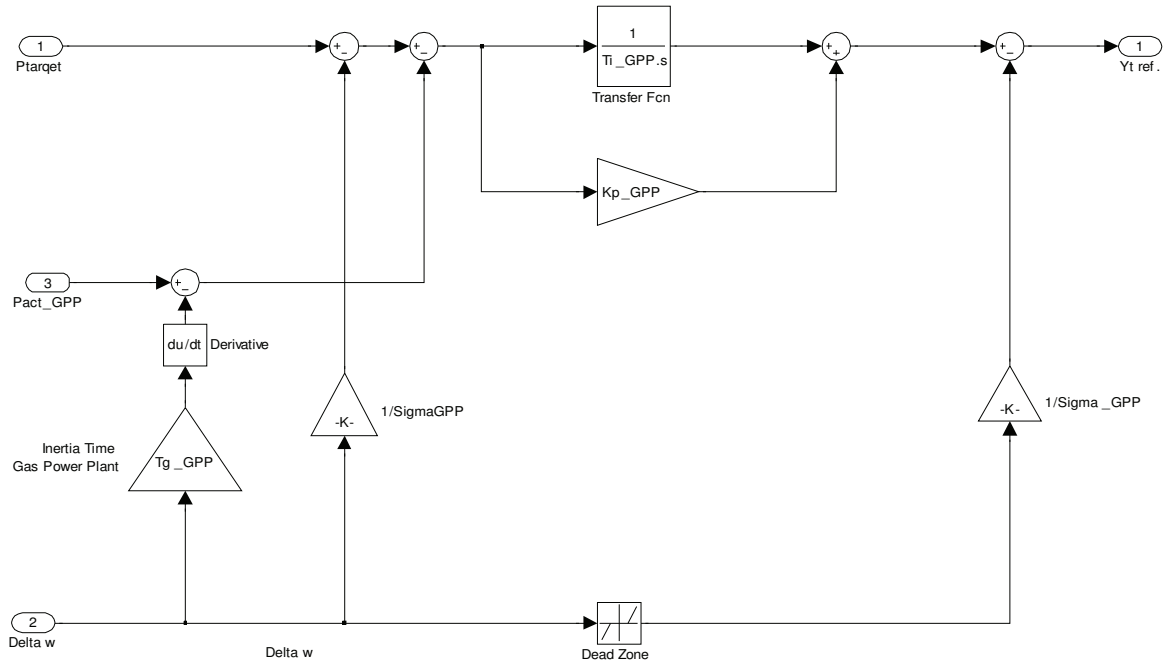


Fig. C-33: Power Control Model.

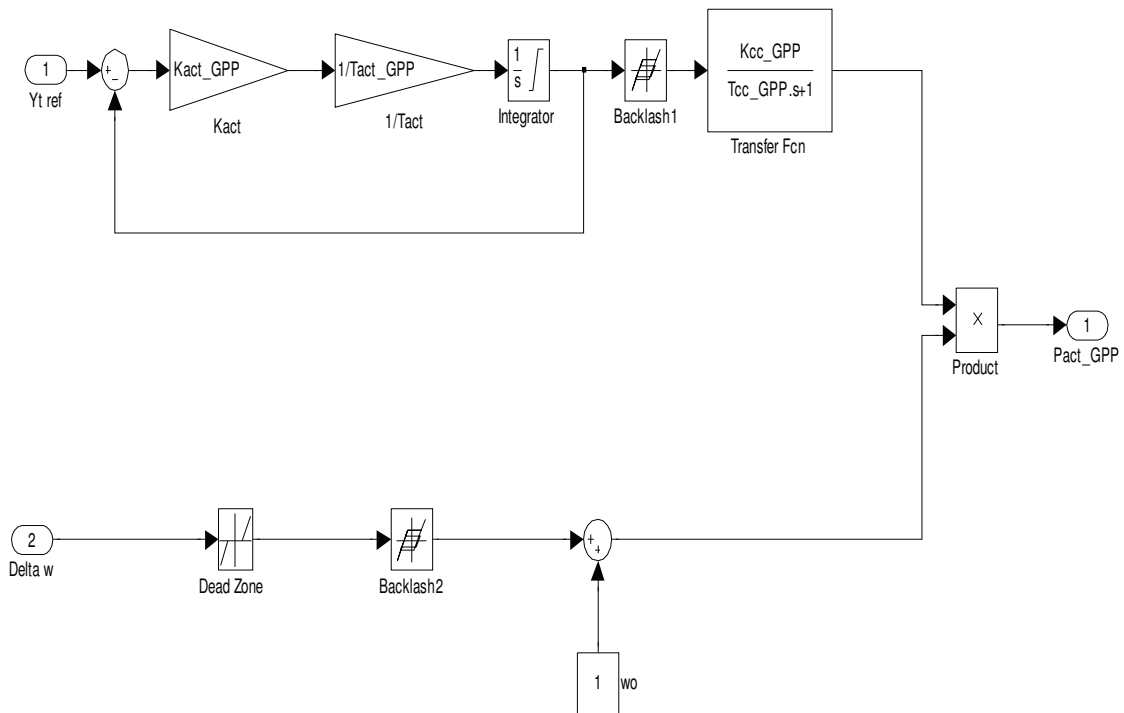


Fig. C-34: Governor Model.

Appendix C

Table C-20, C-21, C-22 and C-23 show the parameters of Ambarli, Bursa, Hamitbat and Unimar GPP.

Table C-20: Parameters of Ambarli Model

Parameters	Variable in Matlab	Definition	Ambarli Value
Mechanical			
	Tg_GPP	Mech. time con.	10
Power Control	GPP_BLT	Backlash	± 50 mHz
	Ti_GPP	Power Control I	25
	Kp_GPP	Power Control P	0.1
	Sigma_GPP	Power Control droop	0.05
	deadband_GPP	Dead band	± 20 mHz
Governor			
	Kact_GPP		10
	Tact_GPP		0.1
Turbine			
	Kcc_GPP		1
	Tcc_GPP		0.5

Table C-21: Parameters of Bursa Model

Parameters	Variable in Matlab	Definition	Bursa Value
Mechanical			
	A_Tg_GPP	Mech. time con.	10
Power Control	A_GPP_BLT	Backlash	± 50 mHz
	A_Ti_GPP	Power Control I	25
	A_Kp_GPP	Power Control P	0.1
	A_Sigma_GPP	Power Control droop	0.05
	deadband_GPP_A	Dead band	± 20 mHz
Governor			
	A_Kact_GPP		10
	A_Tact_GPP		0.1
Turbine			
	A_Kcc_GPP		1
	A_Tcc_GPP		0.5

Appendix C

Table C-22: Parameters of Hamitabat Model

Parameters			Hamitabat
	Variable in Matlab	Definition	Value
Mechanical			
	E_Tg_GPP	Mech. time con.	10
Power Control	E_GPP_BLT	Backlash	± 50 mHz
	E_Ti_GPP	Power Control I	25
	E_Kp_GPP	Power Control P	0.1
	E_Sigma_GPP	Power Control droop	0.05
	deadband_GPP_E	Dead band	± 20 mHz
Governor			
	E_Kact_GPP		10
	E_Tact_GPP		0.1
Turbine			
	E_Kcc_GPP		1
	E_Tcc_GPP		0.5

Table C-23: Parameters of Unimar Model

Parameters			Unimar
	Variable in Matlab	Definition	Value
Mechanical			
	J_Tg_GPP	Mech. time con.	10
Power Control	J_GPP_BLT	Backlash	± 50 mHz
	J_Ti_GPP	Power Control I	25
	J_Kp_GPP	Power Control P	0.1
	J_Sigma_GPP	Power Control droop	0.05
	deadband_GPP_J	Dead band	± 20 mHz
Governor			
	J_Kact_GPP		10
	J_Tact_GPP		0.1
Turbine			
	J_Kcc_GPP		1
	J_Tcc_GPP		0.5

Appendix C

- Structures of Gebze ,Adapazari,Aliaga,Temelli NGCCPP

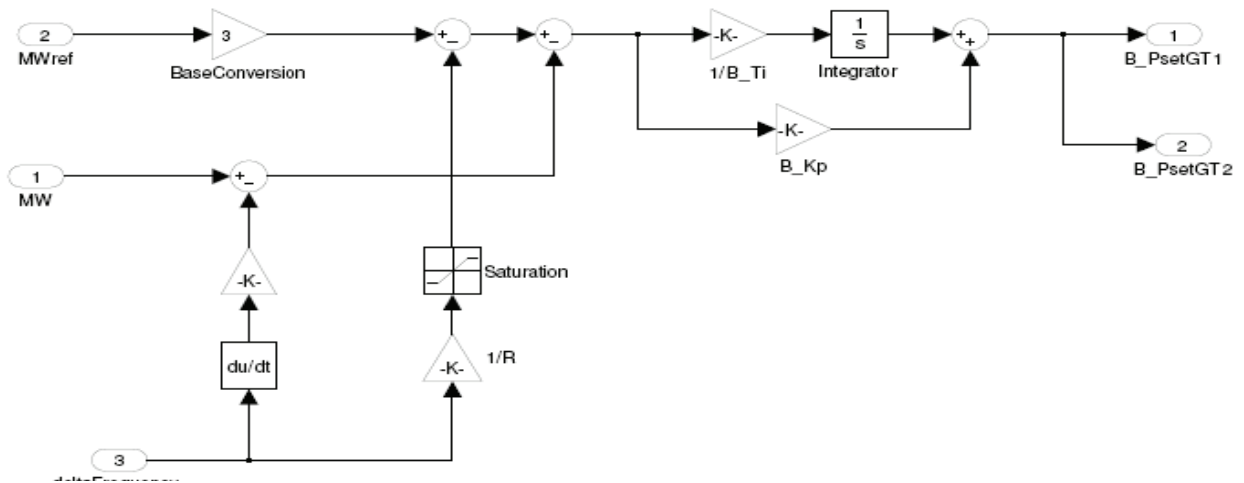


Fig. C-35: Power Control Model of Gebze GPP.

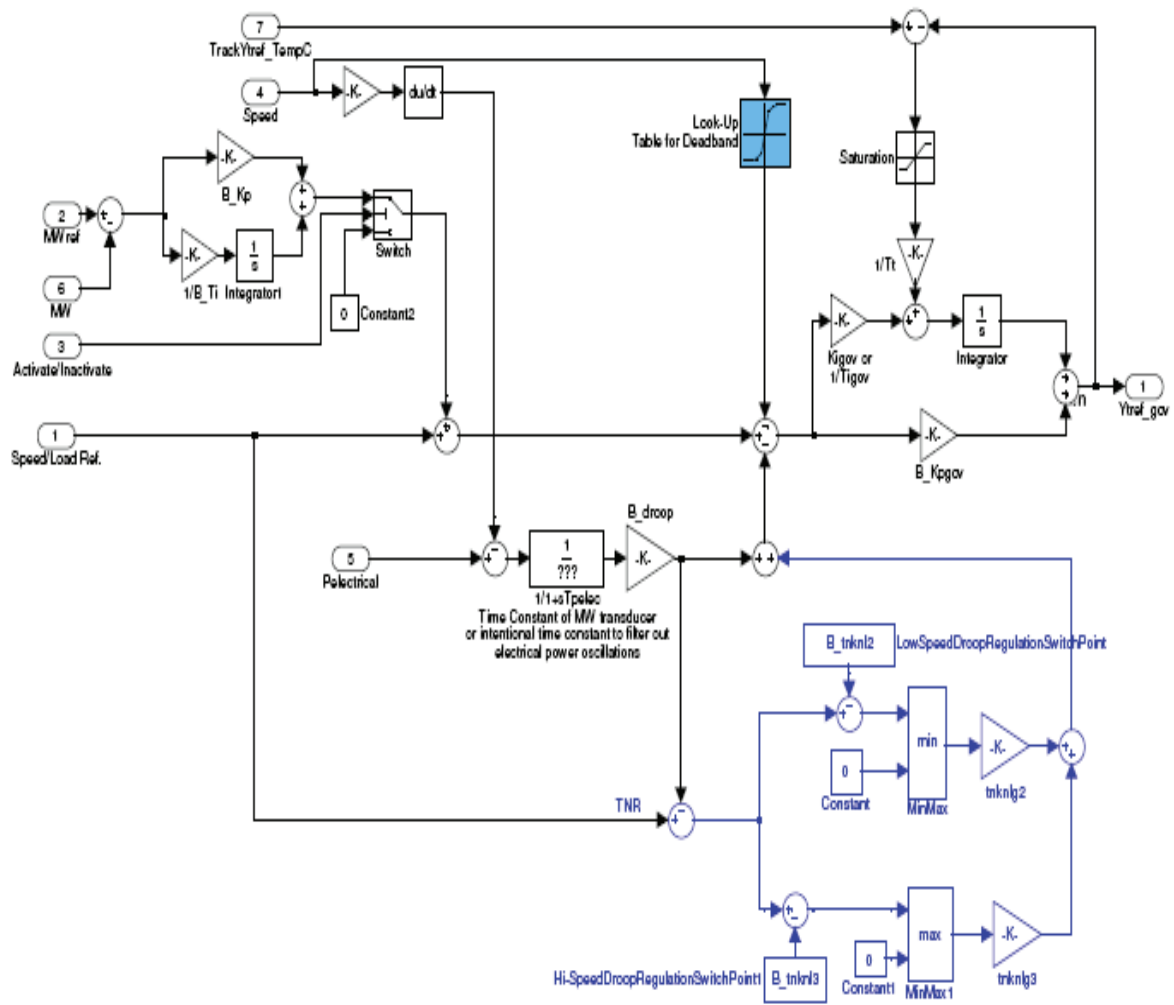


Fig. C-36: Governor Model of Gebze GPP.

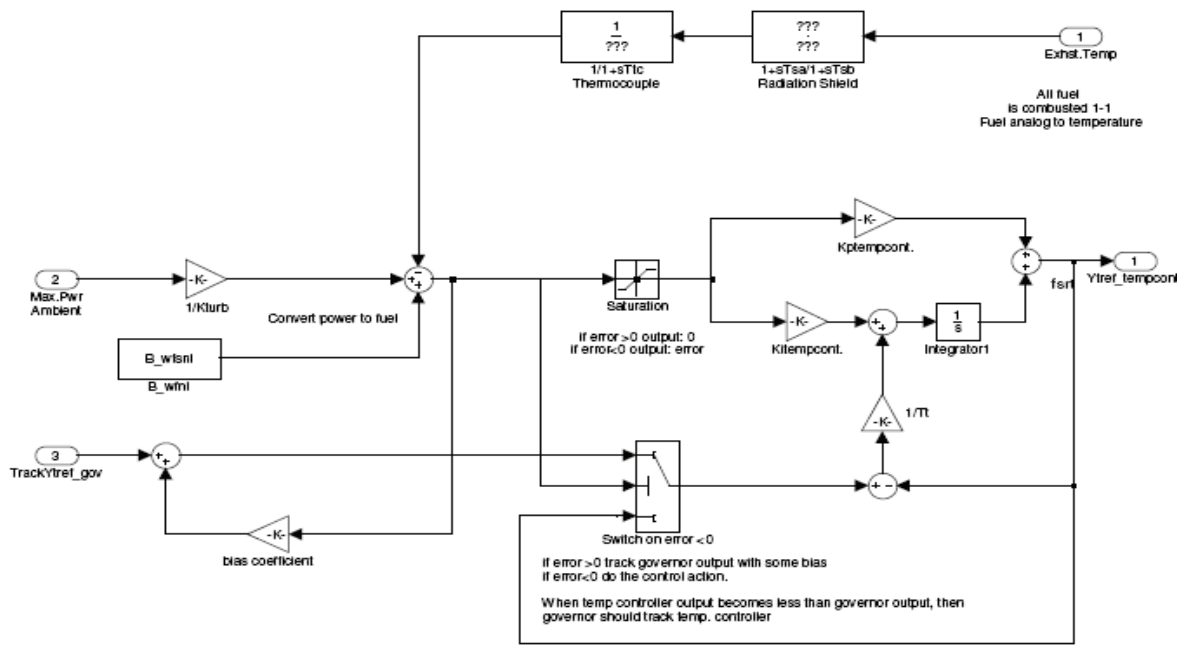


Fig. C-37: Temperature Controller of Gebze GPP.

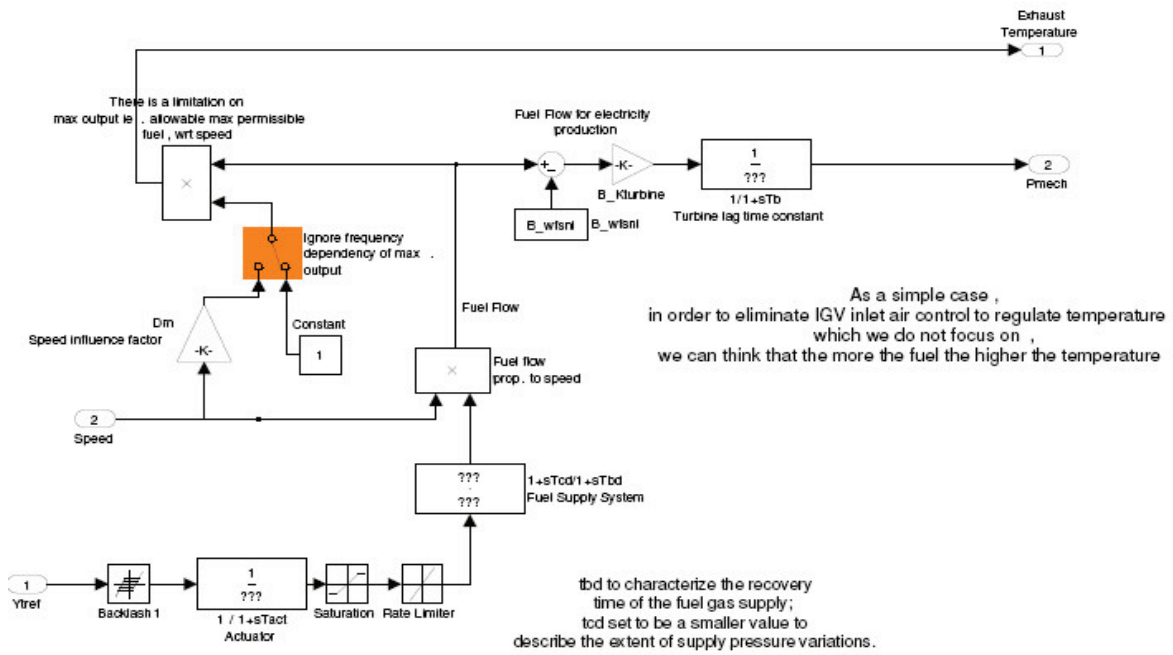


Fig. C-38 Gas: Turbine and Fuel System of Gebze GPP.

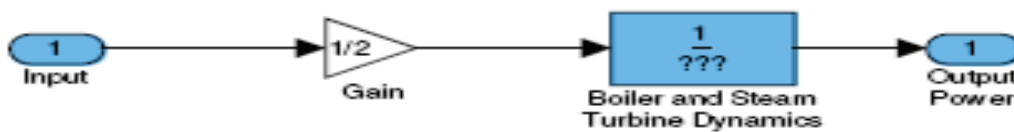


Fig. C-39: Steam Turbine of Gebze GPP.

Appendix C

Table C-24 Gebze ,Adapazari,Aliaga,Temelli Model Parameters

Parameters	Variable in Matlab	Definition	Gebze Value
Mechanical			
	B_Tm_GPP	Mech. time con.	7
	B_GPP_BLT	Backlash	± 50 mHz
Power Control			
	B_Ti_PowerConCC	Power Control I	1000
	B_Kp_PowerConCC	Power Control P	0
	B_PowerConDroopCC	Power Control droop	$0.05 \times (3/2) \times (1/3)$
	B_PowerConFBias_Hi_Lim	Frequency Bias	100
	B_PowerConFBias_Lo_Lim	Frequency Bias	100
Constant P.Con			
	B_Kp_GTCPC		0
	B_Ti_GTCPC		40
	B_ActivateCLC1		0
	B_ActivateCLC2		0
Governor			
	deadband_Gebze	Deadband	± 20 mHz
	B_droop		0.05
	B_Ttc	Thermocouple time constant	3
	B_Tsa	radiation shield transfer function	4
	B_Tsb		5
	B_KpTC	Temperature Controller gain	2
	B_TiTC	Temperature Controller integral time	1.5
	B_trbias	Coefficient for the tracking bias something I introduced	0.5
Gas Turbine and Fuel Sym.			
	B_wfsnl		0.19
	B_Kturbine		1.8
	B_Tact		0.2
	B_Sat_HiLim	Actuator saturation	1
	B_Sat_LowLim		0.15
	B_RateLimR	Actuator rate limiter	3.3
	B_RateLimF		-3.3
	B_Tcd		1
	B_Tbd	Fuel Supply System	1.1
	B_Tb	Turbine lag time constant	0.5
	B_Dm	Speed influence factor	1.05
	B_droop2		0.07

Appendix C

	B_droop3		0.12
	B_tnkn2		0.99875
	B_tnkn3		1.00125
	B_Tpelec		5
	B_Kpgov		9
	B_Tigov		0.6
	B_Tt		1
Steam Turbine			
	B_Tstm	steam turbine time constant	10

Curriculum Vitae

Name Ibrahim Ahmed Ibrahim Nassar

Education, Qualifications, Training and Employment

- 1994 – 1999 Faculty of Engineering Bachelor Degree with final grade "Very Good" Electrical Engineering Department, Al-Azhar University
- 2001 – 2004 M.Sc. Degree in Electrical Engineering (Reactive Power Control In Power Systems Using Neural Network), Faculty of Engineering, Al-Azhar University, Cairo, Egypt.
- 2005-2007 Assistant lecturer in Power and Electrical Machines department , Faculty of Engineering, Al-Azhar University
- Since 2007 PhD student University of Rostock, Faculty of computer science and Electrical Engineering, D-18059 Rostock, Germany

Publications

1. A back-Propagation Neural Network to estimate Reactive Power Control, Sayed.H.El-Banna, Kamel.A. Shoush and Ibrahim.A. Nassar, Al-Azhar Engineering Eighth International Conference, December 24 - 27, 2004, pp.211-227
2. Dynamic Model of Unit 1 of Ataturk Hydro Power Plant in Turkey, Ibrahim A. Nassar , Harald Weber, 13th Middle East Power Systems Conference, MEPCON'2009, Assuit University, Egypt, December 20-23, 2009, pp.259-263
3. Electrical Interconnection between Turkey and Europe: Problems and Solutions, Harald Weber, Ibrahim A. Nassar , 13th Middle East Power Systems Conference, MEPCON'2009, Assuit University, Egypt, December 20-23, 2009, pp.1-11
4. The Overall Frequency Behaviour of the Turkish Power System in Island Operation to Interconnection with European System, Ibrahim A. Nassar , S. Al-Ali and Harald Weber, 13 Symposium Maritime, 2010, Rostock, Germany, pp.155-169
5. Der Anschluss des Türkischen Elektroenergiesys-tems an das Europäische Verbundnetz: Untersu-chung des Erwarteten Pendeldämpfungsverhaltens, S. Al-Ali, Ibrahim A. Nassar and Harald Weber, 13 Symposium Maritime, 2010, Rostock,Germany, pp.179-185

Papers under publications

1. Connection of the Turkish Power system to the European system: Investigation of Primary and Secondary Control Behaviour, Ibrahim A. Nassar , S. Al-Ali and Harald Weber, 17th Power Systems Computation Conference, Stockholm, Sweden,2011
2. Interconnection of the European ENTSO-E-CE System with the Turkish system: Investigation of the Expected Inter-Area-Oscillations Behaviour. S. Al-Ali, Ibrahim A. Nassar and Harald Weber, 17th Power Systems Computation Conference, Stockholm, Sweden, 2011